

PLASTIC RESPONSE OF SHIP SHELL PLATING  
SUBJECTED TO LOADS OF FINITE HEIGHT

CENTRE FOR NEWFOUNDLAND STUDIES

---

**TOTAL OF 10 PAGES ONLY  
MAY BE XEROXED**

(Without Author's Permission)

RICHARD C. HAYWARD











**National Library  
of Canada**

**Acquisitions and  
Bibliographic Services**

**395 Wellington Street  
Ottawa ON K1A 0N4  
Canada**

**Bibliothèque nationale  
du Canada**

**Acquisitions et  
services bibliographiques**

**395, rue Wellington  
Ottawa ON K1A 0N4  
Canada**

*Your file Votre référence*

*Our file Notre référence*

**The author has granted a non-exclusive licence allowing the National Library of Canada to reproduce, loan, distribute or sell copies of this thesis in microform, paper or electronic formats.**

**L'auteur a accordé une licence non exclusive permettant à la Bibliothèque nationale du Canada de reproduire, prêter, distribuer ou vendre des copies de cette thèse sous la forme de microfiche/film, de reproduction sur papier ou sur format électronique.**

**The author retains ownership of the copyright in this thesis. Neither the thesis nor substantial extracts from it may be printed or otherwise reproduced without the author's permission.**

**L'auteur conserve la propriété du droit d'auteur qui protège cette thèse. Ni la thèse ni des extraits substantiels de celle-ci ne doivent être imprimés ou autrement reproduits sans son autorisation.**

**0-612-62388-2**

**Canada**

# **Plastic Response of Ship Shell Plating Subjected to Loads of Finite Height**

**© Richard C. Hayward, B.Eng., B.A.**

**A thesis submitted to the School of Graduate Studies in partial fulfilment  
of the requirements for the degree of Master of Engineering**

**Faculty of Engineering and Applied Science  
Memorial University of Newfoundland  
May 2001**

**St. John's**

**Newfoundland**

**Canada**

## **Abstract**

**The paper addresses the plastic response of plating subjected to loads of finite height. The need for understanding this response arises from the severe loads on midbody plating when ships are caught in compressive ice. However, the results are also applicable to level icebreaking loads in the bow and stern regions. The purpose of the paper is to develop deflection-based response equations for both transversely- and longitudinally-framed plating. Finite element analyses are used to study 344 load cases in which both structural configuration and load extent is varied. The characteristics of the plating response are examined, as well as the influences of the relevant structural and load parameters on permanent set. The plating response equations are developed by comparing finite element results for loads of finite height to results obtained with yield line theory for uniform loads. By comparing the ratios of loads required to obtain equal levels of permanent set for each structural and load configuration, equations for pressure correction factors are obtained. The factors are primarily functions of the load height to frame spacing ratio, but also include secondary influences of structural configuration. The correction factors and yield line theory are then used to examine reported damages to Baltic class vessels and to estimate the damage pressures for assumed load heights.**

## **Acknowledgements**

Like most graduate students, the author is very much indebted to the supervisor of his work. On this occasion, however, given that the thesis was written at a distance, as well as on a part-time basis, the support and patience of Dr. M. Haddara, Associate Dean Graduate Studies at Memorial University, is especially appreciated.

Much appreciation is also due to the author's supervisors and colleagues at Germanischer Lloyd for their assistance. In addition to the abundance of available technical expertise, the provision of the computer hardware and software that was required for the considerable amount of finite element analyses was indispensable.

Finally, the author would like to thank his wife Patricia for her support and encouragement throughout the writing of the thesis, as well as for her patience. Weekdays at work followed by evenings and weekends of study sometimes made for an absent husband.

Hamburg, May 2001  
Richard C. Hayward



## **Contents**

<b>Abstract .....</b>	<b>i</b>
<b>Acknowledgements .....</b>	<b>ii</b>
<b>List of Figures .....</b>	<b>v</b>
<b>List of Tables.....</b>	<b>vii</b>
<b>Nomenclature .....</b>	<b>viii</b>
<b>1.0 Introduction .....</b>	<b>1</b>
1.1 General .....	1
1.2 Developing Concepts of Design Load Heights in the Baltic Sea.....	3
1.3 Scope of Work.....	4
<b>2.0 Literature Review .....</b>	<b>7</b>
2.1 Elastic Design of Plates.....	7
2.2 Elasto-Plastic Studies .....	9
2.3 Experimental Investigations of Plate Behaviour .....	15
2.4 Semi-Empirical Methods.....	19
2.5 Yield Line Theories.....	21
2.6 Application of Finite Element Analyses .....	26
<b>3.0 Methods, Assumptions and Procedure .....</b>	<b>30</b>
3.1 Methods.....	30
3.1.1 General .....	30
3.1.2 Finite Element Analyses.....	32
3.1.3 Yield Line Theory .....	35
3.2 Assumptions .....	36
3.3 Procedure.....	37
3.3.1 Establishment of Test Matrix .....	37
3.3.2 ANSYS Verification.....	38
3.3.3 SHELL43 and Mesh Density Validation.....	39
3.3.4 Boundary Conditions.....	41
3.3.5 Finite Element Analyses.....	42

3.3.6	Determination of Equivalent Uniform Loads.....	43
4.0	Results and Discussion.....	44
4.1	General .....	44
4.2	Characteristics of Plating Response .....	45
4.2.1	Interaction of Bending Moments and Axial Forces .....	45
4.2.2	Patterns of Plasticity .....	50
4.2.3	Distribution of In-Plane Strains and Permanent Set.....	54
4.3	Influences of Structural and Load Parameters on Permanent Set .....	58
4.3.1	Influence of Plate Aspect Ratio.....	58
4.3.2	Influence of Material Yield Stress.....	61
4.3.3	Influence of Frame Spacing to Plate Thickness Ratio .....	63
4.3.4	Influence of Load Height to Frame Spacing Ratio.....	66
4.3.5	Influence of Load Length.....	69
4.4	Plating Response Equations .....	72
4.4.1	General .....	72
4.4.2	Equations for Transversely-Framed Plating.....	75
4.4.3	Equations for Longitudinally-Framed Plating.....	77
4.4.4	Response Equations and Comparison with Finite Element Results.....	79
4.4.5	Sensitivity Analyses .....	81
4.5	Application of Plating Response Equations .....	85
4.5.1	Plating Design Example .....	85
4.5.2	Analysis of Plating Damages to Baltic Class Vessels.....	86
4.5.3	Analysis of Load Heights and Line Load Intensity.....	90
4.5.4	Plastic Design Criteria for Baltic Class Vessels.....	92
4.5.5	Ice Loads for Design of Baltic Class Vessels.....	94
5.0	Summary of Results and Conclusions.....	99
6.0	References .....	106
Appendices		

## List of Figures

Figure 1.1	Conversion of Postulated Ice Load Distributions to Equivalent Uniform Loads of Finite Height.....	5
Figure 2.1	Spread of Plasticity in Clamped Platestrip .....	9
Figure 2.2	Admissible Domain of Load-Deflection Behaviour.....	14
Figure 2.3	Non-Dimensional Load versus Permanent Set.....	20
Figure 2.4	Plastic Hinge Line Patterns.....	22
Figure 3.1	Plastic Collapse Mechanisms .....	30
Figure 3.2	Pressure versus Length of Hinge Mechanism .....	31
Figure 3.3	Material Stress-Strain Curve.....	33
Figure 3.4	Effect of Strain-Hardening .....	34
Figure 3.5	Comparison of Yield Line Theory with Finite Element Results .....	35
Figure 3.6	Validation of ANSYS Results with Experimental Platestrip Results of Young .....	39
Figure 3.7	Validation of SHELL43 Element with SOLID45 Results.....	40
Figure 3.8	Finite Element Model of Shell Plating .....	42
Figure 4.1	Typical Load vs. Permanent Set Results from Finite Element Analyses ..	44
Figure 4.2	Interaction of Bending Moments and Axial Forces - Uniform Load .....	45
Figure 4.3	Interaction of Bending Moments and Axial Forces - Finite Load Height - Transversely-Framed Plating.....	46
Figure 4.4	Interaction of Bending Moments and Axial Forces - Finite Load Height - Longitudinally-Framed Plating.....	46
Figure 4.5	Extent of Bending Moments and Axial Forces - Finite Load Height - Transversely-Framed Plating.....	49
Figure 4.6	Extent of Bending Moments and Axial Forces - Finite Load Height - Longitudinally-Framed Plating.....	50
Figure 4.7	Typical Surface Plasticity Plots.....	51
Figure 4.8	Through-Thickness Plasticity in Platestrips .....	52
Figure 4.9	Load-Deflection Curves for Platestrip ( $b/t = 36$ ).....	53
Figure 4.10	Load-Deflection Curves for Platestrip ( $b/t = 12$ ).....	53
Figure 4.11	In-Plane Strain (x-direction) - Transversely-Framed Plating.....	55
Figure 4.12	In-Plane Strain (x-direction) - Longitudinally-Framed Plating.....	55
Figure 4.13	Normalised Permanent Set in y-Direction - Transversely-Framed Plating .....	57
Figure 4.14	Normalised Permanent Set in x-Direction - Longitudinally-Framed Plating .....	57
Figure 4.15	Influence of Plate Aspect Ratio - Transversely-Framed Plating ( $b/t = 36$ ) .....	59
Figure 4.16	Influence of Plate Aspect Ratio - Transversely-Framed Plating ( $b/t = 12$ ) .....	59

Figure 4.17	Influence of Plate Aspect Ratio - Longitudinally-Framed Plating ( $b/t = 36$ ) .....	60
Figure 4.18	Influence of Plate Aspect Ratio - Longitudinally-Framed Plating ( $b/t = 12$ ) .....	60
Figure 4.19	Influence of Material Yield - Transversely-Framed Plating ( $b/t = 36$ ) .....	62
Figure 4.20	Influence of Material Yield - Transversely- and Longitudinally-Framed Plating ( $b/t = 36$ , $b/t = 12$ ) .....	62
Figure 4.21	Influence of $b/t$ Ratio - Uniform Loading.....	64
Figure 4.22	Influence of $b/t$ Ratio - Transversely-Framed Plating .....	65
Figure 4.23	Influence of $b/t$ Ratio - Longitudinally-Framed Plating .....	65
Figure 4.24	Influence of $f/b$ Ratio - Transversely-Framed Plating .....	67
Figure 4.25	Influence of $f/b$ Ratio - Longitudinally-Framed Plating .....	67
Figure 4.26	Influence of $f/b$ Ratio - Transversely-Framed Plating - Fixed Force.....	68
Figure 4.27	Influence of $f/b$ Ratio - Longitudinally-Framed Plating - Fixed Force .....	68
Figure 4.28	Influence of Load Length - Transversely-Framed Plating .....	70
Figure 4.29	Influence of Load Length - Bending Moments and Axial Forces - Transversely-Framed Plating.....	70
Figure 4.30	Influence of Load Length - Longitudinally-Framed Plating .....	71
Figure 4.31	Sample Determination of $f_b$ .....	72
Figure 4.32	Modified Plate Equation - Transversely-Framed Plating .....	76
Figure 4.33	Beam Equation - Transversely-Framed Plating.....	76
Figure 4.34	Plate Equation - Longitudinally-Framed Plating .....	78
Figure 4.35	Beam Equation - Longitudinally-Framed Plating.....	78
Figure 4.36	Comparison of Equations Against Finite Element Results - Transversely-Framed Plating .....	80
Figure 4.37	Comparison of Equations Against Finite Element Results - Longitudinally-Framed Plating .....	80
Figure 4.38	Sensitivity of Permanent Set to Load Height .....	82
Figure 4.39	Sensitivity of Plate Thickness to Load Height - Transversely-Framed Plating .....	83
Figure 4.40	Sensitivity of Plate Thickness to Load Height - Longitudinally-Framed Plating .....	83
Figure 4.41	Sensitivity of Plate Thickness to Permanent Set - Transversely-Framed Plating .....	84
Figure 4.42	Sensitivity of Plate Thickness to Permanent Set - Longitudinally-Framed Plating .....	84
Figure 4.43	Ice Pressure Analysis of Reported Damages .....	90
Figure 4.44	Line Load Analysis.....	92
Figure 4.45	Analysis of FSICR Plating Requirements - Transversely-Framed Plating .....	97
Figure 4.46	Analysis of FSICR Plating Requirements - Longitudinally-Framed Plating .....	97

## List of Tables

Table 3.1	Test Matrix for Finite Element Analyses.....	38
Table 4.1	Influence of Plate Aspect Ratio on Pressures to Obtain $w_p = 0.025b$ .....	58
Table 4.2	Maximum, Minimum and Average Coefficients of Variation For Individual Load Cases .....	73
Table 4.3	Average Coefficients of Variation for Load Height to Frame Spacing Ratios .....	74
Table 4.4	Equations for $f_b$ and $p_{uniform}$ .....	81
Table 4.5	Assumptions for Sample Design Application.....	86
Table 4.6	Summary of Ice Conditions – Winters 1984 to 1987 .....	87
Table 4.7	Details of Reported Baltic Damages and Estimates of Pressure .....	88

## Nomenclature

$\alpha$	plate (or panel) aspect ratio ( $a/b$ )
$\beta$	plate slenderness ratio
$\Delta$	ship displacement [t]
$\varepsilon$	in-plane strain
$\phi$	curvature of plate hinge [rad/mm]
$\lambda$	load concentration parameter
$\nu$	Poisson's ratio
$\theta$	rotation angle of plate hinge [rad]
$\sigma_y$	material yield strength [N/mm <sup>2</sup> ]
$a$	frame span [mm]
$b$	frame spacing [mm]
$e$	load length [mm]
$D$	flexural rigidity [N·mm]
$D_i$	internal work per unit length [N·mm/mm]
$E$	elastic (Young's) modulus [N/mm <sup>2</sup> ]
$f$	load height [mm]
$f_D$	pressure correction factor
$F$	total ice load [N]
$I$	area moment of inertia [mm <sup>4</sup> ]
$k$	non-dimensional FSICR ship displacement-power factor
$l$	length of plastic hinge [mm]
$M$	bending moment per unit length [N·mm/mm]
$M_p$	fully plastic bending moment per unit length [N·mm/mm]
$N$	in-plane forces per unit length [N/mm/mm]
$N_p$	fully plastic in-plane forces per unit length [N/mm/mm]
$p$	lateral plate pressure [N/mm <sup>2</sup> ]
$p_c$	lateral plate pressure causing three-hinge collapse [N/mm <sup>2</sup> ]
$P_e$	continuous engine output [kW]
$p_{eh}$	lateral plate pressure causing edge hinges [N/mm <sup>2</sup> ]
$p_y$	lateral plate pressure initiating yield [N/mm <sup>2</sup> ]
$q$	line load [N/mm]
$r$	load parameter ratio ( $Q_e/Q_p$ )
$R$	correlation coefficient
$R^2$	coefficient of determination
$Q$	non-dimensional load parameter for uniform pressure
$Q_e$	non-dimensional load parameter for equivalent uniform pressure
$Q_p$	non-dimensional load parameter for concentrated load
$t$	plate thickness [mm]
$w$	central deflection [mm]
$W_e$	external work per unit length [N·mm/mm]
$w_p$	central permanent set [mm]
$w_{x,y}$	deflection [mm]
FSICR	Finnish-Swedish Ice Class Rules
IACS	International Association of Classification Societies

## **1.0 Introduction**

### **1.1 General**

For commercially operated vessels, maximising profits is the commonly accepted objective in structural design optimisation. Accordingly, the design challenge becomes one of maximising the ship's revenue-earning power on one hand, and achieving a balance between repair and construction costs on the other. Costs of repairing an inadequately designed structure are usually compounded by lost revenues during downtime required for the repair, while an overly adequate design results not only in excessive construction costs, but as well a weight penalty which must be borne throughout the life of the ship. Not surprisingly, ship owners increasingly expect classification societies and other regulatory bodies to be aware of these design considerations, and that they be reflected in their ship construction requirements. Increasingly, these rule-based organisations are responding to this expectation.

Once the custodians of time-honoured empirical formulae for ship design, classification societies and regulatory bodies have largely abandoned their experience-based equations in favour of formulae based on first principles. Furthermore, to provide for more efficient designs, and to better assess the margins of safety, this shift has increasingly involved the use of plastic design methods. For ships designed to navigate in ice-covered waters, plastic design is especially important. Given the level of additional strengthening in the icebelt alone, thickness reductions afforded by small levels of permissible deformation can offer significant savings in both steel weight and acquisition costs.



Taking the design optimisation of ice-transiting ships one step further, work is now underway to develop requirements based on multiple ship-ice interaction scenarios. Presently, bow loads in the *Equivalent Standards for the Construction of Arctic Class Ships* (Transport Canada, 1995) are based on a head-on ramming scenario, with loads for other hull areas determined as some fraction of the bow load. In the rules of the Russian Register of Shipping, loads are based on a glancing impact scenario for the forward region, and a compressive ice scenario for the midship and aft regions. Although 1A and 1AS class vessels do sometimes navigate independently, Baltic-class vessels are primarily designed for convoy operations in which the vessels proceed with icebreaker escort. Accordingly, an important scenario for these vessels is that of striking the channel edge during a turning manoeuvre. By combining such ship-ice interaction scenarios with probabilistic estimates of encounter based on season, location and mission profiles, an envelope of design ice loads can be established that will determine the level of strengthening for all areas of the hull. Although tens of scenarios have already been identified (McCallum et al., 1997), one of the scenarios most in need of attention is that of a ship caught in compressive ice.

Surprisingly, the scenario of a ship caught in a compressive ice field has received comparatively little attention. Yet in a recent study of damages to Baltic class vessels (Kujala, 1991), it was revealed that the majority of damages were to the midbody region and that at least 56% of these damages are known to have occurred in compressive ice. The environmental conditions necessary for the development of compressive ice fields include (1) sufficiently high concentrations of ice, (2) the presence of significant driving forces and (3) a stationary or slow-moving boundary that resists the free drift of the ice.

Whether or not a ship is caught under pressure in these conditions depends largely on navigational aspects, such as the experience of the master or ice navigator, and whether or not the ship is under icebreaker escort. However, once a vessel is caught in compressive ice, it can be exposed to significant ice forces for an extended period of time.

In such cases, the interaction normally begins with local crushing of the ice, followed by the failure of large sectors in the ice plate (Kujala et al., 1991). Depending on the flare angle of the ship's sides and the thickness of the ice, these sectors fail as a result either of buckling or bending. In both cases, the global force is transmitted to the hull through direct contact with intact ice and indirectly through an intermediate layer of crushed ice. Sometimes failed ice pieces accumulate above and below the intact ice, thereby stabilising the ice plate so that crushing failure persists. The manner in which ice fails in crushing depends on a number of factors, the most important of which are strain rate and temperature (Riska and Windeler, 1997). When the loading rate is low and/or the ice is relatively warm, plastic failure occurs by means of coalescing micro-cracks. When the loading rate is high and/or the temperature is low, ice fails in a brittle manner. The resulting spalls considerably reduce the vertical extent of ship-ice contact.

## **1.2 Developing Concepts of Design Load Heights in the Baltic Sea**

In the 1920s and 1930s, when Baltic ice class regulations were based on existing classification rules, no reference was made to load height and the scantlings of the ice belt structure were determined by a percentage increase above those for open water ships. Determining hull scantlings on the basis of percentage increases ended with the establishment of the 1971 Finnish-Swedish Ice Class Rules (FSICR), in which the

determination of scantlings was based directly on ship-ice interaction. Parameters of the interaction included a contact height of 800 mm and a design pressure of 3.0 MPa, the assumed thickness and unconfined compression strength of ice, respectively. With the introduction of the 1985 FSICR, the apparent contact heights of the ice were relatively unchanged, but the design height of the area actually under pressure was reduced to 300 mm for 1A vessels, and 350 mm for 1AS vessels. A nominal design pressure of 5.6 MPa means that the assumed contact forces are somewhat lower than the 1971 rules.

Recent observations suggest that contact heights are actually much lower. Laboratory experiments and full-scale testing have shown evidence that contact is line-like, with heights of only a few centimetres (Riska et al., 1990). The ice-failure mechanism for such contact is thought to be flaking due to repetitive shear failures (Daley, 1991). However, there is also evidence to suggest that a spatial heterogeneity of the ice failure process leads to regions of extremely high pressures termed *critical zones* (Jordaan, 1994). In the case of level first-year ice, such critical zones would be expected to appear randomly over the contact length. While both ice-failure models acknowledge that a small portion of the load is transmitted through an adjacent layer of crushed ice, it has also been suggested that the entire load is transmitted through a viscous layer, such that there is no direct contact between the structure and intact ice (Kurdyumov and Kheisin, 1976).

### 1.3 Scope of Work

While the foregoing presents a confusing picture of ice failure mechanisms, it is commonly agreed that spalling results in a vertical extent of effective ice-structure contact that is less than the apparent contact height. To facilitate the design and damage analyses

of structures exposed to such contact, there is presently a need for equations that can determine the response of plating when subjected to loads of finite height. In keeping with the trend towards plastic design, these equations need to address the response of plating in the post-elastic domain. Accordingly, the purpose of the present study is to develop plastic response equations for both transversely- and longitudinally-framed plating subjected to loads of finite height, and to then apply these equations to the design and damage analyses of Baltic class vessels. Given the uncertainties surrounding the horizontal distribution of global loads along the ship's hull, as well as disagreement amongst ice scientists regarding the local ice failure process, a good approximation can be obtained by considering uniformly-distributed loads of finite height and semi-infinite length, as shown in Figure 1.1. In this way, it is possible to proceed with the development of design equations without knowing the details of ice failure mechanisms. Indeed, this approach is one step closer to the actual design condition than ice rules developed to date, which normally convert such line-like loads into equivalent uniform pressures over the entire plate field. Of course, although the study is directed towards first-year ice loads in the midbody, the results can be extended to level icebreaking and any other loads of finite height in the bow and stern regions.

Prefaced by a review of the literature on the plastic response of plating to various loads, the methods, assumptions and procedure of the study are delineated. The characteristics of post-elastic response are then examined, followed by an investigation into the influences of different structural and load parameters on central deflection. Based on these influences, plastic response equations are then developed for both transversely- and longitudinally-framed plating, followed by a limited amount of sensitivity analyses.

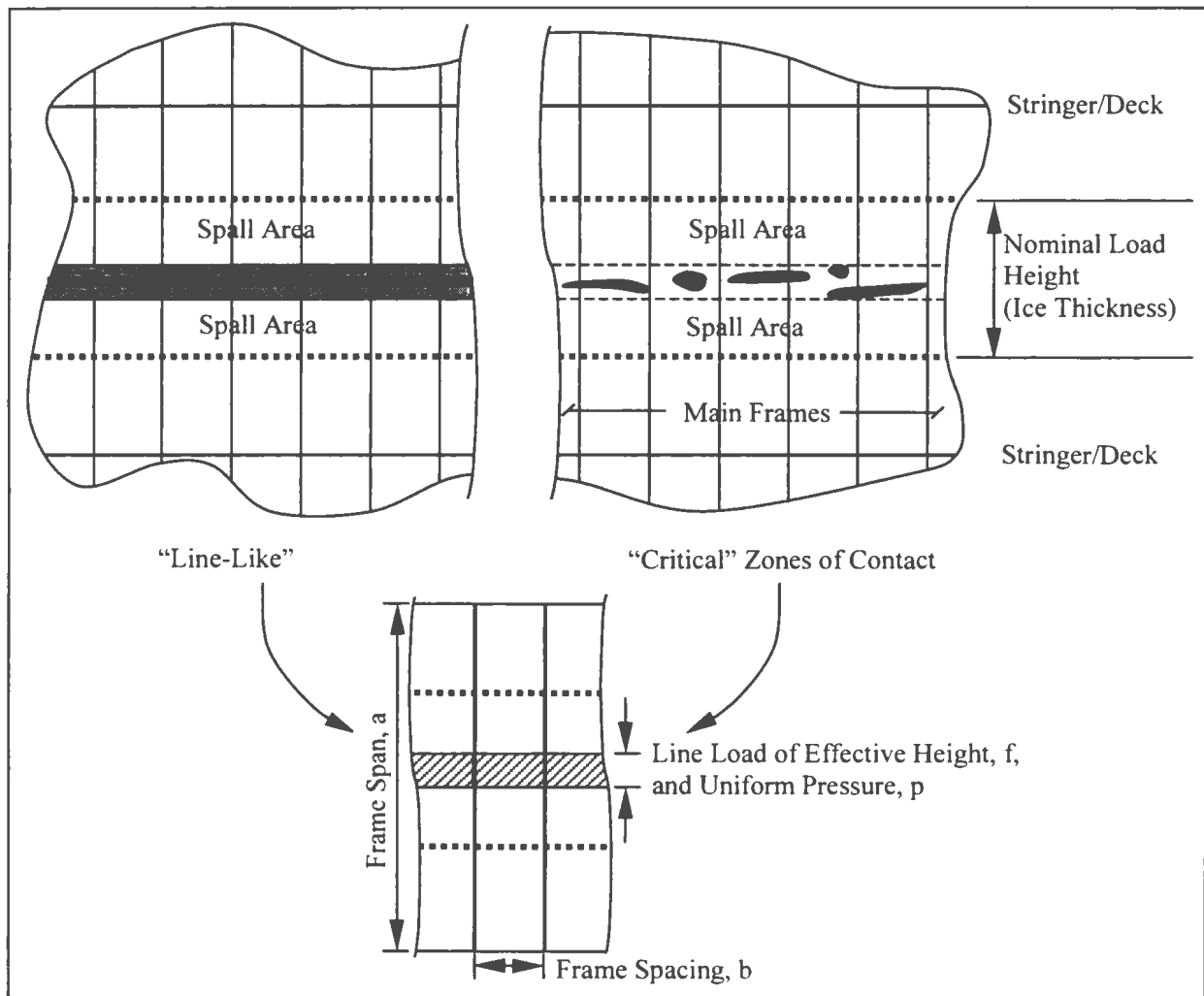


Figure 1.1 Conversion of Postulated Ice Load Distributions to Equivalent Uniform Loads of Finite Height

The equations are subsequently used to evaluate observed damages sustained by Baltic class vessels, including an analysis of load heights and line load intensities. Following a discussion of plastic design criteria, the existing FSICR are examined to determine equivalent plastic design loads. Investigations into the nature of local ice failure are beyond the scope of this study.

## 2.0 Literature Review

### 2.1 Elastic Design of Plates

Timoshenko (1940) first provided a differential equation describing the elastic deflection,  $w$ , of a plating subjected to a uniform load,  $p$

$$\frac{\partial^4 w}{\partial x^4} + 2 \frac{\partial^4 w}{\partial x^2 \partial y^2} + \frac{\partial^4 w}{\partial y^4} = \frac{p}{D} \quad (2.1)$$

The equation is based on the equilibrium of the plate and its solution must satisfy the assumed boundary conditions. Its form is that of the bi-harmonic equation (often abbreviated as  $\nabla^4 w = p/D$ ) and is similar to that for beam bending except for the orthogonal bending terms and the quantity  $D$ , termed the flexural rigidity of the plate

$$D = \frac{Et^3}{12(1-\nu^2)} \quad (2.2)$$

where  $E$  is the elastic (or Young's) modulus,  $t$  is the plate thickness and  $\nu$  is Poisson's ratio. This quantity arises because of the prevention of transverse strain in plating.

Equation (2.1) is valid within the framework of its assumptions, one of which is that the transverse shear strains are negligible (thin plate theory or *Kirchoff approximation*), and another is that deflections remain small (small deflection theory). For a plate of infinite aspect ratio, membrane effects can only occur when the edges of the plate are restrained from moving towards one another. In plates of finite aspect ratios, compression/stretching of the middle plane must occur to achieve a developable surface (hoop compression around the edges of the plate panel and radial tensions in the centre). Accordingly, Equation (2.1) was extended by von Karman (1910) to account for the membrane effects associated with large deflections

$$\nabla^4 w = \frac{1}{D} \left( p + N_x \frac{\partial^2 w}{\partial x^2} + 2N_{xy} \frac{\partial^2 w}{\partial x \partial y} + N_y \frac{\partial^2 w}{\partial y^2} \right) \quad (2.3)$$

where  $N$  is the in-plane force per unit length.

Experiments by Lamble and Choudary (1953) showed good agreement with elastic theory for the case of simply supported plates. And although experience in naval architecture has shown that loads far in excess of those given by elastic theory are commonly acceptable (such that designers would often determine the scantlings of structures based on large and fictitious yield stresses), elastic theory remains an important tool with which to investigate the influence of different parameters on plating behaviour. Riska (1997) used elastic theory to investigate the response of shell plating subjected to line-like ice loads. Assuming the contact to be similar to an elastic body on a Winkler foundation, the influence of the load height on maximum stresses was investigated. To achieve realistic results, the stiffness of the foundation modulus was determined empirically to be between 1.0 GN/m<sup>3</sup> and 4.0 GN/m<sup>3</sup>. A foundation modulus of zero produces a uniform pressure distribution, while non-zero moduli result in pressure drops at mid-span that reduce plate stresses up to 50%.

To illustrate the combined effect of foundation modulus and load height, 21 mm thick plate panels of 400 mm spacing and 2000 mm span were analysed for foundation moduli of zero and 4.0 GN/m<sup>3</sup>. For the transversely-framed panels, an increase in load height from 50 mm to 500 mm (with constant force) resulted in a 47% drop in stresses in the transverse direction for a foundation modulus of zero, and 43% for the quasi-rigid foundation. The longitudinally-framed panel was more sensitive to the foundation modulus, with corresponding reductions in the transverse stresses of 54% and 32% for a



change in load height from 50 mm to 400 mm. Varsta (1983) had performed a similar analysis of transversely-framed plating, in which the stiffening effect of the finite load height was taken into account by increasing the thickness of plating in the uniform load case. The ratio of the plate thicknesses was expressed as an exponential function of the load aspect ratio.

## 2.2 Elasto-Plastic Studies

Clarkson (1956) made one of the first serious theoretical efforts to study post-elastic plate behaviour, checking his theory with limited experimental results and providing design data sheets. Clarkson formulated the problem as an infinite, uniformly-loaded plate with edges that were restrained from rotation and inward movement. Characterising

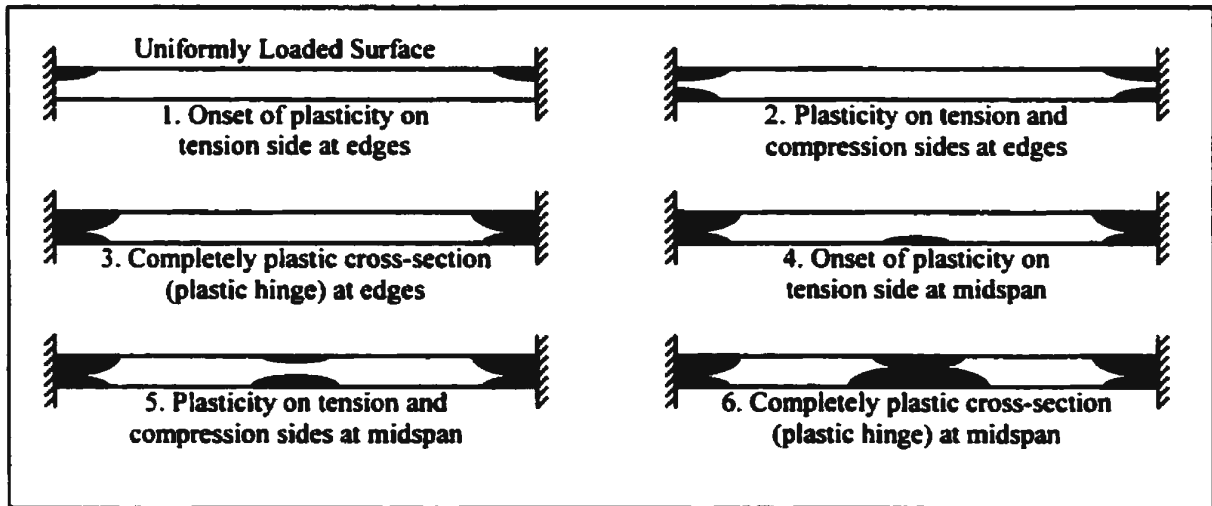


*Figure 2.1 Spread of Plasticity in Clamped Platestrip (Clarkson)*

the spread of plasticity as shown in Figure 2.1, the deflection under a given load was calculated by analysing the central elastic portion according to the corner yield method. The corner yield method addresses the solution of Equation (2.3), with boundary

conditions reflecting the effect of plasticity at the edges. By finite difference integration, the slope at the start of the plastic hinge is then followed through the elasto-plastic zone to the position of zero slope located at the edge of the plate. Since the extent of the plastic hinges is not known a priori, a range of widths is assumed to find that which results in the correct plate width.

However, Clarkson's solution is only valid up to the formation of a central hinge and results in a discernible discontinuity in the slope of the load-deflection curve at the point of departure from elastic theory. Furthermore, in Clarkson's own words, the method is "tedious" and "extremely laborious", usually requiring a graphical solution. Since the method only provides permanent set data for infinitely long plates, the design data sheets for plates of finite aspect ratio are not displacement-based. Accordingly, Clarkson proposed that rectangular plates be designed either to the pressure that forms a plastic hinge along the centreline, or that which results in membrane tension equal to two-thirds the yield stress, whichever is lower. The first condition would be expected to govern for thicker plates, and the second for relatively thinner plates.

Claiming that central deflection depends only slightly on the degree of clamping against edge rotation, Clarkson's proposal is based on a "pinned edges" assumption. This assumption, however, was subsequently challenged in another theoretical and experimental study of long clamped plates (Young, 1959). Specifically, Young criticised the omission in Clarkson's theory of the *plastic* stretching in the plate's middle surface due to combined bending moments and membrane forces. The plastic hinge produced by such a combination permits not only relative rotations within the hinge, but also translations along the geometric centreline. According to an example provided by Young,

Clarkson's predicted deflection is as much as 12 percent too low. However, with the exception of membrane stretching at the plastic hinges, Young's analysis of plate behaviour after the onset of plasticity is essentially the same as that of Clarkson's. Both methods solve Equation (2.3) using boundary conditions that reflect the effect of plasticity at the plate edges. In contrast to Clarkson's rather complicated approach, Young determines this effect by means of the "simple plastic theory of bending". Instead of finite difference integration, simple plastic theory defines the plastic hinge as a point at which all localised plastic flow is assumed to occur.

In Young's treatment of the problem, four distinct stages are identified in the deflection of a loaded plate; wholly elastic, plastic edge hinge formation, plastic central hinge formation and pure plastic membrane action. For solutions within the first two stages, Young derived relationships between non-dimensional parameters of bending moment, membrane tension, applied normal load, central deflection and the ratio of the actual edge moment to the perfectly fixed edge moment. This enabled solutions to be obtained for any degree of rotational restraint at the plate edges, from fully clamped to simply supported. The parametric relationships are presented in graphical form to facilitate the solution of various problems, and are valid up to the onset of plasticity at the plate centre.

Beyond this point, the load-deflection relationship is based on a moment equation which balances the moments due to the load, the edge hinges and those due to the product of the membrane force and eccentricity caused by the plate's deflection. However, a parameter of the membrane force is the ratio between membrane stress and the equivalent yield stress. To express this ratio in terms of deflection, Young assumes that the deflected

form is similar to that of an equivalent membrane, and develops the deflection-stress ratio relationship accordingly. At the change over point to pure plastic membrane action, the assumption is not required since the ratio of membrane and yield stresses is equal to unity. An interesting variation in the development of the deflection-stress ratio relationship is the inclusion of a ratio between the elastic extension of the middle surface and the edge displacement of plates that are not rigidly clamped. In combination with the aforementioned ratio of actual edge moment to the perfectly fixed edge moment, this allows Young's solution to be used for plates with various degrees of edge restraint in terms of both rotation and translation.

Although Young's solution compares well with his full-scale experiments, there exists a discontinuity in the load-deflection curve at the point of central hinge formation. This is due to Young's assumption about the deflected form and to a smaller extent on the neglect of the small inclination of the membrane force at the edge hinges. Furthermore, although the small-scale tests suggest that Young's solution is valid for plates with aspect ratios of three or more, the solution is based on infinitely long plates. As well, the method does not address permanent set. Accordingly, the solution is not readily suited to design purposes, notwithstanding Young's suggestion that plates should be designed according to a total deflection limit criterion. Nevertheless, Young firmly established that the total load-deflection behaviour of plating could be constructed from various load-carrying mechanisms.

Dividing the deflection behaviour of infinite plates into the same four stages as Young, Kamtekar (1981) developed another approximate method for the elasto-plastic analysis of rotationally fixed and axially restrained plates. In the first three stages of

behaviour, a polynomial with five undetermined coefficients is used to represent the deflected form of the plate. The coefficients are all functions of the axial force and the applied lateral load, four of which are determined by satisfying the boundary conditions and the last by satisfying equilibrium at midspan. Response during the pure membrane stage of behaviour is determined solely from static equilibrium. The method shows excellent agreement with experimental results, including the full-scale beam tests of Young and those on long plates by Hooke and Rawlings (1969).

Unlike Young's solution, however, there are no discontinuities in the resulting load-deflection curves of Kamtekar's analysis, since the points that delineate the four stages of behaviour are uniquely defined. Because the method can account for initial imperfections in the plate as well as in-plane displacements, both effects on plate behaviour were investigated. Regarding the former, initial imperfections were seen to increase both the stiffness of the plate and the load required to form the edge hinges, although differences in behaviour become obscured as the membrane stage is approached. To examine the effect of edge displacements, Kamtekar analysed the load-deflection behaviour obtained in one of Young's full-scale tests, assuming edge displacements equal to fractions of the plate thickness,  $t$ . The results showed that the early stages of behaviour are most affected, with significant increases in deflection caused by very small edge displacements. For an edge displacement of  $t/20$ , the central deflection was twice that for the fully restrained platestrip.

Developing further the approach of load-carrying mechanisms, Ratzlaff and Kennedy (1985, 1986) postulated that long rigidly clamped plates exhibit three modes of behaviour under an increasing uniform load; elastic flexural-membrane action, inelastic flexural-

membrane action and inelastic-membrane action. By considering various types of limiting responses, the authors established bounds that define a permissible domain for load-

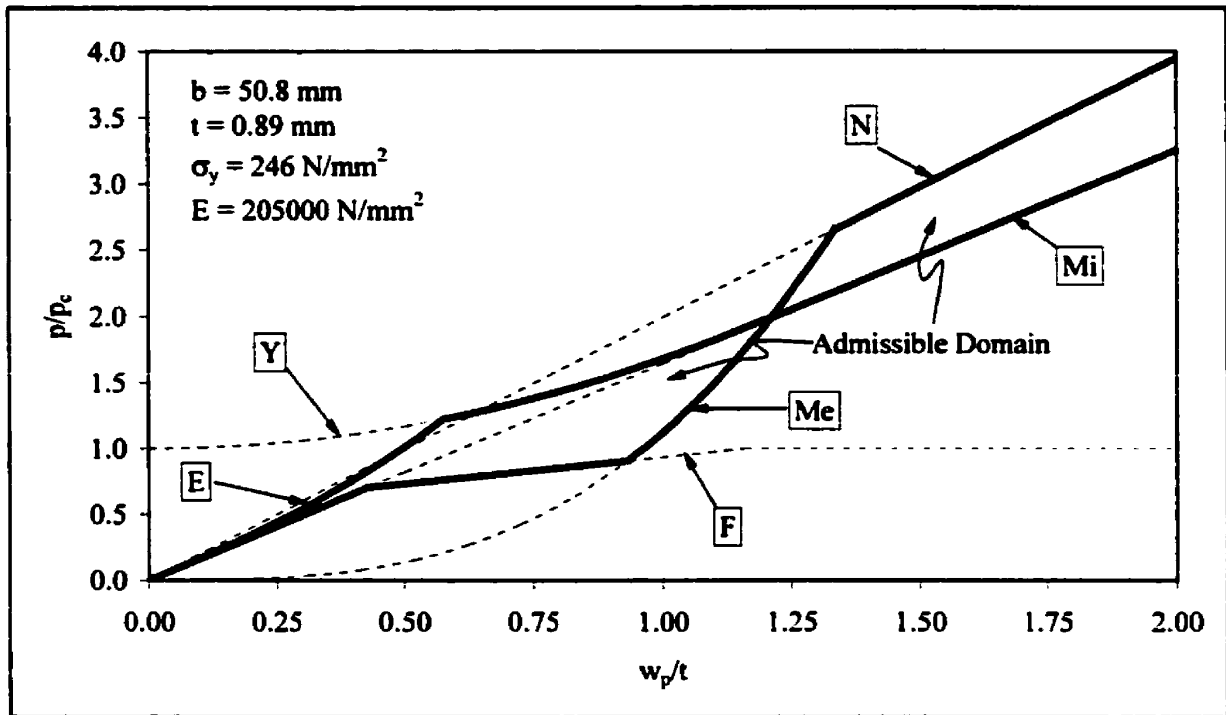


Figure 2.2 Admissible Domain of Load-Deflection Behaviour (Ratzlaff and Kennedy)

deflection behaviour. Referring to Figure 2.2 (in which  $p_c$  denotes the pressure causing three-hinge collapse), curve **E** refers to Timoshenko's elastic solution extended on the basis of a bi-linear moment-curvature relationship. Accordingly, the plastic hinge develops fully and instantaneously at a moment greater than that of first yield, but less than the fully plastic moment due to membrane stresses.

If the edges of the plate are unrestrained, then membrane forces cannot develop in a long plate and the load is resisted by flexural action alone. The load-deflection behaviour of such a mechanism is described by curve **F**, and illustrates the diminished load-carrying capacity of a plate when membrane forces are absent. Alternatively, if the edges

are simply supported, but prevented from approaching one another, then the load is resisted entirely by membrane action. The load-deflection behaviour of such a mechanism is described by curve  $\boxed{Me}$ , and is valid up to the point at which the membrane load at the edges reaches the yield load.

At this point, further loading of the plate results in the progression of a yielded region from the edges towards the centre of plate. Since the value of Poisson's ratio varies throughout the unsupported length, the lower bound of subsequent load-deflection behaviour is obtained assuming an elastic value of 0.3 and an upper bound with a plastic value of 0.5, curves  $\boxed{Mi}$  and  $\boxed{N}$  respectively. The load-deflection behaviour is expected initially near curve  $\boxed{Mi}$  and to then migrate towards  $\boxed{N}$  as the region of plasticity grows. In fact, due to strain-hardening once the edge load exceeds the yield, curve  $\boxed{N}$  will be slightly exceeded. Finally, by considering the interaction of bending moment,  $M$ , and axial force,  $N$ , for a rectangular section, Ratzlaff and Kennedy established an upper bound on the load-deflection behaviour between full yielding of the cross section in flexure and full yielding in tension. Using the maximum normal stress yield criterion, the load-deflection behaviour is described by curve  $\boxed{Y}$ . Experiments and finite element analyses conducted by Ratzlaff and Kennedy compare well with the approach.

### 2.3 Experimental Investigations of Plate Behaviour

In addition to the limited experiments to verify postulated plate theories, a number of experiments have been performed on a more systematic basis. Clarkson (1963) conducted tests of grillages under uniform pressure in order to compare the levels of permanent set to those obtained for a single panel tested with edges clamped against rotation but free to



slide inwards (Clarkson, 1962). Regarding the latter, panels of 5 frame spacing to plate thickness ratios ranging from  $b/t = 50$  to  $b/t = 200$  were tested, with aspect ratios  $\alpha = 1, 1\frac{1}{2}, 2, 3$  and  $5$ . Total deflections and permanent sets were recorded throughout the loading of the plates and reported in a series of non-dimensional load-deflection plots. Design curves based on permanent set were also provided. Unfortunately, in addition to warship-like scantlings, the plates were only provided with margins of  $\frac{3}{4}$  inch. Greater margins would have allowed hoop compressions to develop around the edges, thereby making for a much stiffer structure. Clarkson acknowledged that the boundary conditions of ship structures were different from those considered, but insisted that only reasonable and constant boundary conditions were important. By fitting curves to Clarkson's load-permanent set data, Faulkner et al. (1973) derived the following relationships:

$$p = \frac{6\sigma_y^2}{E\beta^2\sqrt{\alpha}} \left[ 1 + \frac{2w_p}{\alpha} \right] \text{ when } \beta < 2.5 \quad (2.4)$$

$$p = \frac{6\sigma_y^2}{E\beta^2\sqrt{\alpha}} \left[ \frac{4}{3} + \frac{w_p}{\alpha} \right] \text{ when } \beta \geq 2.5 \quad (2.5)$$

where  $\sigma_y$  is the material yield strength,  $\beta$  is the plate slenderness ratio and  $w_p$  is the permanent set at midspan.

Clarkson's investigations of plated grillages consisted of three structures each of  $6 \times 6$  plate panels with aspect ratios of  $1.25$  or  $2.0$ . Each structure was comprised of two grillages connected either back-to-back or front-to-back with a thin steel plate, such that the introduction of pressurised water between the two grillages would load the top platings in either compression or tension. At the outset of the tests, Clarkson anticipated that the panels near the edges of the grillage would behave similar to the single plate

panels with edges free to slide inwards, and that the interior panels would have smaller levels of permanent set due to the restraint offered by the surrounding structure. However, for the grillages loaded such that the top plating was in compression, the interaction of forces in the interior panels from their action as a beam flange with those due to the lateral pressure, resulted in permanent sets up to three times that for a single panel with its edges free to slide inwards. For panels in which the top plating was subjected to substantial tensile forces, the levels of permanent set were less than those predicted by plating with edges free to slide inwards. For Grillage No. 3, tested well beyond normal design pressures, permanent set in the central panel of plating in compression was 38 mm. This compares to a permanent set of only 3.3 mm for the same plating in tension, and 4.8 mm for a similarly tested panel without any edge restraint. For panels in the corners of the grillages, the results were similar to those predicted by the tests on single plates. Since bending stresses near the edges were much smaller, the values for the plates in compression and tension were much more similar, with average permanent deflections of 5.5 mm and 3.2 mm, respectively.

In an effort to develop plastic design criteria for deck plating subjected to large wheel loads, Sandvik (1974) conducted a series of experiments in which fork lift trucks with various loads were driven over two full scale grillage models. Measurements from strain gauges located within the central plate panels were used to validate design curves previously established on the basis of linear elastic theory. Since the measured strains were elasto-plastic, fictitious stresses assuming a perfectly elastic material were used for comparison with the design curves. Permanent sets in the plating, measured after each load case that involved significant plasticity, were then related to a non-dimensional

(elastic) stress parameter. Considering that the levels of permanent set caused by wheel loads should not exceed those due to welding distortions (calculated to be about 0.75% of frame spacing), an allowable design stress of twice the yield was proposed. Since loads of different aspect ratios resulted in different levels of stress (both at the supports and midspan), a simplified design method was proposed using the maximum values of the stress parameters for the various combinations of axle load and tire air pressure.

A more rigorous investigation of deck plating under wheel loads was undertaken by Jackson and Frieze (1980) in a series of lateral patch load tests on a flight deck grillage model. Irregularly spaced stiffeners created plate panels of four different aspect ratios (1, 2, 4 and 8) and two different frame spacings (225 mm, 450 mm). Patch loads were applied with groups of load cells that defined two different areas (150 mm x 75 mm, 250 mm x 125 mm), but which had the same aspect ratio. Numerical studies were conducted in parallel using “dynamic relaxation”, a time-step integration procedure, to solve large-deflection plate equations written in finite difference form. The numerical method included plasticity, initial geometric distortions and residual welding strains. Once the results of the numerical method were validated by the physical tests, the method was then used to generate non-dimensional design curves outside the range of the experimental parameters. A number of interesting conclusions were obtained from the investigation, including the marked increase in the stiffness of load-deflection responses when initial geometrical distortions were in the plating. Another interesting result was that the aspect ratio of the plating was found to have little or no effect on its behaviour, although the ratio of plate and patch widths was found to have a significant influence on residual deflections. The effect of residual stresses on plating behaviour was not clear.

## 2.4 Semi-Empirical Methods

Based largely on the work of Clarkson, Hughes (1981) developed an approximate (semi-empirical) method to facilitate the design of plates subjected to uniform or concentrated loads. Since the edges of the plate are assumed to slide freely, the method is based on the assumption that the commencement and growth of permanent set is due entirely to the development of edge hinges. Although Clarkson characterised the growth of plasticity at the edges in terms of bending stresses and slope, Hughes developed a moment-curvature relationship. For partially plastic cross-sections, the increase in curvature,  $d\phi$ , is found to be  $dM/EI_r$ , where  $I_r$  is the moment of inertia for the reduced (elastic) cross-section of the edge hinge. When the bending moment is removed, the curvature decreases approximately by the amount  $M/EI$ , thereby leaving an amount of permanent curvature,  $\phi_p$ , in the hinge. The permanent angle of rotation at the plate edges,  $\theta_p$ , is obtained by integrating the permanent curvature over the length of the plastic hinge. Since the plate relaxes to an approximately parabolic shape, permanent set is approximated by  $\theta_p b/4$ .

For plates of finite aspect ratio, four edge hinges are developed and the growth of these hinges is more gradual since the plasticity begins at the midpoints of the edges and then spreads along the sides. More importantly, however, geometric compatibility requires stretching of the middle plane such that membrane stresses develop. In view of such “undesirable complexities”, Hughes developed an empirical expression based on the experimental work of Clarkson,

$$Q(p, E, \sigma_y) = Q_y \left( \frac{a}{b}, \beta \right) + T(R_w) \left[ \Delta Q_0 \left( \frac{a}{b}, \beta \right) + \Delta Q_1 \left( \frac{a}{b}, \beta \right) R_w \right] \quad (2.6)$$

in which the round parentheses indicate functional dependence. The quantity  $Q$  is simply a non-dimensional load parameter, while the parameters comprising  $Q$  are developed on the basis of Clarkson's experiments. The parameter  $Q_y$  is the non-dimensional load under which the edge hinges begin to form, with the parameters  $\Delta Q_0$  and  $\Delta Q_1$ , as seen in Figure 2.3, defining the intercept and slope of the load-permanent set behaviour after edge hinge

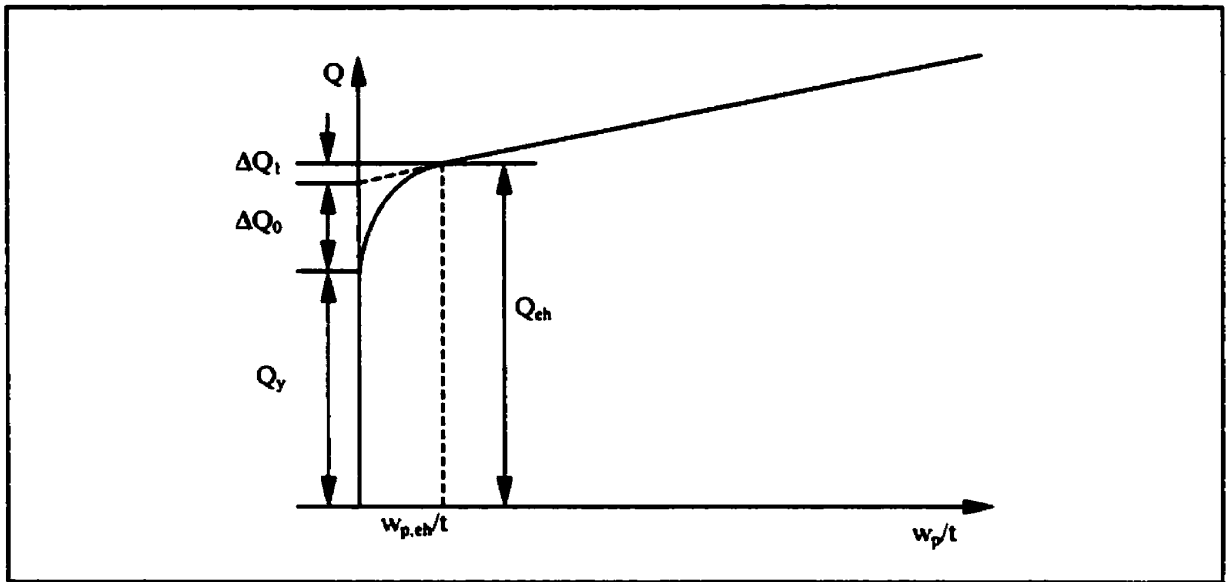


Figure 2.3 Non-Dimensional Load versus Permanent Set (Hughes)

formation. Because there is no further change in the basic nature of the boundary conditions with further increases in load, this behaviour is approximately linear. A non-dimensional transition function  $T(R_w)$ , where  $R_w$  is the ratio of pre- $Q_{eh}$  permanent set to that at  $Q_{eh}$ , is used to describe the load-permanent set behaviour between  $Q_y$  and  $Q_{eh}$ . Accordingly,  $T(R_w)$  takes the value of unity beyond  $Q_{eh}$ . For non-computer aided applications, design curves for the above are provided.

For the design of plating subjected to concentrated loads, Hughes (1983) distinguishes between multiple and single location loads. Multiple location loads refer to pressure patches that are applied several times at different locations such that the plasticity in the plating gradually reaches a final stationary pattern that is similar to that caused by an equivalent uniform load,  $Q_e$ . Accordingly, using a concentrated load parameter,  $Q_p$ , that is related to  $Q_e$  through the load parameter ratio  $r = Q_e/Q_p$ , the maximum permanent set in plating subjected to multiple concentrated loads can be obtained using Equation (2.6). Based on theoretical analyses and the experiments of Sandvik, Hughes developed an equation for  $r$  that was solely a function of the degree of load concentration,  $\lambda$ . Load concentration is defined as the ratio between the geometric average of the load footprint and the frame spacing. Because Sandvik's experiments were based only on plate panels of aspect ratio  $\alpha = 2.5$ , Hughes (1991) later extended the expression for  $r$  to include the influence of the plate aspect ratio. Unfortunately, plating subjected to single-location loads produce complicated plasticity patterns and therefore require a different approach. By performing a regression analysis on the experimental results of Jackson and Frieze, Hughes developed an expression for the concentrated load parameter,  $Q_p$ , that is a function of load concentration, plate slenderness and the ratio of permanent set to frame spacing. As with uniform pressure loads, design curves are provided to facilitate hand calculations.

## 2.5 Yield Line Theories

Yield line theory was originally developed for the design of concrete slabs and was first presented by Wood (1961). The method is energy-based and results in an upper

bound solution. By assuming a kinematically admissible displacement field and a rigid-perfectly plastic material, the external work performed by the load,  $W_e$ , is equated to the internal plastic work performed at the hinges,  $D_i$ . In the case of uniform pressure,

$$\int_A p w_{x,y} dA = \sum_{i=1}^n M \theta_i l_i \quad (2.7)$$

where  $A$  is the area defined by the frame spacing,  $b$ , and the frame span,  $a$ . The quantity  $l_i$  refers to the length of a hinge. For a clamped rectangular plate, Equation (2.7) results in

$$p_c = \frac{48M_p}{b^2 \left( \sqrt{3 + \left( \frac{b}{a} \right)^2} - \frac{b}{a} \right)^2}, \frac{a}{b} < 1 \quad (2.8)$$

for the double-Y-shaped hinge displacement pattern shown in Figure 2.4(a). In Equation (2.8),  $M_p$  refers to the fully plastic moment per unit width of plating

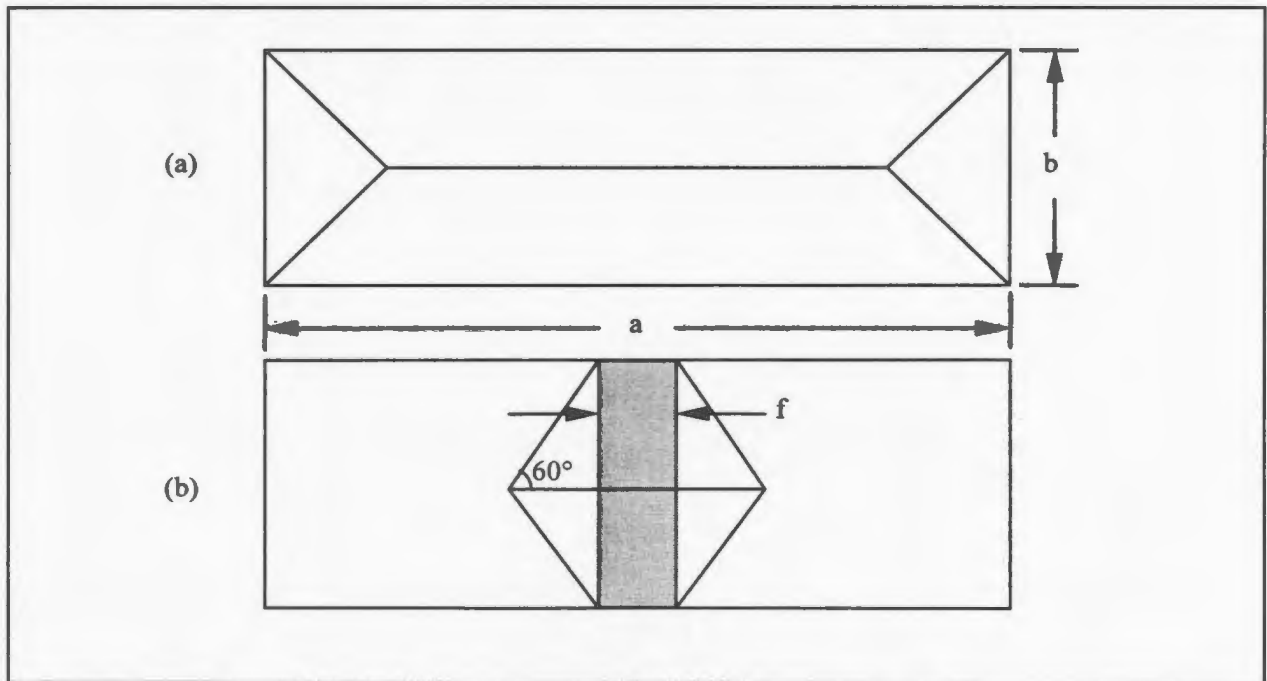


Figure 2.4 Plastic Hinge Line Patterns  
 (a) Uniform Load (Jones)  
 (b) Finite Load Height (Ranki)



$$M_p = \sigma_y \frac{t^2}{4} \quad (2.9)$$

Neglecting the effects of aspect ratio, Johansson (1967) proposed that Equation (2.8) could be used for ice loads of finite height. Assuming a load height of 800 mm, Johansson developed a relationship between frame spacing and a pressure correction coefficient,  $f_D$ , that converts the ice load of finite height to an equivalent uniform pressure. Because the distributing effect would be reduced for smaller frame spacings, the value of  $f_D$  increases from a value of approximately 0.81 at 800 mm frame spacing to unity at a frame spacing of 300 mm.

Sawczuk (1964a) extended the work of Wood to include the membrane forces introduced by lateral deflections beyond the collapse load. Accordingly, the right-hand side of Equation (2.7) was appended to include the combined effects of bending moment and axial force

$$\int_A p w_{x,y} dA = \sum_{i=1}^n (M + N w_p) \theta_i l_i \quad (2.10)$$

where the quantity  $w_p \theta_i$  equals the amount of plastic flow in the middle plane of the hinge.

Based on this result, and using the maximum normal stress yield criterion

$$\frac{M}{M_p} + \left( \frac{N}{N_p} \right)^2 = 1 \quad (2.11)$$

where  $N_p = \sigma_y t$  denotes the fully plastic axial force per unit width of plating, Jones and Walters (1971) found the dissipation function for an interior hinge of a clamped plate to be

$$D_i = \left(1 + 3 \frac{w_p^2}{t^2}\right) M_p \theta_p \quad \frac{w_p}{t} \leq 1 \quad (2.12)$$

$$D_i = 4 \frac{w_p}{t} M_p \theta_p \quad \frac{w_p}{t} \geq 1 \quad (2.13)$$

By substitution of transverse deflections equal to zero, the dissipation functions for the edge hinges are also given by these equations. As a result, the load-permanent set relationship for the double-Y-shaped hinge pattern can be described by

$$\frac{p}{p_c} = 1 + \frac{w_p^2}{3t^2} \left[ \frac{\zeta_0 + (3 - 2\zeta_0)^2}{(3 - \zeta_0)} \right], \quad \frac{w_p}{t} \leq 1 \quad (2.14)$$

$$\frac{p}{p_c} = \frac{2w_p}{t} \left[ 1 + \frac{\zeta_0(2 - \zeta_0)}{(3 - \zeta_0)} \left( \frac{t^2}{3w_p^2} - 1 \right) \right], \quad \frac{w_p}{t} > 1 \quad (2.15)$$

where  $p_c$  is defined by Equation (2.8) and

$$\zeta_0 = \frac{b}{a} \left( \sqrt{3 + \frac{b^2}{a^2}} - \frac{b}{a} \right) \quad (2.16)$$

The principal limitation of yield-line theory is that it ignores the elasto-plastic behaviour that precedes edge hinge formation. Although this becomes decreasingly important as deflection grows, it is not an appropriate method when the design criteria is based on serviceability limits requiring low levels of permanent set.

By examining similar equations for point loads based on the work of Rzhnitsyn (1956), Lehmann and Zhang (1998) modified Equations (2.12) and (2.13) to accommodate partial loading of clamped plates

$$D_i = \left(1 + \frac{cw_p^2}{t^2}\right) M_p \theta_p \quad \frac{w_p}{t} \leq 1 \quad (2.17)$$

$$D_1 = \frac{c_1 w_p}{l} M_p \theta_p \quad \frac{w_p}{l} \geq 1 \quad (2.18)$$

$$\text{where } c = 3 \sqrt{\frac{e^2 + f^2}{a_1^2 + b^2}} + 1, \quad c_1 = 2 + \frac{c}{2} \quad \text{and} \quad a_1 = e + 2(x - x_1)$$

The parameters  $e$  and  $f$  refer to the load length and height, respectively, while  $x$  and  $x_1$  are geometric quantities used to define the length of hinge lines. Although the resulting equations that describe the load-permanent set relationship are quite lengthy, the method can be programmed such that required input is minimal. As well, through appropriate parametric substitution, the equations are valid for both transversely- and longitudinally-framed plating. The method results in an anomaly, however, since the pressure required for a given level of permanent set is minimised at a load length less than that of the frame spacing.

Ranki (1986) also studied partially loaded plate panels, with the aim of developing a simple method by which ice loads could be determined from observed levels of permanent set. In addition to finite element analyses and structural model tests, yield line theory was employed using the hinge line pattern shown in Figure 2.4(b). Based on this collapse mechanism, Ranki determined the collapse pressure for a clamped and partially loaded rectangular plate to be

$$p_c = \frac{8M_p}{b^2} \left( 1 + 2.91 \frac{b}{f} \right) \quad (2.19)$$

For application to observed damages, the load height,  $f$ , is defined as the distance between inflection points on the permanent deflection curve. On the basis of the foregoing, the load-permanent set relationship is described by

$$\frac{p}{p_c} = \left[ \left( 3 + 2\frac{b}{f} \right) \frac{w_p}{t} + 2\frac{b}{f} + 1 \right] \left( 1 + 2.91\frac{b}{f} \right)^{-1} \text{ when } \frac{w_p}{t} \leq 1 \quad (2.20)$$

$$\frac{p}{p_c} = 4 \left( 1 + \frac{b}{f} \right) \frac{w_p}{t} \left( 1 + 2.91\frac{b}{f} \right)^{-1} \text{ when } \frac{w_p}{t} \geq 1 \quad (2.21)$$

The solution is only applicable to transversely-framed plating and, as evidenced by the absence of a parameter for frame span or plate aspect ratio, is not suitable for plates of low aspect ratio where the magnitude of load height approaches that of frame spacing.

Appolonov (2000) also used yield line theory to investigate the effect of load height on the response of transversely-framed plating. Double-Y-shaped hinge patterns were used, although the boundaries of the hinges did not coincide with the boundaries of the plate. For load heights greater than the frame spacing, but less than the frame span, hinge lengths were varied between the two to find that which minimises the energy of collapse. The results show that the hinge length of minimum energy only slightly exceeded the load height. For load heights less than the frame spacing, Appolonov again uses the double-Y-shaped hinge pattern, but with the hinge axis oriented perpendicular to the long side of the plate. It is noted, however, that this can result in “appreciable error” for load heights less than half of the frame spacing. The use of such hinge patterns reveal that the collapse pressure of the plate is approximately proportional to  $(1+b/(2f))^2$  and  $(1/2+b/f)^2$ , respectively, for load heights greater than and less than the frame spacing.

## 2.6 Application of Finite Element Analyses

Katajamäki (1988) applied the finite element method to the analysis of ship shell plating subjected to square loads, the lengths of which were equal to the frame spacing.

The distribution of membrane stresses at mid-span was seen to be very local and concentrated at the location of the load. The effect of in-plane movement at the edges was studied using a finite element model covering several frame spacings, as well as one covering only three frame spacings. When the edges of the latter were fully restrained, the results compared quite well with the load-deflection curves of the larger model in which the membrane effects had been adequately distributed to the surrounding structure. Deflections were exaggerated when the edges of the smaller model were allowed to slide. Katajamäki concluded that the main contribution to the in-plane stiffness of the surrounding structure comes from the adjacent unloaded space.

Chiu et al. (1981) used a non-linear finite element program to develop a simplified plastic design method for plating typical of icebreaking ships. Load-deflection and load-permanent set curves were obtained for uniform pressures applied over every frame bay as well as over every second frame bay, thereby evaluating the effect of different rotations at the edges of the panels. The finite element models were of infinitely long plating that was supported by infinitely rigid framing spaced approximately every 400 mm. Six plate thicknesses were analysed (22 mm to 38 mm), as well as three yield strengths (248 N/mm<sup>2</sup> to 552 N/mm<sup>2</sup>). Permanent set was obtained by subtracting the elastic deflection from the total deflection. Comparison of both the load-deflection and load-permanent set data show that the alternately loaded panels had greater deformation.

In a similar study of icebreaker shell plating, St. John et al. (1992) developed a design method based on allowable permanent set caused by “realistic” ice loads. The shape and size of the ice footprint varied with the assumed ice conditions, but the distribution of pressure was always highly concentrated at the centre of the patch and decaying

exponentially towards the edges. Idealised pressure distributions were applied to finite element models covering five frame spacings and three frame spans. Eighty-four load cases were examined in which plate slenderness ratios were varied along with yield strength, type and spacing of frames, ratio of load width to frame spacing as well as load and plate aspect ratios. The highly concentrated loads were transformed into non-dimensional equivalent uniform pressures based on the work of Hughes. A modified  $r$  factor was developed that is the product of Hughes's original  $r$  factor (for multiple-location loads) and a quantity that is a function of load aspect ratio. Based on the linear regression of non-dimensional, equivalent uniform pressures against non-dimensional ratios of permanent set and plate slenderness, a design equation was developed that relates the plate thickness to the design load and permanent set. An interesting example in the paper showed that plating based on an allowable permanent equal to 0.5% of frame spacing required a thickness that was approximately 44% of that based on first yield criteria.

Zou (1996) also used finite element analyses to study the response of plating to patch loads. Although a uniform distribution of pressure within the ice prints was assumed, single as well as multiple "critical zones" of high-pressure contact areas were investigated. Noting that the plate sections of maximum deformation fail in a manner similar to that of long plates or beams, such "dominant sections" were analysed to account for the lateral support in the original plating. By looking at selected load cases for a 600 mm wide plate of 32 mm thickness ( $\alpha = 2$ ), it was determined that patch load pressures could be converted into equivalent beam pressures using factors that were functionally dependent on the load height to frame span ratio,  $h/a$ . For the cases of three-

hinge collapse and plate rupture, these factors were found to be  $(f/a)^{-0.5582}$  and  $(f/a)^{-0.3563}$ , respectively.

### 3.0 Methods, Assumptions and Procedure

#### 3.1 Methods

##### 3.1.1 General

Because of its simplicity and ease of solution, a yield line formula would be the preferred form of a response equation. Although such an equation would not be appropriate for low values of permanent set, say less than 1% of frame spacing, yield line theory would be suitable for reasonably conservative plastic design criteria and most plating damage analyses. Initially, by assuming the double-Y-shaped collapse mechanism shown in Figure 3.1, it was intended that finite element analyses could be used to

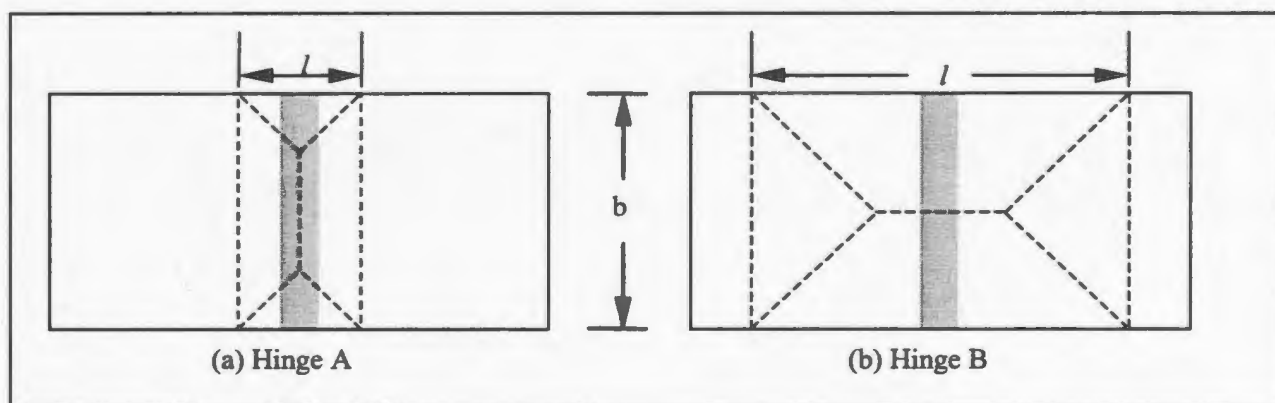


Figure 3.1 Plastic Collapse Mechanisms (a) hinge length,  $l < \text{frame spacing}, b$   
(b) hinge length,  $l > \text{frame spacing}, b$

calibrate the length of the hinge mechanism,  $l$ . However, after some preliminary analyses, it was discovered that significant errors often resulted regardless of the length of the collapse mechanism. To illustrate, Figure 3.2 compares a finite element solution with those of yield line theory when different hinge lengths are assumed. As can be seen for the given load and structural parameters, a hinge length of 425 mm produces the yield



line solution that most closely approaches that of the finite element calculation. However, this yield line solution still has an error of about 31.5%. Similar results for other configurations necessitated consideration of a different collapse mechanism or a different approach.

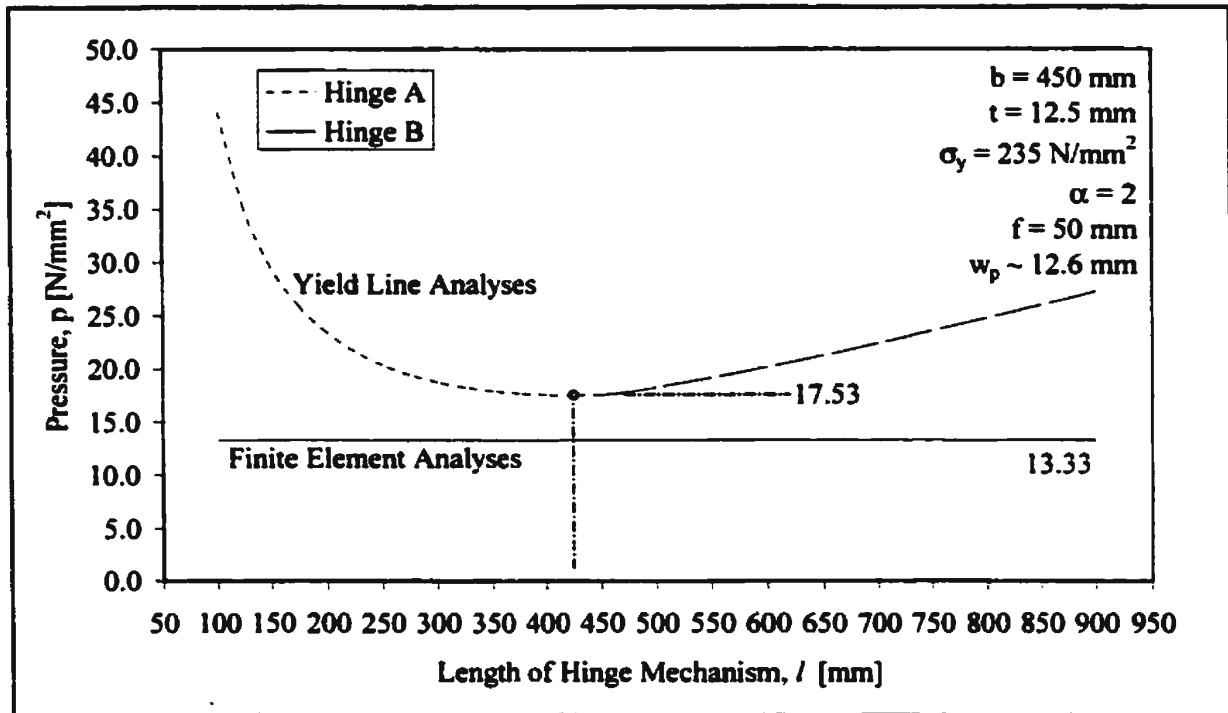


Figure 3.2 Pressure versus Length of Hinge Mechanism

Accordingly, based on Johansson's conversion of a load of finite height to equivalent beam pressures, it was decided to apply loads of various heights to numerous structural configurations and then equate them to equivalent uniform loads. The loads of finite height were evaluated using finite element analyses according to a matrix of test cases in which the parameters of both load and structure were systematically varied. Using yield line theory, the uniform loads required to achieve equivalent levels of permanent set were determined for all load steps within each test case. Since the magnitude of deformations

resulting from loads of finite height would be expected to display a regular and well-behaved relationship to that of uniform loads, such a relationship could be expressed by a single pressure correction coefficient

$$f_D = \frac{P_{\text{uniform}}}{P_{\text{finite height}}} \quad (3.1)$$

that should be almost entirely dependent on the load height to frame spacing ratio. Since plastic response criteria are normally based only on the magnitude of permanent set, it would not be necessary to deal with any differences in the patterns of plasticity between uniform loads and those of finite height.

### 3.1.2 Finite Element Analyses

To determine the response of plating to loads of finite height, plate panels were modelled and analysed using ANSYS Rev. 5.5. Both material and geometric non-linearities were modelled using a plastic shell element (SHELL43) having six degrees of freedom at each node (ANSYS documentation in Appendix A provides a more detailed element description). Solutions of the simultaneous equations were obtained with a frontal solver using Newton-Raphson equilibrium iterations.

Material non-linearity was modelled with a multi-linear option that uses the von Mises yield criteria coupled with an isotropic work hardening assumption. The elastic region of the stress-strain curve was characterised by a Young's modulus of  $E = 2.06 \times 10^5 \text{ N/mm}^2$ , with post-yield behaviour described by a constant (yield) stress straining up to  $\epsilon = 0.02$  and then strain hardening based on a variant of the Ramberg-Osgood relationship up to  $\epsilon = 0.18$

$$\epsilon = \frac{\sigma_y}{E} \left( \frac{\sigma}{\sigma_y} \right)^m \quad (3.2)$$

where  $m = 9.52$  and  $14.42$  for yield stresses of  $235 \text{ N/mm}^2$  and  $355 \text{ N/mm}^2$ , respectively.

Plots of these relationships are shown in Figure 3.3, and a uniform pressure-deflection

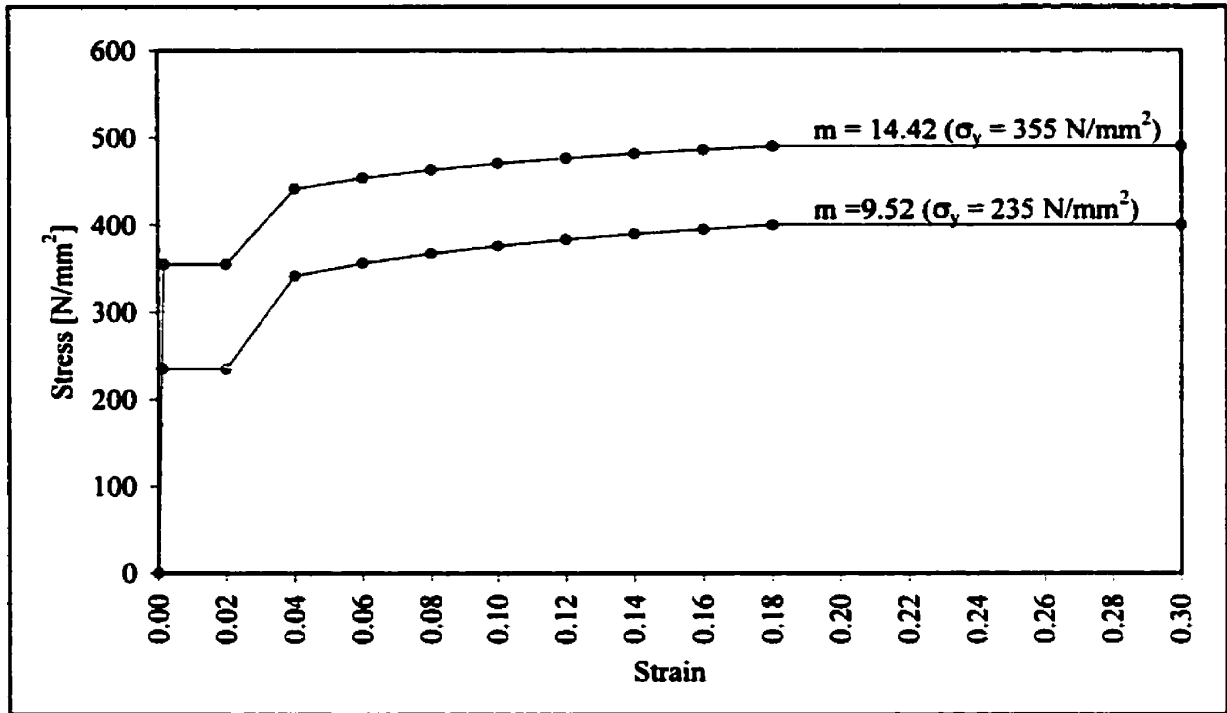


Figure 3.3 Material Stress-Strain Curve (Ramberg-Osgood Relationship)

plot showing the effect of strain-hardening for  $b/t = 36$  plating is shown in Figure 3.4.

Comparing deflections with and without stain hardening, total deflection and permanent set is overestimated by about 18% and 15%, respectively, when strain-hardening is ignored ( $w_p \sim 0.05b$ ). Greater discrepancies of approximately 23% for total deflection and 25% for permanent set were found for  $b/t = 20$  plating at similar  $w_p/b$  values.

The load-deflection history shown in Figure 3.4 also illustrates why residual plate deflections cannot be obtained simply by removing the perfectly elastic portion of

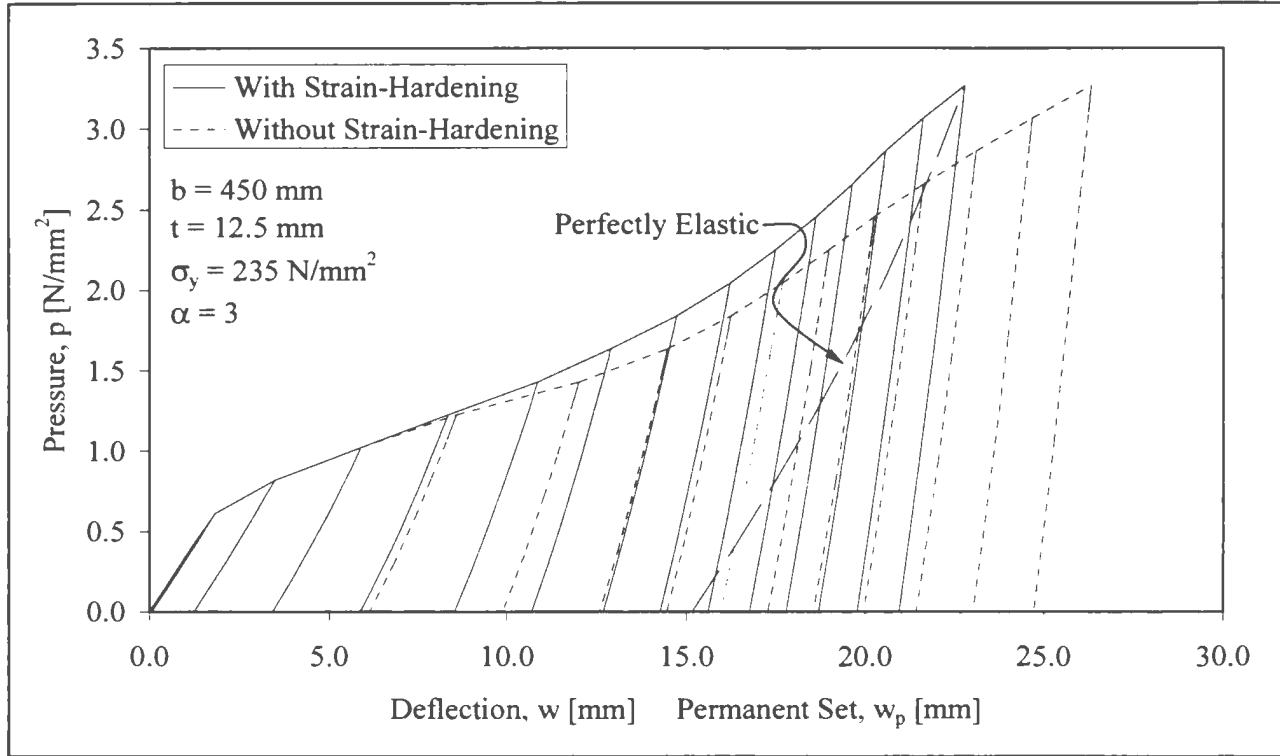


Figure 3.4 Effect of Strain-Hardening

deflection from total elasto-plastic deflections. Permanent set due to residual stresses causes an increased stiffness in the response of plating to lateral loads above that for a flat and stress free plate. Accordingly, the pressure-deflection curve upon load removal is no longer parallel to the originally stress-free elastic curve. Although considerably lessening the calculation times, associated errors become increasingly significant with deflection (about 35% at  $w_p \sim 0.05b$  for the case shown). The slight curvature in the loading/unloading curves is attributable to the non-linear effect of membrane forces.

### 3.1.3 Yield Line Theory

The yield line theory used is that developed by Jones for fully clamped boundaries using the maximum normal stress yield condition. The Equations (2.14) and (2.15) are somewhat cumbersome for the purpose of design, not only because a different equation is required when the permanent set exceeds the thickness of the plate, but also because of the iterative approach that is required to solve for the plate thickness. Nevertheless, as shown in Figure 3.5, the equations well predict the trends, if not always the magnitude, in

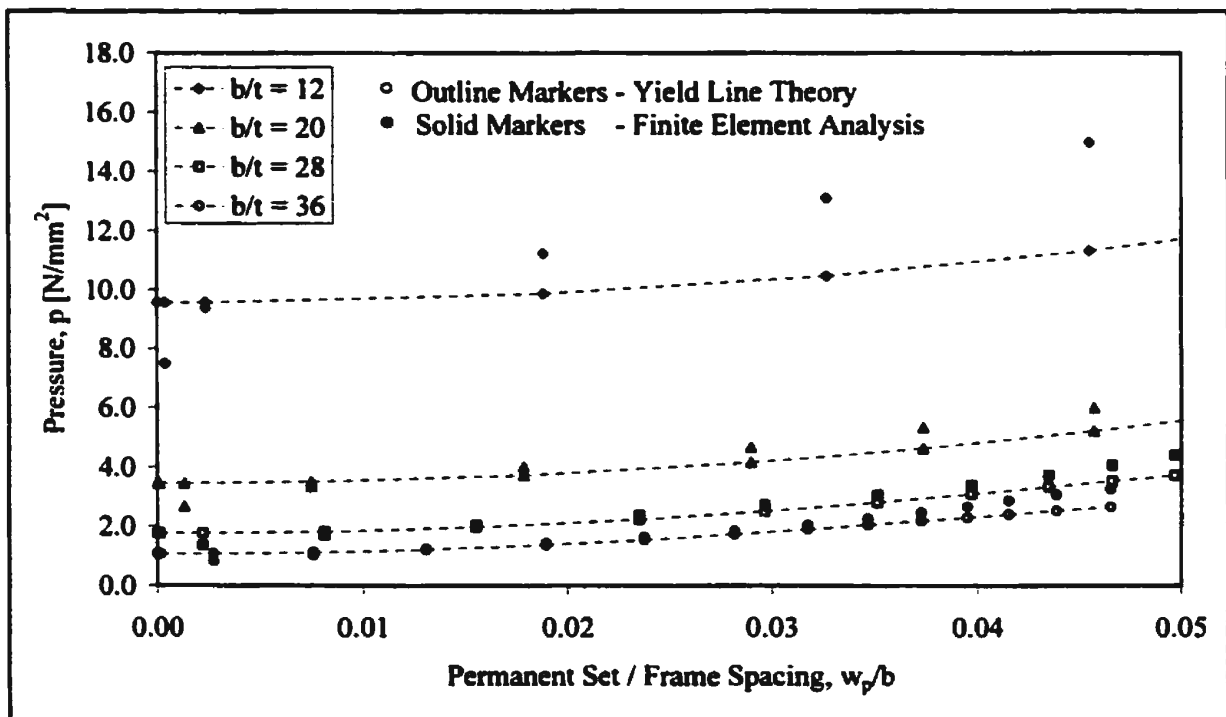


Figure 3.5 Comparison of Yield Line Theory with Finite Element Results

the response of plating to uniform loads, while an iterative solution is easily obtained with the computer programmes now prevalent in ship design and optimisation.

### **3.2 Assumptions**

To simplify the analysis somewhat, the present study makes use of a limited number of assumptions pertaining to the load, structure and their interaction. Most importantly, the plate is assumed to be free of in-plane loads. Given the earlier mentioned effects of in-plane forces on deflection, this is a significant assumption and, theoretically, restricts the applicability of results to areas free from global longitudinal stresses. However, since the icebelt is usually located about the neutral axis of the vessel, global bending stresses are relatively small there compared to those in the upper and lower chords of the ship, while the fore and aft ends of the vessel are also free of significant longitudinal stresses.

Further load assumptions dictate that the load is centred along the unsupported plating span. As well, the distribution of pressure is assumed to be uniform over the entire load patch. This means that the elastic modulus of the ice is effectively zero, and that the so-called 'bridging-effect' assumed in the FSICR, for instance, is not considered. However, since successive ice failure in areas of high stress should result in a quasi-uniform distribution of stresses, this is not an unreasonable assumption.

Regarding the ship structure, it is assumed that the plating has no initial imperfections and no curvature, both of which would reduce levels of plating response. As well, the plate is assumed to behave in a ductile manner throughout the interaction and not to buckle. Furthermore, since stiffeners are modelled by the prevention of out-of-plane displacements, the vertical bending resistance of the stiffeners is assumed to be infinite and their in-plane and torsional stiffness negligible. This also implies that the frames always maintain their load carrying capacities. Although these assumptions have no effect on transversely-framed plating subjected to loads of infinite length (due to symmetry),

there may be some effect on the permanent deflection of the longitudinally-framed plating depending on section properties.

A further assumption, not usually acknowledged, pertains to the omission of modelled stiffeners in the finite element model, such that the reduction in frame spacing due to the thickness and welds of the webs is ignored. Although insignificant for non-ice-strengthened structures, the web thickness of stiffeners in the ice belt region and welds can be as much as 10% of the frame spacing. Since the pressure required to produce a certain amount of permanent set is directly proportional to the frame spacing squared, this effect should be borne in mind when evaluating the frame spacing.

With respect to the interaction between load and structure, the only assumption is that the duration of the interaction is large relative to the natural period of the plate, such that the kinetic energy of the load and the inertia of the plate can be ignored. For the interaction scenario of a ship caught in compressive ice, this assumption is completely valid.

### **3.3 Procedure**

#### **3.3.1 Establishment of Test Matrix**

To study the effect of load heights on the response of ship shell plating, it was first necessary to establish a test matrix for the systematic variation of the relevant parameters describing load and structural configurations. The matrix of 344 test cases, as shown in Table 3.1, is intended to cover structures strengthened for operation in first-year ice, as well as those in second-year and moderate multi-year ice conditions. The smallest load height of 4 times the plate thickness is a corollary of the finite element mesh optimisation,

resulting in small load heights for plating typical of Baltic-class vessels ( $f = 4 \times 12.5 \text{ mm} = 50 \text{ mm}$ ) and relatively higher load heights for Arctic class vessels ( $f = 4 \times 37.5 \text{ mm} = 150 \text{ mm}$ ). Although not included in the development of the plate

Finite Load Height / Infinite Load Length – 280 Test Cases							
$b$ [mm]	$t$ [mm]	$\alpha$ [N/mm <sup>2</sup> ]	$\alpha$	$e/b$	$f/b$	Framing Type	No. Cases
450	37.5	235,355	1,2,3,4,5	$\infty$	3/3,2/3,1/3	Trans/Long	60
500	25.0	235	1,2,3,4,5	$\infty$	5/5,4/5,3/5,2/5,1/5	Trans/Long	50
500	25.0	355	1,2,3,4,5	$\infty$	5/5,3/5,1/5	Trans/Long	30
350	12.5	235,355	1,2,3,4,5	$\infty$	7/7,4/7,1/7	Trans/Long	60
450	12.5	235	1,2,3,4,5	$\infty$	9/9,7/9,5/9,3/9,1/9	Trans/Long	50
450	12.5	355	1,2,3,4,5	$\infty$	9/9,5/9,1/9	Trans/Long	30
Infinite Load Height / Infinite Load Length (Uniform Loads) – 40 Test Cases							
$b$ [mm]	$t$ [mm]	$\alpha$ [N/mm <sup>2</sup> ]	$\alpha$	$e/b$	$f/b$	Framing Type	No. Cases
450	37.5	235,355	1,2,3,4,5	$\infty$	$\infty$	-	10
500	25.0	235,355	1,2,3,4,5	$\infty$	$\infty$	-	10
350	12.5	235,355	1,2,3,4,5	$\infty$	$\infty$	-	10
450	12.5	235,355	1,2,3,4,5	$\infty$	$\infty$	-	10
Finite Load Height / Finite Load Length – 24 Test Cases							
$b$ [mm]	$t$ [mm]	$\alpha$ [N/mm <sup>2</sup> ]	$\alpha$	$e/b$	$f/b$	Framing Type	No. Cases
500	25.0	235	3	1	5/5,3/5,1/5	Trans	3
450	12.5	235	3	1	9/9,5/9,1/9	Trans	3
500	25.0	235	3	1,2,3	5/5,3/5,1/5	Long	9
450	12.5	235	3	1,2,3	9/9,5/9,1/9	Long	9

Table 3.1 Test Matrix for Finite Element Analyses

response equations, loads of finite lengths, as well as uniform loads, were included to evaluate the effect of different boundary conditions. References to  $b/t$  ratios of 12, 20, 28 and 36, refer to the frame spacing and plate thickness combinations of 450/37.5, 500/25.0, 350/12.5 and 450/12.5, respectively, as shown in Table 3.1.

### 3.3.2 ANSYS Verification

Having determined the test cases to be investigated, it was then necessary to verify that the ANSYS program was being using correctly and that the results accurately reflected the physical behaviour of plating loaded into the plastic region. Although previous studies have shown that the ANSYS code is capable of accurately predicting the post-yield behaviour of structures (Bond, 1995), finite element analyses were performed



to reproduce the deflection results obtained by Young (1959) for a fixed-end strip of mild steel plating ( $b/t = 48$ ,  $t \sim 12.8$  mm). The strip was subjected to a load through a linkage that distributed it into four equal concentrations, resulting in displacements similar to those for a uniform load. The results of this verification exercise are shown in Figure 3.6,

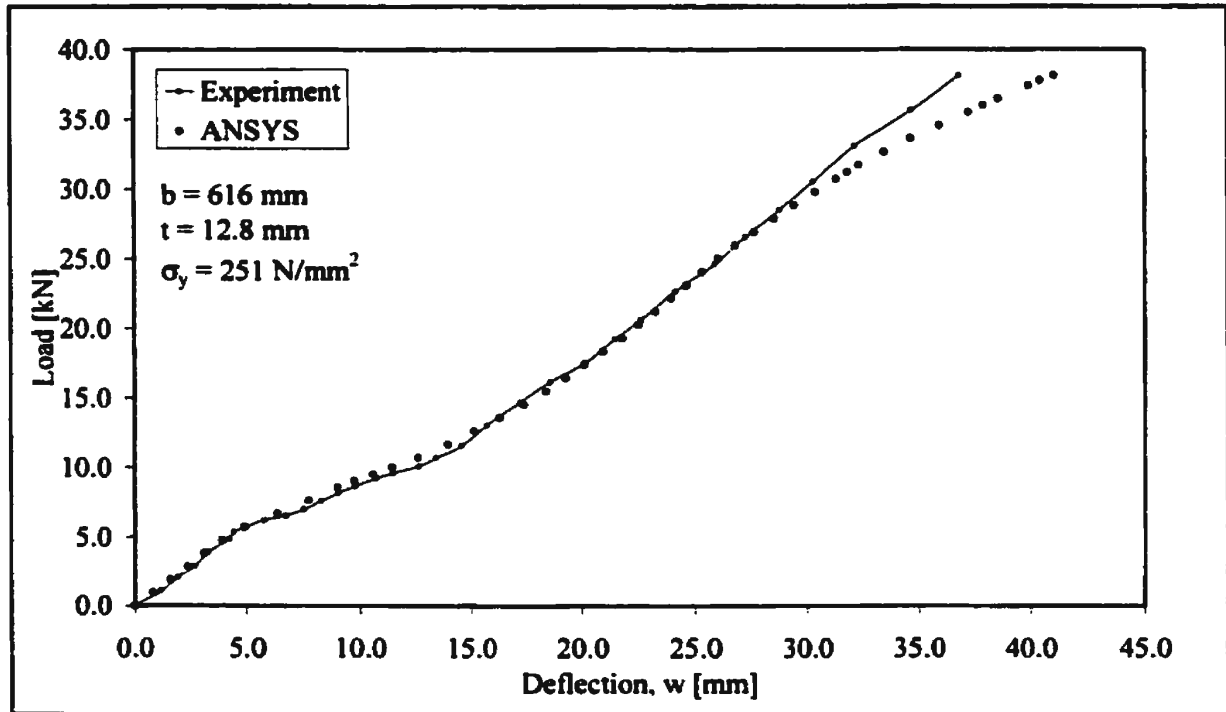


Figure 3.6 Validation of ANSYS Results with Experimental Platestrip Results of Young

and exhibit good agreement with the physical testing. Although the results begin to diverge at deflections of about 30 mm, the maximum deflection of interest is about 31 mm ( $\sim 5.0\%$  of frame spacing).

### 3.3.3 SHELL43 and Mesh Density Validation

Unfortunately, the plating tested by Young, although typical of all such tests, was considerably more slender than the range of plating used in the present study. Although

the SHELL43 element performed well in the verification exercise, it is only recommended for “thin to moderately-thick shell structures”. Since it was desirable from a computation point of view to use shell elements, it was necessary to verify that SHELL43 would perform well with relatively low  $b/t$  values.

Given the absence of physical testing, benchmark results were obtained for uniformly-loaded plates of infinite length using the three-dimensional solid element SOLID45. Given that plating with the least  $b/t$  ratio would most severely test the performance of the SHELL43 element, models with  $b/t = 12$  and  $\alpha = 1, 2$  were constructed with both element types. Models using the SOLID45 element had four through-thickness elements of equal  $x$ -,  $y$ - and  $z$ -dimensions. Based on earlier work with

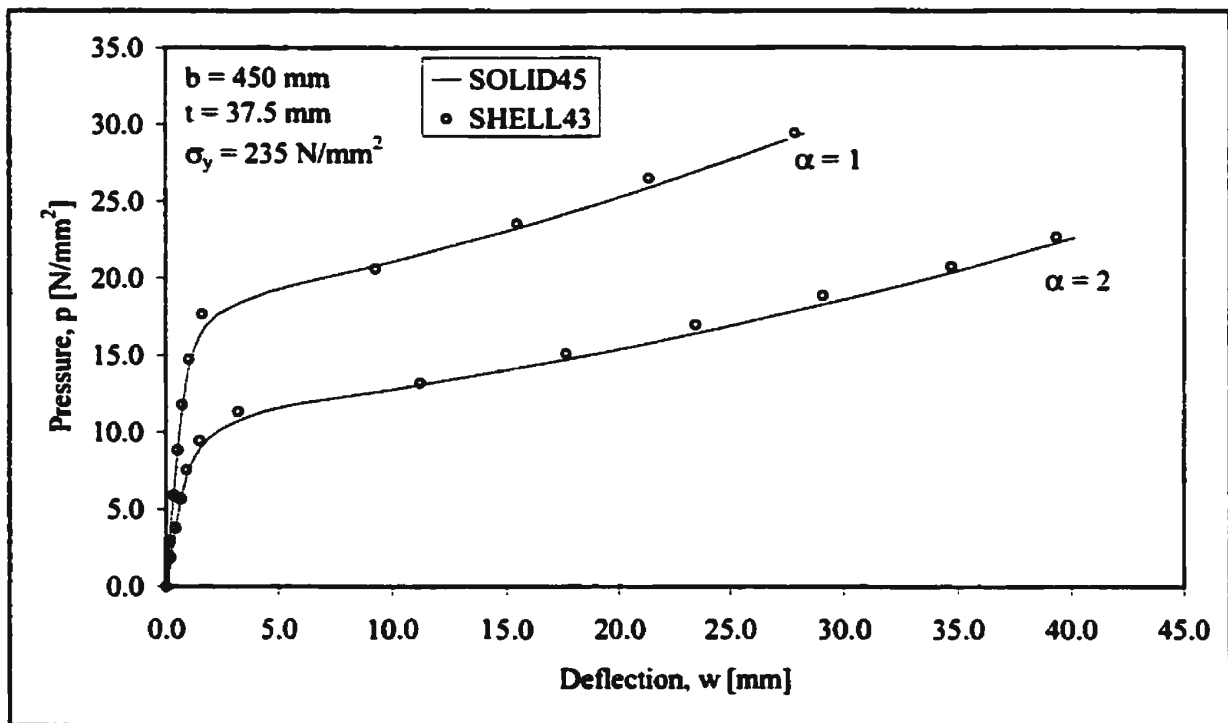


Figure 3.7 Validation of SHELL43 Element with SOLID45 Results

the SHELL43 element (Hayward, 1995), x- and y-dimensions equal to twice the thickness of the plating were found to give a good compromise between mesh density and element aspect ratio. However, elements immediately adjacent to the support experienced high plastic deformation gradients and therefore required a finer mesh density. This was achieved with two elements of an x-dimension equal to the plate thickness, although four such elements were used in the subsequent meshing of plating with  $b/t$  values equal to 28 and 36. As shown in Figure 3.7, good agreement of results was achieved.

#### 3.3.4 Boundary Conditions

Having established a suitable mesh density for the different structural configurations, it was then necessary to determine appropriate boundary conditions. Since boundary conditions are especially important for the analysis of a local structure, all finite element models were of a sufficient extent to permit an adequate redistribution of in-plane strains. Given that the maximum extent of finite loads (in terms of both height and length) was equal to that of the frame spacing,  $b$ , models of a height equal to  $5 \times b$  were used for loads of infinite length (regardless of plate aspect ratios), while both the x- and y- extents of the models were  $5 \times b$  for loads of finite height and width. Differences in the results with models of lengths and widths equal to  $7 \times b$  were negligible. Rotational restraints were not applied at the model edges, except to establish symmetric boundary conditions. In all cases, symmetry allowed  $\frac{1}{4}$  models to be used.

### 3.3.5 Finite Element Analyses

In accordance with the foregoing, Figure 3.8 shows a typical finite element model for a load of finite height and width. By means of load orientation, the model was suitable for

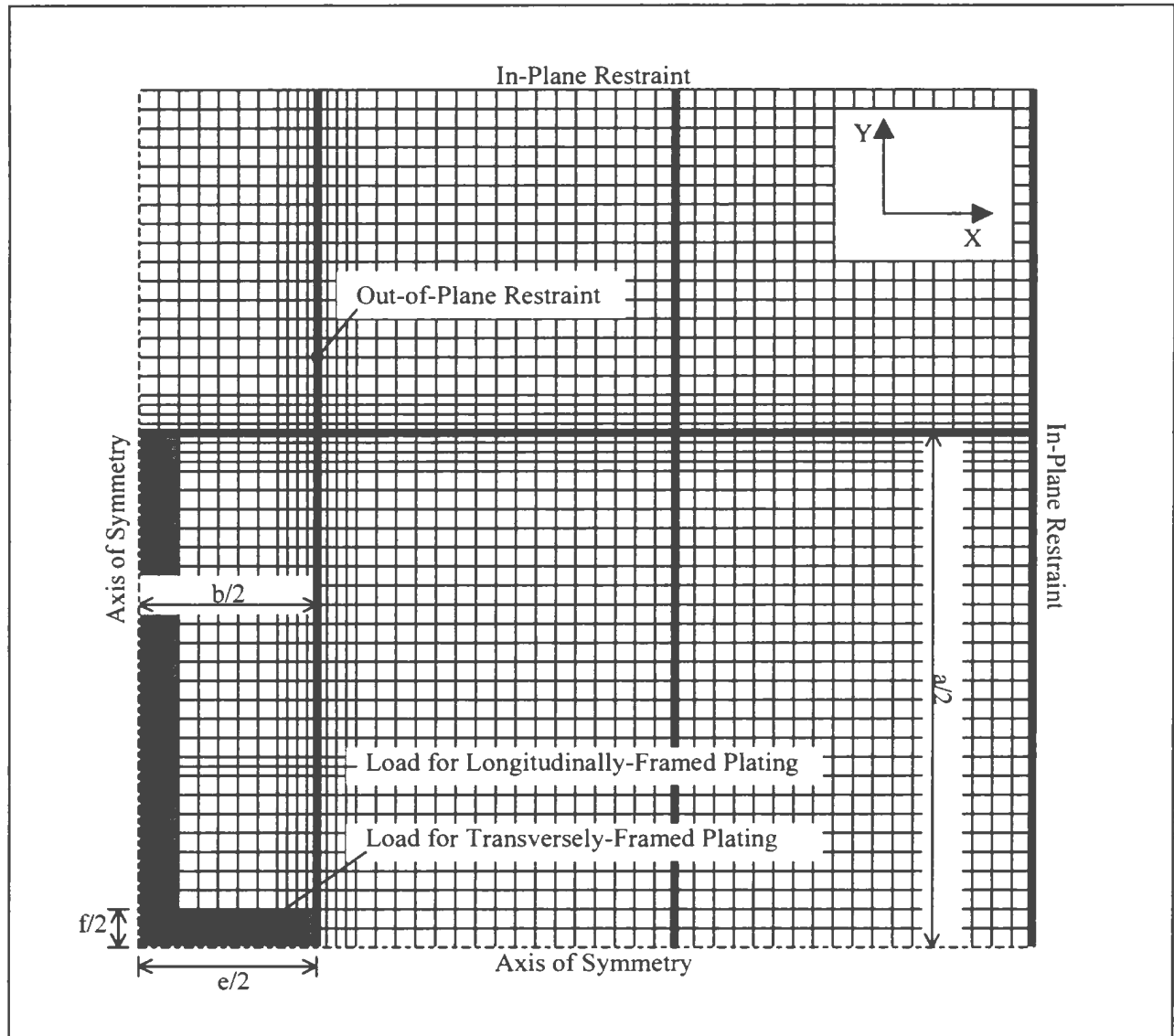


Figure 3.8 Finite Element Model of Shell Plating

both transversely- and longitudinally-framed plating. Loads were first applied to the structure in a linear analysis to determine the pressure required to initiate first yield,  $p_y$ . Subsequently, a non-linear analysis was performed in which loads in increasing multiples

of  $p_y/2$  were applied and then removed. The residual deflection at the centre of the plate panel was then recorded. Loads were applied to a level of  $8 \times p_y$ , or until the analysis failed to meet the convergence criteria. Both force and moment convergence were considered to have been achieved when the square root of the sum of the squares (SRSS) of the force imbalances was less than 0.1% of the SRSS of the applied loads.

### 3.3.6 Determination of Equivalent Uniform Loads

Having obtained the load-permanent set histories for the various combinations of load and structural configurations, equivalent uniform pressures were obtained for each load step of the test cases through substitution of the various structural parameters into Equations (2.14) and (2.15), i.e. yield line theory. By determining the ratio of the applied pressure of finite height to the equivalent uniform pressure, equations for pressure correction factors were subsequently developed for both transversely- and longitudinally-framed plating, thereby defining the stiffening effect of finite load heights.

## 4.0 Results and Discussion

### 4.1 General

As detailed in Table 3.1, 304 load cases were used to investigate the effect of finite load heights on transversely- and longitudinally-framed plating, as well as an additional 40 load cases to examine uniformly-loaded plating<sup>1</sup>. Approximately 30% of the load

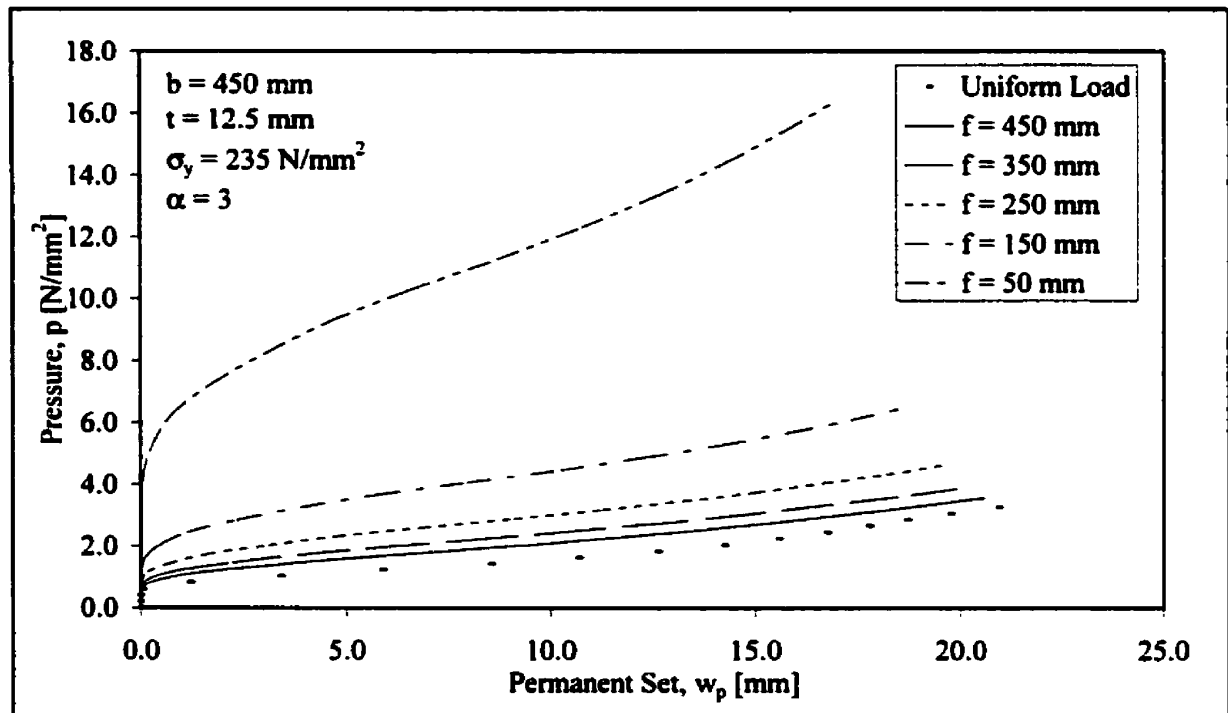


Figure 4.1 Typical Load vs. Permanent Set Results from Finite Element Analyses

cases failed to converge before a load of  $8 \times p_y$  was reached, but only 10% failed to converge before achieving permanent set of at least 5% of the frame spacing. Of this 10%, the average level of permanent set in terms of frame spacing was 4.7% (4.2%

<sup>1</sup> Since framing orientation has no effect on the deflection of uniformly-loaded plates, any references to transversely- and longitudinally-framed plating imply a load of finite height.

minimum). Accordingly, subsequently developed equations for pressure correction factors,  $f_D$ , can be considered valid for levels of permanent set up to  $0.05b$ . Total deflection and permanent set results for all test cases are given in Appendix B, with some typical load-permanent set curves shown in Figure 4.1. As anticipated, the results reveal a well-behaved relationship between pressure, load height and permanent set.

## 4.2 Characteristics of Plating Response

### 4.2.1 Interaction of Bending Moments and Axial Forces

By examining the interaction of local bending moments and axial forces, the load-carrying mechanisms used by the plating throughout the load history can be determined.

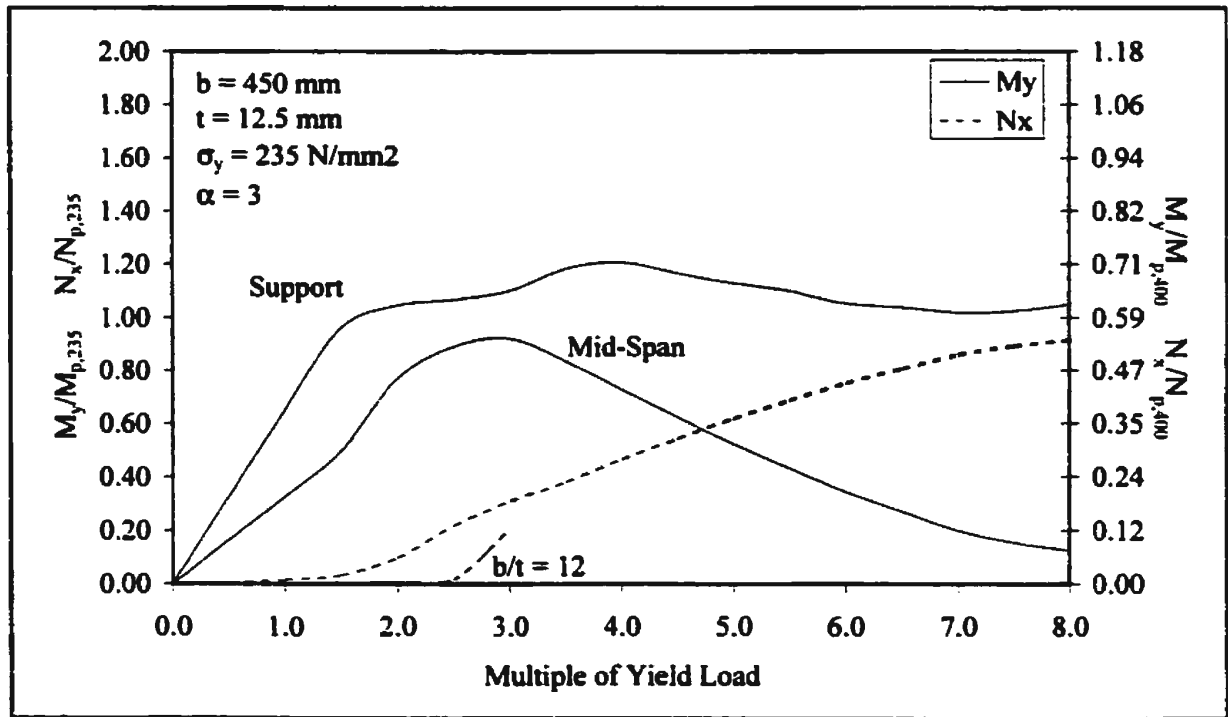


Figure 4.2 Interaction of Bending Moments and Axial Forces – Uniform Load

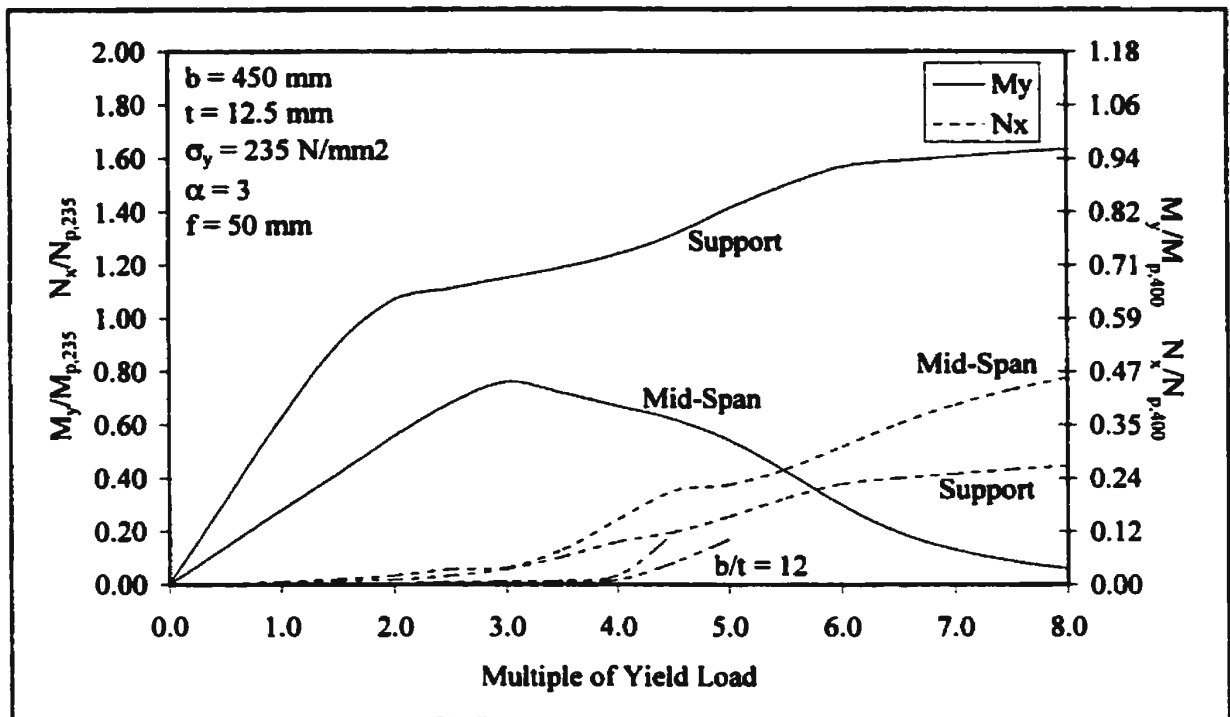


Figure 4.3 Interaction of Bending Moments and Axial Forces – Finite Load Height – Transversely-Framed Plating

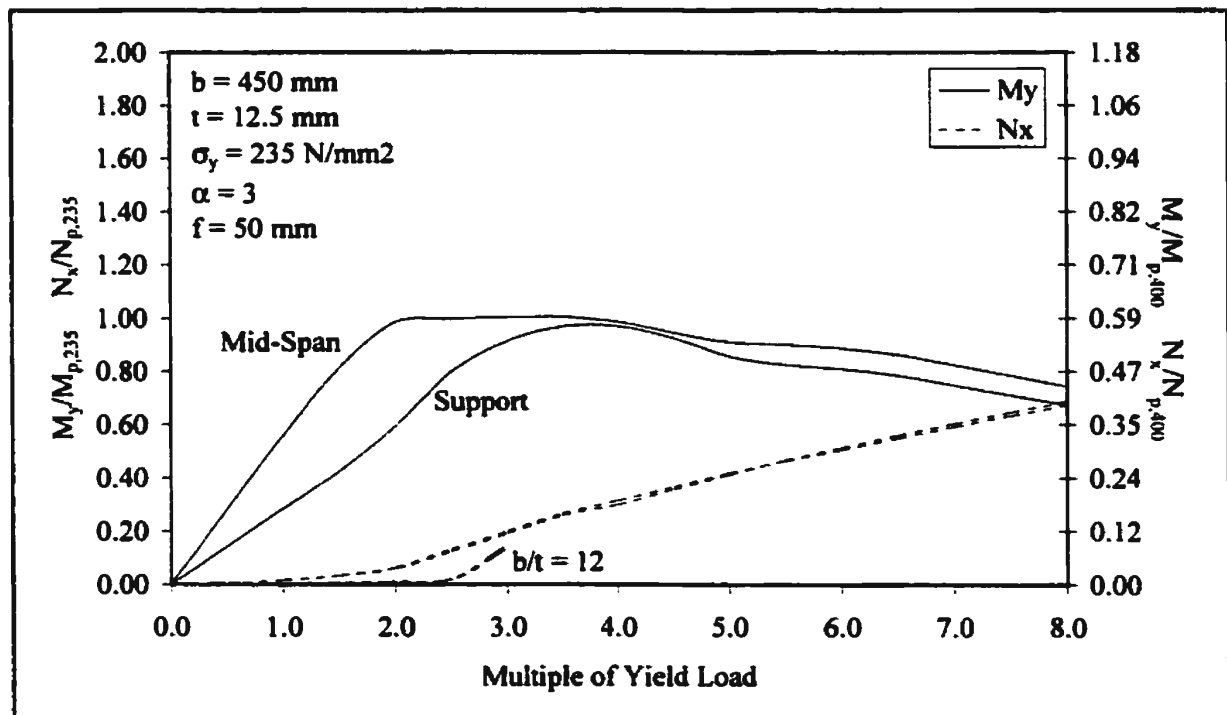


Figure 4.4 Interaction of Bending Moments and Axial Forces – Finite Load Height – Longitudinally-Framed Plating



Figures 4.2 to 4.4 show the interaction of bending moments per unit length,  $M_y$ , and axial forces per unit length,  $N_x$ , for  $b/t = 36$  plating. Also shown is a portion of the axial forces per unit length for  $b/t = 12$  plating. The bending moments and axial forces are shown as ratios of the fully plastic moments,  $M_p$ , and axial loads,  $N_p$ , based on the assumed yield ( $235 \text{ N/mm}^2$ ) and ultimate ( $400 \text{ N/mm}^2$ ) strengths of the material. Contrary to Equation (2.9), the plastic moment and axial loads are here corrected for Poisson's ratio effect using a plastic value of  $\nu = 0.5$

$$M_p = \sigma_y \frac{t^2}{4\sqrt{1+0.5-0.5^2}} \quad (4.1)$$

$$N_p = \sigma_y \frac{t}{\sqrt{1+0.5-0.5^2}} \quad (4.2)$$

These non-dimensional quantities, at mid-span and at the support, are plotted against multiples of the load required to initiate plasticity in the plating.

By comparing the results for uniformly-loaded plating, Figure 4.2, with the spread of plasticity shown in Figure 2.1, it can be seen that the elasto-plastic theories are largely substantiated. Although strain-hardening effects are included in the results shown in Figure 4.2, the bending moments at mid-span remain elastic until the bending moments at the support approach  $M_{p,235}$ . At this point, the bending moment at the support remains relatively constant, although some strain hardening is occurring at the surfaces of the plating. This boundary condition is analogous to the elastic restraint in elasticity theory, wherein the plastic hinge rotates under the effect of a constant moment. Under such boundary conditions, the bending moments at mid-span approach plastic levels and then reduce as membrane forces increasingly begin to carry the load. Of course, the stage at

which the membrane forces begin to carry the load depend largely on the  $b/t$  value. As can be seen, axial forces do not carry any of the load for  $b/t = 12$  plating until the yield load is exceeded by about 150%. Using the interaction formula of Equation (2.11),  $M_y/M_{p,235} + (N_x/N_{p,235})^2$  remains approximately equal to unity at mid-span once a plastic hinge is formed. As the interaction progresses,  $M_y/M_{p,400} + (N_x/N_{p,400})^2$  approaches unity at the support.

For loads of finite height, the interactions are similar except for a few notable characteristics. For transversely-framed plating (see Figure 4.3), the separation between the magnitudes of bending moments at the supports and mid-span is relatively greater, with the latter remaining below the lower plastic moment  $M_{p,235}$  and the former approaching the upper plastic moment  $M_{p,400}$  under the effects of strain-hardening. Correspondingly, the axial forces at the supports remain below those at mid-span throughout the interaction. Conversely, the separation of bending moment magnitudes for longitudinally-framed plating is less than that of the uniformly-loaded plating (see Figure 4.4), with apparently no strain-hardening at the supports (maximum  $M_y/M_{p,235} = 1$ ). Once the bending moments at mid-span and the supports approach  $M_{p,235}$ , the axial force begins to take more of the load and bending moments at both locations are reduced at the approximately the same rate. As in the case of uniformly-loaded plating, the stage at which the axial forces occur depend largely on the ratio of frame spacing to plate thickness. As can be seen, the axial forces in  $b/t = 12$  longitudinally-framed plating occur at the same stage as with uniformly-loaded plating (~ 250% of the yield load). However, for  $b/t = 12$  transversely-framed plating, axial forces are negligible until the yield load is exceeded by approximately 300%.

To illustrate the distribution of bending moments and axial forces over the span of the frame ( $\alpha = 3$ ,  $p = 3 \times p_y$ ), Figures 4.5 and 4.6 show  $M_y/M_{p,235}$  and  $N_x/N_{p,235}$  from the line of load application to the supporting stringer / web frame, respectively, for both transversely- and longitudinally-framed plating. The distribution for uniformly-loaded plating is similar to that for the longitudinally-framed plating. For transversely-framed plating, the bending moments  $M_y$  and axial forces  $N_x$  are significantly reduced beyond a half frame spacing from the line of load application, and zero beyond a frame spacing. For longitudinally-framed plating, the bending moments and axial forces remain constant to within a frame spacing of the support, with bending moments at mid-span nearly unchanged to within one quarter of a frame spacing from the support. These results are significant insofar as they clearly indicate the different influences of plate aspect ratios on

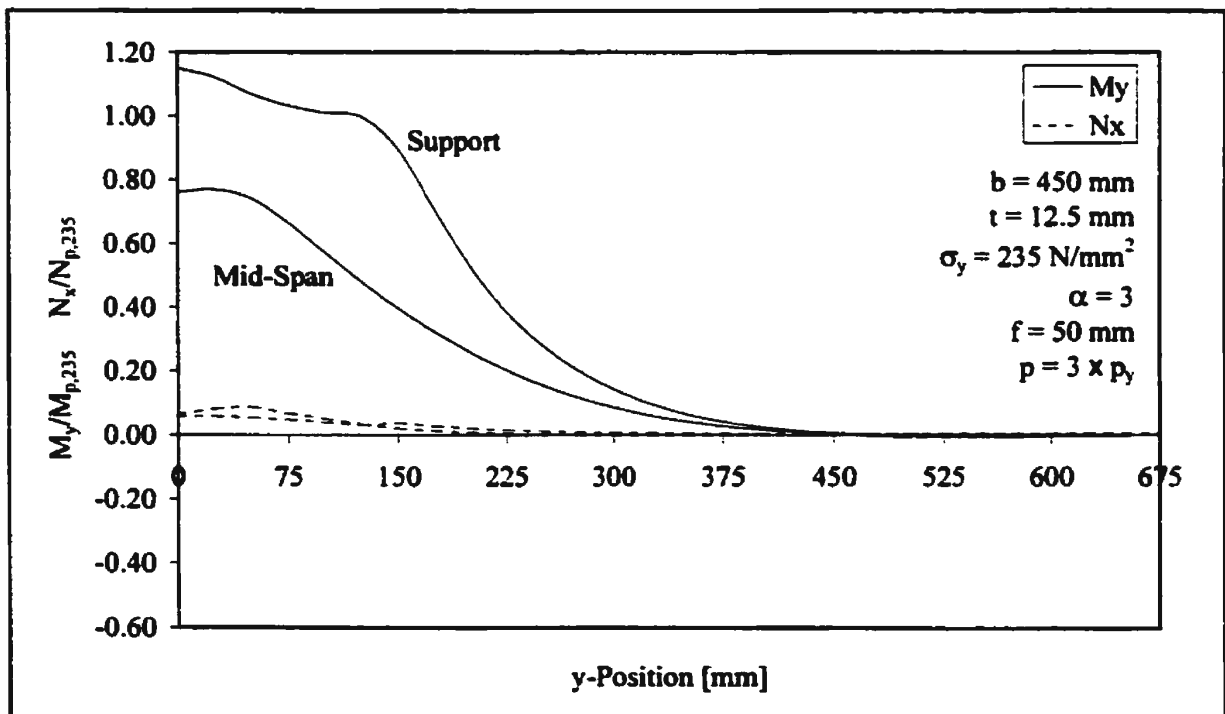


Figure 4.5 Extent of Bending Moments and Axial Forces – Finite Load Height – Transversely-Framed Plating

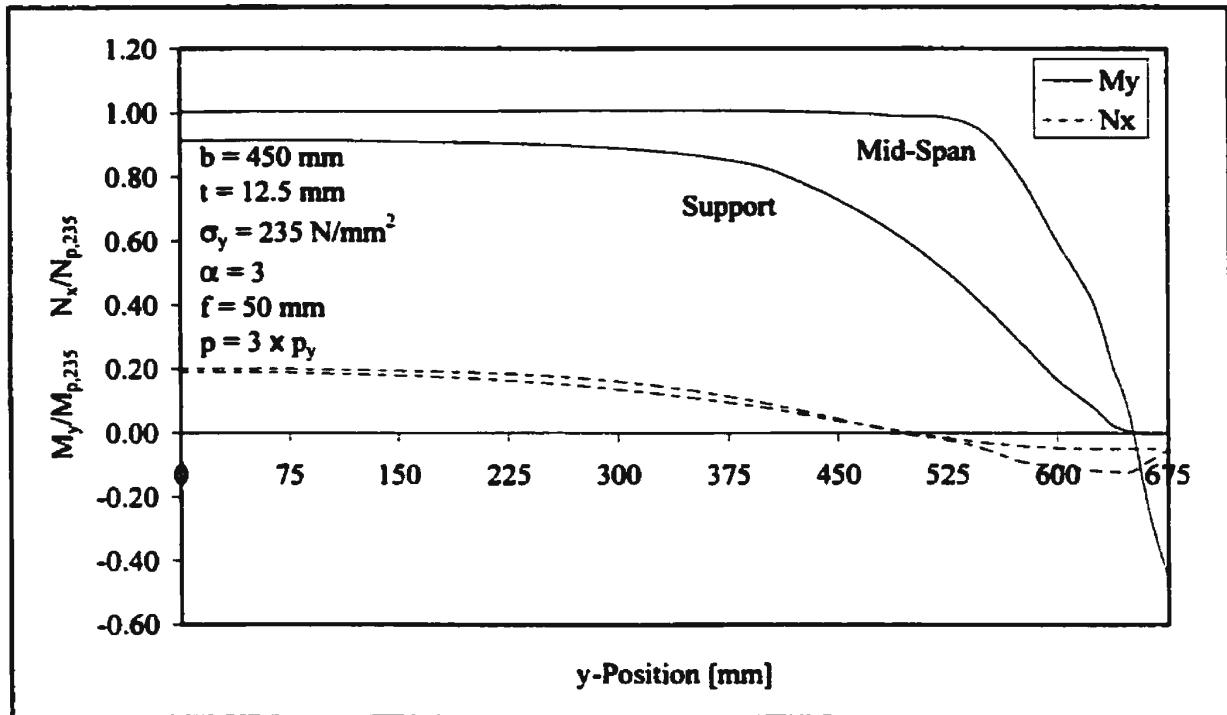


Figure 4.6 Extent of Bending Moments and Axial Forces – Finite Load Height – Longitudinally-Framed Plating

the behaviour of transversely- and longitudinally-framed plating subjected to loads of finite height.

#### 4.2.2 Patterns of Plasticity

Typical patterns of plasticity in the top and bottom surfaces of plating subjected to uniform loads and loads of finite heights are shown in Figure 4.7. The aspect ratio of the shown plating is two, but the plasticity patterns in the transversely-framed plating are identical at greater aspect ratios and very similar, although elongated, for longitudinally-framed and uniformly-loaded plating. While the results shown are those for plating subjected to a load eight times that required to initiate yield, and although the plasticity is a result of both bending moments and axial forces, plasticity distributions shown in Figure 4.7 agree well with those shown for the bending moments alone in Figures 4.5 and

4.6. For the longitudinally-framed plating, the plasticity extends along the support and at mid-span for almost the entire length of the frame. For the transversely-framed plating, the plasticity at the support extends along the frame to about half a frame spacing from

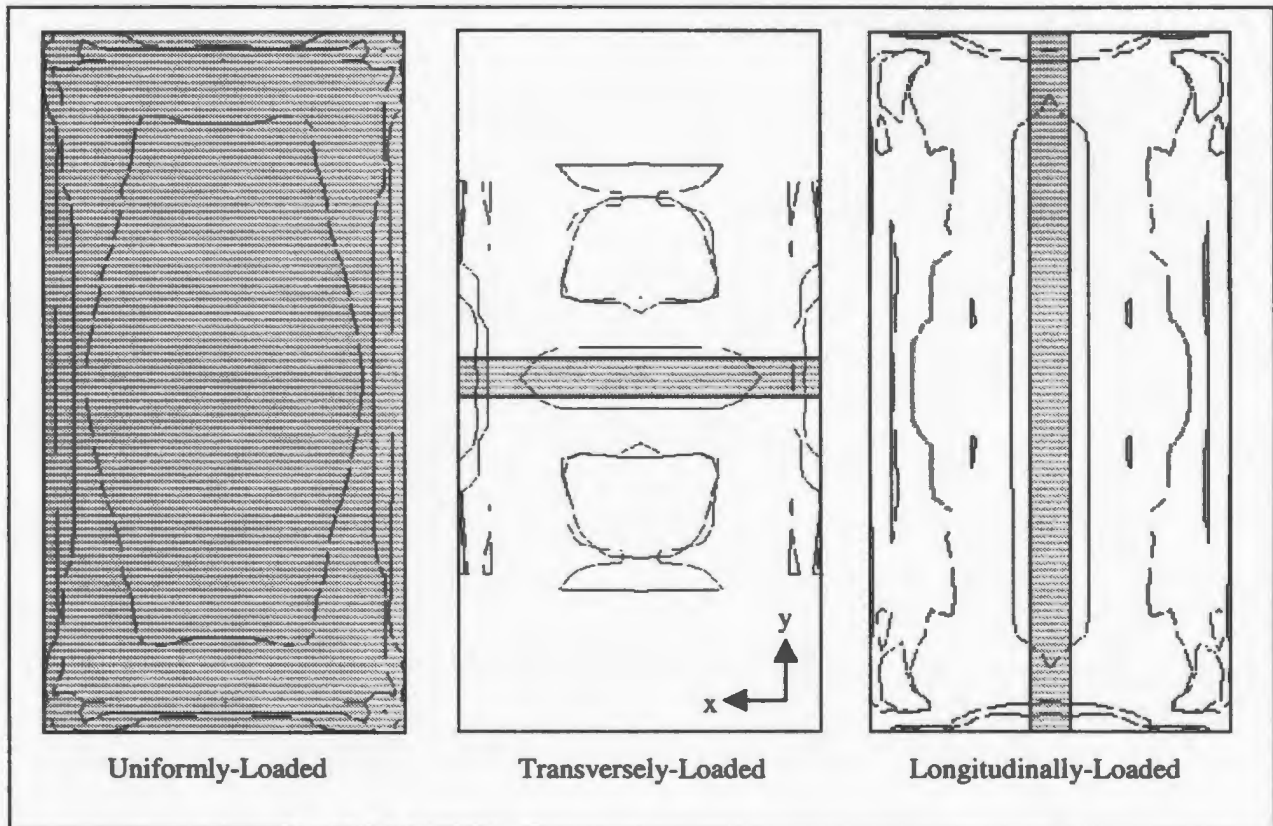


Figure 4.7 Typical Surface Plasticity Plots ( $b = 450 \text{ mm}$ ,  $t = 12.5 \text{ mm}$ ,  $\sigma_y = 235 \text{ N/mm}^2$ ,  $\alpha = 2$ )

the line of load application. The effects of  $M_x$  and  $N_y$ , not shown in Figures 4.5 and 4.6, are here shown to be significant for transversely-framed plating between  $\frac{1}{2}b$  and  $b$  from the line of load application, and only significant for longitudinally-framed plating at the web frame support.

In addition to the foregoing surface plots, through-thickness plots of uniformly-loaded platestrips ( $b/t = 12$  and  $b/t = 36$ ) are shown in Figure 4.8, with and without edge restraint, to illustrate the effects of membrane forces. These effects become increasingly

significant as deformation grows and, according to yield line theory, mid-span bending moments vanish in a fully restrained plate when deflection equals that of the plate

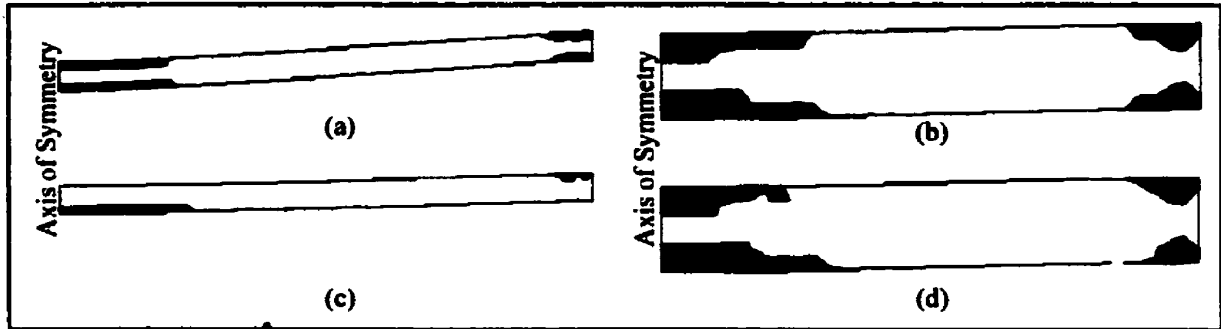


Figure 4.8 Through-Thickness Plasticity in Platestrips

thickness. Therefore, within the practical range of permanent set to frame spacing ratios, say 1% to 5%, the significance of membrane forces should be markedly different for plating of  $b/t = 36$  then it is for  $b/t = 12$ .

The effect of membrane forces in the former can be directly observed by comparing the through-thickness plasticity of a clamped platestrip with edges free to slide (Figure 4.8 (a)), to that in which edge displacements are prevented (Figure 4.8 (c)). These figures show the extent of plasticity at the theoretical load (corrected for Poisson's ratio effect) required to form edge hinges in a platestrip with unrestrained edge displacements

$$p_{ch} = \frac{3\sigma_y (t/b)^2}{\sqrt{1 - 0.5 + 0.5^2}} \quad (4.3)$$

The presence of membrane forces in Figure 4.8 (c) is evidenced by the absence of plasticity in the areas of compressive bending forces. The membrane effect, in terms of the load deflection history, is also shown in Figure 4.9. The effect of membrane forces on the plasticity in the sturdier  $b/t = 12$  plating can be seen in Figures 4.8 (b) and 4.8 (d). In

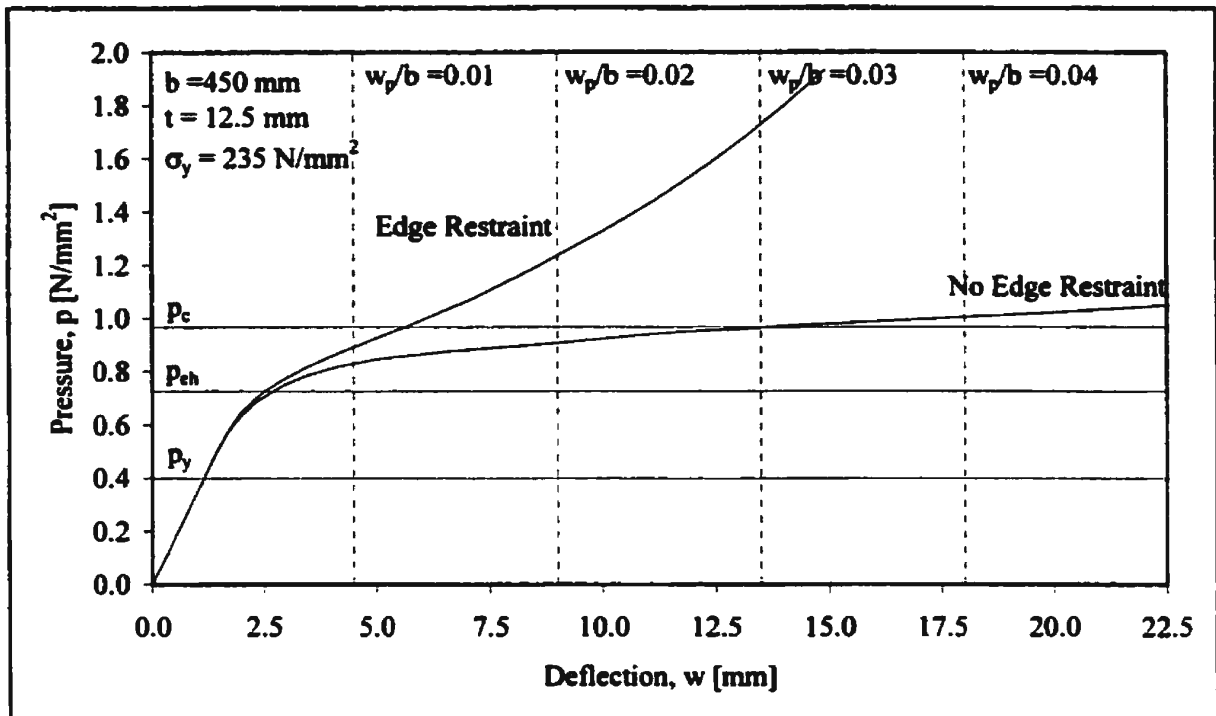


Figure 4.9 Load-Deflection Curves for Platestrip ( $b/t = 36$ )

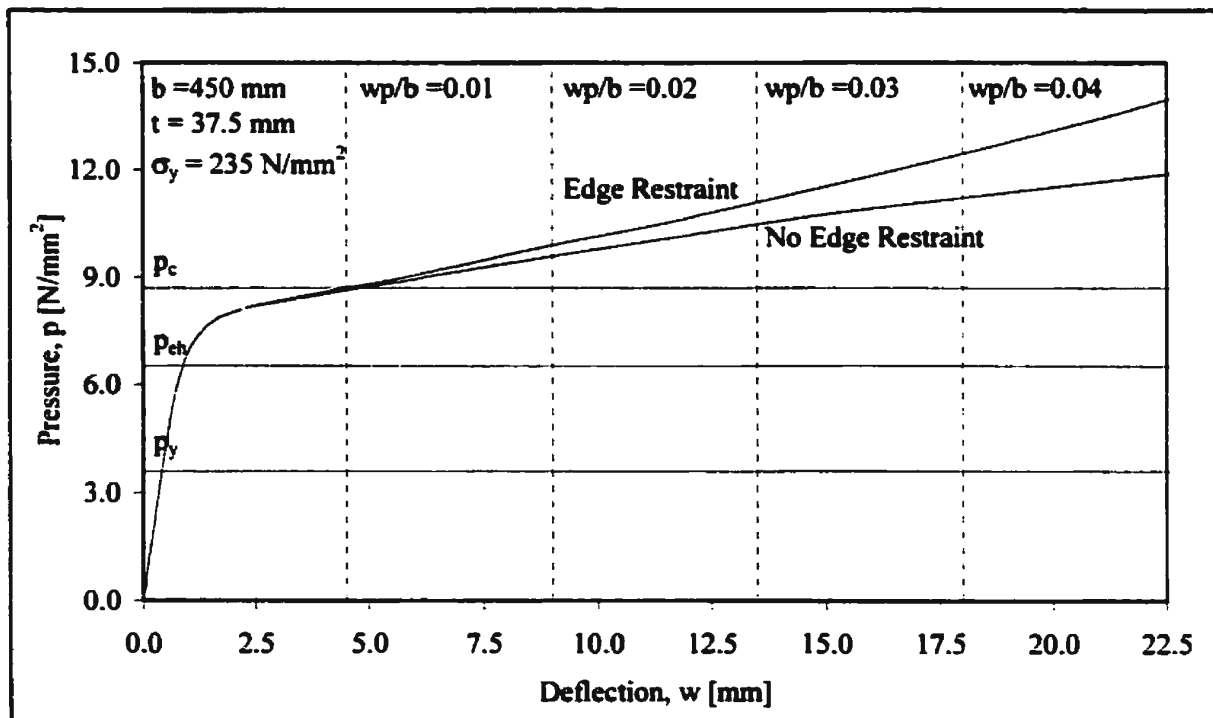


Figure 4.10 Load-Deflection Curves for Platestrip ( $b/t = 12$ )

contrast to the relatively slender plating, the distribution of plasticity under load  $p_{eh}$  is quite similar regardless of the edge condition. This absence of significant membrane effect results in similar load-deflection curves for both cases, as shown in Figure 4.10.

#### 4.2.3 Distribution of In-Plane Strains and Permanent Set

Another means by which to observe the interaction of bending moments and axial forces is to measure the in-plane strains. Assuming that the plastic neutral axis remains near the centre of the plate, the differences between strains at mid-plane and those at the surface are indicative of the bending moments that are present. There is, however, a very practical reason for examining in-plane strains at the top and bottom surfaces of the plating, since both the exterior and interior coatings that protect the steel are susceptible to breakdown when subjected to excessive strains. Although it is very difficult to ascertain the amount of straining that is “excessive”, a function of temperature, chemical composition, coating age and thickness, some approximation of the strains that occur under the design condition is required for a responsible design criterion.

Accordingly, Figures 4.11 and 4.12 show plane strains in the x-direction at  $y = 0$  for transversely- and longitudinally-framed plating, respectively. The strains shown are those at the top, middle and bottom surfaces of the plating. Results are shown for loads that cause permanent sets equal to about 1% of frame spacing. Although the strains shown are for  $b/t = 36$  plating, the positive strains for plating with lesser  $b/t$  values are similar, since greater strains due to bending moments compensate for lower membrane forces. The distribution of strains under loads of increased load height differ only slightly for both transversely-and longitudinally-framed plating. As can be seen for the plating under



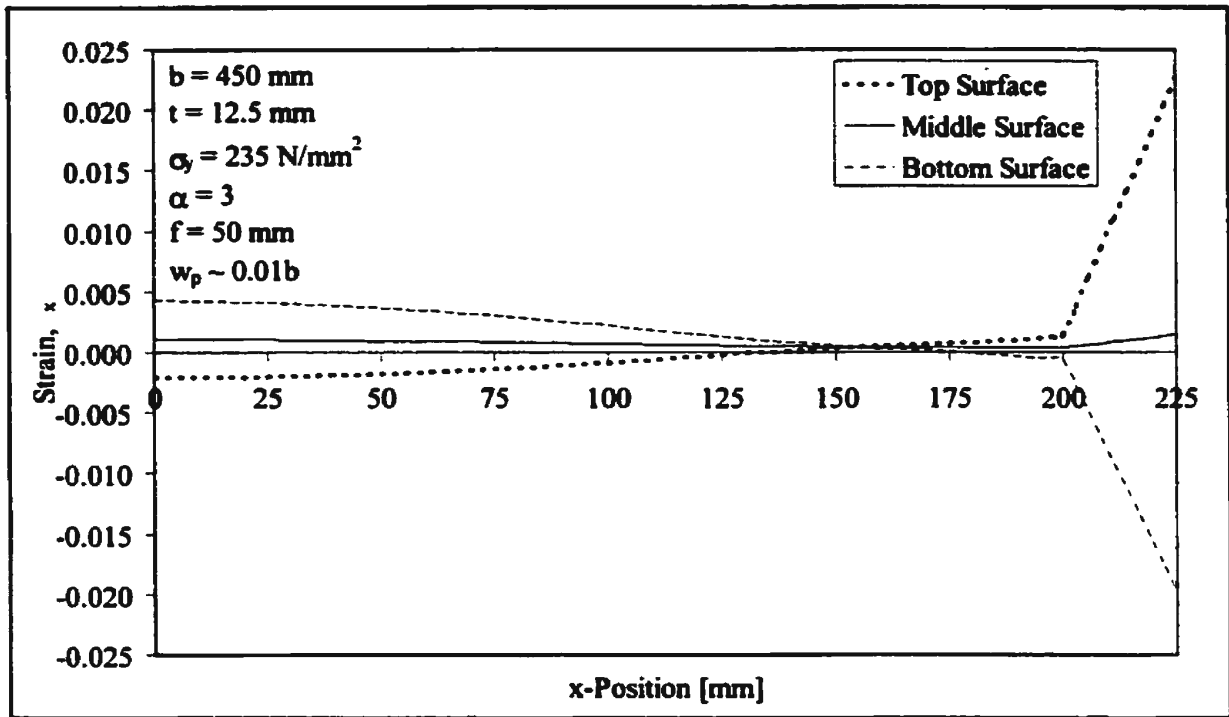


Figure 4.11 In-Plane Strain (x-direction) – Transversely-Framed Plating

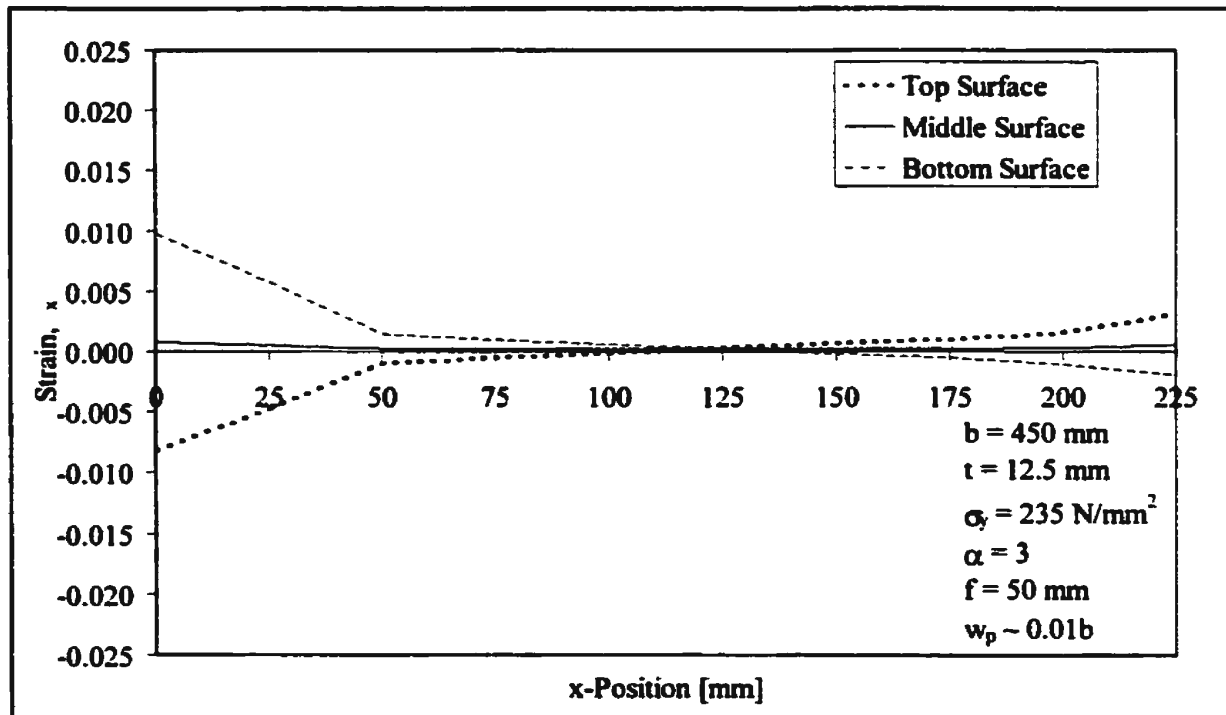


Figure 4.12 In-Plane Strain (x-direction) – Longitudinally-Framed Plating

consideration, the maximum level of strain when transversely-framed is about 2.3%, and occurs at the support. For longitudinally-framed plating, the maximum level of strain is about 1.0% and occurs at mid-span.

In Figures 4.13 and 4.14, patterns of permanent set are shown for transversely- and longitudinally-framed plating, respectively. Patterns are shown for  $b/t = 36$  plating subjected to uniform loads and loads of height equal to  $b/9$ ,  $5b/9$  and  $b$ . Results are shown for loads that cause permanent set equal to about 5% of frame spacing. The displacements are normalised against those at mid-span, and plotted over a distance orthogonal to the direction of the load. It can be seen that patterns of permanent set for longitudinally-framed plating are quite similar to plating subjected to a uniform load, while displacement patterns for transversely-framed plating are markedly different. Results for plating of lower  $b/t$  values are similar, with the plots of different load heights gradually converging towards one another. Except for the case of the uniformly-loaded plate, patterns of permanent set for greater plate aspect ratios remain unchanged, with displacements for the transversely-framed plating continuing to converge at zero about one and a half frame spacings from the line of load application. Unfortunately, in terms of damage analyses, Figures 4.13 and 4.14 illustrate the difficulty in determining load heights from the vertical extent of permanent set. Although a close examination reveals that the vertical extents of the loads roughly coincide with the points of inflection in the plots of permanent set, determining ice load heights in this manner is very difficult in practice. This is especially true since damages could very likely have been caused by multiple moving loads of different heights, intensities and vertical locations.

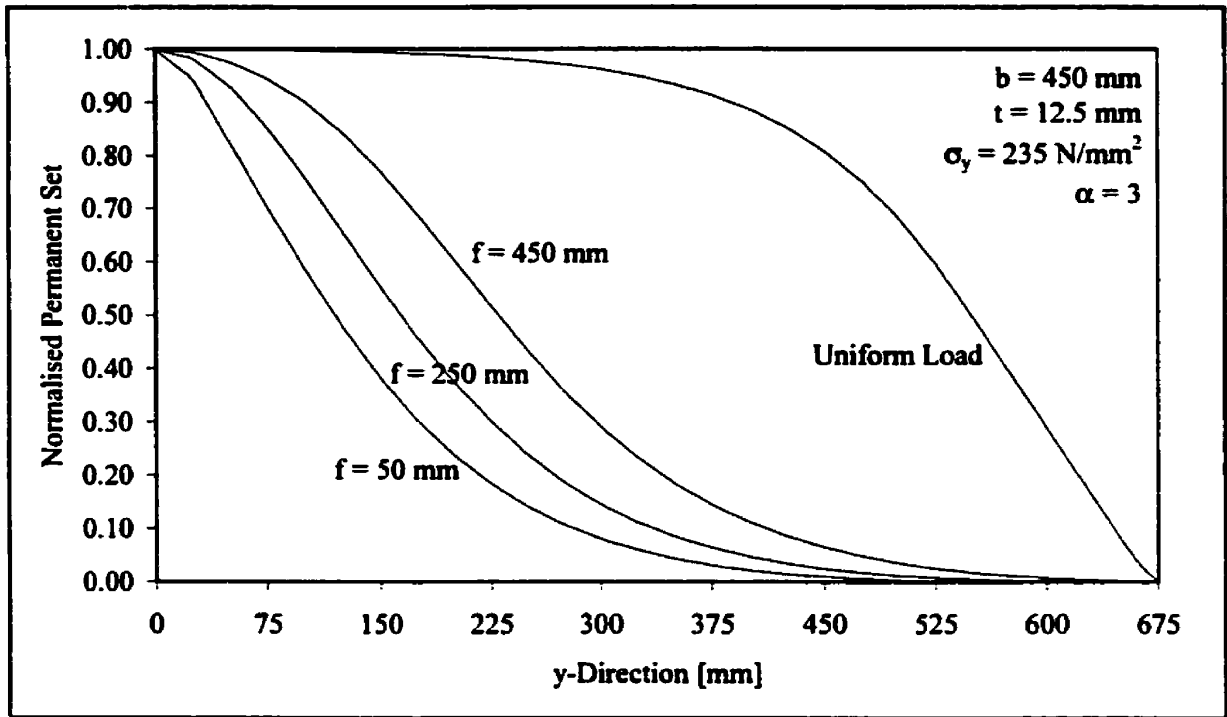


Figure 4.13 Normalised Permanent Set in y-Direction – Transversely-Framed Plating

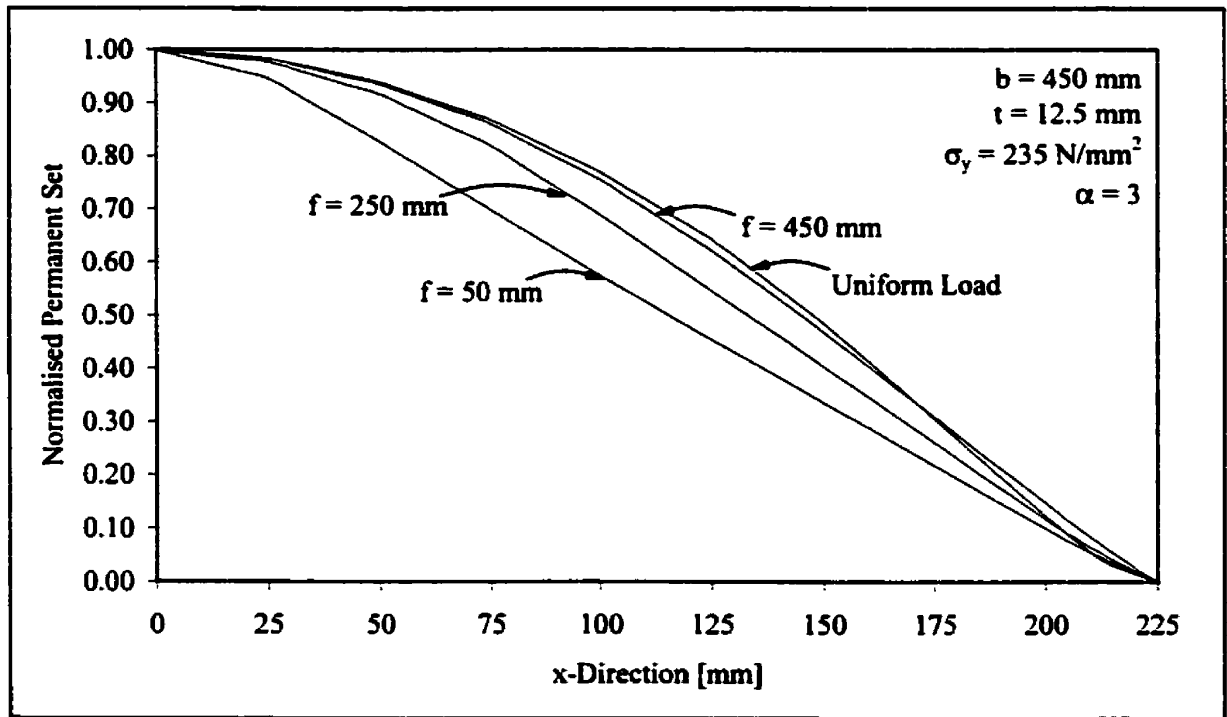


Figure 4.14 Normalised Permanent Set in x-Direction – Longitudinally-Framed Plating

### 4.3 Influences of Structural and Load Parameters on Permanent Set

#### 4.3.1 Influence of Plate Aspect Ratio

The influence of plate aspect ratio on permanent set depends jointly on load height, framing orientation and whether or not the aspect ratio exceeds the “critical” value. The “critical” value of plate aspect ratio can be defined as the value beyond which aspect ratio ceases to influence the magnitude of central deflection. For a uniform load, the critical value depends largely on the ratio of frame spacing to plate thickness. As can be seen in Figures 4.15 and 4.16, a plate aspect ratio beyond three ceases to influence the magnitude of load required to achieve  $w_p = 0.025b$  for  $b/t = 36$  plating, but continues beyond an aspect ratio of five to influence the required load for  $b/t = 12$  plating. As shown in Table 4.1, Equations (2.14) and (2.15) from yield line theory reasonably capture the influence of aspect ratio on the behaviour of uniformly-loaded plates.

$\alpha$	$b/t = 12$			$b/t = 36$		
	YLT	YLT*	FEA	YLT	YLT*	FEA
1	2.76	2.93	3.00	20.17	24.12	22.14
2	1.80	1.91	1.88	12.06	14.42	13.62
3	1.59	1.69	1.69	10.10	12.08	12.08
4	1.51	1.60	1.66	9.24	11.06	11.60
5	1.46	1.55	1.66	8.77	10.49	11.36
YLT* Adjusted to Coincide with Finite Element Results for Plate Aspect Ratio of 3						

Table 4.1 Influence of Plate Aspect Ratio on Pressures to Obtain  $w_p = 0.025b$

For loads of finite height, the effect of plate aspect ratio on permanent set depends largely on the orientation of the framing. For transversely-framed plating, as shown in Figures 4.15 and 4.16, the influence of plate aspect ratio beyond a value of two is negligible. Because the deformations are limited to the mid-span area of the plate, the

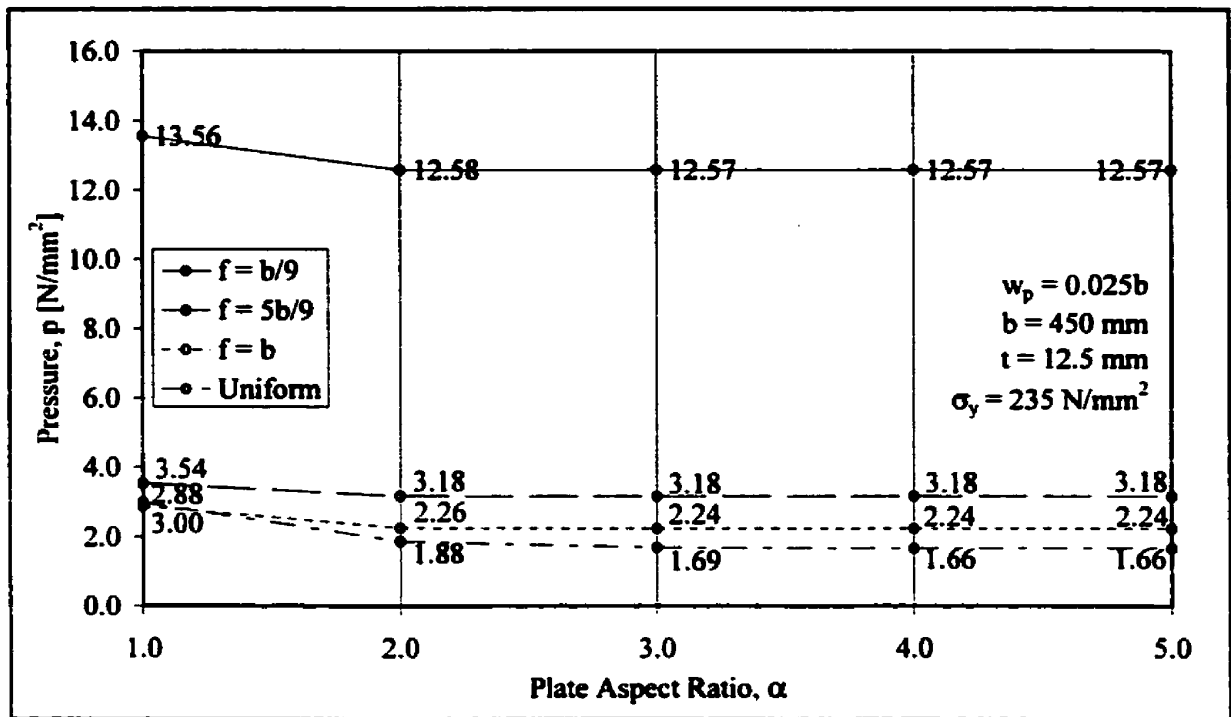


Figure 4.15 Influence of Plate Aspect Ratio – Transversely-Framed Plating ( $b/t = 36$ )

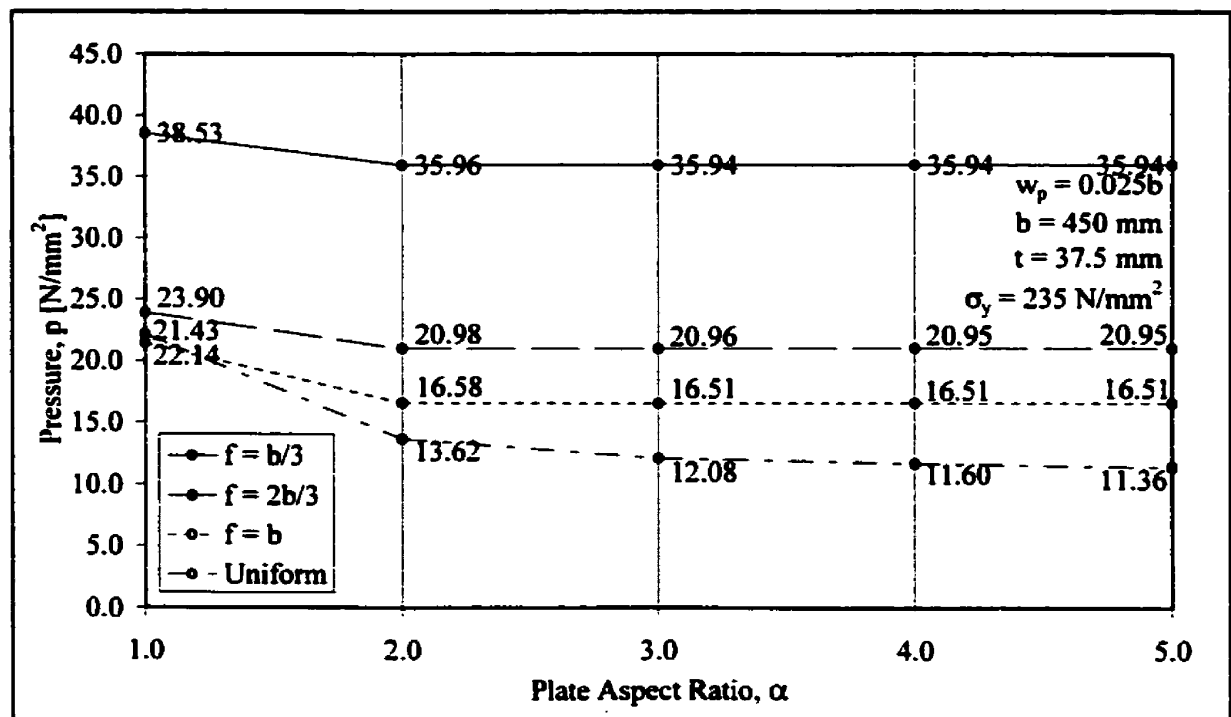


Figure 4.16 Influence of Plate Aspect Ratio – Transversely-Framed Plating ( $b/t = 12$ )

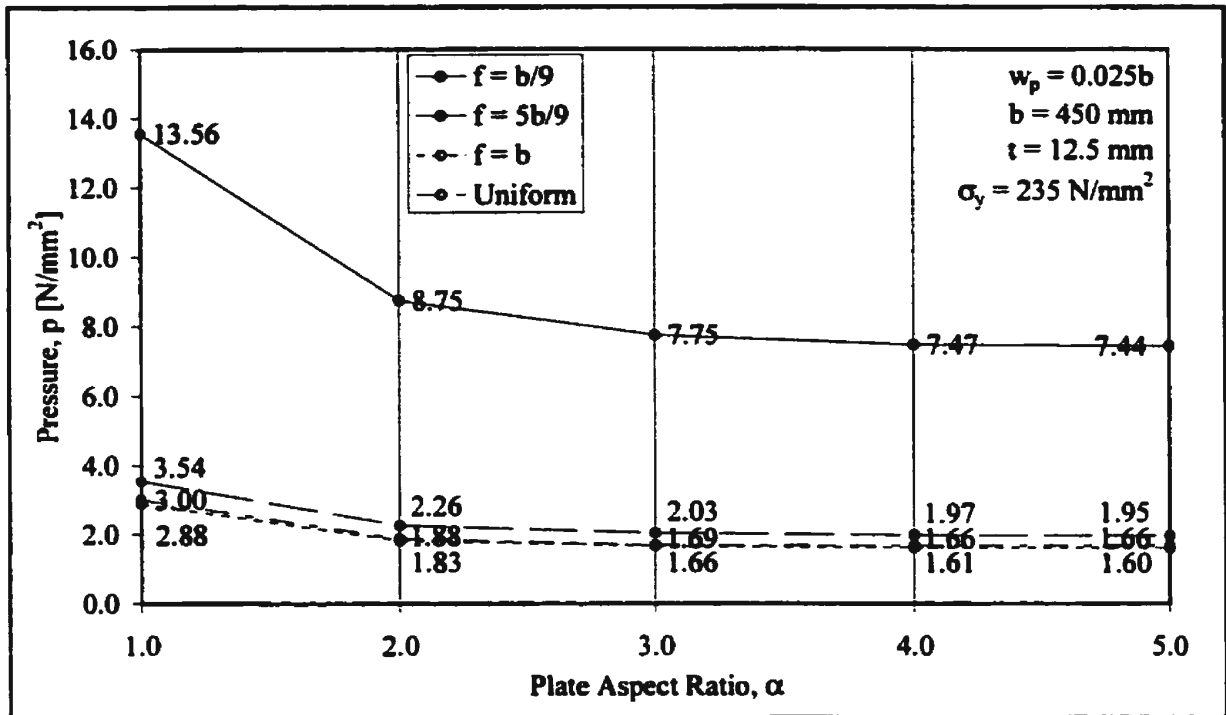


Figure 4.17 Influence of Plate Aspect Ratio – Longitudinally-Framed Plating ( $b/t = 36$ )

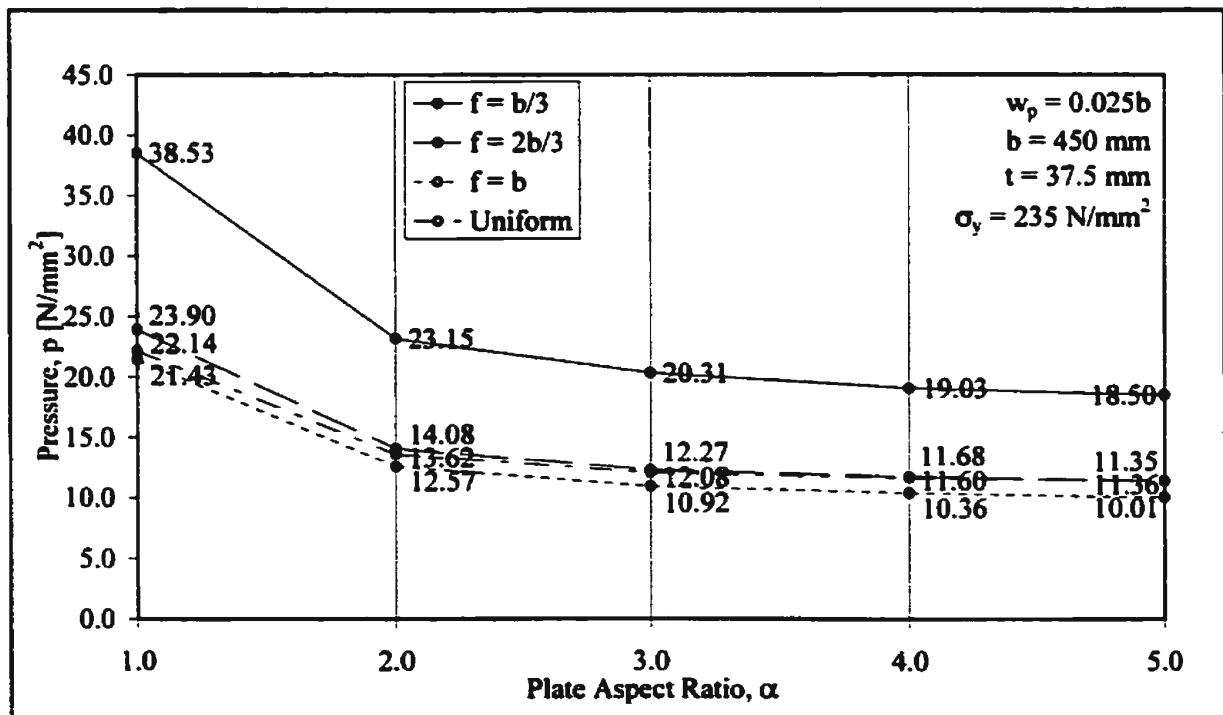


Figure 4.18 Influence of Plate Aspect Ratio – Longitudinally-Framed Plating ( $b/t = 12$ )

stiffening effect of the stringers does not influence the magnitude of permanent set. In contrast, the deformations of the longitudinally-framed plating occur over the entire span. As can be seen in Figures 4.17 and 4.18, the influence of plate aspect ratio extends beyond  $\alpha = 2$  and closely resembles the aspect ratio effects for uniformly-loaded plates. Correspondingly, the critical value of the aspect ratio is about three for  $b/t = 36$  plating and beyond  $\alpha = 5$  for plating with  $b/t = 12$ . As with uniformly-loaded plating, the increase in the pressure required to obtain a given level of permanent set in a square plate is considerable compared to that for a longitudinally-framed plate with an aspect ratio of two (55% to 65% depending on  $b/t$ ). For transversely-framed plating, the increase is considerably less (about 7% to 8% for the examined level of permanent set). An interesting anomaly in the results is that the pressures required to obtain  $w_p = 0.025b$  are noticeably higher for  $b/t = 12$  plating when uniformly-loaded than for the plating when longitudinally-framed and subjected to loads of height equal to the frame spacing.

#### 4.3.2 Influence of Material Yield Stress

According to linear-elastic theory, the pressure required to obtain a given level of plating response is inversely proportional to the yield stress of the material. Similarly, in terms of yield line theory, if the right-hand sides of Equations (2.14) and (2.15) are kept constant while the yield strength of the material is changed, then the magnitude of applied uniform pressure must be inversely proportional to this change (since the collapse pressure,  $p_c$ , is directly proportional to the yield strength of the material). Figure 4.19 shows the degree of correlation between this assumption and results of the finite element analyses. Since the applied pressures for the  $\sigma_y = 355\text{N/mm}^2$  plating are plotted on a scale

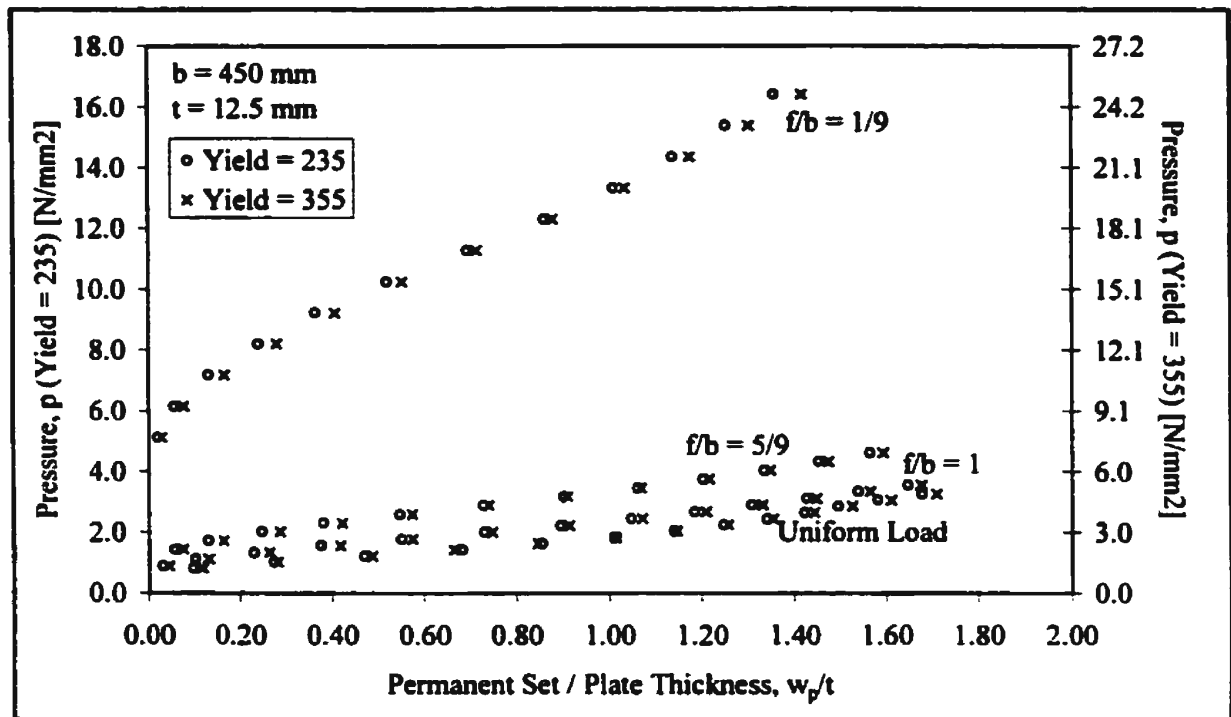


Figure 4.19 Influence of Material Yield – Transversely-Framed Plating ( $b/t = 36$ )

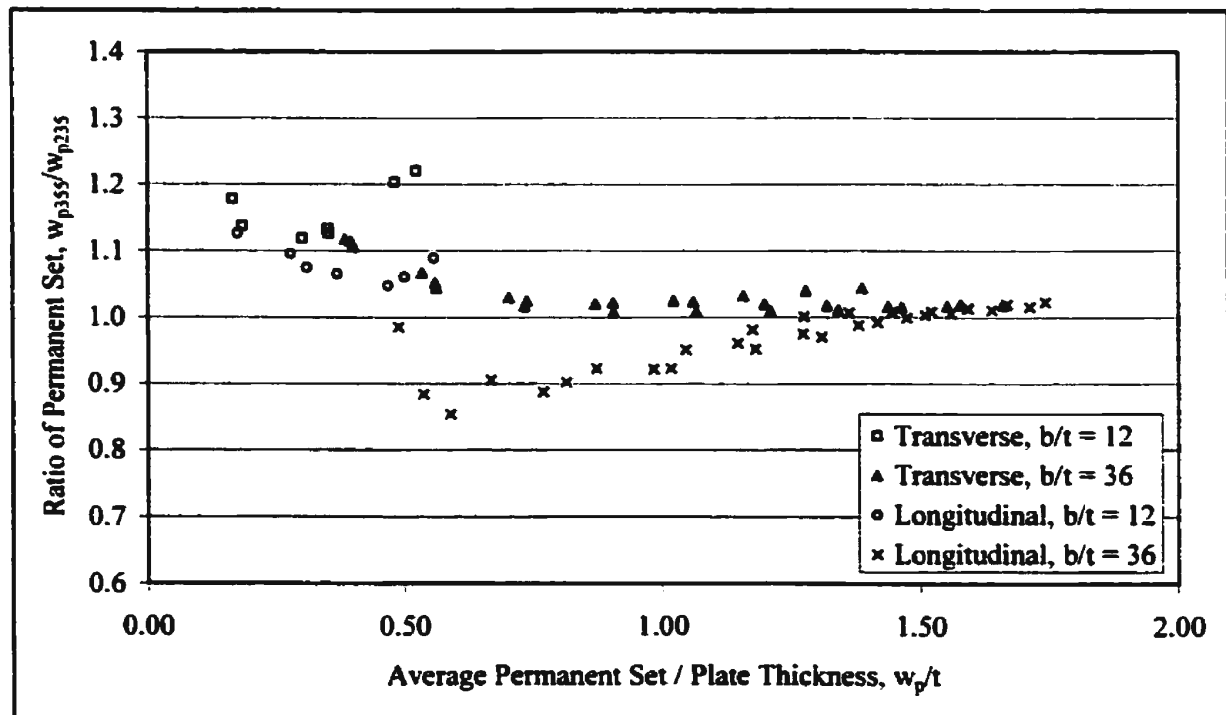


Figure 4.20 Influence of Material Yield – Transversely- and Longitudinally-Framed Plating ( $b/t = 36$ ,  $b/t=12$ )



condensed by  $355/235 = 1.51$ , the data points for the uniform load should lay on top of one another if the treatment of material strength within yield line theory is correct. As can be seen, the agreement is quite good for the  $b/t = 36$  plating, with the mean of pressure ratios equal to 1.01. However, the agreement deteriorates progressively with reducing  $b/t$  ratios, with mean ratios of 1.05, 1.10 and 1.20 for  $b/t$  values of 28, 20 and 12, respectively (based on  $w_p/t$  values above 0.1).

With respect to plating subjected to loads of finite height, Figure 4.19 also shows results for  $f = b$ ,  $f = 5b/9$  and  $f = b/9$ . As can be seen, the level of agreement is similar to that for uniformly-loaded plating. However, to gain a more complete picture of the influence of yield strength on the permanent set of plates subjected to line-like loads, Figure 4.20 shows the ratios of permanent set,  $w_{p355}/w_{p235}$ , for both transversely- and longitudinally-framed plating, where  $p_{355} = 355/235 p_{235}$ . It is evident that the ratios of permanent set for both  $b/t = 12$  and  $b/t = 36$  plating approach unity as the values of  $w_p/t$  increase. Except for longitudinally-framed plating of  $b/t = 36$ , the magnitudes of permanent set for plates of higher yield strength are greater than for plates of lower yield strength subjected to correspondingly lower pressures.

#### 4.3.3 Influence of Frame Spacing to Plate Thickness Ratio

To assess the influence, according to yield line theory, of frame spacing to plate thickness ratios on levels of permanent set, Equations (2.14) and (2.15) are again examined with the right-hand sides of the equations kept constant. Since  $p_c = 16M_p/b^2 = 4\sigma_y t^2/b^2$ , any change to the magnitude of  $b/t$  must be balanced with a change in  $p$  by a factor of  $([b/t]_{old} / [b/t]_{new})^2$ . For example, to maintain a given level of  $w_p/t$ , a change from

$b/t = 36$  to  $b/t = 12$  requires an increase in pressure by a factor of  $(36/12)^2 = 9$ . Using such increases in uniformly-applied pressures (shown as multiples of yield loads since they also follow this relationship), Figure 4.21 compares the values of  $w_p/t$  for the frame spacing to plate thickness ratios of 12, 20, 28 and 36, obtained with finite element

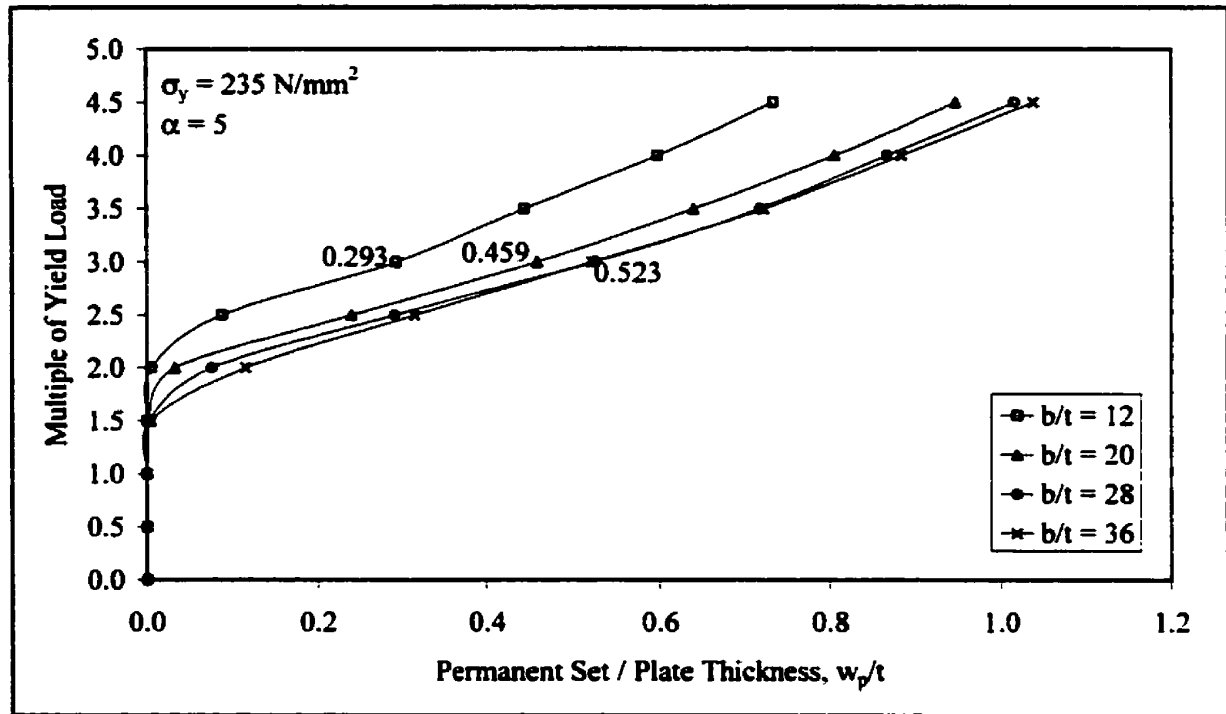


Figure 4.21 Influence of  $b/t$  Ratio – Uniform Loading

analyses. As with the analysis of material yield, the data points should lay on top of one another. However, it can be seen that the assumed relationship within yield line theory works reasonably well for  $b/t = 28$  and  $b/t = 36$ , but that the relatively thicker plates incur correspondingly lower levels of  $w_p/t$ .

For plating subjected to loads of finite height, Figures 4.22 and 4.23 show comparisons similar to those for uniformly-loaded plates. Plating with  $b/t$  ratios of 12 and 36 are shown for which all other plate and load parameters are equal. Similar to the

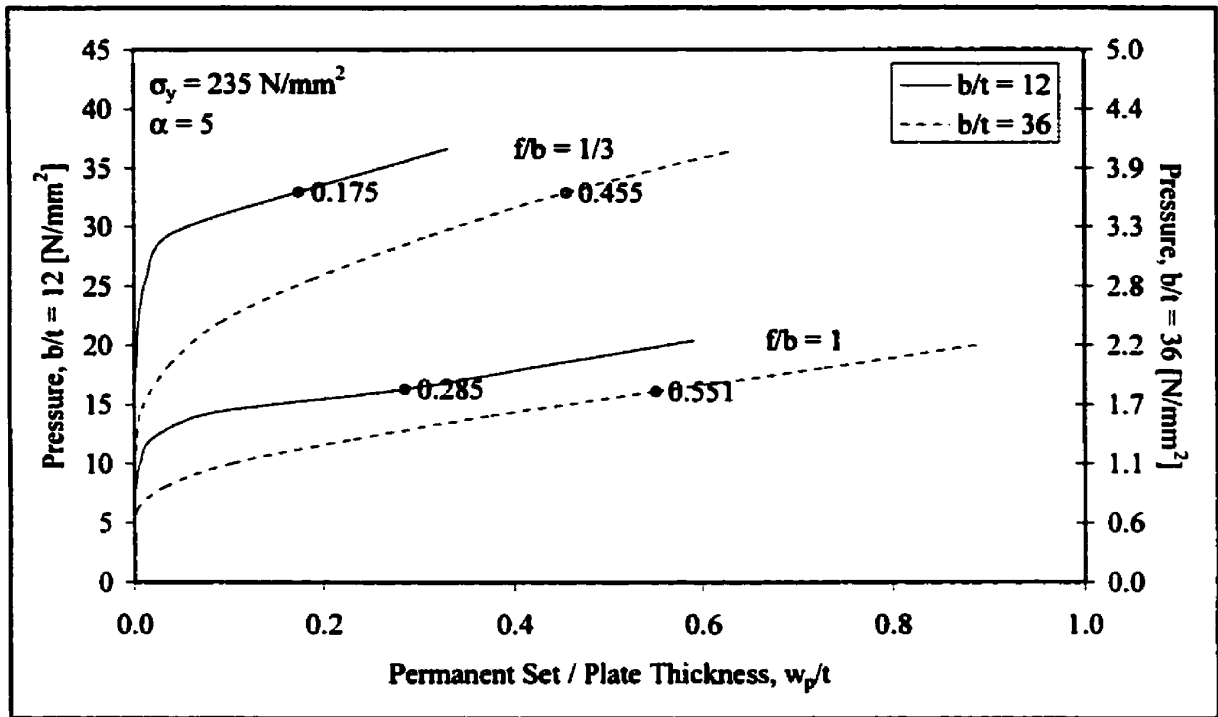


Figure 4.22 Influence of  $b/t$  Ratio – Transversely-Framed Plating

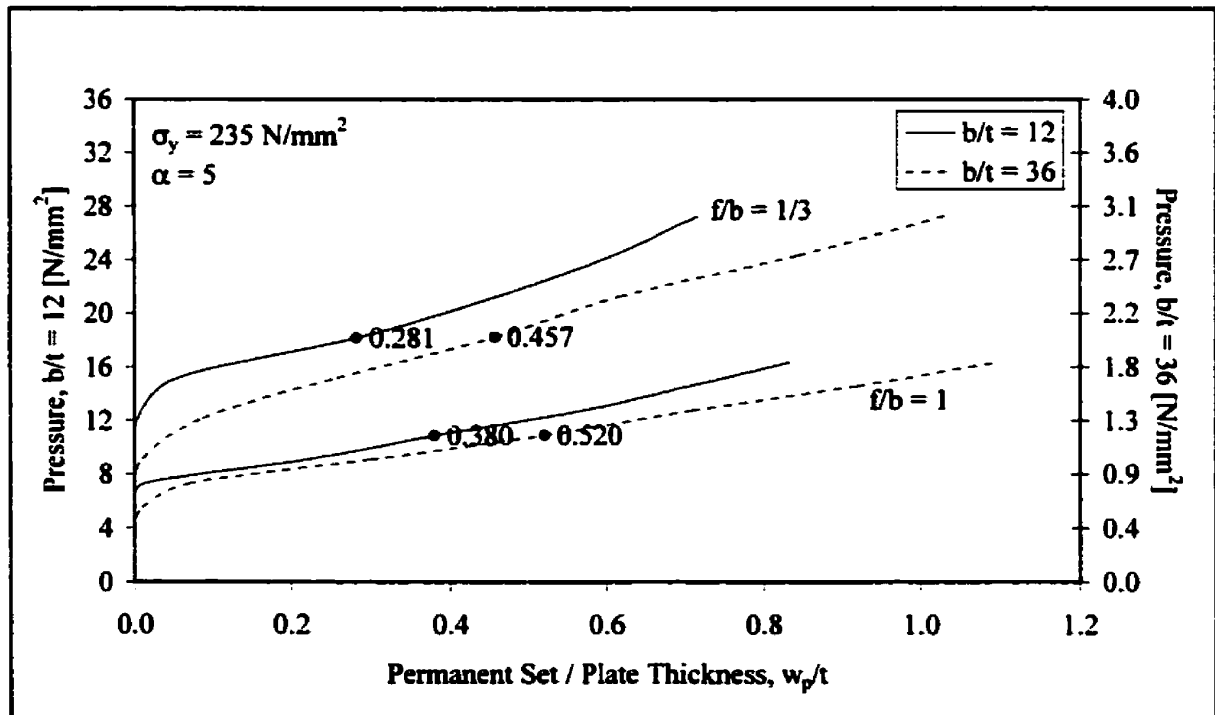


Figure 4.23 Influence of  $b/t$  Ratio – Longitudinally-Framed Plating

comparisons for material strength, the applied pressures for the  $b/t = 36$  plating are plotted on an axis expanded by a factor of  $(36/12)^2 = 9$ , so that the data points should again lay on top of one another. As can be seen, the results for both transversely- and longitudinally-framed plating do not verify the influence of  $b/t$  values on permanent set according to yield line theory. Although, the longitudinally-framed plating shows marginally better agreement than that for transversely-framed plating, the equations for the pressure correction factors will need to reflect these influences of the  $b/t$  ratios.

#### 4.3.4 Influence of Load Height to Frame Spacing Ratio

In Figures 4.24 and 4.25, the pressures required to produce  $w_p = 0.025b$  are plotted against the load height to frame spacing ratios for plates of different slenderness ratios. The results are typical for different aspect ratios and levels of permanent set. Equations fitted to the data points verify the well-behaved relationship between load height and pressure for transversely-framed plating and a given level of permanent set. As evidenced by the differing values of  $f/b$  exponents, the change in required pressure for different load heights is moderately dependent on the  $b/t$  values. Equations fitted to the data points for longitudinally-framed plating also verify a well-behaved relationship between load height and pressure, although the effect of  $b/t$  values is more pronounced than for transversely-framed plating. While there is evidence of a linear relationship between pressure and  $f/b$  ratios at higher values of the latter, for both transversely- and longitudinally-framed plating, this is not so once the load heights approach half the spacing of the frames. Comparing the results of Figure 4.24 to those of Figures 4.15 and 4.16 (transversely-framed plating,  $\alpha = 3$ ,  $w_p = 0.025b$ ), it can be seen that the pressures associated with loads

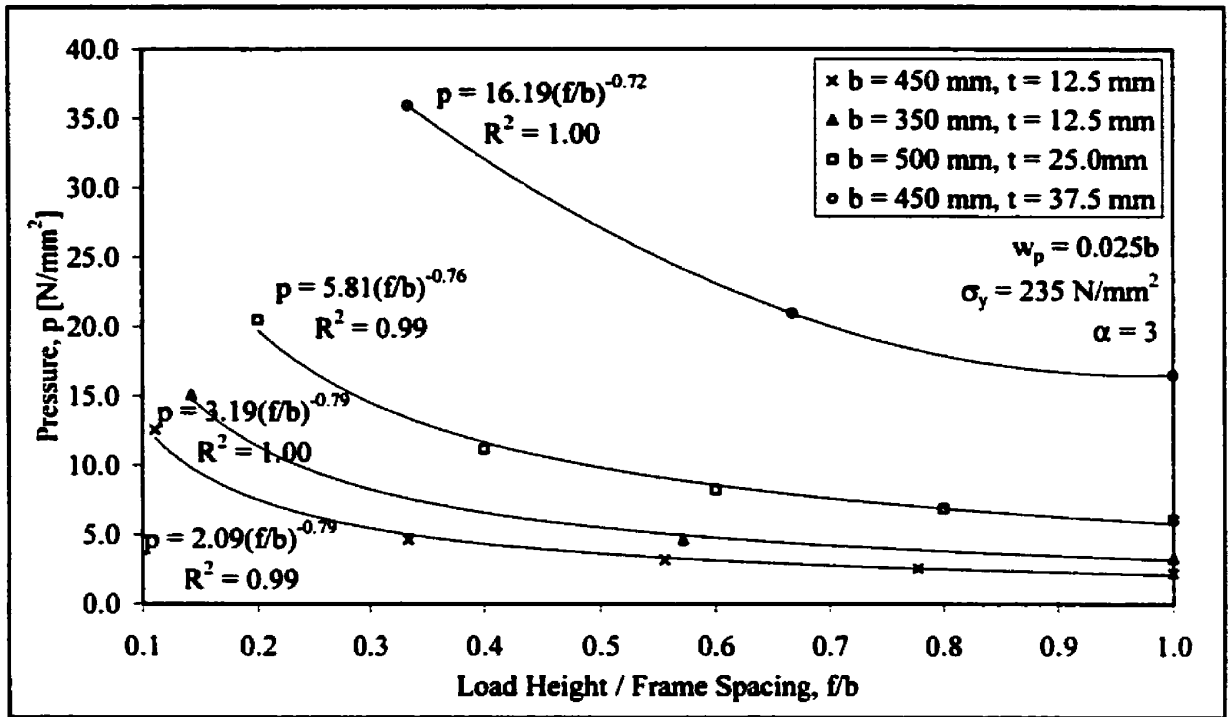


Figure 4.24 Influence of  $f/b$  Ratio – Transversely-Framed Plating

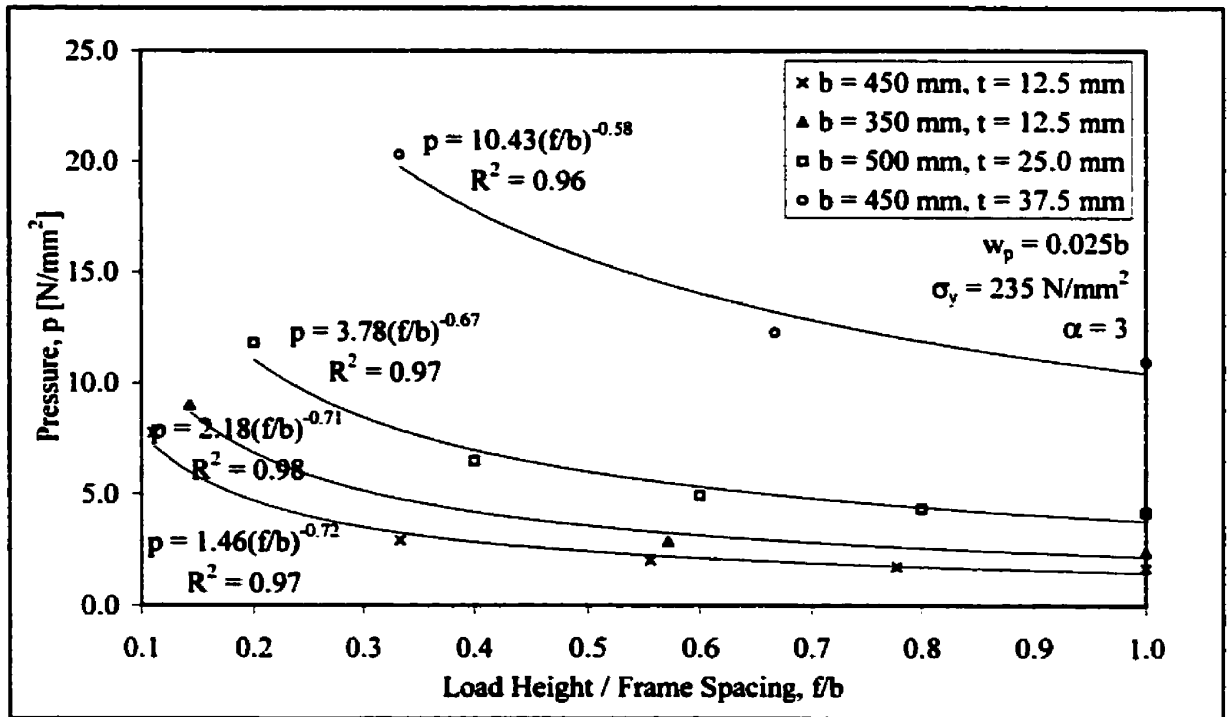


Figure 4.25 Influence of  $f/b$  Ratio – Longitudinally-Framed Plating

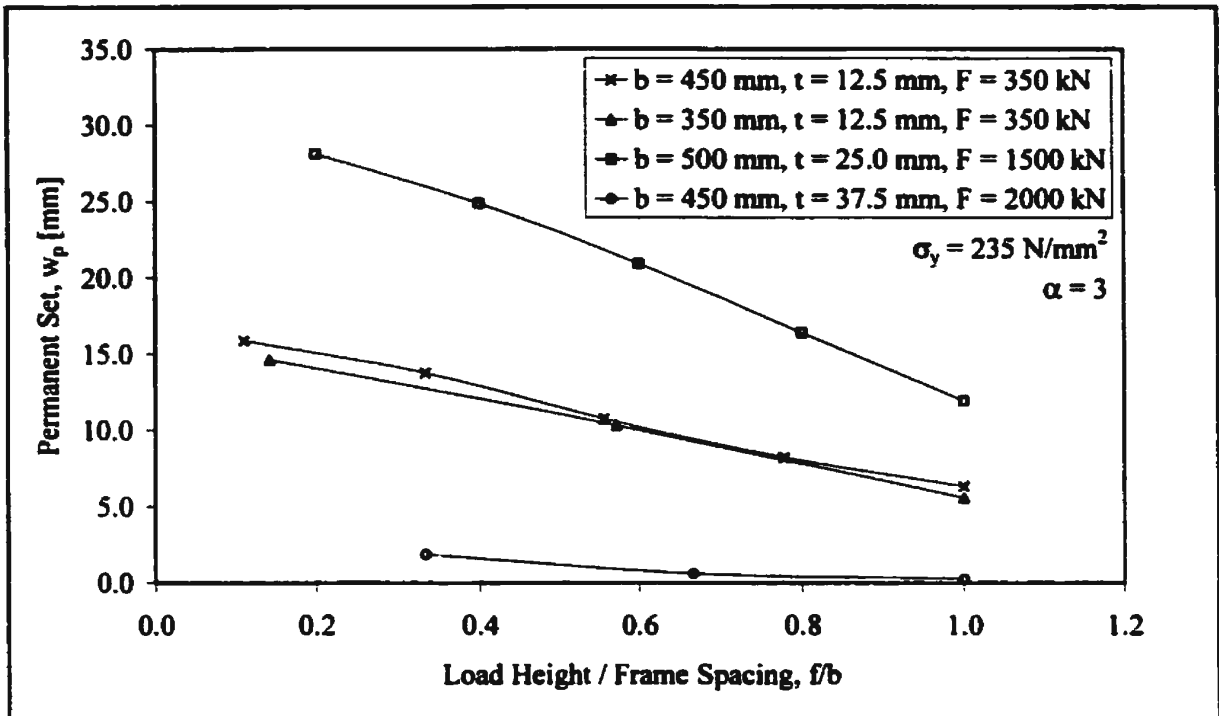


Figure 4.26 Influence of  $f/b$  Ratio – Transversely-Framed Plating – Fixed Force

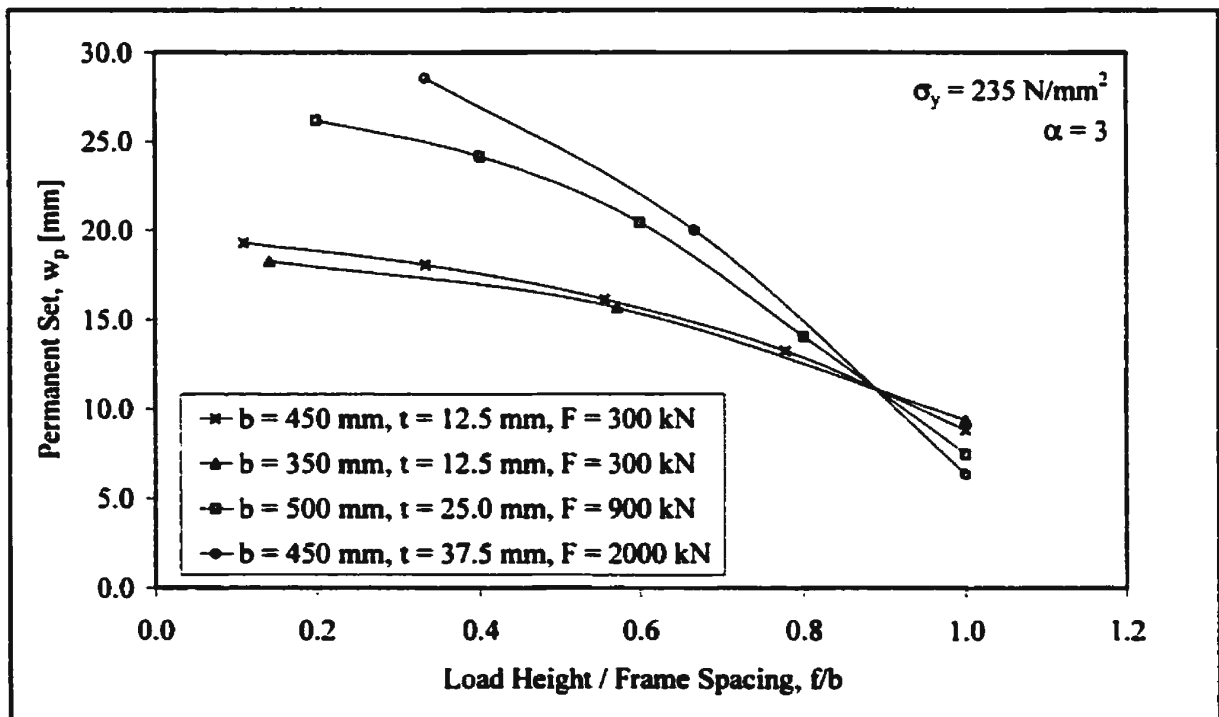


Figure 4.27 Influence of  $f/b$  Ratio – Longitudinally-Framed Plating – Fixed Force

of height equal to the frame spacing are 75% to 80% of those when the load is applied uniformly.

An interesting issue to be addressed is whether or not there exists a critical load height, below which the level of permanent set remains constant for a given force. This question is addressed in Figures 4.26 and 4.27 which show the levels of permanent set in both transversely- and longitudinally-framed plating, respectively, when subjected to line loads of various heights, but a constant force. As can be seen, even for load heights approaching  $f = 0.1b$ , the slope of the line load curves remain non-zero throughout, although in almost all cases there is a reduction in slope at the lower levels of load height. This reduction is quite marked for longitudinally-framed plating.

#### 4.3.5 Influence of Load Length

The influence of load length on the permanent set of transversely-framed plating is shown in Figure 4.28. For plating loaded only over the span of the frame spacing, it can be seen that the load-permanent set histories for various load heights differ little from plating subjected to loads of infinite length. This is a very different situation compared to the elastic domain, in which the absence of a load in the adjacent frame bay would result in greater levels of response in the plating under load. Certainly, as can be seen in Figure 4.28, total deflections are greater in the plating subjected to a load of finite length. However, as seen in Figure 4.29, the bending moments and axial forces are also different in comparison to the case of infinite load length. The result is that the increased level of work performed by the load of finite length is balanced with an increased level of plastic

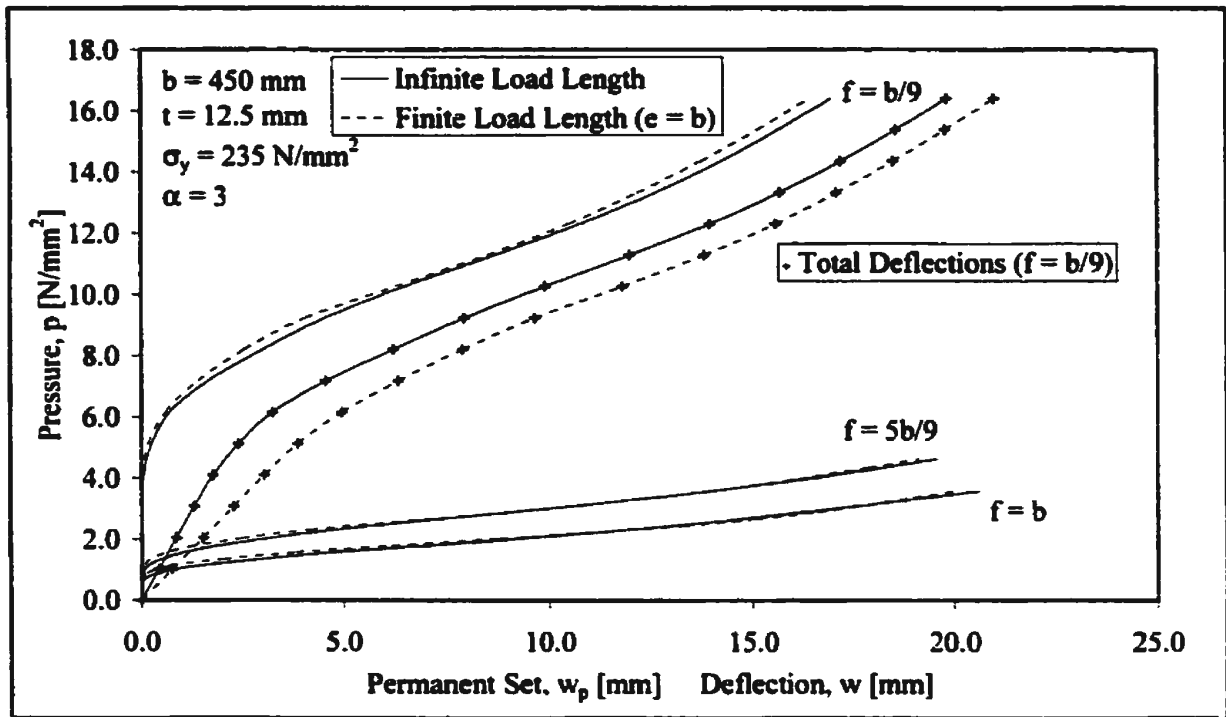


Figure 4.28 Influence of Load Length – Transversely-Framed Plating

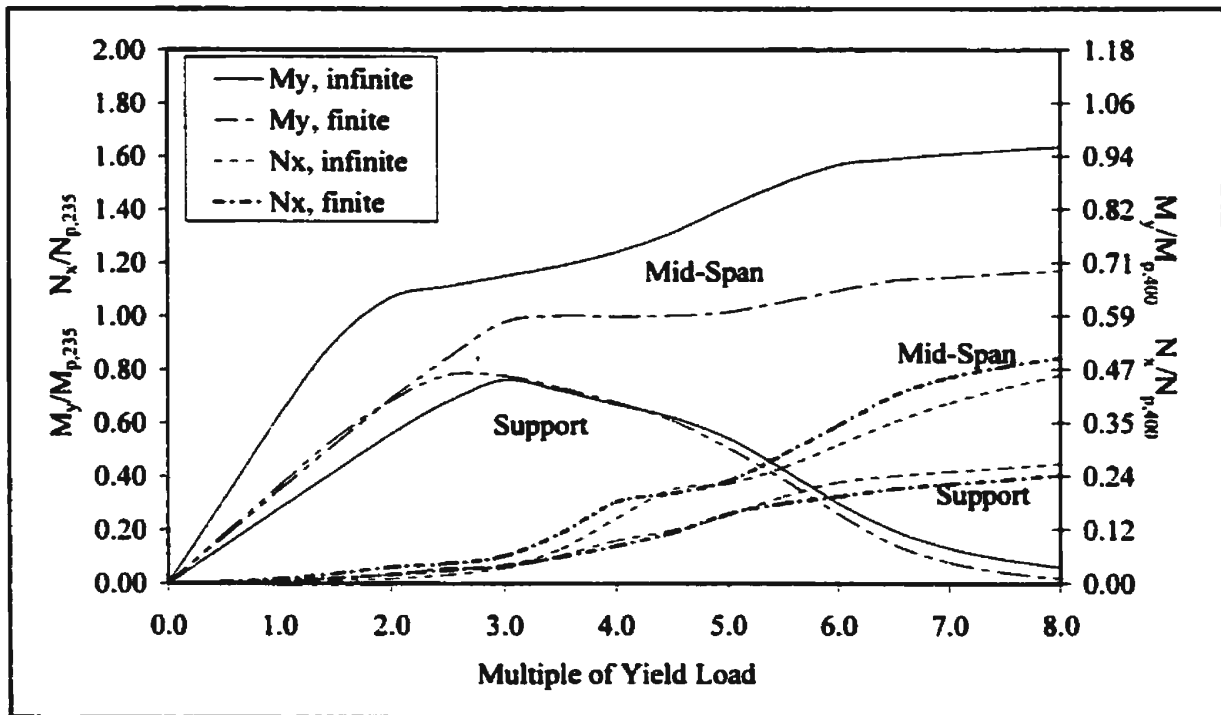


Figure 4.29 Influence of Load Length - Bending Moments and Axial Forces – Transversely-Framed Plating



work, such that the permanent deformations are similar to those resulting from a load of infinite length. Similarly, the residual response of alternately loaded panels in the plastic domain would not be expected to differ significantly from a singly loaded panel.

In the case of longitudinally-framed plating, Figure 4.30 compares the load-permanent set histories of plating subjected to loads of infinite length to those for loads of

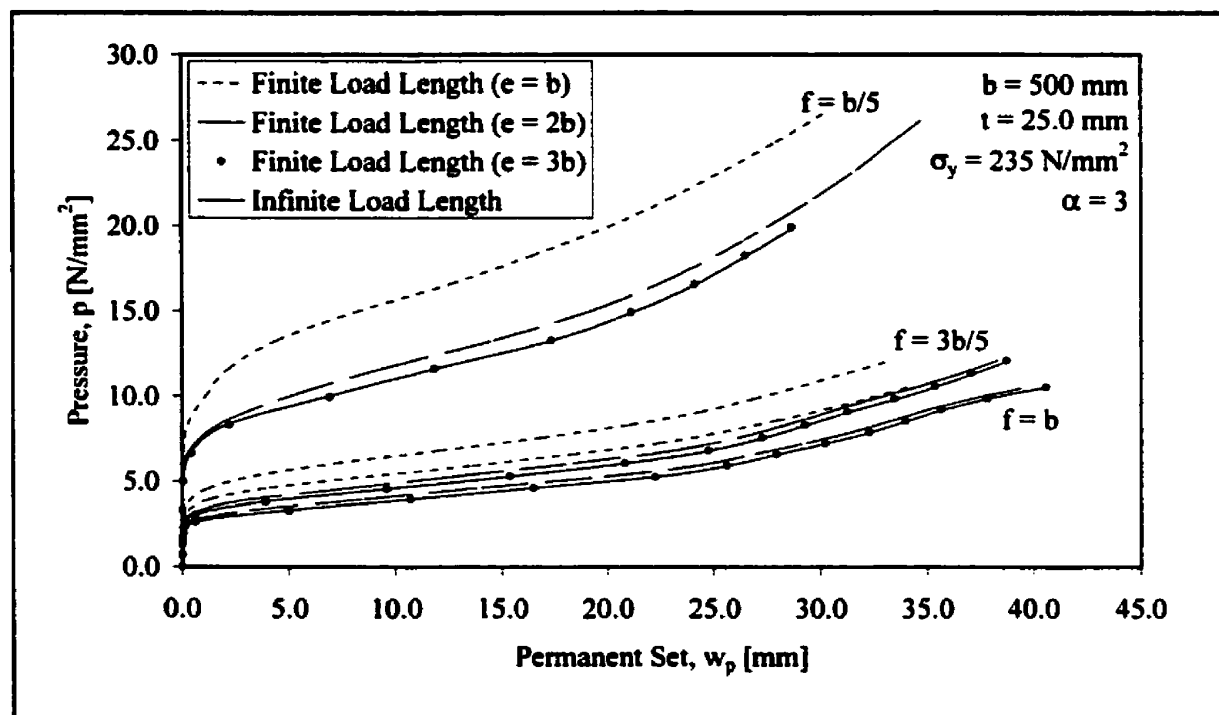


Figure 4.30 Influence of Load Length – Longitudinally-Framed Plating

length equal to one, two and three times the frame spacing. For the load heights shown, it can be seen that the permanent set resulting from loads equal in length to a single frame spacing are substantially less than those from loads of infinite length. The difference is lessened considerably when the load length is doubled, and becomes negligible when the length is trebled. Analyses were performed with plating of lesser  $b/t$  values, both transversely- and longitudinally-framed, and were found to produce similar results.

## 4.4 Plating Response Equations

### 4.4.1 General

The development of a design equation for plating subjected to line-like loads first requires a determination of the average correction factors,  $f_D$ , for each individual load case. As shown in Figure 4.31, the correction factors are the ratios of the uniform load,

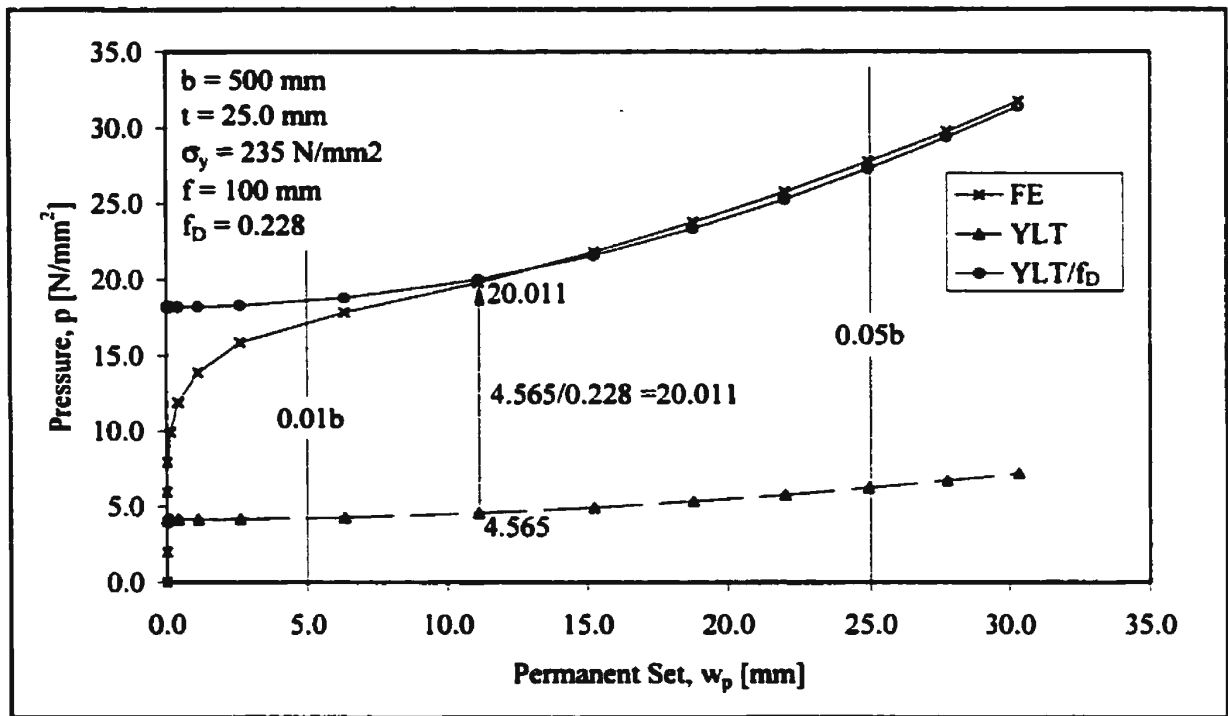


Figure 4.31 Sample Determination of  $f_D$

according to yield line theory, to loads of finite height, as determined by finite element analysis, necessary to achieve a given level of permanent set. The average of these ratios for levels of permanent set between 1% and 5% of frame spacing is taken as the correction value for the load case in question. The lower bound of 1% is considered sufficient to avoid in large part the influence of elasticity present in the finite element

results (but neglected in yield line theory), while the upper bound of 5% should be sufficient for any reasonable design criteria as well as most damage analyses. To measure the spread of individual correction factors within a load case, the coefficient of variation (ratio of the standard deviation to the mean) was obtained for all 280 load cases of finite load height and infinite load length. The maximum, minimum and average values of these coefficients are presented in Table 4.2. Within this table, *Plate* equations refer to yield line Equations (2.14) and (2.15) when the plate aspect ratio is treated normally ( $\alpha = \alpha$ ),

Framing Type	Transverse			Longitudinal	
Equation	Plate	Modified Plate	Beam	Plate	Beam
Max	7.29%	6.40%	11.98%	7.37%	11.83%
Min	0.22%	1.10%	0.01%	0.84%	0.01%
Mean	3.49%	2.80%	7.54%	3.66%	5.56%

Table 4.2 Maximum, Minimum and Average Coefficients of Variation For Individual Load Cases

and *Beam* equations when the plate aspect ratio is set to infinity ( $\alpha = \infty$ ). Because the aspect ratio of transversely-framed plating has a negligible effect beyond a value of two (see §4.3.1), a *Modified Plate* equation was also used in which this value of plate aspect ratio was fixed in the yield line equations. As indicated by the coefficients of variation, yield line theory better captures the trend of the finite element results when a finite plate aspect ratio is used. Although not shown in Table 4.2, the variation of results with the *Beam* equation noticeably increased with plate slenderness.

Having established the correction factors for each of the individual load cases, the next step was to assess the agreement of these correction factors within each grouping of the load height to frame spacing ratios. The mean values of the coefficients of variation for the groupings of  $f/b$  ratios are shown in Table 4.3. Upon examination of the individual

load height to frame spacing ratios, it was discovered that the variation coefficients for plate aspect ratios of unity were significantly higher than for all other plate aspect ratios. Accordingly, the error assessment was redone omitting the plate aspect ratio  $\alpha = 1$ , with the resulting coefficients shown for comparison in Table 4.3. The significant reduction in variation coefficients combined with the rarity of square plate panels was sufficient to warrant the omission of such plating in subsequent curve fitting.

Framing Equations	Transverse			Longitudinal	
	Plate	Modified Plate	Beam	Plate	Beam
$\alpha = 1$ to 5	22.8%	14.5%	6.6%	2.9%	20.6%
$\alpha = 2$ to 5	10.0%	1.8%	3.7%	2.9%	7.2%

*Table 4.3 Average Coefficients of Variation for Load Height to Frame Spacing Ratios*

The results of Table 4.3 can be understood when the functional dependencies of the different yield line equations are compared to those of the finite element analyses. For transversely-framed plating, the *Plate* equation is influenced by the panel aspect ratio while the finite element results, for load heights less than the frame spacing, exhibit no such dependency beyond  $\alpha = 2$ . Accordingly, the *Modified Plate* equation with a constant aspect ratio of  $\alpha = 2$ , and the beam equation with  $\alpha = \infty$ , produce results which exhibit little variation in trends compared to those of the finite element results. In contrast, the finite element results for longitudinally-framed plating exhibit a dependence on plate aspect ratio up to about  $\alpha = 5$ . Accordingly, the *Plate* equation shows far less variation than the *Beam* equation, which takes no account of plate aspect ratio. A common attribute of all equations for both transversely- and longitudinally-framed plating was the relative increase in variation for  $b/t = 12$  plating compared to all other frame spacing to thickness ratios.

#### 4.4.2 Equations for Transversely-Framed Plating

Since the plate equation performs best for transversely-framed plating when the panel aspect ratio is fixed at  $\alpha = 2$ , only the *Modified Plate* equation, along with the *Beam* equation, was used in the curve fitting applications. Due to a lesser, or secondary, correlation between the  $f_D$  correction factors and frame spacing to plate thickness ratios, the dependent variable for the curve fitting applications of both the *Modified Plate* and *Beam* equations contained  $f/b$  and  $b/t$ . The curve fitting for the *Modified Plate* equation results in a second-order polynomial

$$f_D = -0.1330x^2 + 0.6701x \quad R = 0.9981 \quad (4.4)$$

$$\text{where } x = \frac{f}{b} \left( \frac{b}{t} \right)^{0.2}$$

and for the *Beam* equation

$$f_D = -0.0120x^2 + 0.1728x \quad R = 0.9971 \quad (4.5)$$

$$\text{where } x = \frac{f}{b} \left( \frac{b}{t} \right)^{0.5}$$

The correlation coefficient,  $R$ , is the square root of the coefficient of determination,  $R^2$ , defined as

$$R^2 = \frac{\sum_i^n (f_{D,i} - \bar{f}_D)^2 - \sum_i^n (f_{D,i} - f_D(x_i))^2}{\sum_i^n (f_{D,i} - \bar{f}_D)^2} \quad (4.6)$$

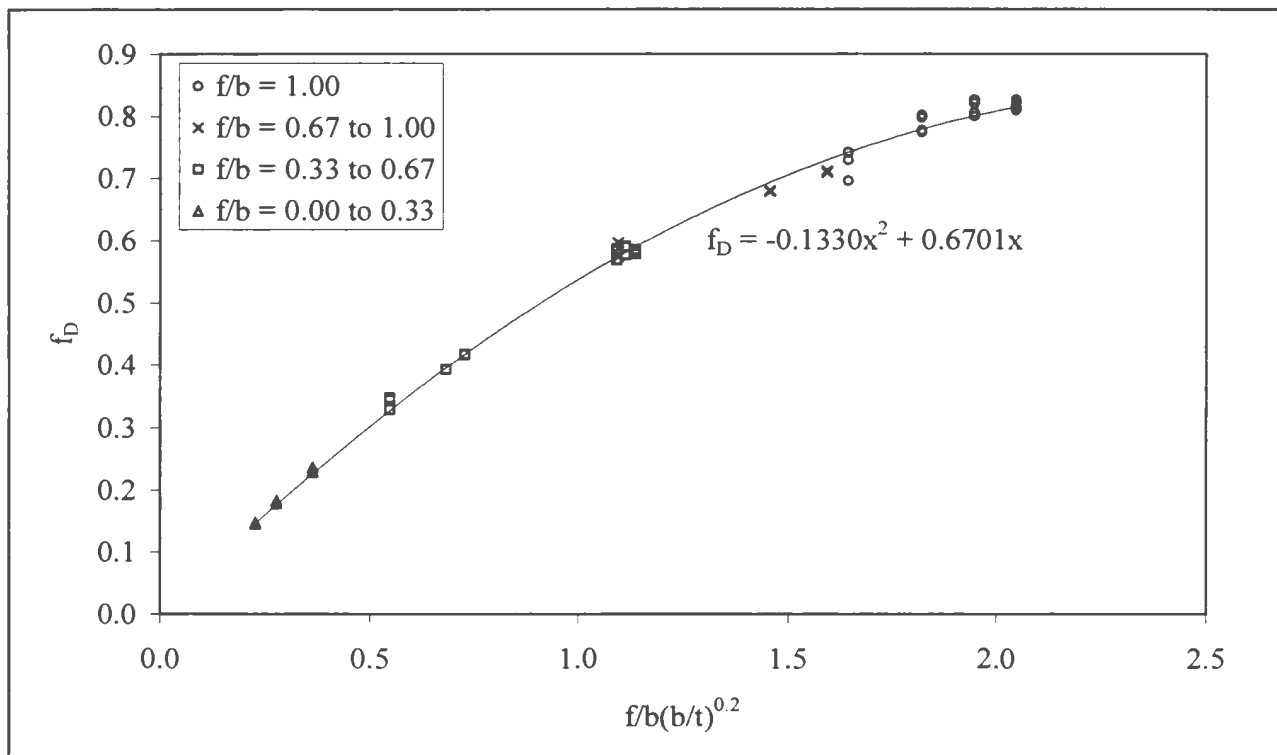


Figure 4.32 Modified Plate Equation – Transversely-Framed Plating

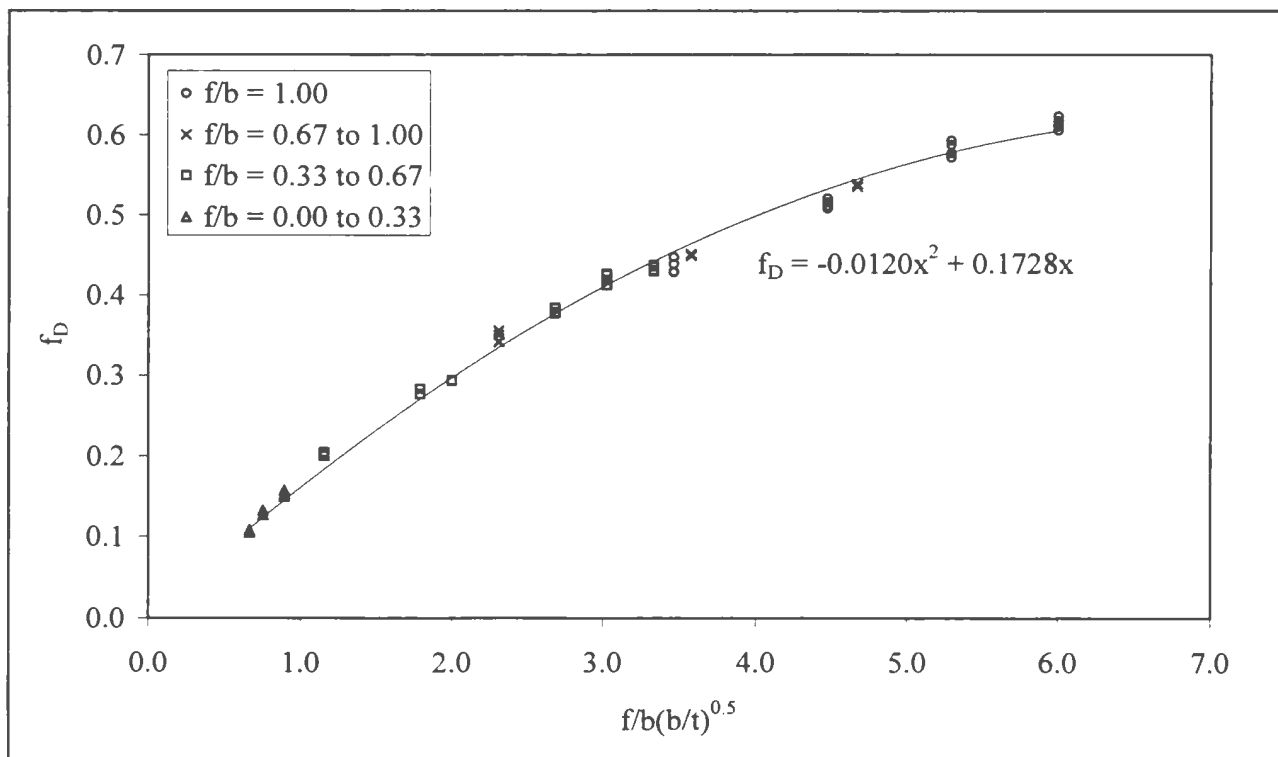


Figure 4.33 Beam Equation – Transversely-Framed Plating

where  $f_{Di}$ , including the corresponding mean value, are obtained from the finite element results, and  $f_D(x_i)$  from the equation of the fitted curve. As can be seen from Equations (4.4) and (4.5), the influence of  $b/t$  is greater for the *Beam* equation than for the *Modified Plate* equation. Plots of these equations can be seen in Figures 4.32 and 4.33. The coefficients of correlation for both equations are consistent for all values of  $\alpha$  and  $b/t$ .

#### 4.4.3 Equations for Longitudinally-Framed Plating

In a manner similar to that used for transversely-framed plating, mean values of correction factors,  $f_D$ , were plotted against the load height to frame spacing ratio,  $f/b$ . Like the transversely-framed plating, some correlation to  $b/t$  was also evident. However, the plate aspect ratio also exhibited some influence on the  $f_D$  correction factors, since the equations based on yield line theory do not fully capture the effect of plate aspect ratio for longitudinally-framed plating. This is reflected in the curve fitting application to the results based on the *Plate* equation

$$f_D = -0.6263x^2 + 1.5363x \quad R = 0.9951 \quad (4.7)$$

$$\text{where } x = \frac{f}{b} \left( \frac{b}{t} \frac{b}{a} \right)^{0.1}$$

as well as those based on the *Beam* equation

$$f_D = -0.0357x^2 + 0.3372x \quad R = 0.9897 \quad (4.8)$$

$$\text{where } x = \frac{f}{b} \left( \frac{b}{t} \frac{a}{b} \right)^{0.33}$$

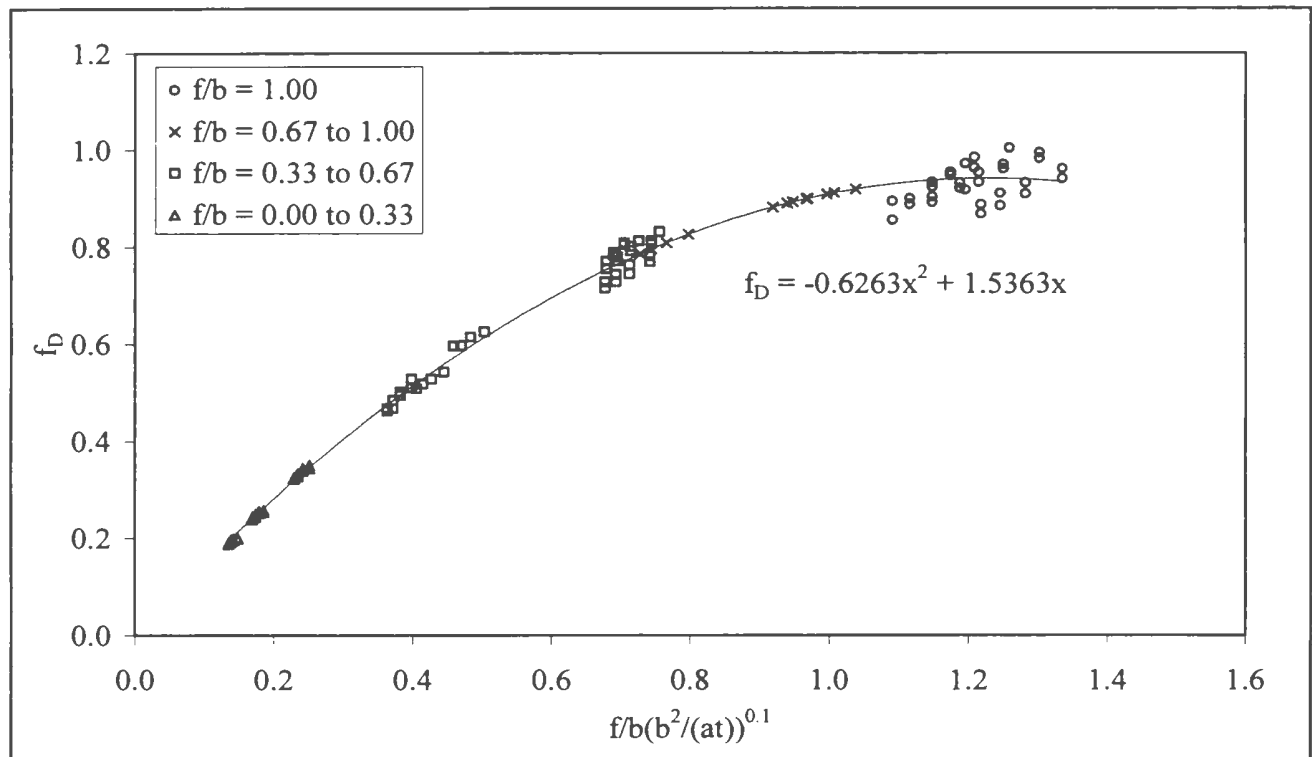


Figure 4.34 Plate Equation – Longitudinally-Framed Plating

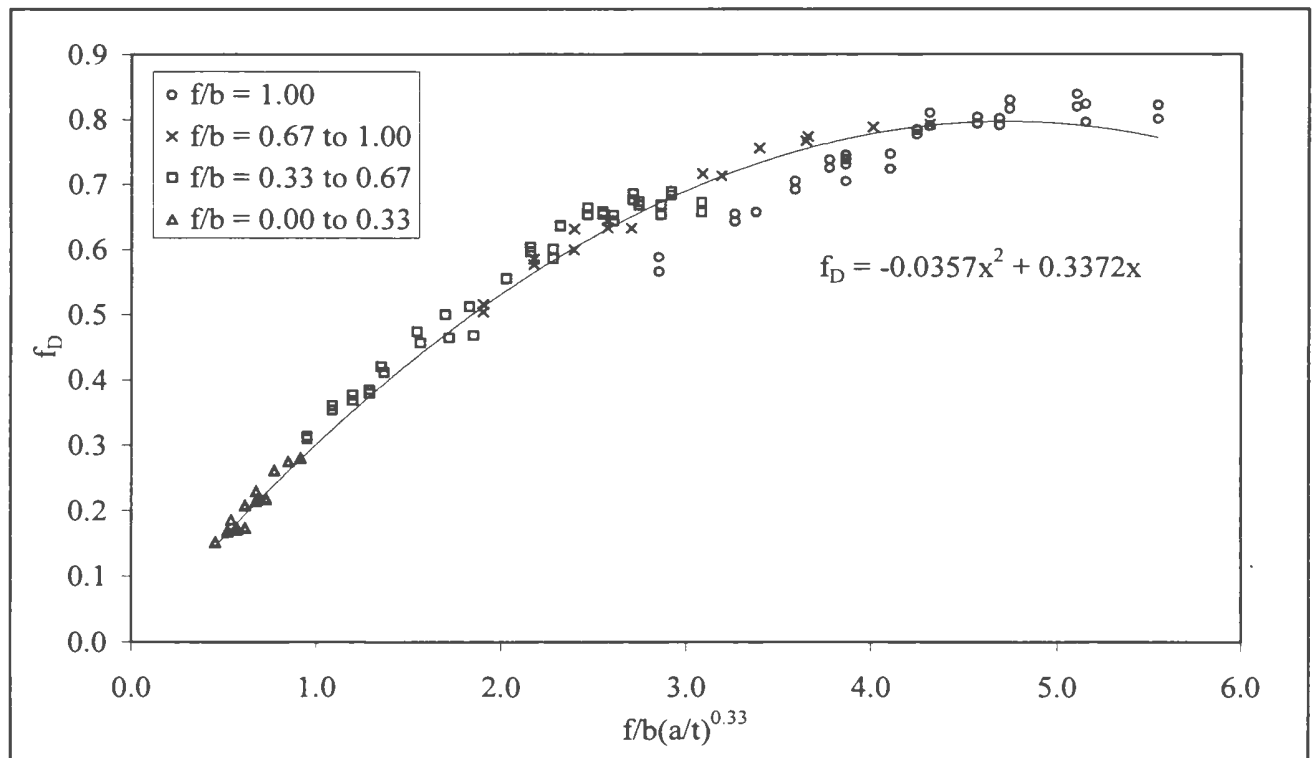


Figure 4.35 Beam Equation – Longitudinally-Framed Plating



Compared to transversely-framed plating, pressure correction factors for longitudinally-framed plating show less dependence on secondary influences beyond  $f/b$ . Plots of Equations (4.7) and (4.8), both second-order polynomials, can be seen in Figures 4.34 and 4.35. The correlation coefficients for both equations are reasonably consistent for all values of  $\alpha$  and  $b/t$ , with slight deterioration for the lower values of each. As can be seen in Figures 4.34 and 4.35, there is also some degradation in agreement for load height to frame spacing ratios of unity.

#### 4.4.4 Response Equations and Comparison with Finite Element Results

The obvious advantage of the *Beam* equation over the *Plate* or *Modified Plate* equations is its simplicity of solution. With a plate aspect ratio of  $\alpha = \infty$ , Equations (2.14) and (2.15) reduce to

$$\frac{P}{P_c} = 1 + \frac{w_p^2}{t^2}, \quad \frac{w_p}{t} \leq 1 \quad (4.9)$$

$$\frac{P}{P_c} = \frac{2w_p}{t}, \quad \frac{w_p}{t} > 1 \quad (4.10)$$

and Equation (2.8) to

$$P_c = \frac{16M_p}{b^2}, \quad \frac{a}{b} < 1 \quad (4.11)$$

Such equations would allow calculations to be made quickly by hand. However, the drawback of such an approach is a loss of accuracy. Despite the high degree of correlation between Equations (4.5) and (4.8) with the average values of correction factors,  $f_D$ , the variations within these average values carry through to the equations, and manifest

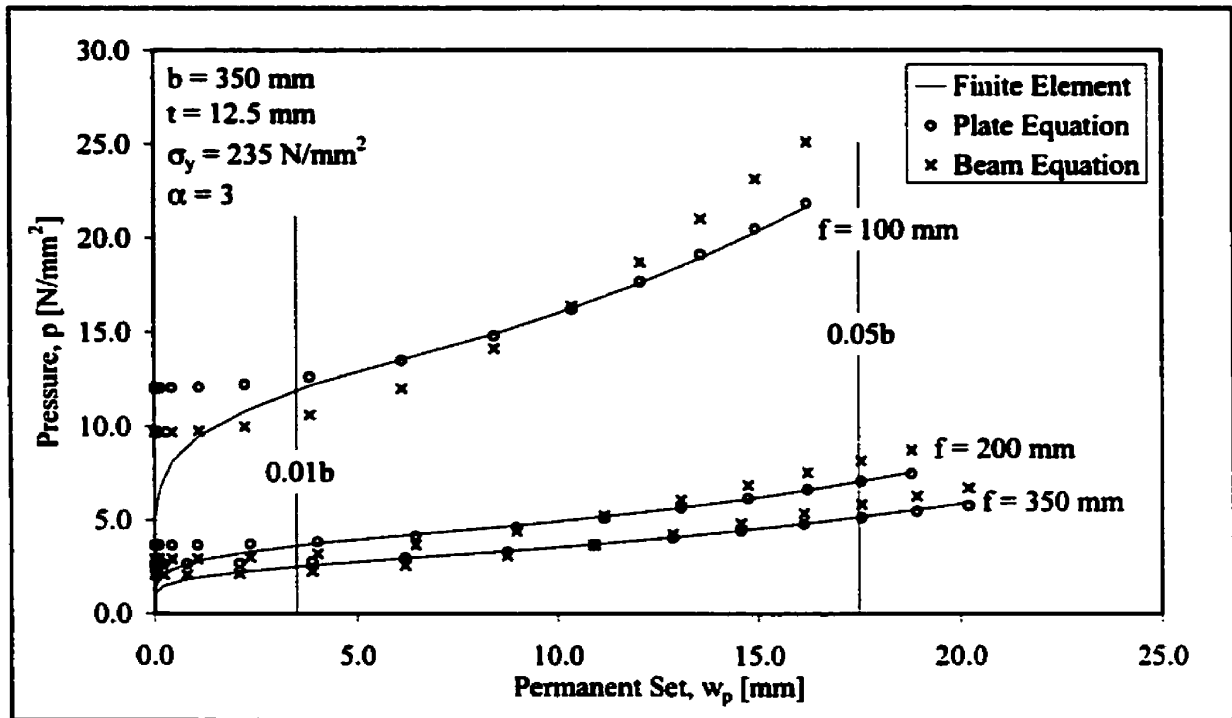


Figure 4.36 Comparison of Equations Against Finite Element Results – Transversely-Framed Plating

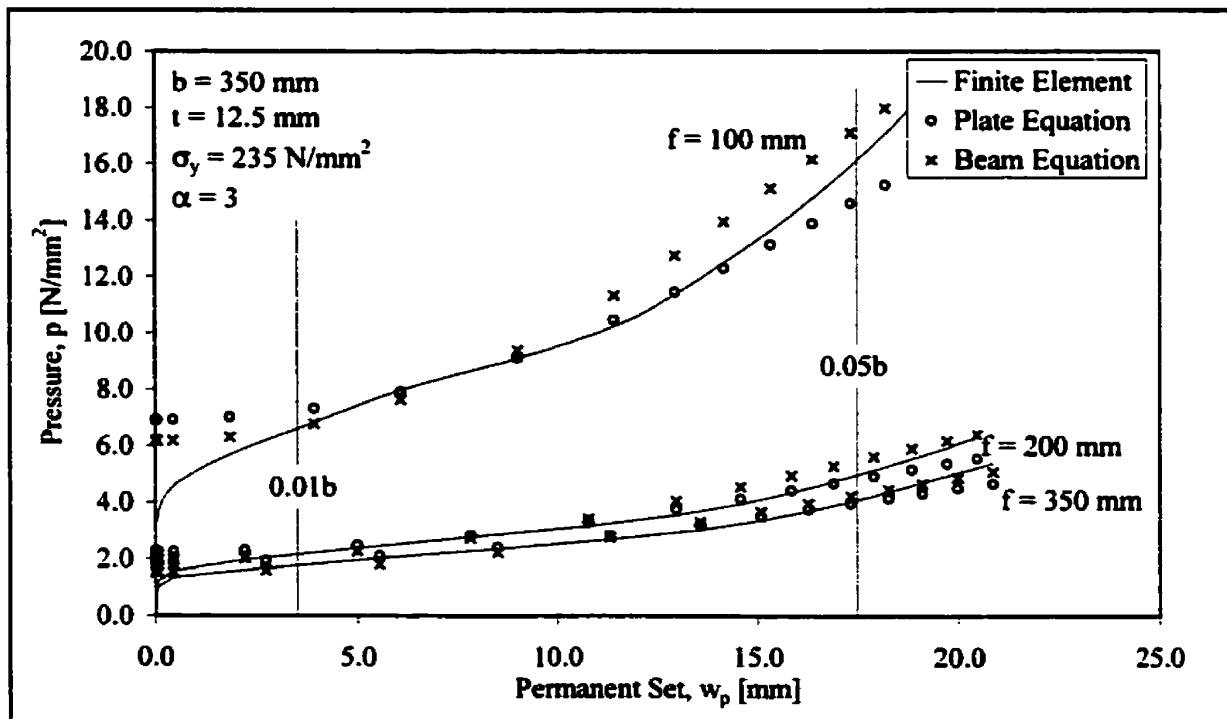


Figure 4.37 Comparison of Equations Against Finite Element Results – Longitudinally-Framed Plating

themselves when compared to the finite element results. As shown in Figures 4.36 and 4.37, the beam equations generally underestimate the loads causing residual deflections approaching 1% of frame spacing, and overestimate loads resulting in deflections approaching 5%. Accordingly, the *Beam* equation should only be used to obtain quick estimates of plating response, and the *Plate* and *Modified Plate* equations for purposes of design and damage analyses, as summarised in Table 4.4. In the applications that follow,

Purpose	Quick Estimate		Design / Damage Analyses	
Quantity	$f_D$	$p_{uniform}$	$f_D$	$p_{uniform}$
Transverse Framing	Eqn. 4.5	Eqns. 4.9 / 4.10	Eqn. 4.4	Eqns. 2.14 / 2.15 ( $\alpha = 2$ )
Longitudinal Framing	Eqn. 4.8	Eqns. 4.9 / 4.10	Eqn. 4.7	Eqns. 2.14 / 2.15

Table 4.4 Equations for  $f_D$  and  $p_{uniform}$

only the *Plate* and *Modified Plate* equations are used for longitudinally- and transversely-framed plating, respectively.

#### 4.4.5 Sensitivity Analyses

The response equations generated in the previous section can now be used to study the relationships between various parameters. Those of primary interest are the relationships between permanent set ( $w_p$ ), load height ( $f$ ), plate thickness ( $t$ ) and frame spacing ( $b$ ). Neglecting in the first instance the influence of changes in the latter two, the relationship between permanent set and load height can be seen in Figure 4.38. Results for both transversely- and longitudinally-framed plating are shown for a typical structural configuration and a line load of  $q = 1500$  kN/m. The results are typical of other configurations and show that permanent set for longitudinally-framed plating is on average twice that for transversely-framed plating. The increase in permanent set for

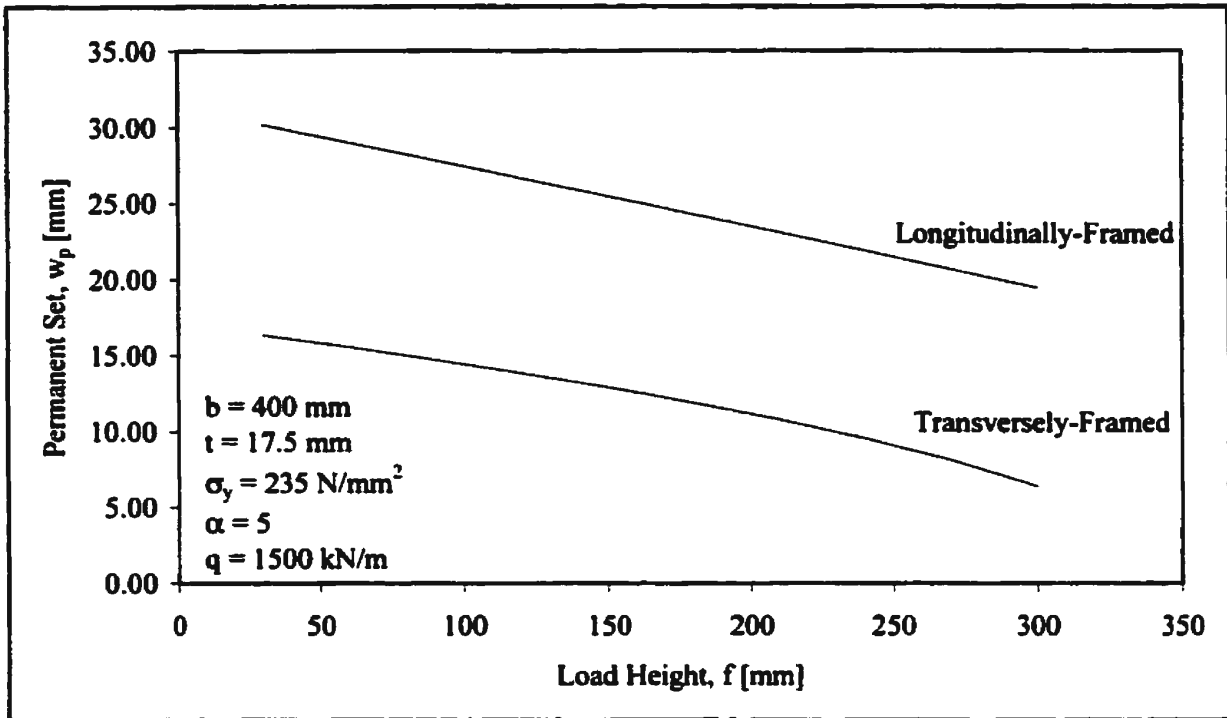


Figure 4.38 Sensitivity of Permanent Set to Load Height

longitudinally-framed plating when the load height is reduced from 300 mm to 30 mm is about 55%. The corresponding increase for transversely-framed plating is about 157%. Accordingly, if the design load height for transversely-framed plating were 300 mm, then an additional 10 mm of permanent set would occur if the vessel encountered a line load of the same intensity, but with a vertical extent of only 30 mm.

The relationships between load height and plate thickness for a given level of permanent set are shown for both transversely- and longitudinally-framed plating in Figures 4.39 and 4.40, respectively. As with permanent set and load height, the relationship between plate thickness and load height is very nearly linear, although the increases in plate thickness are not as substantial when the load height is reduced. For instance, with a reduction in load height from 300 mm to 30 mm ( $w_p = 6.0 \text{ mm}$ ), the required plate thickness for transversely-framed plating is increased between 9% and 23%

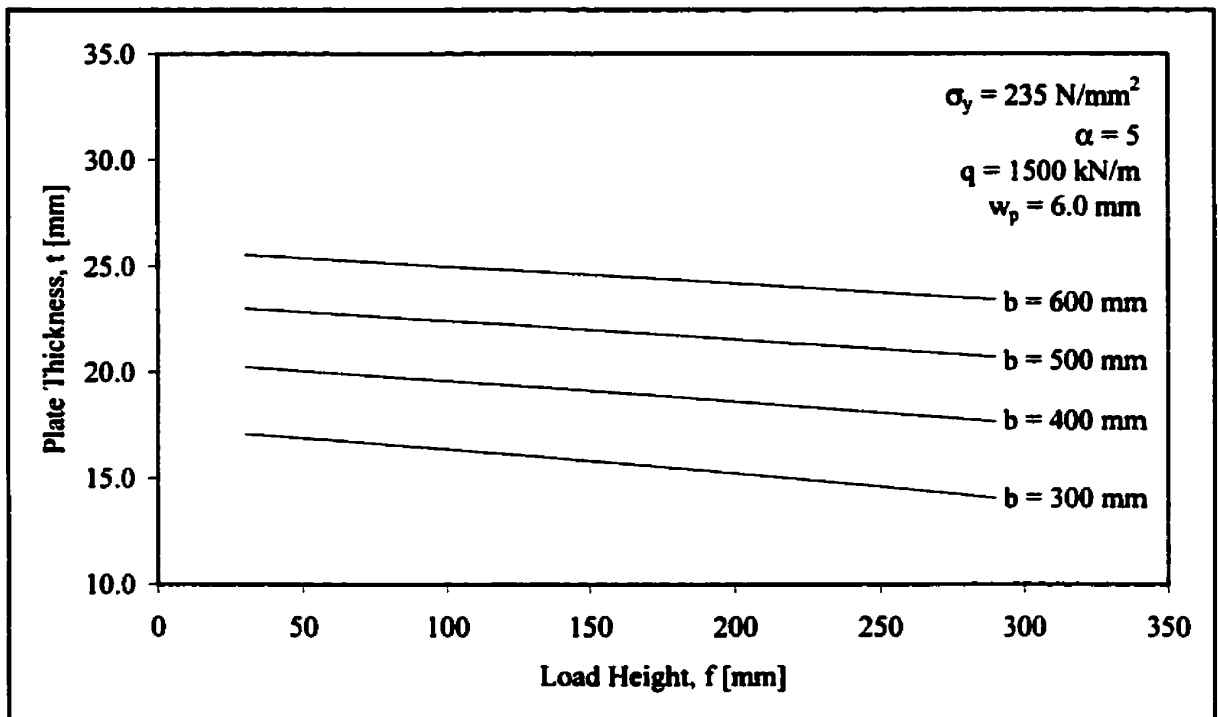


Figure 4.39 Sensitivity of Plate Thickness to Load Height – Transversely-Framed Plating

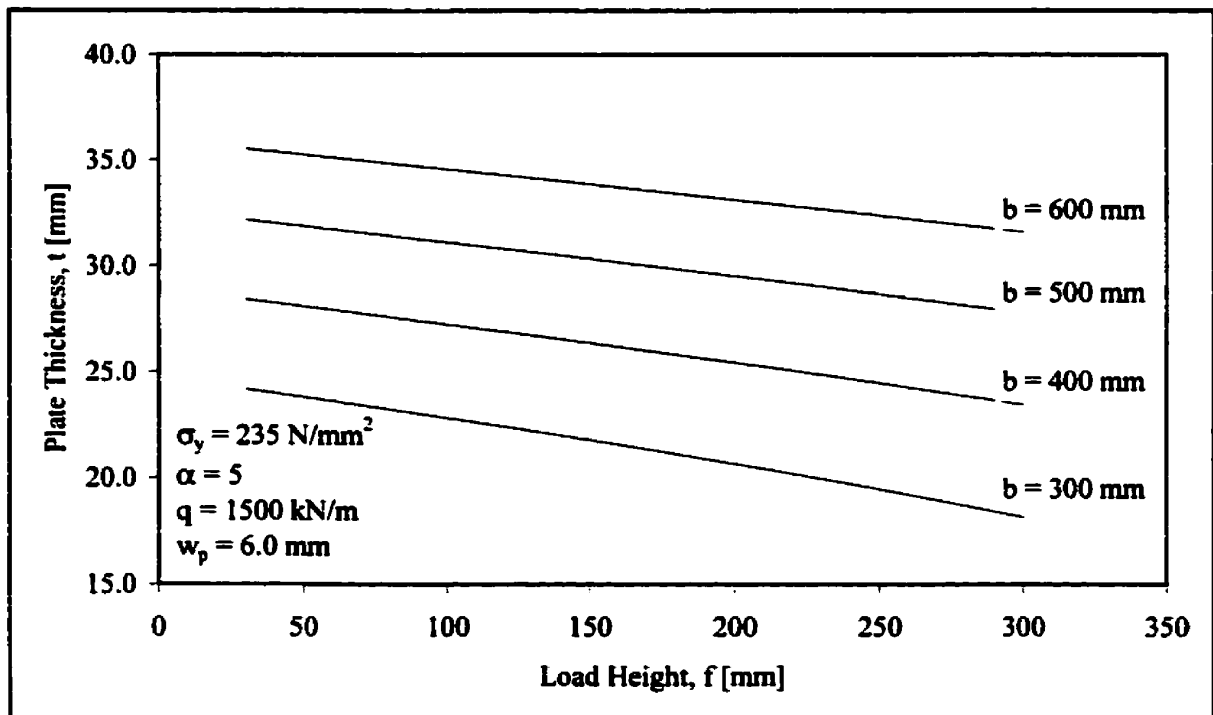


Figure 4.40 Sensitivity of Plate Thickness to Load Height – Longitudinally-Framed Plating

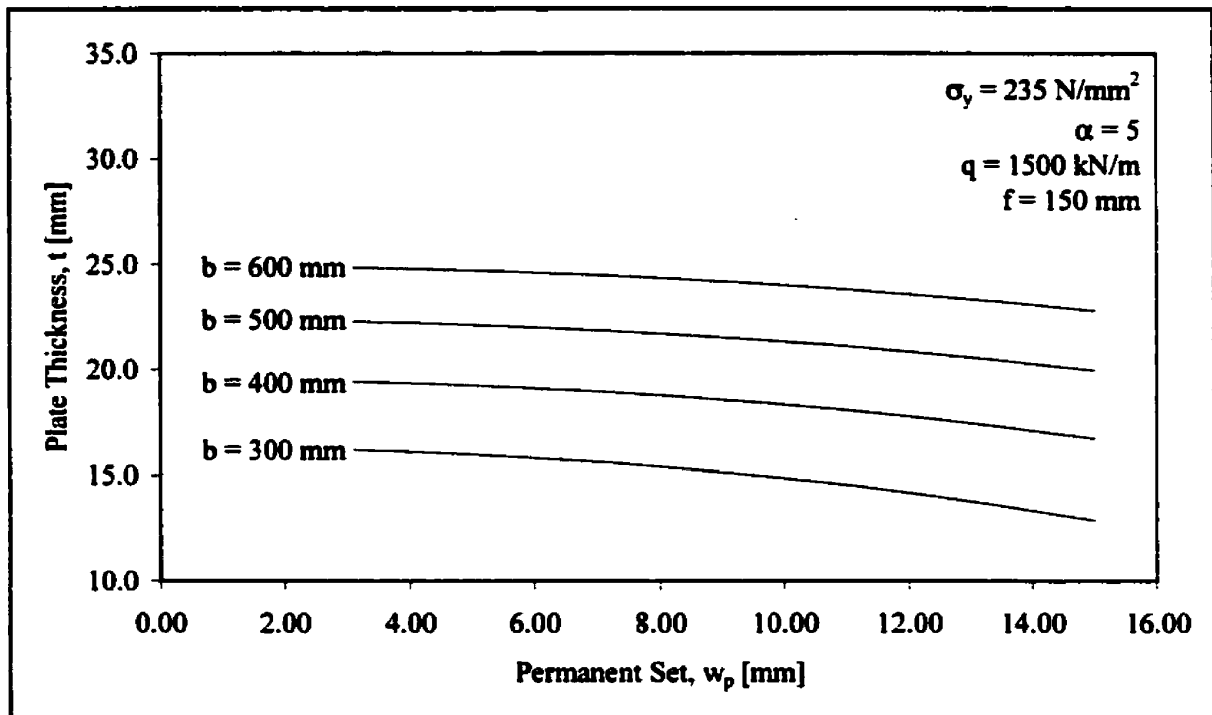


Figure 4.41 Sensitivity of Plate Thickness to Permanent Set – Transversely-Framed Plating

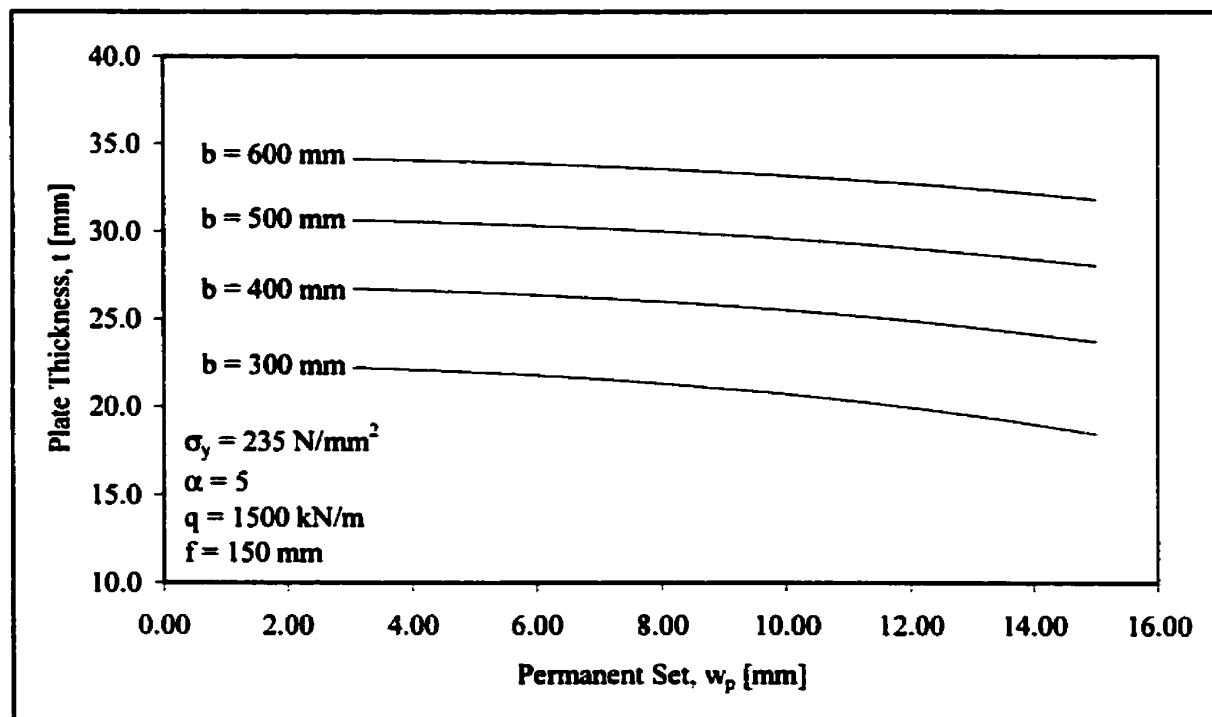


Figure 4.42 Sensitivity of Plate Thickness to Permanent Set – Longitudinally-Framed Plating

(depending on frame spacing), and for longitudinally-framed plating between 13% and 33%. Continuing with the design case for transversely-framed plating ( $b = 400$  mm,  $t = 17.5$  mm), it can be seen from Figure 4.39 that a plating thickness of about 20 mm is required to maintain levels of permanent set at 6 mm, if the encountered line load height is reduced from 300 mm to 30 mm.

Finally, the thickness of transversely- and longitudinally-framed plating, subjected to a given line load, is shown in Figures 4.41 and 4.42 as a function of permanent set. The relationships are again mostly linear, with only a modest amount of non-linearity. In the case of transversely-framed plating, increases in plate thickness for an allowable permanent set reduction from 15 mm to 3 mm are similar, about 9% to 26%, to those for a load height reduction from 300 mm to 30 mm. For longitudinally-framed plating, thickness increases are marginally less for the same reduction in allowable permanent set, ranging from 7% to 20%.

## 4.5 Application of Plating Response Equations

### 4.5.1 Plating Design Example

To illustrate the procedure for determining the required plate thickness for a given structural configuration, design load and criteria, the equations developed in the preceding section will now be used in a sample design application. The assumed structural and load parameters, as well as the design criteria, are given in Table 4.5. Beginning with a trial thickness of 15.0 mm, Equation (4.4) is used to determine a pressure correction factor of  $f_D = 0.522$ . With a lateral plate pressure  $p = 6.0$  N/mm<sup>2</sup> over the finite height of the ice load, the equivalent uniform pressure that results in the same

level of permanent set is equal to  $6.0 \text{ N/mm}^2 \times 0.522 = 3.13 \text{ N/mm}^2$ . Using Equation (2.14), with  $\alpha_{\max} = 2$ , it can be determined that the plate thickness required to

Structural Parameters	Framing Type	Transverse
	Frame Spacing, $b$	400 mm
	Frame Span, $a$	1200 mm
	Material Yield Strength, $\sigma_y$	235 N/mm <sup>2</sup>
Load Parameters	Ice Load Height, $f$	200 mm
	Lateral Plate Pressure, $p$	6.0 N/mm <sup>2</sup>
Design Criteria	Permissible Permanent Set, $w_p$	1% of Frame Spacing

*Table 4.5 Assumptions for Sample Design Application*

obtain a permanent set of 4.0 mm (1% of  $b$ ) is 17.1 mm. Since this thickness is greater than the trial plate thickness of 15.0 mm, a greater trial thickness needs to be taken. Accordingly, for a trial thickness of 20.0 mm, the corresponding pressure correction factor and equivalent uniform load is 0.500 and 3.00 N/mm<sup>2</sup>, respectively. For this level of uniform pressure, the plate thickness required to obtain a permanent set of 4.0 mm is 16.8 mm. Since this thickness is less than the trial thickness, the desired plate thickness must be somewhere between 15.0 mm and 20.0 mm. Continuing in this way, the optimum thickness of 17.0 mm is ultimately obtained. When performed using a computer application, this determination requires only a fraction of a second in calculation time. Of course, corrosion and wear additions have to be added to obtain the as-built plate thickness.

#### 4.5.2 Analysis of Plating Damages to Baltic Class Vessels

As mentioned earlier, response equations such as those developed in §4.4.2 and §4.4.3 are very useful in the analysis of plating damages. Combined with assumptions about the ice load height, the equations can be used to “back-out” the pressures required



to cause measured levels of permanent set. The most comprehensive assemblage of damage statistics to date is that contained in a study commissioned by the Winter Navigation Research Board in support of the FSICR; *Damage Statistics of Ice-Strengthened Ships in the Baltic Sea, 1984 – 1987* (Kujala, 1991). The report describes and analyses the ice damages of ships navigating in the Baltic during the winters of 1984 to 1987. Although the winter of 1984 was slightly below average in terms of maximum ice extent in the Bothnian Bay and Sea ( $\sim 190 \text{ km}^2$ ), the winters of 1985 to 1987 were relatively harsh ( $\sim 335 \text{ km}^2$  to  $\sim 415 \text{ km}^2$ ). A summary of ice conditions for the various Baltic sea areas is included in the report and reproduced in Table 4.6.

Year	Sea Area	Maximum Sea Ice Thickness [cm]	Maximum Fast Ice Thickness [cm]	Duration of Ice Cover (Days)
1984	Baltic Proper	20	60	30
	Gulf of Finland	50	50	97
	Bothnian Sea	40	55	102
	Bothnian Bay	70	80	150
1985	Baltic Proper	40	50	107
	Gulf of Finland	50	90	136
	Bothnian Sea	60	75	136
	Bothnian Bay	70	110	143
1986	Baltic Proper	30	50	70
	Gulf of Finland	40	60	121
	Bothnian Sea	60	55	130
	Bothnian Bay	60	70	145
1987	Baltic Proper	40	70	100
	Gulf of Finland	50	70	127
	Bothnian Sea	60	90	140
	Bothnian Bay	70	100	145

*Table 4.6 Summary of Ice Conditions – Winters 1984 to 1987*

Although the report examines plating, framing and web frame damages in the bow, midship and stern areas, the focus of the present study is on plating damages in the midship area. As noted in the report, most damages were within the midship area and occurred when the ships had been caught in compressive ice. Of the ships studied, almost all of which were built according to the 1971 FSICR, 19 incidents of damage to plating in the midship area were documented (similar damages to sister vessels counted as a single

incident). These damages occurred both within the icebelt and below, and are summarised in Table 4.7. The ice class and  $k$  factor for each vessel are included in the table, since these quantities are used in the FSICR to determine the design ice pressure. The factor  $k$  is a measure of the displacement and engine power of the vessel

$$k = \frac{\sqrt{\Delta P_e}}{1000} \quad (4.12)$$

where  $\Delta$  is the displacement [t] of the ship at maximum ice class draught and  $P_e$  is the continuous engine output [kW].

Ship No.	Ship Type	Ice Class	k	Framing	b [mm]	a [mm]	t [mm]	$\sigma_y$ [N/mm <sup>2</sup> ]	$w_o$	p [MPa] Present Study	p [MPa] Ranki
45	Cargo Ferry	IAS	8.32	Long	300	2800	14.5	290	30	208.1	171.1
7	Dry Cargo	IAS	6.21	Long	450	3040	20.0	290	10	85.6	70.4
22 - 25	Bulk Carrier	IA	12.81	Long	400	3300	16.5	290	30	173.1	145.4
13	Tanker	IAS	6.70	Long	350	2800	10.0	290	20	76.8	67.2
48 - 50	Tanker	IAS	15.92	Trans	343	2100	17.0	290	30	335.8	355.0
4	Dry Cargo	IAS	12.30	Trans	400	3000	19.0	290	10	172.6	163.2
13	Tanker	IAS	6.70	Trans	350	3200	16.0	290	10	145.9	141.4
35	Bulk Carrier	IA	4.27	Trans	350	2500	15.5	290	15	167.2	161.1
51	Tanker	IAS	5.94	Trans	350	2100	15.5	290	15	167.2	161.1
7	Dry cargo	IAS	6.21	Trans	380	3000	16.5	290	10	140.0	136.6
14	Bulk Carrier	IA	8.08	Trans	350	2375	14.0	290	15	143.2	143.2
21	Cargo Ferry	IAS	16.12	Trans	400	2200	13.5	290	10	91.1	94.1
16	Dry Cargo	IA	5.18	Trans	350	3500	10.0	290	25	140.3	170.4
43 - 44	Passenger Ferry	IA	13.00	Trans	400	1750	9.5	350	25	135.1	170.4
14	Bulk Carrier	IA	8.08	Trans	700	2375	13.0	290	25	85.0	109.3
48 - 50	Tanker	IAS	15.92	Trans	700	2100	12.5	290	50	155.8	210.1
21	Cargo Ferry	IAS	16.12	Trans	800	2200	13.5	290	15	50.1	59.5
43 - 44	Passenger Ferry	IA	13.00	Trans	800	1750	9.5	350	30	69.6	101.0
45	Cargo Ferry	IAS	8.32	Long	300	2800	10.5	290	24	116.6	99.1
<i>Italicised – Plating below Icebelt</i>											

Table 4.7 Details of Reported Baltic Damages and Estimates of Pressure

In his analysis of the damages, Kujala used Ranki's Equations (2.20) and (2.21) to determine the ice-induced pressure for an assumed load height of 10 mm. The apparent load length was set equal to the frame spacing for transversely-framed plating and the frame span for plating framed longitudinally. The resulting pressures are shown in Table 4.7, although the results shown for the longitudinally-framed plating are not the same as

those in the report. As mentioned earlier, Ranki's Equations (2.20) and (2.21) are only applicable to transversely-framed plating. Accordingly, the values shown in Table 4.7 are based on unpublished equations developed by Ranki (2000) for longitudinally-framed plating

$$p = 2\sigma_y \frac{t^2}{fb \left(1 - \frac{f}{2b}\right)} \left(1.3 \frac{w_p}{t} + 0.7\right) \text{ when } \frac{w_p}{t} \leq 1 \quad (4.13)$$

$$p = 4\sigma_y \frac{tw_p}{fb \left(1 - \frac{f}{2b}\right)} \text{ when } \frac{w_p}{t} \geq 1 \quad (4.14)$$

For comparison, resulting pressures similarly obtained with Equations (4.4) and (4.7) of the present study are included in Table 4.7. As can be seen, the agreement for the transversely-framed plating within the icebelt is very good with an average difference of about 3.4%. The agreement for the longitudinally-framed plating is not as good with an average difference of 16%, but is within measurement tolerances. The average difference for the more slender plating outside the icebelt is about 24.1%. In all calculations, the actual yield stress of mild steel was assumed to be 290 N/mm<sup>2</sup>, based on statistical characteristics of measured yield stresses for plating with a nominal strength of 235 N/mm<sup>2</sup> (Kujala, 1990). A yield strength of 350 N/mm<sup>2</sup> was assumed for the NVA-32 plating of ships 43 and 44. Of course, there is always some uncertainty associated with the yield strength of the plating, as well as with the assumption that there has been no diminution of the as-built plate thicknesses.

#### **4.5.3 Analysis of Load Heights and Line Load Intensity**

Regarding the foregoing analysis, the assumed load height of 10 mm was based on contemporary research results which indicated that the contact between ship and ice was line-like (Riska et al., 1990). Full-scale results were obtained visually through a transparent lexan window cut in the ice belt of the icebreaker Sampo, as well as with a PVDF-plate mounted nearby. During measurements conducted in the northern Baltic in February 1989, the maximum pressure recorded in 60 cm thick ice was about 54 MPa. Simultaneous observations and measurements indicated that there were two types of contact; direct line-like contact of high pressure and an adjacent low-pressure region of crushed ice. However, as can be seen from Table 4.7, the pressures associated with a 10 mm load height would need to be very high to cause the observed damages (in fact, pressure melting would occur at such levels). Such pressures have never been measured, suggesting that the height of the high pressure contact must have been greater, or that the pressures in the low-pressure region were comparably higher. To investigate this matter further, Figure 4.43 shows the pressures backed-out of the reported damages using Equations (4.4) and (4.7), assuming load heights of 25 mm, 50 mm, 100 mm, as well as a load height equal to the frame spacing. Also shown in the figure are the 90th percentiles of these values obtained for each of the four load heights. Accordingly, if 54 MPa is considered to be an extreme pressure (although higher values, especially in ice thicker than 60 cm, are possible), then the minimum load height to cause the observed damages would need to be about 40 mm. Of course, such a result ignores the randomness of the local contact and is based on an average pressure over the assumed height and length of the contact area.

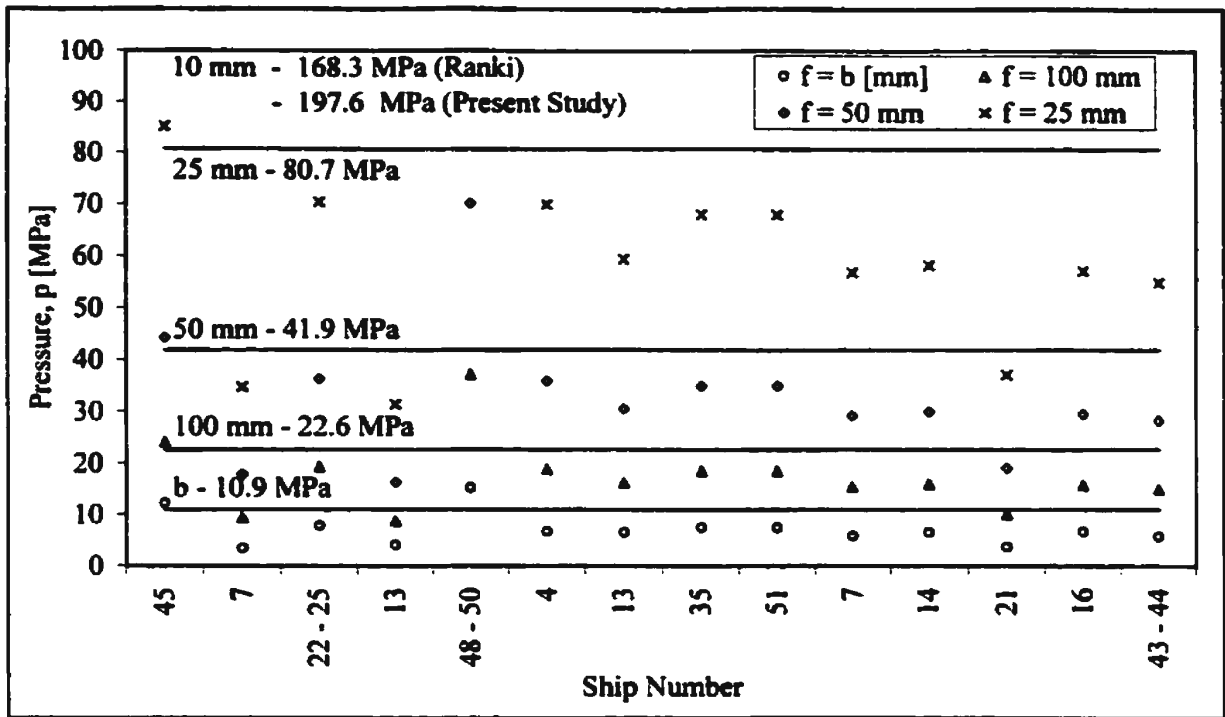


Figure 4.43 Ice Pressure Analysis of Reported Damages

In the report of the Winter Navigation Research Board, the data in Table 4.7 was presented in a plot of line load intensity,  $q$ , against the apparent load length,  $e$ , in which the former is simply the pressure multiplied by the load height. This plot is reproduced in Figure 4.44 along with the curve that was fitted to the data points

$$q = 814e^{-0.71} \quad (4.15)$$

Such a plot suggests that line load intensity is a function of load length. However, as can be seen, these results are based essentially on two distinct groups of data points;  $e < 400$  mm (transversely-framed plating) and  $e > 2800$  mm (longitudinally-framed plating). Since the results for the second group were obtained with equations intended only for transversely-framed plating, the relatively low level of line-load intensities can be attributed to the absence at the time of a readily available response equation for

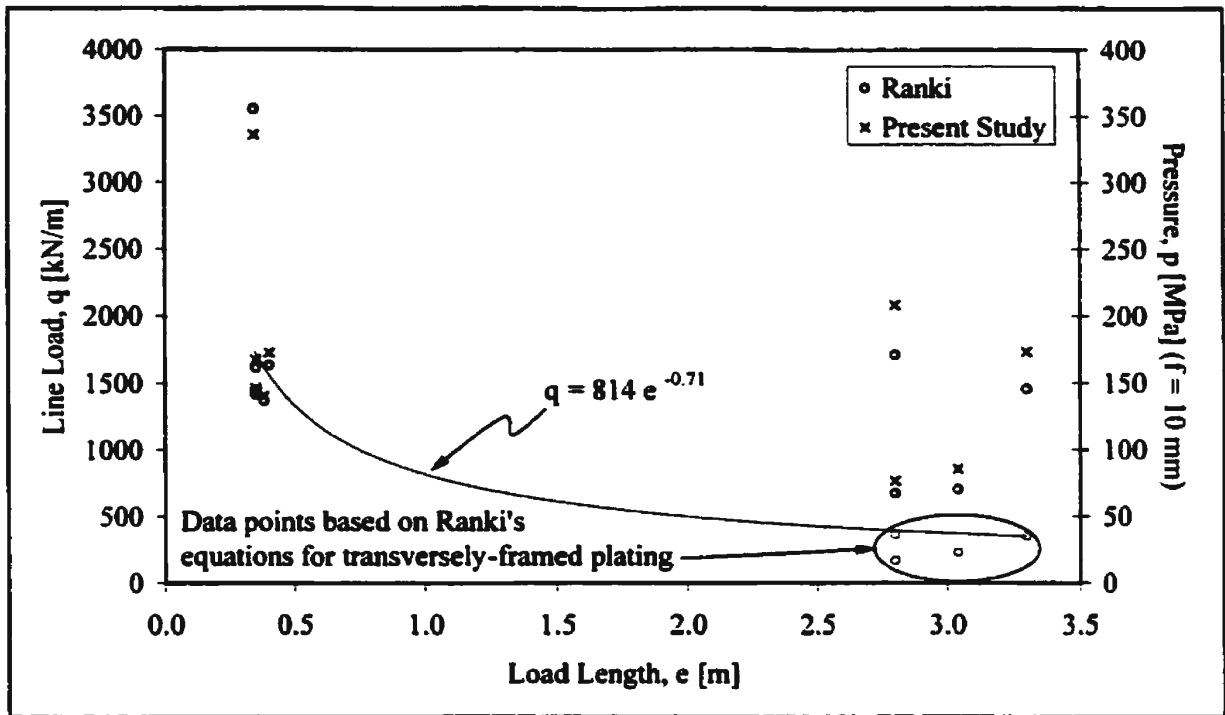


Figure 4.44 Line Load Analysis

longitudinally-framed plating. Higher levels of line load intensity are obtained on the basis of Equations (4.4) and (4.7) of the present study, as well as Ranki's Equations (4.13) and (4.14), as shown in Figure 4.44. As can be seen, there is no readily apparent relationship between line load intensity and load length.

#### 4.5.4 Plastic Design Criteria for Baltic Class Vessels

Although plastic design criteria can be based on a number of responses, the design of ship shell plating is almost always based on allowable permanent set. The measure of permanent set is sometimes given in absolute terms or as a ratio of plate thickness, but is best expressed as a function of frame spacing. When determining an acceptable level of permanent set, the issue of safety needs always to be resolved before matters of

serviceability are addressed. This means that any design criteria based on serviceability limits should ensure an adequate margin against ultimate failure of the plating when subjected to local loads, and that the eccentricity of plating has been considered in terms of the compressive in-plane stresses arising from hull girder bending.

Assuming that safety issues have been addressed, one of the serviceability considerations when defining an acceptable level of deformation is the increased resistance of shell plating. Most vessels with an ice class spend more time navigating in open water than in ice. Accordingly, owners normally wish to avoid excessive “hungry-horse” effects, not simply on aesthetic grounds, but to reduce voyage times and fuel costs. A further consideration, mentioned earlier in §4.2.3, is the preservation of both interior and exterior coatings by limiting deformation of the base material. It has been observed, for instance, that the breakdown mechanism of INERTA 160 begins with excessive deformation of the shell plating. The high degree of curvature at the frames then leads to cracks in the coating which eventually results in its loss (Mäkinen, 1994).

Unfortunately, it is very difficult to establish acceptable design criteria based on such serviceability issues, although “rule of thumb” values for permanent set have been established between 0.5% and 2.0% of frame spacing. However, for the purposes of the present study, the allowable level of permanent set will be based on fabrication tolerances. Since the plating of newly constructed and repaired ships always has some degree of unfairness, a function of welding distortions and general workmanship, a sensible design criteria would permit deflections just slightly beyond those allowed by fabrication tolerances. The *Shipbuilding and Repair Quality Standard* of the International Association of Classification Societies (IACS, 1996) prescribes 4 mm as the standard for

the fairness of shell plating between frames (midship region), with a limit of 8 mm for a small percentage of plate fields. Based on the damaged ships studied in the report of the Winter Navigation Research Board, the average spacing of frames is about 400 mm. Accordingly, in the analyses which follows, allowable permanent set is taken to be 1% of frame spacing based on the standard fairness of 4 mm ( $4 \text{ mm} / 400 \text{ mm} = 1.0\%$ ), although permanent set equal to 2.0% of frame spacing based on the fairness limit of 8 mm will be shown for comparison ( $8 \text{ mm} / 400 \text{ mm} = 2.0\%$ ). Similar fairness values are obtained using the production standards of the German Shipbuilding Industry (Verband für Schiffbau und Meerestechnik), which defines fairness as a maximum deviation from straight line of 4 mm in 95% of the shell plating, and a maximum of 7 mm in the remaining 5%.

#### 4.5.5 Ice Loads for Design of Baltic Class Vessels

As noted in the report of the Winter Navigation Research Board, there is no clear relationship for the studied vessels between ice class and the number of voyages in various sea areas. This is reflected in Table 4.7 by the lack of correlation between ice class and calculated levels of encountered ice pressure. However, since all 1A class ships with more than 3 voyages to Bothnian Bay during the winter of 1985 experienced damages, the report considers navigation frequency of ships to the Northern Baltic to be an important parameter. Accordingly, ice loads for 1AS Baltic class vessels need to be distinguished from those for ice class 1A.

In terms of the extent of such loads, an assumption of the present study is that the load length is at least equal to the frame spacing or span, respectively, for transversely-



and longitudinally-framed plating. As shown in §4.3.5, the load length for longitudinally-framed plating has little effect once it exceeds twice the frame spacing, and a negligible effect when it exceeds the spacing of transversely-framed plating. In terms of load height, plating displacement patterns vary little with the vertical extent of the ice load such that the assumed height is not critical so long as the design ice pressure is adjusted accordingly. Therefore, the primary task is to determine the magnitude of 1A and 1AS line loads or, for an assumed load height, the design ice pressures. Since it is not economically feasible to design against all of the extreme ice loads calculated in Table 4.6, a compromise between construction and repair costs must be found.

Fortunately, although the FSICR are based on elastic theory with adjusted levels of design ice loads, the in-service experience has been very good. Even though the height and magnitude of design ice loads were revised in 1985, the basic level of ice-strengthening according to the 1971 rules was considered to be satisfactory, notwithstanding the increased scantling requirements for longitudinally-framed structures. Currently, although some changes are intended for strength levels in the stern quarter of Baltic class vessels, impending modifications do not include any changes to structures in the midship area. This implies that both owners and administrations continue to be satisfied with the present level of strengthening in the midbody. Accordingly, for a specified plastic design criterion, design ice loads can be determined such that the resulting plate thicknesses correspond to those prescribed by the FSICR.

On the basis of this, Figure 4.45 shows the required midbody plate thicknesses based on the 1985 FSICR for transversely-framed plating, excluding corrosion additions ( $\sigma_y = 235 \text{ N/mm}^2$ ,  $a = 3.0 \text{ m}$ ). Two curves each are shown for 1A and 1AS class vessels.

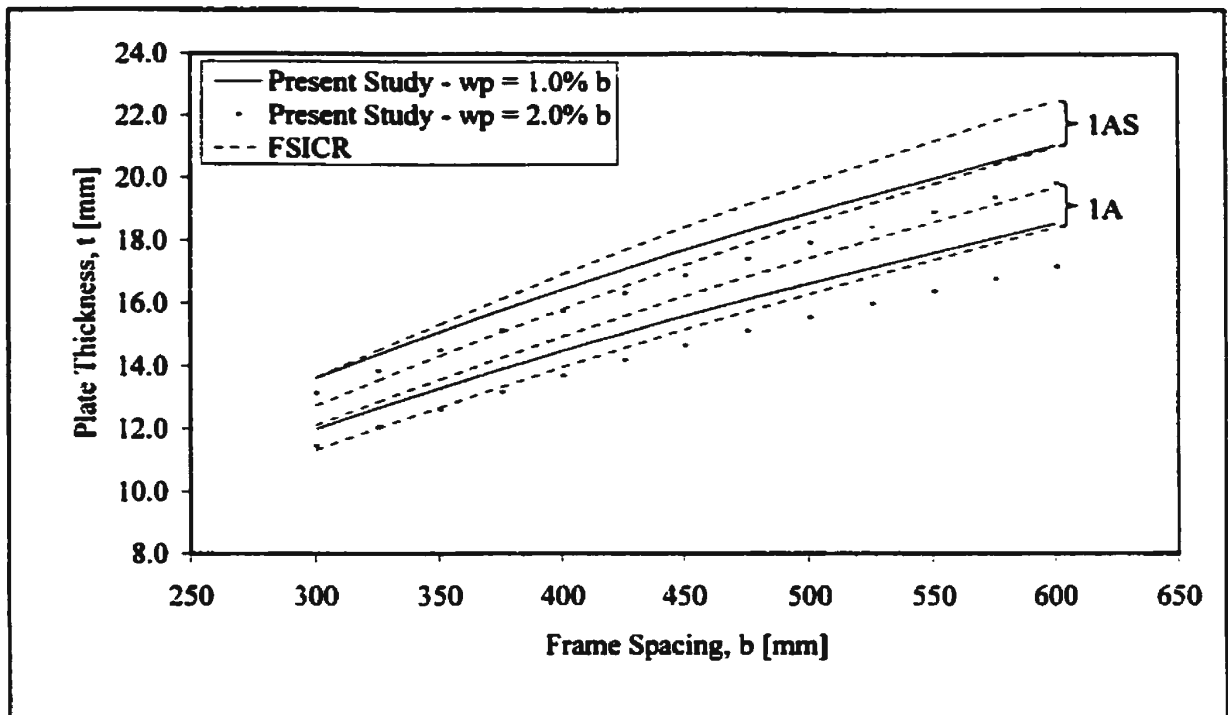


Figure 4.45 Analysis of FSICR Plating Requirements – Transversely-Framed Plating

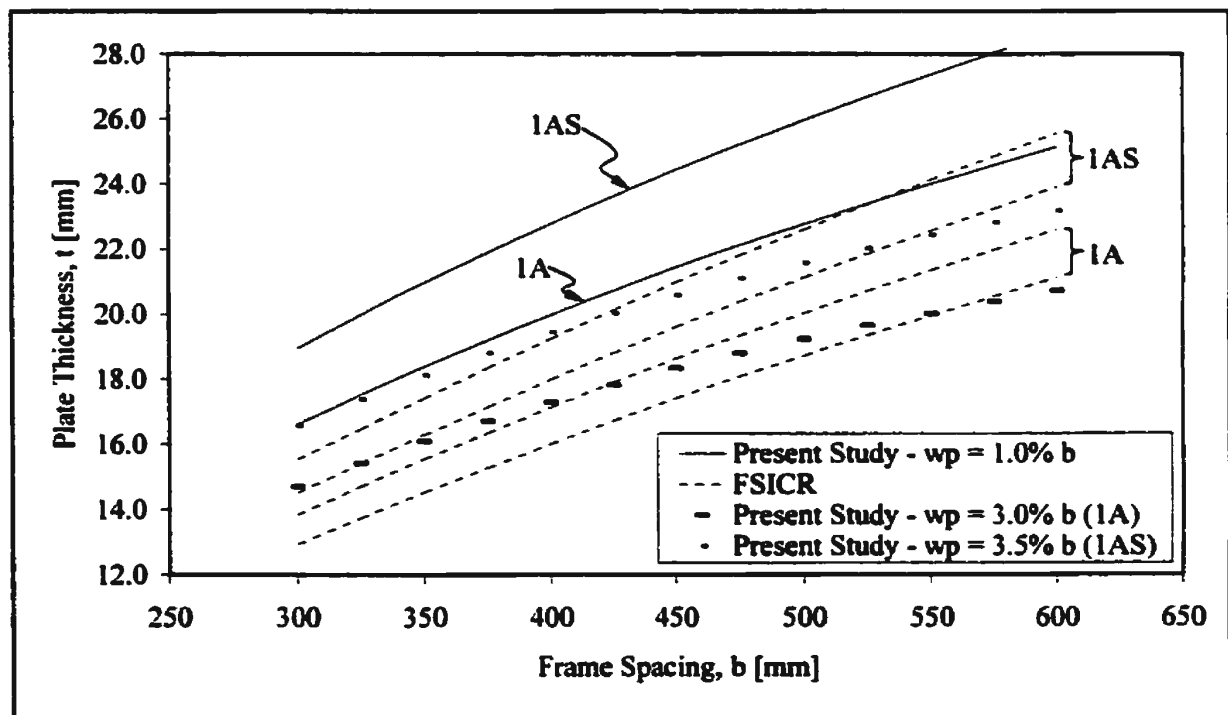


Figure 4.46 Analysis of FSICR Plating Requirements – Longitudinally-Framed Plating

The upper curve is based on a  $k$  factor of 14.62 (third quartile of  $k$  factors for the 61 ships in the study of the Winter Navigation Research Board), and a lower  $k$  factor of 7.62 (first quartile of  $k$  factors). Although the trends of plate thicknesses are dissimilar over the range of frame spacings ( $w_p/b = 0.01$ ), a reasonable fit was obtained with design line loads of  $q = 1120$  kN/m ( $p = 5.6$  MPa for  $f = 200$  mm) and  $q = 860$  kN/m ( $p = 4.3$  MPa for  $f = 200$  mm) for 1AS and 1A vessels, respectively. For load heights of 200 mm, 5.6 MPa corresponds to the 15<sup>th</sup> percentile of loads calculated from observed damages, while 4.3 MPa is less than any of the calculated loads at that height. Thicknesses based on a design criteria of  $w_p/b = 0.02$  are also shown, and reduce the required thicknesses by about 0.5 mm at a frame spacing of 300 mm and about 1.3 mm at a frame spacing of 600 mm.

In Figure 4.46, the design pressures obtained from the foregoing analysis of transversely-framed plating have been applied to longitudinally-framed plating. The results show that the thicknesses required to obtain permanent sets equal to 1% of frame spacing are significantly greater than those presently required by the 1985 FSICR. Correspondence with the existing FSICR requirements could only be obtained with allowable permanent set criteria equal to 3.0% and 3.5% of frame spacing for 1A and 1AS class vessels, respectively. This situation occurs partly because the FSICR design pressure for longitudinally-framed structures is a compromise between plating and framing, and as well because it was thought necessary to avoid large differences compared to the 1971 FSICR. It should be noted that the above results include an impending modification to the FSICR that restricts the length of longitudinal frames to twice that of the frame spacing when calculating the design ice pressure. This change

increases the design ice pressure for plating of aspect ratios greater than two, and hence the required thickness of the plating. According to the results shown in Figure 4.46, it is not surprising that all the longitudinally-framed ships included in the study of the Winter Navigation Research Board have sustained damages when navigating in Bothnian Bay (especially given the lighter scantlings prescribed by the 1971 FSICR). However, since the implementation of stricter requirements in the 1985 FSICR for longitudinally-framed ships, Baltic class ships are increasingly framed transversely in the icebelt region (when practical). Accordingly, it is becoming increasingly difficult to obtain in-service experience with which to evaluate the impact of the above discrepancy.

## **5.0 Summary of Results and Conclusions**

The present study was undertaken to better understand the influence of load height on the plastic response of ship shell plating. The primary aim of the study was to develop response equations for both transversely- and longitudinally-framed plating. This was considered to be important not only for the aspect of design, but also damage analysis. By examining the permanent deformation of ship shell plating, further insight was sought into the levels of ice loads occurring in the Baltic Sea.

Following a comprehensive review of the pertinent literature to date, the methods, assumptions and procedure of the study were delineated. Regarding the methods of analysis, a yield line formula was sought because of its simplicity. However, it was determined that the traditional double-Y-shaped collapse mechanism resulted in significant errors with loads of finite height. Accordingly, based on a method of converting loads of finite height to equivalent beam pressures, loads of finite height were applied to various structural configurations and then converted to equivalent uniform plate loads. Finite element analyses were used to determine the former, and yield line theory the latter. Regarding the finite element analyses, it was shown important to include the effects of strain-hardening and to obtain levels of permanent set by incrementally loading and unloading the plating. Simply removing the perfectly elastic portion from the total deflection resulted in significant errors as the deformation grew. The yield line equations used to obtain the equivalent uniform load were those developed by Jones for fully clamped boundaries using the maximum normal stress yield condition.

Assumptions pertaining to the load, structure and their interaction were then identified. The most important of these was that the plating was assumed to be free of global in-plane loads. In-plane loads can have a significant influence on the levels of deformation, and become increasingly important in the upper and lower extents of the icebelt in the midship area.

The procedure to be followed throughout the study was then delineated. The test matrix was described, followed by the ANSYS verification measures. The test matrix consisted of 344 load cases of various load and structural configurations. Based on experimental results of Young, the ANSYS code was found to well predict the load-deflection behaviour of a 12.8 mm plate strip under a quasi-uniform load. To ensure that the shell element used in this verification exercise would perform equally well at the lower limits of the  $b/t$  ratios in the test matrix, load-deflection results were also compared to finite element analyses using finely meshed solid elements. Model extents of 5 x 5 frame spacing enabled an adequate redistribution of in-plane strains. Ninety percent of these load cases obtained the target level of permanent set, which was set at 5% of frame spacing.

The analysis of the finite element results began with an examination of the interaction between bending moments and axial forces. As predicted with elasto-plastic theory, the load is carried primarily by the edge moments in the early stages of loading, followed by a centre moment, and then progressively by in-plane straining. This sequence of load-carrying mechanisms is common regardless of the load height and framing orientation. However, the load at which in-plane forces become significant is very dependent on the plate thickness to frame spacing ratio. In-plane forces for  $b/t = 36$  plating normally

appeared soon after the yield load had been reached. For  $b/t = 12$  plating, such forces only appeared after the yield load was exceeded by 150% to 300%, depending on the orientation of the framing. The same effect could be seen in through-thickness plasticity plots. The extent of bending moments and axial forces were examined over the span of the plate panel, near load levels at which the former reached their plastic values. While the magnitudes of the bending moments for the longitudinally-framed plating remained unchanged over much of the span, the magnitudes for transversely-framed plating were negligible within a frame spacing of the applied load. This effect could again be seen in plasticity patterns, this time on the surfaces of the plating.

Describing the distribution of in-plane strains and permanent set then concluded the characterisation of plating response. The former was considered to be important from a practical standpoint, because of the potential for coating breakdown under excessive straining. The strains across the frame spacing were found to be similar for all  $b/t$  ratios. For a level of permanent set equal to about 1% of frame spacing, a maximum strain value of approximately 2.3% occurred at the support for transversely-framed plating, and a maximum strain of 1.0% at midspan for longitudinally-framed plating. Patterns of permanent set were also examined to see if it was possible to determine load heights from the displacements. Unfortunately, in terms of determining load heights from observed damages, this was found to be very difficult.

The influences of structural and load parameters on permanent set were then examined, beginning with the effects of aspect ratio. For uniformly-loaded plating, and longitudinally-framed plating subjected to loads of finite height, the effect of aspect ratio on the pressures required to obtain a certain level of permanent set were noticeable up to

$\alpha = 3, 4$  or  $5$ , depending on the ratio of frame spacing to plate thickness. On the other hand, for transversely-framed plating, the effects of aspect ratio were negligible beyond  $\alpha = 2$ . Regarding the effect of material yield strength, results of the finite element analyses verified to a large extent the assumption in yield line theory that the uniform pressure required to achieve a given level of permanent set was directly proportional to material strength. However, the assumption becomes progressively erroneous as the  $b/t$  ratio decreases. The foregoing is also true for both transversely- and longitudinally-framed plating subjected to loads of finite height. Also investigated was the assumption in yield line theory that the pressure required to obtain a given level of permanent set is inversely proportional to the squared ratio of frame spacing to plate thickness. The results of the finite element analyses showed good agreement between the uniformly-loaded plating of  $b/t = 28$  and  $b/t = 36$ , but not for the relatively thicker plating of  $b/t = 12$  and  $b/t = 20$ . As well, the assumption could not be verified for plating subjected to loads of finite height.

The influence of load height on levels of permanent set was an important aspect of the present study. For both transversely- and longitudinally-framed plating, it was determined that the effect of load height on the pressure required to obtain a specified level of permanent set was nearly linear for load heights greater than half of the frame spacing. Generally speaking, the pressures increased proportionally between  $(f/b)^{-0.58}$  to  $(f/b)^{-0.79}$ , depending on the  $b/t$  ratio and framing orientation. As well, the issue was investigated as to whether or not there exist critical load heights below which the levels of permanent set remain constant for a given force. However, although the rate of change in



permanent sets continually declined as load heights were reduced, no critical load heights were found.

Loads of finite lengths were also examined for both transversely- and longitudinally-framed plating. The former was subjected to loads of length equal to the frame spacing. No significant differences in central deflection compared to loads of infinite length were observed. Longitudinally-framed plating was subjected to loads of length equal to 1, 2 and 3 times the frame spacing. The results indicated that changes to central deflection became negligible once the load length reached three times the frame spacing.

Plating response equations were subsequently developed, and required that average correction factors,  $f_D$ , for each load case be developed. For a given level of permanent set, the correction factors are the ratios of the uniform load, according to yield line theory, to loads of finite height, determined by finite element analyses. This was done on the basis of *Plate* equations, in which the actual value of aspect ratio was used in the equations of yield line theory, as well as *Beam* equations, in which the aspect ratio was assumed to be infinite. A *Modified Plate* equation for the transversely-framed plating was also examined in which the aspect ratio was set to two. By examining the average coefficients of variation for each of these equation types, it was determined that the least amount of error resulted from the *Modified Plate* equation for the transversely-framed plating, and from the *Plate* equation for plating framed longitudinally. Based on a similar analysis comparing plate aspect ratios, it was determined that the considerable scatter associated with square plate panels warranted their omission from further analyses.

When plotting the average correction factors for transversely-framed plating against the load height to frame spacing ratio, a higher degree of correlation was obtained by

including a factor of  $(b/t)^{0.2}$  in the independent variable. Accordingly, the following second-order polynomial was fitted to the results

$$f_D = -0.1330x^2 + 0.6701x$$

$$\text{where } x = \frac{f}{b} \left( \frac{b}{t} \right)^{0.2}$$

with a correlation coefficient of  $R = 0.9981$ . For longitudinally-framed plating, a high degree of correlation could be achieved by including the influence of  $b/a$  in addition to  $b/t$ . Accordingly, the following curve was fitted to the results for longitudinally-framed plating

$$f_D = -0.6263x^2 + 1.5363x$$

$$\text{where } x = \frac{f}{b} \left( \frac{b}{t} \frac{b}{a} \right)^{0.1}$$

with a correlation coefficient of  $R = 0.9951$ . Simplified *Beam* equations with lesser correlation coefficients were also obtained for approximate hand calculations. However, in comparison to the finite element results, the *Modified Plate* and *Plate* equations were shown to better capture the trends between pressure and permanent set. Sensitivity analyses were carried to study the relationships between permanent set, load height, plate thickness and frame spacing. The relationships between load height and plate thickness for a given line load and level of permanent set, as well as between permanent set and plate thickness for a given line load and load height, were seen to be nearly linear. The most interesting result, however, was that the permanent set for longitudinally-framed plating was on average twice that for a transversely-loaded plate, over a wide range of load heights.

Damage statistics of ice-strengthened Baltic class ships were next examined to determine the pressures necessary to cause damage under different load height assumptions. Based on load measurements obtained during transit through 60 cm thick ice in the northern Baltic, the analysis showed that load heights of a least 40 mm would be necessary to cause the observed damages. Re-examination of an earlier line load analysis questioned the assertion that line load intensity is related to load length. Finally, the current FSICR were evaluated using a plastic design philosophy. Based on fabrication tolerances, the allowable permanent set was assumed to be 1% of frame spacing. With such a design criteria, and an assumed load height of 200 mm, design pressures of  $p = 5.6$  MPa (line load  $q = 1120$  kN/m) and  $p = 4.3$  MPa (line load  $q = 860$  kN/m) were required to align the prescribed thicknesses of transversely-framed plating for 1AS and 1A vessels, respectively. When these same design pressures were applied to longitudinally-framed plating, the thicknesses required by the FSICR were far below those based on plastic design ( $w_p/b = 0.01$ ). The two sets of design curves could only be aligned by allowing permanent sets equal to 3.0% of frame spacing for 1A vessels, and 3.5% for those with ice class 1AS.

## **6.0 References**

**Aalami, B. (1972). "Large Deflection of Plates Under Hydrostatic Pressure", Journal of Ship Research 16, pp. 261 - 270.**

**Aalami, B., Moukhtarzade, A. and Mahmudi-Saati, P. (1972). "On the Strength Design of Ship Plates Subjected to In-Plane and Transverse Loading", RINA Transactions 114, pp. 519 - 534.**

**ANSYS, Inc. (1995). ANSYS User's Manual, Rev. 5.2, Volumes I – IV, Houston, PA.**

**Appolonov, E. (2000). "Background Notes to Shell Plating Thickness", Prepared for IACS Ad-Hoc Group on Polar Ship Rules.**

**Bond, J., Kennedy, S., Srinivasan, J., Basu, R., Toscano, D. and Stocks, D. (1995). "Post-Yield Strength of Icebreaking Ship Structures", Proceedings of the Third Canadian Marine Hydrodynamics and Structures Conference, Halifax/Dartmouth, pp. 157 - 166.**

**Brown, P.W., Jordaan, I.J., Maher A.N. and Haddara, M.R. (1996). "Optimisation of Bow Plating for Icebreakers", Journal of Ship Research 40, pp. 70 - 78.**

**Bunting, S., Briscoe, P.H., Subbiah, B.E. and Glenton, S.J. (1972). "Flat Plates Subject to Localised Loads", RINA Transactions 114, pp. 499 - 506.**

**Chapra, S.C. and Canale, R.P. (1988). Numerical Methods for Engineers, Second Ed., McGraw-Hill Publishing Co., New York.**

**Chiu, R., Haciski, E. and Hirsimaki, P. (1981). "Application of Plastic Analysis to U.S. Coast Guard Icebreaker Shell Plating", SNAME Transactions 89 (pre-print).**

**Christodoulides, J.C. and de Oliveira, J.G. (1982). "Plastic Collapse of Orthotropic Plates", Journal of Ship Research 24, pp. 286 - 295.**

**Chu, C-J, and Vorus, W.S. (1984). "Plastic Reserve Strength of Rectangular Plates", Journal of Ship Research 28, pp. 173 - 185.**

**Clarkson, J. (1956). "A New Approach to the Design of Plates to Withstand Lateral Pressure", RINA Transactions 98, pp. 443 - 463.**

**Clarkson, J. (1959). "Tests of Flat Plated Grillages under Concentrated Loads", RINA Transactions 101, pp. 129 - 142.**

- Clarkson, J. (1962). "Uniform Pressure Tests on Plates with Edges Free to Slide Inwards", RINA Transactions 104, pp. 67 - 76.
- Clarkson, J. (1963). "Tests of Flat Plated Grillages Under Uniform Pressure", RINA Transactions 105, pp. 467 - 484.
- Daidola, J.C. and Sheinberg, R. (1988). "A Procedure for the Structural Design of Icebreakers and Other Ships Navigating in Ice", SNAME Transactions 96 (pre-print).
- Daley, C. (1991). "Ice Edge Contact – A Brittle Failure Process Model", Doctor of Technology Thesis, Acta Polytechnica Scandinavica, Mechanical Engineering Series No. 100, Espoo.
- Drucker, D.C. (1957). "Plastic Design Methods - Advantages and Limitations", SNAME Transactions 65, pp. 172 - 190.
- Egge, E.D. and Böckenhauer, M. (1991). "Calculation of the Collision Resistance of Ships and its Assessment for Classification Purposes", Marine Structures: Design, Construction and Safety, Vol. 4, No. 1, pp. 35 - 56.
- Faulkner, D., Adamchak, J.C., Snyder, G.J. and Vetter, M.F. (1973). "Synthesis of Welded Grillages to Withstand Compression and Normal Loads", Journal of Computers and Structures 3, pp. 221 - 246.
- Finnish Board of Navigation (1985). Finnish-Swedish Ice Class Rules.
- Hakala, M.K. (1980). "A Non-Linear Finite Element Analysis of an Ice-Strengthened Ship Shell Structure", Computers and Structures 12, pp. 541 - 547.
- Hayward, R. (1995). "Finite Element Analyses of Icebreaker Shell Plating Subjected to Realistic Ice Loads", Engineering 8000 Project, Memorial University of Newfoundland, St. John's.
- Hodge, P.G. (1959). Plastic Analysis of Structures, McGraw-Hill, New York.
- Hooke, R. and Rawlings, B. (1969). "An Experimental Investigation of the Behaviour of Clamped, Rectangular, Mild Steel Plates Subjected to Uniform Transverse Pressure", Proceedings Institution of Civil Engineers 42, pp. 75 - 103.
- Hooke, R. (1970). "Post-Elastic Deflection Prediction of Plates", Proceedings ASCE 96, pp. 757 - 771.
- Hughes, O.F. (1981). "Design of Laterally Loaded Plating - Uniform Pressure Loads", Journal of Ship Research 25, pp. 77 - 89.

- Hughes, O.F. (1983). "Design of Laterally-Loaded Plating - Concentrated Loads", *Journal of Ship Research* 27, pp. 252 - 264.
- Hughes, O.F. (1988). *Ship Structural Design: A Rationally-Based, Computer-Aided Optimisation Approach*, SNAME.
- Hughes, O. and Caldwell, J.B. (1991). *Ship Structural Design - Supplement to Chapter 9 - Plate Bending*, SNAME.
- International Association of Classification Societies (1996). *Shipbuilding and Repair Quality Standard*, London.
- Jackson, R.I. and Frieze, P.A. (1981). "Design of Deck Structures Under Wheel Loads", *RINA Transactions* 123, pp. 119 - 144.
- Johansson, B.M. (1967). "On the Ice-Strengthening of Ship Hulls", *International Shipbuilding Progress* 14, pp. 231 - 245.
- Johnson, W. and Mellor, P.B. (1962). *Plasticity for Mechanical Engineers*, D. Van Nostrand Company Ltd., London.
- Jones, N. (1971). "A Theoretical Study of the Dynamic Plastic Behaviour of Beams and Plates with Finite Deflections", *International Journal of Solids and Structures* 7, pp. 1007 - 1029.
- Jones, N. and Walters, R.M. (1971). "Large Deflections of Rectangular Plates", *Journal of Ship Research* 15, pp. 164 - 171, p. 288.
- Jones, N. (1972). "Review of the Plastic Behaviour of Beams and Plates ", *International Shipbuilding Progress* 19, pp. 313 - 327.
- Jones, N. (1973). "Influence of In-Plane Displacements at the Boundaries of Rigid-Plastic Beams and Plates", *International Journal of Mechanical Sciences* 15, pp. 547 - 561.
- Jones, N. (1976). "Plastic Behaviour of Ship Structures", *SNAME Transactions* 84, pp. 115 - 145.
- Jordaan, I.J., Maes, M.A., Brown, P.W. and Hermans, I.P. (1993). "Probabilistic Analysis of Local Ice Pressures". *Journal of Offshore Mechanics and Arctic Engineering* 115, pp. 83 - 89.
- Jordaan, I.J., Xiao, J. and Zou, B. (1993). "Fracture and Damage of Ice: Towards Practical Implementation", *First Joint Mechanics Meeting of ASME-ASCE-SES, Charlottesville* (pre-print).

**Jordaan, I.J. and Singh, S.K. (1994). "Compressive Ice Failure: Critical Zones of High Pressure", IAHR Ice Symposium, Trondheim (pre-print).**

**Kamtekar, A.G. (1981). "An Approximate Analysis of the Behaviour of Laterally Loaded, Fully Fixed Beams and Plates", International Journal of Mechanical Sciences 23, pp. 437 - 455.**

**Katajamäki, K. (1988). "Analysis of Permanent Deflection on Ship Shell Plating". 5<sup>th</sup> Marine Technology Symposium, Technical Research Centre of Finland, Espoo, pp. 43 - 71.**

**Kendrick, A. (1997). "Definition of Ice Loads Under the Pressured Ice Scenario", Fleet Technology Report FTL-4643A6DR, Kanata.**

**Kheisin, D.E. and Cherepanov, N.V. (1970). "Change of Ice Structure in the Zone of Impact of a Solid Body Against the Ice Cover Surface", Problemy Arktiki i Antarktiki No. 34, pp. 239 - 245.**

**Kmiecik, M. (1995). "Usefulness of the Yield Line Theory in Design of Ship Plating". Marine Structures 8, pp. 67 - 79.**

**Kujala, P. (1990). "Safety of Ice-Strengthened Ship Hulls in the Baltic Sea", RINA Spring Meeting, Paper No. 9, London (pre-print).**

**Kujala, P. (1991). "Damage Statistics of Ice-Strengthened Ships in the Baltic Sea, 1984 - 1987", Winter Navigation Research Board, Research Report No. 50, Helsinki.**

**Kujala, P., Goldstein, R., Osipenko, N. and Danilenko, V. (1991) "A Ship in Compressive Ice - Preliminary Model Test Results and Analysis of the Process", Helsinki University of Technology, Laboratory of Naval Architecture and Marine Engineering, Report M-111, Otaniemi.**

**Kujala, P., Goldstein, R., Osipenko, N. and Danilenko, V. (1993) "A Ship in Compressive Ice - Analysis of the Ice Failure Process", Helsinki University of Technology, Laboratory of Naval Architecture and Marine Engineering, Report M-165, Otaniemi.**

**Kujala, P. Tuhkuri, J. and Varsta, P. (1994). "Ship-Ice Contact and Design Ice Loads", SNAME IceTech '94, Fifth International Conference on Ships and Marine Structures in Cold Regions, Paper A, Calgary.**

**Kurdyumov V.A. and Kheisin, D.E. (1976). "Hydrodynamic Model of the Impact of a Solid on Ice", AARI, Leningrad, translated from Prikladnaya Mekhanika 12, pp. 103 - 109.**

Lamble, J.H. and Choudhary, J.P. (1953). "Support Reactions, Stresses and Deflections for Plates Subjected to Uniform Transverse Loading", RINA Transactions 95, pp. 329 - 349.

Lehmann, E. and Zhang, L. (1998). Non-Linear Behaviour of Stiffened Structures (in German, *Nichtlineares Verhalten von ausgesteiften Tragwerken*), Springer-Verlag, Berlin.

Mäkinen, E., Liukkonen, S., Nortala-Hoikkanen, A. and Harjula A. (1994). "Friction and Hull Coatings in Ice Operations", SNAME IceTech'94, Fifth International Conference on Ships and Marine Structures in Cold Regions, Paper E, Calgary.

Manolakos, D.E. and Mamalis, A.G. (1988). "Limit Analysis for Laterally Loaded Stiffened Plates", International Journal of Mechanical Sciences 30, pp. 441 - 447.

McCallum, J., Lapp, D. and Gorman R. (1997). "Ship-Ice Interaction Scenarios", TP 12992, Minister of Supply and Services, Ottawa.

Muckle, W. (1967). Strength of Ships' Structures, Edward Arnold, London.

Mürer, C. (1983). "Strengthening of Hull Structures in Ice", WEGEMT 7<sup>th</sup> Graduate School on Ships and Structures in Ice, Helsinki University of Technology, Paper XII.

Nagasawa, H. and Aoki, G. (1968). "Orthogonally Stiffened Plates Under Lateral Loads" Japan Shipbuilding and Marine Engineering (July), pp. 19 - 25.

Ranki, E. (1986). "The Determination of Ice Loads from the Permanent Deformations of the Shell Structure in Ships", Licentiate Thesis (in Finnish, *Jääkuormituksen Määrittäminen Laivan Laidoitusrakenteen Pysyvistä Muodonmuutoksista*), Helsinki University of Technology, Espoo.

Ranki, E. (2000). Personal Communications (September).

Ratzlaff, K.P. and Kennedy, D.J.L. (1985). "Analysis of Continuous Steel Plates Subjected to Uniform Transverse Loads", Canadian Journal of Civil Engineering 12, pp. 685 - 699.

Ratzlaff, K.P. and Kennedy, D.J.L. (1986). "Behaviour and Ultimate Strength of Continuous Steel Plates Subjected to Uniform Transverse Loads", Canadian Journal of Civil Engineering 13, pp. 76 - 85.

Riska, K. and Varsta, P. (1983). "Structural Ice Loads in the Baltic", WEGEMT 7<sup>th</sup> Graduate School on Ships and Structures in Ice, Helsinki University of Technology, Paper IX.



**Riska, K., Rantala, H. and Joensuu, A. (1990). "Full Scale Observations of Ship-Ice Contact", Helsinki University of Technology, Laboratory of Naval Architecture and Marine Engineering, Report M-97, Otaniemi.**

**Riska, K. and Windeler, M. (1997). "Ice-Induced Stresses in the Shell Plating of Ice-Going Vessels", Helsinki University of Technology, Ship Laboratory, Report M-219, Otaniemi.**

**Rzhanitsyn, A.R. (1956). "The Design of Plates and Shells by the Kinematical Method of Limit Equilibrium", 9eme Congr. Mecanique Applique, Universite de Bruxelles 6, pp. 331 - 343.**

**Sandvik, P.C. (1974). "Deck Plates Subject to Large Wheel Loads", Report SK/M 28, University of Trondheim.**

**Sawczuk, A. (1964a). "On Initiation of the Membrane Action in Rigid-Plastic Plates", Proc. Journal de Mecanique 3, pp. 15 - 23.**

**Sawczuk, A. (1964b). "Large Deflections of Rigid-Plastic Plates", Proceedings from 11<sup>th</sup> International Congress of Applied Mechanics, pp. 224 - 228.**

**Soreide, T.H. (1983). "Collapse Analysis of Ship Shell Panels", WEGEMT 7<sup>th</sup> Graduate School on Ships and Structures in Ice, Helsinki University of Technology, Paper XI.**

**Soreide, T.H., Moan, T. and Nordsve, N.T. (1978). "On the Behaviour and Design of Stiffened Plates in Ultimate Limit State", Journal of Ship Research 22, pp. 238 - 244.**

**SSC (1981). "A Rational Basis for the Selection of Ice Strengthening Criteria for Ships - Volume I, SSC 309.**

**SSC (1981). "A Rational Basis for the Selection of Ice Strengthening Criteria for Ships - Volume II, SSC 310.**

**SSC (1995). "Post-Yield Strength of Icebreaking Ship Structural Members", SSC 384.**

**St. John, J. and Minnick, P. (1990). "A Design Method for Icebreaker Hull Loads Due to Level Icebreaking", SNAME IceTech '90, Fourth International Conference on Ships and Marine Structures in Cold Regions, Paper O.**

**St. John, J., Minnick, P. and Sheinberg, R. (1992). "Plastic Design Method for Icebreaker Shell Plating Subjected to Measured Ice Loads", SNAME Transactions 100, pp. 117 - 141.**

**Szilar, R. (1974). Theory and Analysis of Plates, Prentice-Hall.**

**Timoshenko, S. and Woinowsky-Krieger, S. (1959). Theory of Plates and Shells, 2<sup>nd</sup> ed., McGraw-Hill Kogakusha Ltd., Tokyo.**

**Transport Canada (1989). Proposal for the Revision of the Arctic Shipping Pollution Prevention Regulations, TP 9981, Minister of Supply and Services, Ottawa.**

**Transport Canada (1995). Equivalent Standards for the Construction of Arctic Class Ships, TP 12260, Minister of Supply and Services, Ottawa.**

**Tsoy, L.G. and Karavanov, S.B. (1992). "Investigation and Analysis of Ice Damages to the Hulls of Cargo Ships Operating on the Northern Sea Route", CNIIMF, St. Petersburg.**

**Varsta, P. (1983). On the Mechanics of Ice Load on Ships in Level Ice in the Baltic Sea, VTT, Espoo.**

**Verband für Schiffbau und Meerestechnik. Production Standard of the German Shipbuilding Industry – 5<sup>th</sup> Edition, VSM, Hamburg.**

**Viner, A.C. "Development of Ship Strength Formulations", unknown publication details.**

**Von Karman, T. (1910). Encyclopædia of Mathematical Sciences (in German, *Encyklopädie der Mathematischen Wissenschaften*), Vol. IV.**

**Wah, T. (1960). "A Theory for the Plastic Design of Ship Plating Under Uniform Pressure", Journal of Ship Research 4, pp. 17 - 24.**

**Wells, D., Keinonen, A. and Revill, C. (1994). "Analysis of Ice Damages Sustained by ASPPR Type Vessels in the Canadian Arctic 1976 to 1992", TP 11691E, Minister of Supply and Services, Ottawa.**

**Wiernicki, C.J. (1987). "Damage to Ship Plating Due to Ice Impact Loads", SNAME Transactions 24, pp. 43 - 58.**

**Wood, R.H. (1961). Plastic and Elastic Design of Slabs and Plates, Ronald Press, New York.**

**Xirouchakis, P.C. and Stortstrom, R. (1981). "On the Structural Analysis of Ice-Transiting Vessels", SNAME Star Symposium, Ottawa, pp. 133 - 143.**

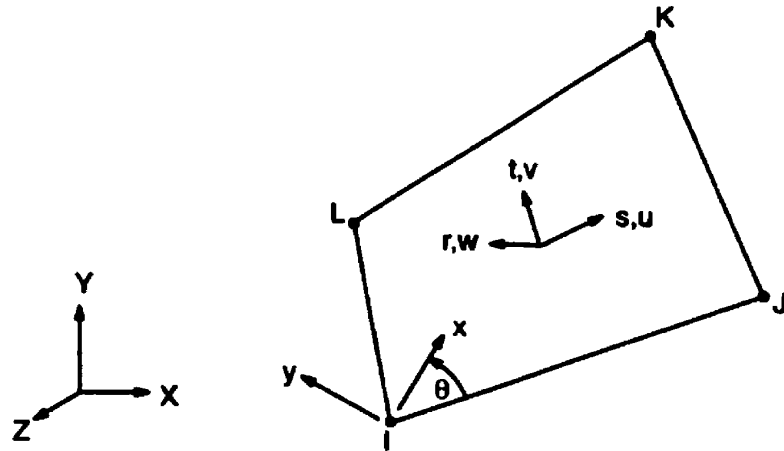
**Young, A.G. (1959). "Ship Plating Loaded Beyond the Elastic Limit", RINA Transactions 101, pp. 143 - 165.**

**Young, W.C. (1989). Roark's Formulas for Stress and Strain - 6<sup>th</sup> Ed., McGraw-Hill Book Company, New York.**

**Zou, B. (1996). "Ships in Ice: The Interaction Process and Principles of Design", PhD. Thesis, Memorial University of Newfoundland, St. John's.**

## **Appendix A**

## 14.43 SHELL43 — Plastic Shell



Matrix or Vector	Geometry	Shape Functions	Integration Points
Stiffness Matrix	Quad	Equations (12.5.13-1), (12.5.13-2), and (12.5.13-3)	In-plane: 2 x 2 Thru-the-thickness: 2 (linear material) 5 (nonlinear material)
	Triangle	Equations (12.5.4-1), (12.5.4-2), and (12.5.4-3)	In-plane: 1 Thru-the-thickness: 2 (linear material) 5 (nonlinear material)
Mass Matrix	Quad	Equations (12.5.8-1), (12.5.8-2), and (12.5.8-3)	Same as stiffness matrix
	Triangle	Equations (12.5.1-1), (12.5.1-2), and (12.5.1-3)	Same as stiffness matrix
Stress Stiffness Matrix	Same as mass matrix		Same as stiffness matrix

Matrix or Vector	Geometry	Shape Functions	Integration Points
Thermal Load Matrix	Same as stiffness matrix		Same as stiffness matrix
Transverse Pressure Load Vector	Quad	Equation (12.5.8–3)	2 x 2
	Triangle	Equation (12.5.1–3)	1
Edge Pressure Load Vector	Quad	Equations (12.5.8–1) and (12.5.8–2) specialized to the edge	2
	Triangle	Equations (12.5.1–1) and (12.5.1–2) specialized to the edge	2

Load Type	Distribution
Element Temperature	Bilinear in plane of element, linear thru thickness
Nodal Temperature	Bilinear in plane of element, constant thru thickness
Pressure	Bilinear in plane of element and linear along each edge

References: Ahmad(1), Cook(5), Dvorkin(96), Dvorkin(97), Bathe and Dvorkin(98), Allman(113), Cook(114), MacNeal and Harder(115)

### 14.43.1 Other Applicable Sections

Chapter 2 describes the derivation of structural element matrices and load vectors as well as stress evaluations. Section 13.1 describes integration point locations.

### 14.43.2 Assumptions and Restrictions

Normals to the centerplane are assumed to remain straight after deformation, but not necessarily normal to the centerplane.

Each pair of integration points (in the  $r$  direction) is assumed to have the same element (material) orientation.

This element does not generate a consistent mass matrix; only the lumped mass matrix is available.

### 14.43.3 Assumed Displacement Shape Functions

The assumed displacement and transverse shear strain shape functions are given in Chapter 12. The basic shape functions are essentially a condensation of those used for SHELL93. The basic functions for the transverse shear strain have been changed to avoid shear locking (Dvorkin(96), Dvorkin(97), Bathe and Dvorkin(98)) and are pictured in Figure 14.43-1. One result of the use of these displacement and strain shapes is that elastic rectangular elements give constant curvature results for flat elements, and also, in the absence of membrane loads, for curved elements. Thus, for these cases, nodal stresses are the same as centroidal stresses. Both SHELL63 and SHELL93 can have linearly varying curvatures.

### 14.43.4 Stress-Strain Relationships

The material property matrix [D] for the element is:

$$[D] = \begin{bmatrix} AE_x & Av_{xy}E_x & 0 & 0 & 0 & 0 \\ Av_{xy}E_x & AE_y & 0 & 0 & 0 & 0 \\ 0 & 0 & 0 & 0 & 0 & 0 \\ 0 & 0 & 0 & G_{xy} & 0 & 0 \\ 0 & 0 & 0 & 0 & \frac{G_{yz}}{1.2} & 0 \\ 0 & 0 & 0 & 0 & 0 & \frac{G_{xz}}{1.2} \end{bmatrix} \quad (14.43-1)$$

where:

- $$A = \frac{E_y}{E_y - (v_{xy})^2 E_x}$$
- $E_x$  = Young's modulus in element x-direction (input as EX on MP command)
- $v_{xy}$  = Poisson's ratio in element x-y plane (input as NUXY on MP command)
- $G_{xy}$  = shear modulus in element x-y plane (input as GXY on MP command)
- $G_{yz}$  = shear modulus in element y-z plane (input as GYZ on MP command)
- $G_{xz}$  = shear modulus in element x-z plane (input as GXZ on MP command)

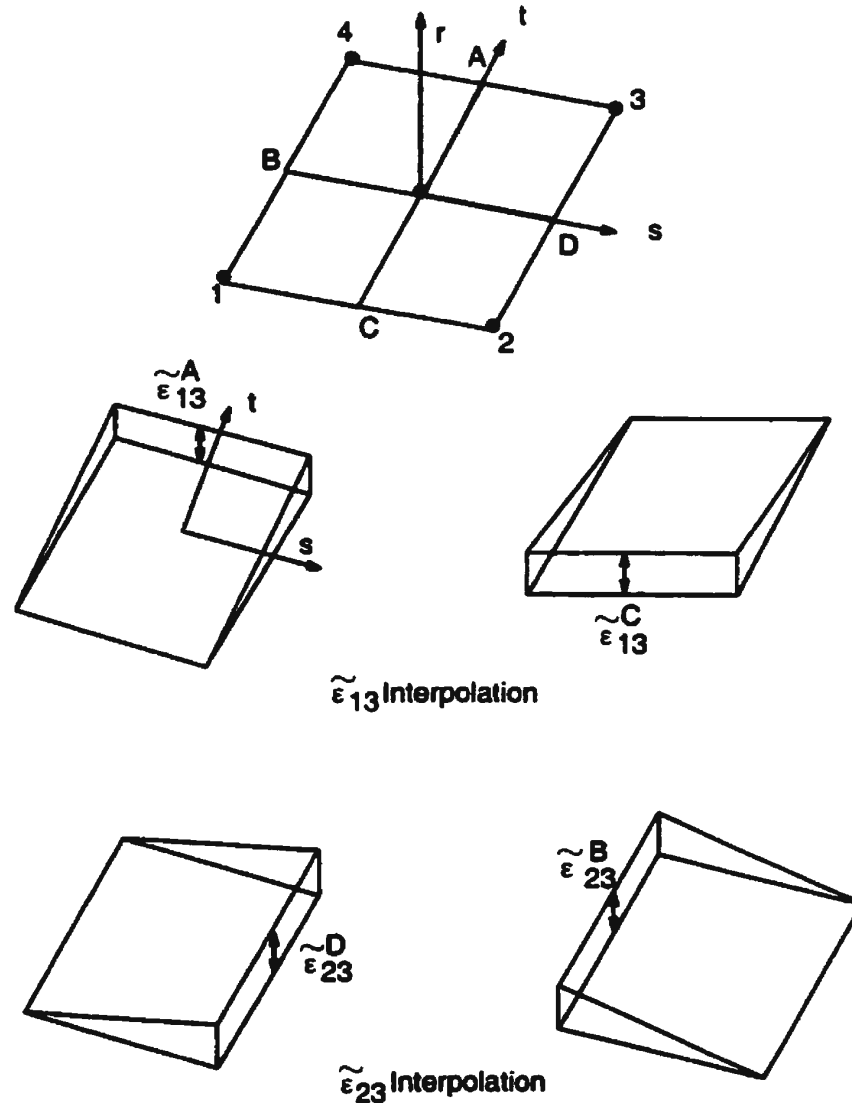


Figure 14.43-1 Shape Functions for the Transverse Strains

### 14.43.5 In-Plane Rotational DOF

If KEYOPT(3) is 0 or 1, there is no significant stiffness associated with the in-plane rotation DOF (rotation about the element  $r$  axis). A nominal value of stiffness is present (as described with SHELL63), however, to prevent free rotation at the node. KEYOPT(3) = 2 is used to include the Allman-type rotational DOFs (as described by



Allman(113) and Cook(114)). Such rotations improve the in-plane and general 3-D shell performance of the element. However, one of the outcomes of using the Allman rotation is that the element stiffness matrix contains up to two spurious zero energy modes (discussed below).

### 14.43.6 Spurious Mode Control with Allman Rotation

The first spurious mode is associated with constant rotations (Figure 14.43-2). The second spurious mode coincides with the well-known hourglass mode induced by reduced order integration (Figure 14.43-3). It is interesting to note that the hourglass spurious mode is elastically restrained for nonrectangular and multi-element configurations.

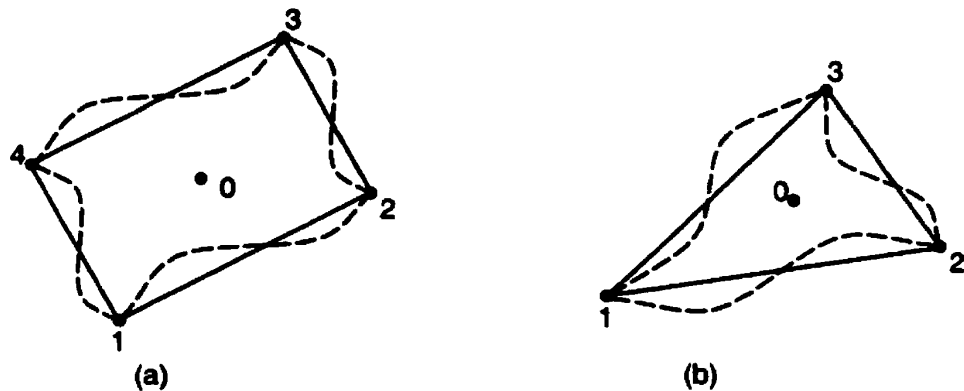


Figure 14.43-2 Constant out-of-plane rotation spurious mode  
( $\theta_{z1} = \theta_{z2} = \theta_{z3} = \theta_{z4}$ )

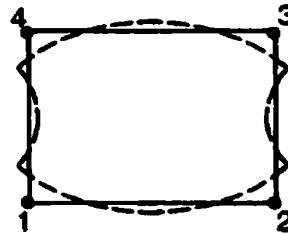


Figure 14.43-3 Hourglass mode ( $\theta_{z1} = -\theta_{z2} = \theta_{z3} = -\theta_{z4}$ )

The spurious modes are controlled on an elemental level using the concept suggested by MacNeal and Harder(115). For the constant rotation (Figure 14.43-2) spurious mode control, an energy penalty is defined as:

$$P_I = \delta_1 V \theta_I G_{xy} \theta_I \quad (14.43-2)$$

where:

- $P_I$  = energy penalty I
- $\delta_1$  = penalty parameter (input quantity ZSTIF1 on R command)
- $V$  = element volume
- $G_{xy}$  = shear modulus (input on MP command)
- $\theta_I$  = relative rotation, defined below

The relative rotation is computed at the element center as,

$$\theta_I = \theta_o - \frac{1}{n} \sum_{i=1}^n \theta_{zi} \quad (14.43-3)$$

where:

- $\theta_o = \frac{1}{2} \left( \left. \frac{\partial v}{\partial x} \right|_o - \left. \frac{\partial u}{\partial y} \right|_o \right)$
- $u, v$  = in-plane motions assuming edges remain straight
- $\theta_{zi}$  = in-plane rotation at node i
- $n$  = number of nodes per element
- $\left|_o\right.$  = evaluated at center of element

For the hourglass spurious modes which occur only for 4-noded elements, the energy penalty is taken as the inner product of the constraint force vector and the alternating rotational mode shapes as,

$$P_{II} = \delta_2 V \theta_{II} G_{xy} \theta_{II} \quad (14.43-4)$$

where:

- $P_{II}$  = energy penalty II
- $\delta_2$  = penalty parameter (input quantity ZSTIF2 on RMORE command)
- $\theta_{II} = \frac{1}{4} (\theta_{z1} - \theta_{z2} + \theta_{z3} - \theta_{z4})$

Once the energy penalties ( $P_I$  and  $P_{II}$ ) are defined, the associated stiffness augmentations can be calculated as,

$$[K_{ij}^e]_a = \frac{\partial^2 P_I}{\partial u_i \partial u_j} + \frac{\partial^2 P_{II}}{\partial u_i \partial u_j} \quad (14.43-5)$$

where:  $u_i$  = nodal displacement vector

This augmented stiffness matrix when added to the regular element stiffness matrix results in an effective stiffness matrix with no spurious modes.

### 14.43.7 Natural Space Extra Shape Functions with Allman Rotation

One of the outcomes of the Allman rotation is the dissimilar displacement variation along the normal and tangential directions of the element edges. The result of such variation is that the in-plane bending stiffness of the elements is too large by a factor  $1/(1-\nu^2)$  and sometimes termed as Poisson's ratio locking. To overcome this difficulty, two natural space (s and t) nodeless in-plane displacement shape functions are added in the element stiffness matrix formulation and then condensed out at the element level. The element thus generated is free of Poisson's ratio locking. For details of a similar implementation, refer to Yunus et al (117).

### 14.43.8 Warping

A warping factor is computed as:

$$\phi = \frac{D}{t} \quad (14.43-6)$$

where:  $D$  = component of the vector from the first node to the fourth node parallel to the element normal  
 $t$  = average thickness of the element

If  $\phi > 1.0$ , a warning message is printed.

### 14.43.9 Stress Output

The stresses at the center of the element are computed by taking the average of the four integration points on that plane.

The output forces and moments are computed as described in Section 2.3.

## **Appendix B**

Run ID >	001	002	003	004	005
0.00	0.00	0.00	0.00	0.00	0.00
0.50	0.17	0.20	0.20	0.20	0.20
0.00	0.00	0.00	0.00	0.00	0.00
1.00	0.34	0.41	0.41	0.41	0.41
0.00	0.00	0.00	0.00	0.00	0.00
1.50	0.52	0.63	0.63	0.63	0.63
0.00	0.00	0.01	0.02	0.02	0.02
2.00	0.71	0.90	0.99	1.02	1.02
0.00	0.02	0.08	0.17	0.20	0.21
2.50	1.00	1.48	2.08	3.15	4.28
0.00	0.14	0.46	1.06	2.14	3.27
3.00	1.59	3.17	9.63	11.31	12.09
0.00	0.55	1.92	8.47	10.19	10.98
3.50	9.29	11.25	15.90	17.36	17.82
0.00	8.12	9.92	14.68	16.18	16.66
4.00	15.46	17.62	21.74	23.13	23.59
0.00	14.20	16.24	20.50	21.95	22.42
4.50	21.35	23.46	27.12	28.24	28.64
0.00	20.06	22.08	25.91	27.07	27.49
5.00	27.89	29.10	32.79	33.78	34.08
0.00	Convergence Failure	27.76	31.62	Convergence Failure	Convergence Failure
5.50	Convergence Failure	34.71	38.32	Convergence Failure	Convergence Failure
0.00	Convergence Failure	33.44	Convergence Failure	Convergence Failure	Convergence Failure
6.00	Convergence Failure	39.34	Convergence Failure	Convergence Failure	Convergence Failure
0.00	Convergence Failure	Convergence Failure	Convergence Failure	Convergence Failure	Convergence Failure
6.50	Convergence Failure	Convergence Failure	Convergence Failure	Convergence Failure	Convergence Failure
0.00	Convergence Failure	Convergence Failure	Convergence Failure	Convergence Failure	Convergence Failure
7.00	Convergence Failure	Convergence Failure	Convergence Failure	Convergence Failure	Convergence Failure
0.00	Convergence Failure	Convergence Failure	Convergence Failure	Convergence Failure	Convergence Failure
7.50	Convergence Failure	Convergence Failure	Convergence Failure	Convergence Failure	Convergence Failure
0.00	Convergence Failure	Convergence Failure	Convergence Failure	Convergence Failure	Convergence Failure
8.00	Convergence Failure	Convergence Failure	Convergence Failure	Convergence Failure	Convergence Failure
0.00	Convergence Failure	Convergence Failure	Convergence Failure	Convergence Failure	Convergence Failure



Multiples of  $p_y$  - Uniformly Loaded

b [mm]	450	450	450	450	450
t [mm]	37.5	37.5	37.5	37.5	37.5
$\sigma_y$ [N/mm <sup>2</sup> ]	235	235	235	235	235
$\alpha$	1	2	3	4	5
e/b	infinite	infinite	infinite	infinite	infinite
f/b	infinite	infinite	infinite	infinite	infinite
$p_y$ [N/mm <sup>2</sup> ]	5.8913	3.7768	3.7472	3.7568	3.7568

Run ID >	006	007	008	009	010
0.00	0.00	0.00	0.00	0.00	0.00
0.50	0.30	0.37	0.37	0.37	0.37
0.00	0.00	0.00	0.00	0.00	0.00
1.00	0.61	0.73	0.74	0.74	0.74
0.00	0.00	0.00	0.00	0.00	0.00
1.50	0.92	1.13	1.15	1.15	1.15
0.00	0.01	0.03	0.04	0.04	0.04
2.00	1.29	1.77	2.14	2.27	2.30
0.00	0.08	0.31	0.67	0.80	0.83
2.50	1.98	3.02	5.54	7.08	7.68
0.00	0.47	1.20	3.75	5.37	6.00
3.00	3.77	6.58	10.80	12.59	13.18
0.00	1.95	4.45	8.93	10.84	11.47
3.50	11.32	12.24	16.29	17.42	17.65
0.00	9.47	10.11	14.49	15.73	15.98
4.00	16.99	17.54	20.39	21.39	21.74
0.00	15.21	15.53	18.67	19.77	20.15
4.50	21.03	21.78	24.48	25.10	25.19
0.00	19.31	19.90	22.90	23.58	23.67
5.00	24.70	25.36	27.18	27.57	27.61
0.00	23.04	23.60	25.63	26.07	26.11
5.50	28.14	28.09	29.75	30.18	30.26
0.00	26.56	26.40	28.24	28.70	28.79
6.00	30.94	30.70	32.35	32.54	32.47
0.00	29.41	29.06	30.88	31.09	31.01
6.50	33.47	33.26	34.52	34.45	34.27
0.00	31.97	31.67	33.06	32.99	32.80
7.00	35.98	35.57	36.99	37.02	36.86
0.00	34.52	34.01	35.56	35.60	35.43
7.50	38.61	37.97	39.71	39.82	39.68
0.00	37.19	36.46	38.33	38.43	38.28
8.00	41.08	40.51	42.06	41.98	41.81
0.00	39.69	Convergence Failure	40.70	40.61	40.43



Multiples of  $p_y$  - Uniformly Loaded

b [mm]	500	500	500	500	500
t [mm]	25.0	25.0	25.0	25.0	25.0
$\sigma_y$ [N/mm <sup>2</sup> ]	235	235	235	235	235
$\alpha$	1	2	3	4	5
e/b	infinite	infinite	infinite	infinite	infinite
f/b	infinite	infinite	infinite	infinite	infinite
$p_y$ [N/mm <sup>2</sup> ]	2.1631	1.3476	1.3342	1.3367	1.3367

Run ID >	011	012	013	014	015
0.00	0.00	0.00	0.00	0.00	0.00
0.50	0.29	0.36	0.36	0.36	0.36
0.00	0.00	0.00	0.00	0.00	0.00
1.00	0.58	0.71	0.72	0.72	0.72
0.00	0.00	0.00	0.00	0.00	0.00
1.50	0.88	1.09	1.12	1.11	1.11
0.00	0.01	0.03	0.04	0.04	0.04
2.00	1.27	1.78	2.19	2.32	2.34
0.00	0.11	0.38	0.77	0.92	0.95
2.50	1.99	3.01	4.48	5.03	5.16
0.00	0.56	1.29	2.85	3.48	3.63
3.00	3.67	5.19	7.08	7.87	8.06
0.00	1.99	3.29	5.43	6.34	6.57
3.50	7.04	7.75	9.78	10.32	10.40
0.00	5.39	5.86	8.23	8.88	8.97
4.00	10.11	10.41	11.83	12.16	12.20
0.00	8.59	8.67	10.38	10.77	10.83
4.50	12.30	12.42	13.64	13.94	13.99
0.00	10.86	10.81	12.28	12.65	12.70
5.00	14.09	14.21	15.18	15.43	15.45
0.00	12.73	12.72	13.90	14.18	14.20
5.50	15.78	15.68	16.49	16.66	16.65
0.00	14.50	14.27	15.24	15.43	15.42
6.00	17.35	16.96	17.57	17.66	17.63
0.00	16.12	15.59	16.33	16.43	16.40
6.50	18.74	18.11	18.63	18.66	18.60
0.00	17.56	16.78	17.39	17.42	17.35
7.00	20.05	19.31	19.73	19.71	19.64
0.00	18.90	18.01	18.52	18.49	18.41
7.50	21.30	20.55	20.93	20.90	20.82
0.00	20.18	19.30	19.74	19.69	19.61
8.00	22.51	21.80	22.21	22.16	22.10
0.00	21.41	20.59	21.04	20.99	20.91



Multiples of  $p_y$  - Uniformly Loaded

b [mm]	350	350	350	350	350
t [mm]	12.5	12.5	12.5	12.5	12.5
$\sigma_y$ [N/mm <sup>2</sup> ]	235	235	235	235	235
$\alpha$	1	2	3	4	5
e/b	infinite	infinite	infinite	infinite	infinite
f/b	infinite	infinite	infinite	infinite	infinite
$p_y$ [N/mm <sup>2</sup> ]	1.1023	0.6844	0.6772	0.6783	0.6783

Run ID >	016	017	018	019	020
0.00	0.00	0.00	0.00	0.00	0.00
0.50	0.48	0.58	0.59	0.59	0.59
0.00	0.00	0.00	0.00	0.00	0.00
1.00	0.95	1.16	1.18	1.18	1.18
0.00	0.00	0.00	0.00	0.00	0.00
1.50	1.44	1.78	1.82	1.82	1.82
0.00	0.02	0.04	0.06	0.06	0.06
2.00	2.10	2.91	3.47	3.62	3.64
0.00	0.22	0.65	1.23	1.41	1.44
2.50	3.26	4.60	5.90	6.23	6.29
0.00	0.96	1.93	3.42	3.86	3.94
3.00	5.35	6.84	8.35	8.78	8.86
0.00	2.76	3.99	5.88	6.43	6.54
3.50	8.16	9.18	10.87	11.20	11.23
0.00	5.59	6.36	8.53	8.98	9.02
4.00	11.13	11.52	12.89	13.12	13.14
0.00	8.80	8.88	10.70	11.02	11.04
4.50	13.40	13.54	14.72	14.93	14.94
0.00	11.23	11.10	12.68	12.96	12.98
5.00	15.22	15.29	16.20	16.32	16.32
0.00	13.18	13.03	14.27	14.43	14.42
5.50	16.84	16.78	17.48	17.55	17.54
0.00	14.90	14.65	15.59	15.68	15.66
6.00	18.41	18.08	18.62	18.65	18.63
0.00	16.57	16.04	16.76	16.79	16.76
6.50	19.89	19.21	19.64	19.64	19.61
0.00	18.13	17.22	17.77	17.77	17.74
7.00	21.32	20.26	20.57	20.53	20.50
0.00	19.62	18.30	18.70	18.64	18.60
7.50	22.71	21.30	21.63	21.56	21.50
0.00	21.08	19.36	19.77	19.68	19.61
8.00	24.05	22.47	22.79	22.74	22.68
0.00	22.46	20.57	20.96	20.89	20.82



Multiples of  $p_y$  - Uniformly Loaded

b [mm]	450	450	450	450	450
t [mm]	12.5	12.5	12.5	12.5	12.5
$\sigma_y$ [N/mm <sup>2</sup> ]	235	235	235	235	235
$\alpha$	1	2	3	4	5
e/b	infinite	infinite	infinite	infinite	infinite
f/b	infinite	infinite	infinite	infinite	infinite
$p_y$ [N/mm <sup>2</sup> ]	0.6668	0.4132	0.4088	0.4094	0.4094



Run ID >	021	022	023	024	025
0.00	0.00	0.00	0.00	0.00	0.00
0.50	0.26	0.31	0.31	0.31	0.31
0.00	0.00	0.00	0.00	0.00	0.00
1.00	0.52	0.62	0.62	0.62	0.62
0.00	0.00	0.00	0.00	0.00	0.00
1.50	0.78	0.95	0.96	0.95	0.95
0.00	0.00	0.02	0.03	0.03	0.03
2.00	1.07	1.36	1.50	1.54	1.55
0.00	0.03	0.13	0.26	0.31	0.31
2.50	1.51	2.23	3.12	4.52	5.71
0.00	0.22	0.69	1.57	2.99	4.19
3.00	2.39	4.69	11.07	13.27	14.10
0.00	0.83	2.81	9.35	11.62	12.48
3.50	10.40	12.97	19.31	21.68	22.52
0.00	8.65	10.98	17.56	20.05	20.93
4.00	18.54	21.48	27.38	29.17	29.82
0.00	16.70	19.51	25.74	27.63	28.31
4.50	27.86	29.25	34.03	35.24	35.51
0.00	Convergence Failure	27.41	32.50	33.77	Convergence Failure
5.00	Convergence Failure	35.87	40.33	41.26	Convergence Failure
0.00	Convergence Failure	Convergence Failure	Convergence Failure	Convergence Failure	Convergence Failure
5.50	Convergence Failure	Convergence Failure	Convergence Failure	Convergence Failure	Convergence Failure
0.00	Convergence Failure	Convergence Failure	Convergence Failure	Convergence Failure	Convergence Failure
6.00	Convergence Failure	Convergence Failure	Convergence Failure	Convergence Failure	Convergence Failure
0.00	Convergence Failure	Convergence Failure	Convergence Failure	Convergence Failure	Convergence Failure
6.50	Convergence Failure	Convergence Failure	Convergence Failure	Convergence Failure	Convergence Failure
0.00	Convergence Failure	Convergence Failure	Convergence Failure	Convergence Failure	Convergence Failure
7.00	Convergence Failure	Convergence Failure	Convergence Failure	Convergence Failure	Convergence Failure
0.00	Convergence Failure	Convergence Failure	Convergence Failure	Convergence Failure	Convergence Failure
7.50	Convergence Failure	Convergence Failure	Convergence Failure	Convergence Failure	Convergence Failure
0.00	Convergence Failure	Convergence Failure	Convergence Failure	Convergence Failure	Convergence Failure
8.00	Convergence Failure	Convergence Failure	Convergence Failure	Convergence Failure	Convergence Failure
0.00	Convergence Failure	Convergence Failure	Convergence Failure	Convergence Failure	Convergence Failure



Multiples of  $p_y$  - Uniformly Loaded

b [mm]	450	450	450	450	450
t [mm]	37.5	37.5	37.5	37.5	37.5
$\sigma_y$ [N/mm <sup>2</sup> ]	355	355	355	355	355
$\alpha$	1	2	3	4	5
e/b	infinite	infinite	infinite	infinite	infinite
f/b	infinite	infinite	infinite	infinite	infinite
$p_y$ [N/mm <sup>2</sup> ]	8.8997	5.7054	5.6607	5.6752	5.6751

Run ID >	026	027	028	029	030
0.00	0.00	0.00	0.00	0.00	0.00
0.50	0.46	0.55	0.56	0.56	0.56
0.00	0.00	0.00	0.00	0.00	0.00
1.00	0.91	1.10	1.12	1.11	1.11
0.00	0.00	0.00	0.00	0.00	0.00
1.50	1.39	1.70	1.74	1.73	1.73
0.00	0.02	0.04	0.06	0.06	0.06
2.00	1.95	2.66	3.19	3.36	3.40
0.00	0.13	0.46	0.98	1.16	1.20
2.50	2.98	4.49	7.17	8.41	8.80
0.00	0.70	1.76	4.54	5.90	6.33
3.00	5.41	8.50	12.25	13.97	14.55
0.00	2.70	5.40	9.53	11.44	12.09
3.50	12.36	13.74	18.28	19.63	19.97
0.00	9.61	10.63	15.73	17.28	17.66
4.00	18.80	19.55	23.31	24.41	24.67
0.00	16.23	16.69	21.01	22.26	22.55
4.50	23.63	24.50	27.19	27.72	27.73
0.00	21.23	21.93	25.06	25.66	25.68
5.00	27.66	27.98	29.91	30.33	30.36
0.00	25.41	25.58	27.82	28.29	28.32
5.50	31.20	30.89	32.53	32.85	32.87
0.00	29.07	28.59	30.48	30.83	30.84
6.00	34.27	33.50	34.89	35.01	34.91
0.00	32.21	31.27	32.85	32.98	32.87
6.50	37.22	36.04	37.53	37.61	37.47
0.00	35.24	33.87	35.52	Convergence Failure	Convergence Failure
7.00	40.17	38.70	40.49	Convergence Failure	Convergence Failure
0.00	38.27	36.58	38.55	Convergence Failure	Convergence Failure
7.50	43.03	41.49	43.17	Convergence Failure	Convergence Failure
0.00	41.19	Convergence Failure	Convergence Failure	Convergence Failure	Convergence Failure
8.00	45.71	Convergence Failure	Convergence Failure	Convergence Failure	Convergence Failure
0.00	43.92	Convergence Failure	Convergence Failure	Convergence Failure	Convergence Failure



Multiples of  $p_y$  - Uniformly Loaded

b [mm]	500	500	500	500	500
t [mm]	25.0	25.0	25.0	25.0	25.0
$\sigma_y$ [N/mm <sup>2</sup> ]	355	355	355	355	355
$\alpha$	1	2	3	4	5
e/b	infinite	infinite	infinite	infinite	infinite
f/b	infinite	infinite	infinite	infinite	infinite
$p_y$ [N/mm <sup>2</sup> ]	3.2677	2.0357	2.0156	2.0192	2.0192

Run ID >	031	032	033	034	035
0.00	0.00	0.00	0.00	0.00	0.00
0.50	0.44	0.54	0.55	0.54	0.54
0.00	0.00	0.00	0.00	0.00	0.00
1.00	0.88	1.07	1.09	1.08	1.08
0.00	0.00	0.00	0.00	0.00	0.00
1.50	1.33	1.63	1.68	1.67	1.67
0.00	0.02	0.04	0.06	0.06	0.06
2.00	1.90	2.62	3.13	3.26	3.28
0.00	0.17	0.53	1.04	1.20	1.23
2.50	2.93	4.21	5.52	5.88	5.94
0.00	0.79	1.71	3.18	3.64	3.72
3.00	4.88	6.40	7.87	8.32	8.42
0.00	2.44	3.70	5.50	6.08	6.21
3.50	7.78	8.76	10.68	11.14	11.21
0.00	5.35	6.07	8.49	9.09	9.17
4.00	10.91	11.34	13.02	13.38	13.42
0.00	8.70	8.86	11.03	11.49	11.54
4.50	13.32	13.61	14.90	15.10	15.10
0.00	11.29	11.37	13.05	13.30	13.30
5.00	15.33	15.47	16.33	16.45	16.44
0.00	13.44	13.40	14.55	14.69	14.68
5.50	17.02	16.93	17.60	17.66	17.64
0.00	15.24	14.97	15.85	15.92	15.90
6.00	18.54	18.20	18.68	18.70	18.67
0.00	16.84	16.31	16.94	16.95	16.92
6.50	19.97	19.34	19.79	19.79	19.75
0.00	18.33	17.49	18.05	18.04	18.00
7.00	21.35	20.46	20.91	20.88	20.82
0.00	19.75	18.64	19.19	19.14	19.06
7.50	22.70	21.70	22.23	22.21	22.15
0.00	21.15	19.92	20.53	20.50	20.43
8.00	24.02	23.05	23.59	23.55	23.48
0.00	22.51	21.32	21.93	21.88	21.79



Multiples of  $p_y$  - Uniformly Loaded

b [mm]	350	350	350	350	350
t [mm]	12.5	12.5	12.5	12.5	12.5
$\sigma_y$ [N/mm <sup>2</sup> ]	355	355	355	355	355
$\alpha$	1	2	3	4	5
e/b	infinite	infinite	infinite	infinite	infinite
f/b	infinite	infinite	infinite	infinite	infinite
$p_y$ [N/mm <sup>2</sup> ]	1.6652	1.0339	1.0230	1.0247	1.0247

Run ID >	036	037	038	039	040
0.00	0.00	0.00	0.00	0.00	0.00
0.50	0.72	0.88	0.90	0.89	0.89
0.00	0.00	0.00	0.00	0.00	0.00
1.00	1.43	1.75	1.78	1.77	1.77
0.00	0.00	0.00	0.00	0.00	0.00
1.50	2.16	2.64	2.70	2.70	2.69
0.00	0.03	0.06	0.09	0.09	0.09
2.00	3.10	4.14	4.72	4.82	4.83
0.00	0.31	0.84	1.48	1.64	1.65
2.50	4.60	6.03	7.02	7.19	7.20
0.00	1.26	2.24	3.52	3.80	3.82
3.00	6.83	8.27	9.55	9.76	9.76
0.00	3.17	4.30	6.09	6.44	6.45
3.50	9.19	10.47	11.62	11.79	11.79
0.00	5.53	6.57	8.30	8.59	8.59
4.00	11.83	12.52	13.70	13.84	13.83
0.00	8.41	8.80	10.59	10.82	10.81
4.50	14.23	14.51	15.58	15.70	15.69
0.00	11.10	11.04	12.68	12.86	12.85
5.00	16.26	16.31	17.11	17.16	17.15
0.00	13.37	13.11	14.33	14.42	14.40
5.50	18.02	17.83	18.42	18.46	18.44
0.00	15.30	14.80	15.71	15.76	15.73
6.00	19.53	19.15	19.60	19.61	19.59
0.00	16.93	16.24	16.92	16.93	16.90
6.50	20.96	20.33	20.71	20.72	20.70
0.00	18.47	17.50	18.06	18.05	18.01
7.00	22.35	21.42	21.75	21.73	21.71
0.00	19.93	18.64	19.09	19.06	19.03
7.50	23.74	22.47	22.79	22.76	22.72
0.00	21.40	19.72	20.14	20.08	20.03
8.00	25.12	23.57	23.99	Convergence Failure	23.86
0.00	22.85	20.85	21.37	Convergence Failure	21.19



Multiples of  $p_y$  - Uniformly Loaded

b [mm]	450	450	450	450	450
t [mm]	12.5	12.5	12.5	12.5	12.5
$\sigma_y$ [N/mm <sup>2</sup> ]	355	355	355	355	355
$\alpha$	1	2	3	4	5
e/b	infinite	infinite	infinite	infinite	infinite
f/b	infinite	infinite	infinite	infinite	infinite
$p_y$ [N/mm <sup>2</sup> ]	1.0072	0.6242	0.6175	0.6185	0.6184

Run ID >	101	102	103	104	105
0.00	0.00	0.00	0.00	0.00	0.00
0.50	0.18	0.20	0.20	0.20	0.20
0.00	0.00	0.00	0.00	0.00	0.00
1.00	0.36	0.40	0.40	0.40	0.40
0.00	0.00	0.00	0.00	0.00	0.00
1.50	0.55	0.60	0.60	0.60	0.60
0.00	0.00	0.01	0.01	0.01	0.01
2.00	0.74	0.84	0.84	0.84	0.84
0.00	0.02	0.05	0.05	0.05	0.05
2.50	1.01	1.26	1.27	1.27	1.27
0.00	0.10	0.27	0.27	0.27	0.27
3.00	1.33	1.96	1.98	1.98	1.98
0.00	0.24	0.76	0.78	0.78	0.78
3.50	2.06	4.30	4.48	4.48	4.48
0.00	0.77	2.88	3.05	3.06	3.06
4.00	10.02	11.98	12.17	12.17	12.17
0.00	8.59	10.48	10.67	10.67	10.67
4.50	16.19	17.84	17.95	17.95	17.95
0.00	14.66	16.25	16.36	16.36	16.36
5.00	22.03	23.69	23.76	23.76	23.76
0.00	Convergence Failure	22.07	22.14	22.14	22.14
5.50	Convergence Failure	29.69	29.76	29.76	29.76
0.00	Convergence Failure	28.10	Convergence Failure	Convergence Failure	Convergence Failure
6.00	Convergence Failure	34.97	Convergence Failure	Convergence Failure	Convergence Failure
0.00	Convergence Failure	Convergence Failure	Convergence Failure	Convergence Failure	Convergence Failure
6.50	Convergence Failure	Convergence Failure	Convergence Failure	Convergence Failure	Convergence Failure
0.00	Convergence Failure	Convergence Failure	Convergence Failure	Convergence Failure	Convergence Failure
7.00	Convergence Failure	Convergence Failure	Convergence Failure	Convergence Failure	Convergence Failure
0.00	Convergence Failure	Convergence Failure	Convergence Failure	Convergence Failure	Convergence Failure
7.50	Convergence Failure	Convergence Failure	Convergence Failure	Convergence Failure	Convergence Failure
0.00	Convergence Failure	Convergence Failure	Convergence Failure	Convergence Failure	Convergence Failure
8.00	Convergence Failure	Convergence Failure	Convergence Failure	Convergence Failure	Convergence Failure
0.00	Convergence Failure	Convergence Failure	Convergence Failure	Convergence Failure	Convergence Failure



Multiples of  $p_y$  - Transversely Loaded

b [mm]	450	450	450	450	450
t [mm]	37.5	37.5	37.5	37.5	37.5
$\sigma_y$ [N/mm <sup>2</sup> ]	235	235	235	235	235
$\alpha$	1	2	3	4	5
e/b	infinite	infinite	infinite	infinite	infinite
f/b	1.000	1.000	1.000	1.000	1.000
$p_y$ [N/mm <sup>2</sup> ]	5.0792	4.0769	4.0766	4.0766	4.0766

Run ID >	106	107	108	109	110
0.00	0.00	0.00	0.00	0.00	0.00
0.50	0.32	0.35	0.35	0.35	0.35
0.00	0.00	0.00	0.00	0.00	0.00
1.00	0.64	0.71	0.71	0.71	0.71
0.00	0.00	0.00	0.00	0.00	0.00
1.50	0.97	1.08	1.08	1.08	1.08
0.00	0.01	0.02	0.02	0.02	0.02
2.00	1.34	1.59	1.59	1.59	1.59
0.00	0.05	0.17	0.18	0.18	0.18
2.50	1.86	2.49	2.51	2.51	2.51
0.00	0.25	0.72	0.74	0.74	0.74
3.00	2.60	4.28	4.37	4.37	4.37
0.00	0.67	2.15	2.24	2.24	2.24
3.50	5.09	7.79	8.01	8.01	8.01
0.00	2.84	5.37	5.60	5.60	5.60
4.00	12.02	12.87	13.16	13.16	13.16
0.00	9.71	10.41	10.73	10.73	10.73
4.50	17.47	17.97	18.15	18.15	18.15
0.00	15.22	15.61	15.81	15.81	15.81
5.00	21.66	22.27	22.41	22.41	22.41
0.00	19.46	20.02	20.18	20.18	20.18
5.50	25.01	25.91	26.03	26.03	26.03
0.00	22.85	23.77	23.90	23.90	23.90
6.00	27.93	28.90	29.03	29.03	29.03
0.00	25.80	26.83	26.97	26.97	26.97
6.50	30.52	31.73	31.89	31.89	31.89
0.00	28.42	29.72	29.89	29.89	29.89
7.00	32.79	34.19	34.37	34.37	34.37
0.00	30.70	32.23	32.42	32.42	32.42
7.50	34.94	36.43	36.59	36.59	36.59
0.00	32.87	34.49	34.67	34.67	34.67
8.00	37.11	38.75	38.87	38.87	38.87
0.00	35.06	36.86	36.99	36.99	36.99



Multiples of  $p_y$  - Transversely Loaded

b [mm]	500	500	500	500	500
t [mm]	25.0	25.0	25.0	25.0	25.0
$\sigma_y$ [N/mm <sup>2</sup> ]	235	235	235	235	235
$\alpha$	1	2	3	4	5
e/b	infinite	infinite	infinite	infinite	infinite
f/b	1.000	1.000	1.000	1.000	1.000
$p_y$ [N/mm <sup>2</sup> ]	1.8472	1.4575	1.4569	1.4569	1.4569

Run ID >	111	112	113	114	115
0.00	0.00	0.00	0.00	0.00	0.00
0.50	0.31	0.34	0.34	0.34	0.34
0.00	0.00	0.00	0.00	0.00	0.00
1.00	0.62	0.69	0.69	0.69	0.69
0.00	0.00	0.00	0.00	0.00	0.00
1.50	0.93	1.05	1.05	1.05	1.05
0.00	0.01	0.02	0.02	0.02	0.02
2.00	1.30	1.58	1.59	1.59	1.59
0.00	0.07	0.22	0.22	0.22	0.22
2.50	1.81	2.47	2.49	2.49	2.49
0.00	0.28	0.78	0.80	0.80	0.80
3.00	2.53	4.00	4.07	4.07	4.07
0.00	0.70	2.02	2.09	2.09	2.09
3.50	4.35	5.93	6.04	6.04	6.04
0.00	2.26	3.75	3.88	3.88	3.88
4.00	7.56	8.24	8.38	8.38	8.38
0.00	5.47	6.05	6.21	6.21	6.21
4.50	10.40	10.67	10.79	10.79	10.79
0.00	8.43	8.60	8.75	8.75	8.75
5.00	12.60	12.76	12.86	12.86	12.86
0.00	10.72	10.81	10.92	10.92	10.92
5.50	14.49	14.61	14.68	14.68	14.68
0.00	12.68	12.76	12.86	12.86	12.86
6.00	16.08	16.23	16.30	16.30	16.30
0.00	14.33	14.47	14.56	14.56	14.56
6.50	17.49	17.70	17.78	17.78	17.78
0.00	15.79	16.03	16.12	16.12	16.12
7.00	18.78	19.08	19.18	19.18	19.18
0.00	17.12	17.47	17.58	17.58	17.58
7.50	19.94	20.37	20.47	20.47	20.47
0.00	18.31	18.81	18.93	18.93	18.93
8.00	21.02	21.58	21.70	21.70	21.70
0.00	19.41	20.07	20.19	20.19	20.19



Multiples of  $p_y$  - Transversely Loaded

b [mm]	350	350	350	350	350
t [mm]	12.5	12.5	12.5	12.5	12.5
$\alpha_y$ [N/mm <sup>2</sup> ]	235	235	235	235	235
$\alpha$	1	2	3	4	5
e/b	infinite	infinite	infinite	infinite	infinite
f/b	1.000	1.000	1.000	1.000	1.000
$p_y$ [N/mm <sup>2</sup> ]	0.9397	0.7399	0.7396	0.7396	0.7396

Run ID >	116	117	118	119	120
0.00	0.00	0.00	0.00	0.00	0.00
0.50	0.50	0.56	0.56	0.56	0.56
0.00	0.00	0.00	0.00	0.00	0.00
1.00	1.01	1.12	1.13	1.13	1.13
0.00	0.00	0.00	0.00	0.00	0.00
1.50	1.52	1.71	1.71	1.71	1.71
0.00	0.01	0.03	0.03	0.03	0.03
2.00	2.13	2.61	2.62	2.62	2.62
0.00	0.13	0.39	0.40	0.40	0.40
2.50	2.95	3.95	3.98	3.98	3.98
0.00	0.48	1.27	1.30	1.30	1.30
3.00	4.07	5.85	5.92	5.92	5.92
0.00	1.14	2.81	2.88	2.88	2.88
3.50	6.04	7.82	7.91	7.91	7.91
0.00	2.76	4.58	4.69	4.69	4.69
4.00	8.83	9.96	10.10	10.09	10.09
0.00	5.56	6.71	6.88	6.88	6.88
4.50	11.61	12.06	12.19	12.19	12.19
0.00	8.55	8.94	9.11	9.11	9.11
5.00	13.85	14.03	14.13	14.13	14.13
0.00	10.96	11.06	11.20	11.20	11.20
5.50	15.75	15.79	15.89	15.89	15.89
0.00	13.00	12.98	13.11	13.11	13.11
6.00	17.43	17.37	17.46	17.46	17.46
0.00	14.79	14.70	14.82	14.82	14.82
6.50	18.93	18.79	18.88	18.88	18.88
0.00	16.39	16.24	16.35	16.35	16.35
7.00	20.32	20.17	20.26	20.26	20.26
0.00	17.87	17.72	17.84	17.84	17.84
7.50	21.60	21.49	21.59	21.59	21.59
0.00	19.21	19.12	19.24	19.24	19.24
8.00	22.79	22.75	22.86	22.86	22.86
0.00	20.45	20.45	20.58	20.58	20.58



Multiples of  $p_y$  - Transversely Loaded

b [mm]	450	450	450	450	450
t [mm]	12.5	12.5	12.5	12.5	12.5
$\sigma_y$ [N/mm <sup>2</sup> ]	235	235	235	235	235
$\alpha$	1	2	3	4	5
e/b	infinite	infinite	infinite	infinite	infinite
f/b	1.000	1.000	1.000	1.000	1.000
$p_y$ [N/mm <sup>2</sup> ]	0.5680	0.4467	0.4465	0.4465	0.4465



Run ID >	121	122	123	124	125
0.00	0.00	0.00	0.00	0.00	0.00
0.50	0.18	0.19	0.19	0.19	0.19
0.00	0.00	0.00	0.00	0.00	0.00
1.00	0.35	0.38	0.38	0.38	0.38
0.00	0.00	0.00	0.00	0.00	0.00
1.50	0.53	0.57	0.57	0.57	0.57
0.00	0.00	0.00	0.00	0.00	0.00
2.00	0.72	0.78	0.78	0.78	0.78
0.00	0.01	0.02	0.02	0.02	0.02
2.50	0.96	1.09	1.09	1.09	1.09
0.00	0.08	0.15	0.15	0.15	0.15
3.00	1.26	1.53	1.53	1.53	1.53
0.00	0.20	0.40	0.40	0.40	0.40
3.50	1.87	2.59	2.60	2.60	2.60
0.00	0.62	1.25	1.26	1.26	1.26
4.00	7.52	7.20	7.29	7.29	7.29
0.00	6.11	5.68	5.77	5.77	5.77
4.50	14.33	13.97	14.04	14.04	14.04
0.00	12.83	12.38	12.45	12.45	12.45
5.00	19.88	19.30	19.37	19.37	19.37
0.00	18.29	17.62	17.69	17.69	17.69
5.50	25.55	25.08	25.12	25.12	25.12
0.00	23.94	Convergence Failure	Convergence Failure	Convergence Failure	Convergence Failure
6.00	30.46	Convergence Failure	Convergence Failure	Convergence Failure	Convergence Failure
0.00	Convergence Failure	Convergence Failure	Convergence Failure	Convergence Failure	Convergence Failure
6.50	Convergence Failure	Convergence Failure	Convergence Failure	Convergence Failure	Convergence Failure
0.00	Convergence Failure	Convergence Failure	Convergence Failure	Convergence Failure	Convergence Failure
7.00	Convergence Failure	Convergence Failure	Convergence Failure	Convergence Failure	Convergence Failure
0.00	Convergence Failure	Convergence Failure	Convergence Failure	Convergence Failure	Convergence Failure
7.50	Convergence Failure	Convergence Failure	Convergence Failure	Convergence Failure	Convergence Failure
0.00	Convergence Failure	Convergence Failure	Convergence Failure	Convergence Failure	Convergence Failure
8.00	Convergence Failure	Convergence Failure	Convergence Failure	Convergence Failure	Convergence Failure
0.00	Convergence Failure	Convergence Failure	Convergence Failure	Convergence Failure	Convergence Failure



Multiples of  $p_y$  - Transversely Loaded

b [mm]	450	450	450	450	450
t [mm]	37.5	37.5	37.5	37.5	37.5
$\sigma_y$ [N/mm <sup>2</sup> ]	235	235	235	235	235
$\alpha$	1	2	3	4	5
e/b	infinite	infinite	infinite	infinite	infinite
f/b	0.667	0.667	0.667	0.667	0.667
$p_y$ [N/mm <sup>2</sup> ]	5.4542	4.7514	4.7514	4.7514	4.7514

Run ID >	126	127	128	129	130
0.00	0.00	0.00	0.00	0.00	0.00
0.50	0.31	0.33	0.33	0.33	0.33
0.00	0.00	0.00	0.00	0.00	0.00
1.00	0.62	0.66	0.66	0.66	0.66
0.00	0.00	0.00	0.00	0.00	0.00
1.50	0.94	1.01	1.01	1.01	1.01
0.00	0.01	0.01	0.01	0.01	0.01
2.00	1.28	1.41	1.41	1.41	1.41
0.00	0.04	0.08	0.08	0.08	0.08
2.50	1.76	2.05	2.05	2.05	2.05
0.00	0.22	0.40	0.40	0.40	0.40
3.00	2.42	3.05	3.05	3.05	3.05
0.00	0.55	1.04	1.05	1.05	1.05
3.50	3.74	5.11	5.14	5.14	5.14
0.00	1.55	2.77	2.80	2.80	2.80
4.00	9.74	9.15	9.20	9.20	9.20
0.00	7.39	6.58	6.63	6.63	6.63
4.50	15.68	14.33	14.41	14.42	14.42
0.00	13.37	11.78	11.87	11.87	11.87
5.00	20.08	19.02	19.10	19.10	19.10
0.00	17.82	16.55	16.63	16.63	16.63
5.50	23.66	22.97	23.06	23.06	23.06
0.00	21.44	20.57	20.67	20.67	20.67
6.00	26.67	26.29	26.38	26.38	26.38
0.00	24.47	23.95	24.05	24.05	24.05
6.50	29.39	29.22	29.33	29.33	29.33
0.00	27.22	26.93	27.05	27.05	27.05
7.00	31.86	31.89	32.00	32.00	32.00
0.00	29.70	29.65	29.77	29.77	29.77
7.50	34.17	34.22	34.32	34.32	34.32
0.00	32.03	32.01	32.12	32.12	32.12
8.00	36.37	36.47	36.56	36.56	36.56
0.00	Convergence Failure	34.29	34.39	34.39	34.39



Multiples of  $p_y$  - Transversely Loaded

b [mm]	500	500	500	500	500
t [mm]	25.0	25.0	25.0	25.0	25.0
$\sigma_y$ [N/mm <sup>2</sup> ]	235	235	235	235	235
$\alpha$	1	2	3	4	5
e/b	infinite	infinite	infinite	infinite	infinite
f/b	0.600	0.600	0.600	0.600	0.600
$p_y$ [N/mm <sup>2</sup> ]	2.0782	1.8071	1.8069	1.8069	1.8069

Run ID >	131	132	133	134	135
0.00	0.00	0.00	0.00	0.00	0.00
0.50	0.30	0.32	0.32	0.32	0.32
0.00	0.00	0.00	0.00	0.00	0.00
1.00	0.59	0.64	0.64	0.64	0.64
0.00	0.00	0.00	0.00	0.00	0.00
1.50	0.89	0.97	0.97	0.97	0.97
0.00	0.01	0.01	0.01	0.01	0.01
2.00	1.24	1.37	1.37	1.37	1.37
0.00	0.06	0.10	0.10	0.10	0.10
2.50	1.71	2.01	2.01	2.01	2.01
0.00	0.23	0.43	0.43	0.43	0.43
3.00	2.35	2.94	2.95	2.95	2.95
0.00	0.58	1.05	1.06	1.06	1.06
3.50	3.51	4.50	4.52	4.52	4.52
0.00	1.46	2.34	2.36	2.36	2.36
4.00	6.18	6.32	6.34	6.34	6.34
0.00	4.02	3.99	4.01	4.01	4.01
4.50	9.25	8.74	8.77	8.77	8.77
0.00	7.17	6.44	6.47	6.47	6.47
5.00	11.69	11.13	11.17	11.17	11.17
0.00	9.71	8.95	8.99	8.99	8.99
5.50	13.61	13.20	13.23	13.23	13.23
0.00	11.71	11.12	11.16	11.16	11.16
6.00	15.28	15.00	15.04	15.04	15.04
0.00	13.44	13.01	13.06	13.06	13.06
6.50	16.76	16.58	16.64	16.64	16.64
0.00	14.97	14.67	14.73	14.73	14.73
7.00	18.09	17.99	18.06	18.06	18.06
0.00	16.33	16.14	16.21	16.21	16.21
7.50	19.29	19.28	19.35	19.35	19.35
0.00	17.57	17.48	17.56	17.56	17.56
8.00	20.41	20.47	20.56	20.56	20.56
0.00	18.71	18.71	18.80	18.80	18.80



Multiples of  $p_y$  - Transversely Loaded

b [mm]	350	350	350	350	350
t [mm]	12.5	12.5	12.5	12.5	12.5
$\sigma_y$ [N/mm <sup>2</sup> ]	235	235	235	235	235
$\alpha$	1	2	3	4	5
e/b	infinite	infinite	infinite	infinite	infinite
f/b	0.571	0.571	0.571	0.571	0.571
$p_y$ [N/mm <sup>2</sup> ]	1.0794	0.9425	0.9423	0.9423	0.9423

Run ID >	136	137	138	139	140
0.00	0.00	0.00	0.00	0.00	0.00
0.50	0.48	0.52	0.52	0.52	0.52
0.00	0.00	0.00	0.00	0.00	0.00
1.00	0.97	1.04	1.04	1.04	1.04
0.00	0.00	0.00	0.00	0.00	0.00
1.50	1.46	1.57	1.58	1.58	1.58
0.00	0.01	0.02	0.02	0.02	0.02
2.00	2.02	2.25	2.25	2.25	2.25
0.00	0.10	0.19	0.19	0.19	0.19
2.50	2.78	3.24	3.25	3.25	3.25
0.00	0.40	0.70	0.71	0.71	0.71
3.00	3.78	4.60	4.61	4.61	4.61
0.00	0.95	1.63	1.64	1.64	1.64
3.50	5.32	6.39	6.41	6.41	6.41
0.00	2.10	3.08	3.09	3.09	3.09
4.00	7.54	8.24	8.26	8.26	8.26
0.00	4.14	4.73	4.76	4.76	4.76
4.50	10.34	10.30	10.33	10.33	10.33
0.00	7.06	6.79	6.83	6.83	6.83
5.00	12.80	12.43	12.45	12.45	12.45
0.00	9.72	9.06	9.09	9.09	9.09
5.50	14.81	14.44	14.47	14.47	14.47
0.00	11.88	11.25	11.29	11.29	11.29
6.00	16.56	16.27	16.30	16.30	16.30
0.00	13.76	13.23	13.28	13.28	13.28
6.50	18.13	17.89	17.94	17.94	17.94
0.00	15.43	15.00	15.05	15.05	15.05
7.00	19.59	19.40	19.45	19.45	19.45
0.00	16.97	16.61	16.68	16.68	16.68
7.50	20.92	20.79	20.85	20.85	20.85
0.00	18.38	18.09	18.17	18.17	18.17
8.00	22.15	22.08	22.16	22.16	22.16
0.00	19.65	19.46	19.55	19.55	19.55



Multiples of  $p_y$  - Transversely Loaded

b [mm]	450	450	450	450	450
t [mm]	12.5	12.5	12.5	12.5	12.5
$\sigma_y$ [N/mm <sup>2</sup> ]	235	235	235	235	235
$\alpha$	1	2	3	4	5
e/b	infinite	infinite	infinite	infinite	infinite
f/b	0.556	0.556	0.556	0.556	0.556
$p_y$ [N/mm <sup>2</sup> ]	0.6612	0.5784	0.5783	0.5783	0.5783

Run ID >	141	142	143	144	145
0.00	0.00	0.00	0.00	0.00	0.00
0.50	0.16	0.17	0.17	0.17	0.17
0.00	0.00	0.00	0.00	0.00	0.00
1.00	0.32	0.34	0.34	0.34	0.34
0.00	0.00	0.00	0.00	0.00	0.00
1.50	0.48	0.51	0.51	0.51	0.51
0.00	0.00	0.00	0.00	0.00	0.00
2.00	0.65	0.69	0.69	0.69	0.69
0.00	0.01	0.01	0.01	0.01	0.01
2.50	0.84	0.90	0.90	0.90	0.90
0.00	0.04	0.06	0.06	0.06	0.06
3.00	1.09	1.21	1.21	1.21	1.21
0.00	0.13	0.20	0.20	0.20	0.20
3.50	1.47	1.71	1.71	1.71	1.71
0.00	0.35	0.52	0.52	0.52	0.52
4.00	2.21	2.78	2.78	2.78	2.78
0.00	0.92	1.41	1.41	1.41	1.41
4.50	9.22	8.07	8.09	8.09	8.09
0.00	7.80	6.55	6.56	6.56	6.56
5.00	14.90	13.94	13.96	13.97	13.97
0.00	13.39	12.33	12.36	12.36	12.36
5.50	19.76	18.86	18.89	18.89	18.89
0.00	18.17	17.17	Convergence Failure	Convergence Failure	Convergence Failure
6.00	25.11	24.17	Convergence Failure	Convergence Failure	Convergence Failure
0.00	Convergence Failure	22.45	Convergence Failure	Convergence Failure	Convergence Failure
6.50	Convergence Failure	29.60	Convergence Failure	Convergence Failure	Convergence Failure
0.00	Convergence Failure	27.88	Convergence Failure	Convergence Failure	Convergence Failure
7.00	Convergence Failure	34.22	Convergence Failure	Convergence Failure	Convergence Failure
0.00	Convergence Failure	Convergence Failure	Convergence Failure	Convergence Failure	Convergence Failure
7.50	Convergence Failure	Convergence Failure	Convergence Failure	Convergence Failure	Convergence Failure
0.00	Convergence Failure	Convergence Failure	Convergence Failure	Convergence Failure	Convergence Failure
8.00	Convergence Failure	Convergence Failure	Convergence Failure	Convergence Failure	Convergence Failure
0.00	Convergence Failure	Convergence Failure	Convergence Failure	Convergence Failure	Convergence Failure



Multiples of  $p_y$  - Transversely Loaded

b [mm]	450	450	450	450	450
t [mm]	37.5	37.5	37.5	37.5	37.5
$\sigma_y$ [N/mm <sup>2</sup> ]	235	235	235	235	235
$\alpha$	1	2	3	4	5
e/b	infinite	infinite	infinite	infinite	infinite
f/b	0.333	0.333	0.333	0.333	0.333
$p_y$ [N/mm <sup>2</sup> ]	8.0134	7.3282	7.3282	7.3282	7.3282

Run ID >	146	147	148	149	150
0.00	0.00	0.00	0.00	0.00	0.00
0.50	0.27	0.29	0.29	0.29	0.29
0.00	0.00	0.00	0.00	0.00	0.00
1.00	0.54	0.57	0.57	0.57	0.57
0.00	0.00	0.00	0.00	0.00	0.00
1.50	0.81	0.86	0.86	0.86	0.86
0.00	0.00	0.00	0.00	0.00	0.00
2.00	1.09	1.17	1.17	1.17	1.17
0.00	0.02	0.03	0.03	0.03	0.03
2.50	1.45	1.58	1.58	1.58	1.58
0.00	0.11	0.15	0.15	0.15	0.15
3.00	1.92	2.13	2.13	2.13	2.13
0.00	0.31	0.42	0.42	0.42	0.42
3.50	2.77	3.13	3.14	3.14	3.14
0.00	0.88	1.12	1.13	1.13	1.13
4.00	4.16	4.93	4.93	4.93	4.93
0.00	2.00	2.63	2.63	2.63	2.63
4.50	9.47	8.86	8.87	8.87	8.87
0.00	7.15	6.35	6.36	6.36	6.36
5.00	14.60	13.64	13.66	13.66	13.66
0.00	12.30	11.11	11.13	11.13	11.13
5.50	18.38	17.75	17.77	17.77	17.77
0.00	16.07	15.25	15.27	15.28	15.28
6.00	21.71	21.26	21.30	21.30	21.30
0.00	19.41	18.79	18.83	18.83	18.83
6.50	24.94	24.47	24.51	24.51	24.51
0.00	22.67	22.03	22.07	22.07	22.07
7.00	28.07	27.36	27.41	27.41	27.41
0.00	25.85	24.95	25.01	25.01	25.01
7.50	30.80	30.09	30.15	30.15	30.15
0.00	Convergence Failure	27.73	27.79	27.79	27.79
8.00	Convergence Failure	32.65	32.71	32.71	32.71
0.00	Convergence Failure	30.33	30.38	30.38	30.38



Multiples of  $p_y$  - Transversely Loaded

b [mm]	500	500	500	500	500
t [mm]	25.0	25.0	25.0	25.0	25.0
$\sigma_y$ [N/mm <sup>2</sup> ]	235	235	235	235	235
$\alpha$	1	2	3	4	5
e/b	infinite	infinite	infinite	infinite	infinite
f/b	0.200	0.200	0.200	0.200	0.200
$p_y$ [N/mm <sup>2</sup> ]	4.3203	3.9654	3.9652	3.9651	3.9651

Run ID >	151	152	153	154	155
0.00	0.00	0.00	0.00	0.00	0.00
0.50	0.25	0.27	0.27	0.27	0.27
0.00	0.00	0.00	0.00	0.00	0.00
1.00	0.50	0.54	0.54	0.54	0.54
0.00	0.00	0.00	0.00	0.00	0.00
1.50	0.76	0.81	0.81	0.81	0.81
0.00	0.00	0.00	0.00	0.00	0.00
2.00	1.02	1.10	1.10	1.10	1.10
0.00	0.02	0.03	0.03	0.03	0.03
2.50	1.37	1.50	1.50	1.50	1.50
0.00	0.12	0.16	0.16	0.16	0.16
3.00	1.86	2.04	2.04	2.04	2.04
0.00	0.35	0.43	0.43	0.43	0.43
3.50	2.65	2.96	2.96	2.96	2.96
0.00	0.90	1.10	1.10	1.10	1.10
4.00	3.82	4.33	4.33	4.33	4.33
0.00	1.83	2.23	2.23	2.23	2.23
4.50	5.93	6.08	6.08	6.08	6.08
0.00	3.82	3.83	3.83	3.83	3.83
5.00	8.57	8.38	8.38	8.38	8.38
0.00	6.50	6.12	6.13	6.13	6.13
5.50	10.79	10.60	10.60	10.61	10.61
0.00	8.79	8.42	8.43	8.43	8.43
6.00	12.47	12.46	12.47	12.47	12.47
0.00	10.51	10.36	10.37	10.37	10.37
6.50	14.02	14.09	14.11	14.11	14.11
0.00	12.08	12.03	12.05	12.05	12.05
7.00	15.48	15.55	15.57	15.57	15.57
0.00	13.59	13.53	13.56	13.56	13.56
7.50	16.85	16.87	16.90	16.90	16.90
0.00	14.99	14.89	14.92	14.92	14.92
8.00	18.11	18.10	18.14	18.14	18.14
0.00	16.28	16.15	16.19	16.19	16.19



Multiples of  $p_y$  - Transversely Loaded

b [mm]	350	350	350	350	350
t [mm]	12.5	12.5	12.5	12.5	12.5
$\sigma_y$ [N/mm <sup>2</sup> ]	235	235	235	235	235
$\alpha$	1	2	3	4	5
e/b	infinite	infinite	infinite	infinite	infinite
f/b	0.143	0.143	0.143	0.143	0.143
$p_y$ [N/mm <sup>2</sup> ]	2.9362	2.7053	2.7052	2.7052	2.7052

Run ID >	156	157	158	159	160
0.00	0.00	0.00	0.00	0.00	0.00
0.50	0.41	0.43	0.43	0.43	0.43
0.00	0.00	0.00	0.00	0.00	0.00
1.00	0.81	0.87	0.87	0.87	0.87
0.00	0.00	0.00	0.00	0.00	0.00
1.50	1.22	1.31	1.31	1.31	1.31
0.00	0.00	0.01	0.01	0.01	0.01
2.00	1.65	1.78	1.78	1.78	1.78
0.00	0.04	0.05	0.05	0.05	0.05
2.50	2.20	2.40	2.40	2.40	2.40
0.00	0.19	0.26	0.26	0.26	0.26
3.00	2.99	3.26	3.26	3.26	3.26
0.00	0.60	0.70	0.70	0.70	0.70
3.50	4.18	4.57	4.57	4.57	4.57
0.00	1.43	1.65	1.65	1.65	1.65
4.00	5.68	6.21	6.21	6.21	6.21
0.00	2.62	3.01	3.01	3.01	3.01
4.50	7.47	7.93	7.93	7.93	7.93
0.00	4.24	4.54	4.54	4.54	4.54
5.00	9.78	9.90	9.90	9.90	9.90
0.00	6.56	6.47	6.48	6.48	6.48
5.50	12.01	11.98	11.99	11.99	11.99
0.00	8.93	8.66	8.67	8.67	8.67
6.00	13.89	13.94	13.94	13.95	13.95
0.00	10.92	10.76	10.76	10.77	10.77
6.50	15.44	15.68	15.69	15.69	15.69
0.00	12.54	12.62	12.63	12.63	12.63
7.00	16.86	17.19	17.21	17.21	17.21
0.00	14.01	14.21	14.23	14.23	14.23
7.50	18.20	18.54	18.57	18.57	18.57
0.00	15.41	15.63	15.65	15.65	15.65
8.00	19.48	19.80	19.83	19.83	19.83
0.00	16.73	16.93	16.97	16.97	16.97



Multiples of  $p_y$  - Transversely Loaded

b [mm]	450	450	450	450	450
t [mm]	12.5	12.5	12.5	12.5	12.5
$\sigma_y$ [N/mm <sup>2</sup> ]	235	235	235	235	235
$\alpha$	1	2	3	4	5
e/b	infinite	infinite	infinite	infinite	infinite
f/b	0.111	0.111	0.111	0.111	0.111
$p_y$ [N/mm <sup>2</sup> ]	2.2222	2.0511	2.0510	2.0510	2.0510



Run ID >	201	202	203	204	205
0.00	0.00	0.00	0.00	0.00	0.00
0.50	0.28	0.30	0.30	0.30	0.30
0.00	0.00	0.00	0.00	0.00	0.00
1.00	0.55	0.60	0.60	0.60	0.60
0.00	0.00	0.00	0.00	0.00	0.00
1.50	0.83	0.91	0.91	0.91	0.91
0.00	0.00	0.01	0.01	0.01	0.01
2.00	1.12	1.27	1.27	1.27	1.27
0.00	0.02	0.07	0.07	0.07	0.07
2.50	1.52	1.91	1.91	1.91	1.91
0.00	0.14	0.41	0.41	0.41	0.41
3.00	2.01	2.96	2.99	2.99	2.99
0.00	0.36	1.14	1.17	1.17	1.17
3.50	3.11	6.18	6.38	6.39	6.39
0.00	1.16	4.05	4.26	4.26	4.26
4.00	11.52	13.91	14.18	14.18	14.18
0.00	9.39	11.66	11.94	11.94	11.94
4.50	19.15	21.79	21.98	21.98	21.98
0.00	16.91	Convergence Failure	19.69	19.69	19.69
5.00	27.16	Convergence Failure	29.94	29.94	29.94
0.00	Convergence Failure	Convergence Failure	Convergence Failure	Convergence Failure	Convergence Failure
5.50	Convergence Failure	Convergence Failure	Convergence Failure	Convergence Failure	Convergence Failure
0.00	Convergence Failure	Convergence Failure	Convergence Failure	Convergence Failure	Convergence Failure
6.00	Convergence Failure	Convergence Failure	Convergence Failure	Convergence Failure	Convergence Failure
0.00	Convergence Failure	Convergence Failure	Convergence Failure	Convergence Failure	Convergence Failure
6.50	Convergence Failure	Convergence Failure	Convergence Failure	Convergence Failure	Convergence Failure
0.00	Convergence Failure	Convergence Failure	Convergence Failure	Convergence Failure	Convergence Failure
7.00	Convergence Failure	Convergence Failure	Convergence Failure	Convergence Failure	Convergence Failure
0.00	Convergence Failure	Convergence Failure	Convergence Failure	Convergence Failure	Convergence Failure
7.50	Convergence Failure	Convergence Failure	Convergence Failure	Convergence Failure	Convergence Failure
0.00	Convergence Failure	Convergence Failure	Convergence Failure	Convergence Failure	Convergence Failure
8.00	Convergence Failure	Convergence Failure	Convergence Failure	Convergence Failure	Convergence Failure
0.00	Convergence Failure	Convergence Failure	Convergence Failure	Convergence Failure	Convergence Failure



Multiples of  $p_y$  - Transversely Loaded

b [mm]	450	450	450	450	450
t [mm]	37.5	37.5	37.5	37.5	37.5
$\sigma_y$ [N/mm <sup>2</sup> ]	355	355	355	355	355
$\alpha$	1	2	3	4	5
e/b	infinite	infinite	infinite	infinite	infinite
f/b	1.000	1.000	1.000	1.000	1.000
$p_y$ [N/mm <sup>2</sup> ]	7.6729	6.1587	6.1583	6.1583	6.1583

Run ID >	206	207	208	209	210
0.00	0.00	0.00	0.00	0.00	0.00
0.50	0.48	0.53	0.54	0.54	0.54
0.00	0.00	0.00	0.00	0.00	0.00
1.00	0.97	1.07	1.07	1.07	1.07
0.00	0.00	0.00	0.00	0.00	0.00
1.50	1.46	1.63	1.63	1.63	1.63
0.00	0.01	0.03	0.03	0.03	0.03
2.00	2.02	2.39	2.40	2.40	2.40
0.00	0.08	0.26	0.26	0.26	0.26
2.50	2.79	3.72	3.75	3.75	3.75
0.00	0.38	1.07	1.09	1.09	1.09
3.00	3.89	6.15	6.26	6.26	6.26
0.00	0.99	2.98	3.09	3.09	3.09
3.50	6.80	9.90	10.12	10.12	10.12
0.00	3.45	6.38	6.62	6.62	6.62
4.00	13.47	14.80	15.10	15.10	15.10
0.00	10.06	11.21	11.56	11.56	11.56
4.50	19.28	20.23	20.50	20.50	20.50
0.00	15.99	16.84	17.15	17.15	17.15
5.00	23.92	24.97	25.19	25.19	25.19
0.00	20.77	21.82	22.06	22.06	22.06
5.50	27.64	28.64	28.81	28.81	28.81
0.00	Convergence Failure	25.64	25.84	25.84	25.84
6.00	Convergence Failure	31.89	32.05	32.05	32.05
0.00	Convergence Failure	29.01	29.21	29.21	29.21
6.50	Convergence Failure	34.84	35.02	35.02	35.02
0.00	Convergence Failure	32.07	32.28	32.28	32.28
7.00	Convergence Failure	37.47	37.67	37.67	37.67
0.00	Convergence Failure	34.77	35.00	35.00	35.00
7.50	Convergence Failure	40.02	40.25	40.25	40.25
0.00	Convergence Failure	37.38	37.64	37.64	37.64
8.00	Convergence Failure	42.60	42.84	42.85	42.85
0.00	Convergence Failure	40.03	40.29	40.30	40.30



Multiples of  $p_y$  - Transversely Loaded

b [mm]	500	500	500	500	500
t [mm]	25.0	25.0	25.0	25.0	25.0
$\sigma_y$ [N/mm <sup>2</sup> ]	355	355	355	355	355
$\alpha$	1	2	3	4	5
e/b	infinite	infinite	infinite	infinite	infinite
f/b	1.000	1.000	1.000	1.000	1.000
$p_y$ [N/mm <sup>2</sup> ]	2.7904	2.2017	2.2009	2.2009	2.2009

Run ID >	211	212	213	214	215
0.00	0.00	0.00	0.00	0.00	0.00
0.50	0.47	0.52	0.52	0.52	0.52
0.00	0.00	0.00	0.00	0.00	0.00
1.00	0.93	1.03	1.04	1.04	1.04
0.00	0.00	0.00	0.00	0.00	0.00
1.50	1.40	1.57	1.58	1.58	1.58
0.00	0.01	0.03	0.03	0.03	0.03
2.00	1.95	2.36	2.37	2.37	2.37
0.00	0.10	0.32	0.32	0.32	0.32
2.50	2.70	3.59	3.61	3.61	3.61
0.00	0.41	1.09	1.12	1.12	1.12
3.00	3.72	5.40	5.46	5.46	5.46
0.00	1.00	2.54	2.61	2.61	2.61
3.50	5.57	7.36	7.45	7.45	7.45
0.00	2.51	4.30	4.41	4.41	4.41
4.00	8.46	9.57	9.70	9.70	9.70
0.00	5.38	6.48	6.66	6.66	6.66
4.50	11.38	11.87	11.99	11.99	11.99
0.00	8.50	8.94	9.10	9.10	9.10
5.00	13.70	14.06	14.17	14.17	14.17
0.00	10.99	11.33	11.46	11.46	11.46
5.50	15.66	15.95	16.04	16.04	16.04
0.00	13.08	13.38	13.50	13.50	13.50
6.00	17.31	17.54	17.63	17.63	17.63
0.00	14.83	15.10	15.21	15.21	15.21
6.50	18.75	18.99	19.08	19.08	19.08
0.00	16.35	16.64	16.76	16.76	16.76
7.00	20.08	20.39	20.49	20.49	20.49
0.00	17.73	18.14	18.25	18.25	18.25
7.50	21.32	21.72	21.83	21.83	21.83
0.00	19.03	19.53	19.66	19.66	19.66
8.00	22.51	23.01	23.13	23.13	23.13
0.00	20.26	20.87	21.01	21.01	21.01



Multiples of  $p_y$  - Transversely Loaded

b [mm]	350	350	350	350	350
t [mm]	12.5	12.5	12.5	12.5	12.5
$\sigma_y$ [N/mm <sup>2</sup> ]	355	355	355	355	355
$\alpha$	1	2	3	4	5
e/b	infinite	infinite	infinite	infinite	infinite
f/b	1.000	1.000	1.000	1.000	1.000
$p_y$ [N/mm <sup>2</sup> ]	1.4195	1.1177	1.1173	1.1173	1.1173

Run ID >	216	217	218	219	220
0.00	0.00	0.00	0.00	0.00	0.00
0.50	0.76	0.85	0.85	0.85	0.85
0.00	0.00	0.00	0.00	0.00	0.00
1.00	1.52	1.69	1.69	1.69	1.69
0.00	0.00	0.00	0.00	0.00	0.00
1.50	2.28	2.55	2.56	2.56	2.56
0.00	0.02	0.05	0.05	0.05	0.05
2.00	3.17	3.80	3.81	3.81	3.81
0.00	0.19	0.53	0.54	0.54	0.54
2.50	4.31	5.48	5.51	5.51	5.51
0.00	0.66	1.62	1.65	1.65	1.65
3.00	5.74	7.49	7.54	7.54	7.54
0.00	1.51	3.23	3.30	3.30	3.30
3.50	7.72	9.56	9.63	9.63	9.63
0.00	3.08	5.12	5.22	5.22	5.22
4.00	10.04	11.50	11.60	11.60	11.60
0.00	5.33	7.05	7.19	7.19	7.19
4.50	12.59	13.49	13.60	13.60	13.60
0.00	8.11	9.18	9.34	9.34	9.34
5.00	14.88	15.39	15.50	15.50	15.50
0.00	10.68	11.28	11.44	11.44	11.44
5.50	16.86	17.15	17.25	17.25	17.25
0.00	12.89	13.26	13.41	13.41	13.41
6.00	18.60	18.70	18.80	18.80	18.80
0.00	14.83	14.98	15.12	15.12	15.12
6.50	20.13	20.10	20.19	20.19	20.19
0.00	16.50	16.51	16.64	16.64	16.64
7.00	21.54	21.45	21.55	21.55	21.55
0.00	18.04	17.98	18.11	18.11	18.11
7.50	22.87	22.78	22.89	22.89	22.89
0.00	19.47	19.42	19.56	19.56	19.56
8.00	24.13	24.07	24.19	24.19	24.19
0.00	20.81	20.79	20.95	20.95	20.95



Multiples of  $p_y$  - Transversely Loaded

b [mm]	450	450	450	450	450
t [mm]	12.5	12.5	12.5	12.5	12.5
$\sigma_y$ [N/mm <sup>2</sup> ]	355	355	355	355	355
$\alpha$	1	2	3	4	5
e/b	infinite	infinite	infinite	infinite	infinite
f/b	1.000	1.000	1.000	1.000	1.000
$p_y$ [N/mm <sup>2</sup> ]	0.8580	0.6748	0.6745	0.6745	0.6745

Run ID >	221	222	223	224	225
0.00	0.00	0.00	0.00	0.00	0.00
0.50	0.27	0.28	0.28	0.28	0.28
0.00	0.00	0.00	0.00	0.00	0.00
1.00	0.53	0.57	0.57	0.57	0.57
0.00	0.00	0.00	0.00	0.00	0.00
1.50	0.80	0.85	0.85	0.85	0.85
0.00	0.00	0.00	0.00	0.00	0.00
2.00	1.09	1.17	1.17	1.17	1.17
0.00	0.02	0.04	0.04	0.04	0.04
2.50	1.45	1.64	1.64	1.64	1.64
0.00	0.12	0.22	0.22	0.22	0.22
3.00	1.90	2.31	2.31	2.31	2.31
0.00	0.30	0.60	0.60	0.60	0.60
3.50	2.82	3.88	3.89	3.89	3.89
0.00	0.94	1.86	1.87	1.87	1.87
4.00	8.89	9.00	9.06	9.07	9.07
0.00	6.77	6.73	6.80	6.80	6.80
4.50	16.68	16.31	16.39	16.39	16.39
0.00	14.44	13.93	14.02	14.02	14.02
5.00	24.73	23.90	24.02	24.02	24.02
0.00	22.45	Convergence Failure	21.59	21.60	21.60
5.50	31.36	Convergence Failure	31.58	31.58	31.58
0.00	Convergence Failure	Convergence Failure	29.23	29.23	29.23
6.00	Convergence Failure	Convergence Failure	37.28	37.28	37.28
0.00	Convergence Failure	Convergence Failure	Convergence Failure	Convergence Failure	Convergence Failure
6.50	Convergence Failure	Convergence Failure	Convergence Failure	Convergence Failure	Convergence Failure
0.00	Convergence Failure	Convergence Failure	Convergence Failure	Convergence Failure	Convergence Failure
7.00	Convergence Failure	Convergence Failure	Convergence Failure	Convergence Failure	Convergence Failure
0.00	Convergence Failure	Convergence Failure	Convergence Failure	Convergence Failure	Convergence Failure
7.50	Convergence Failure	Convergence Failure	Convergence Failure	Convergence Failure	Convergence Failure
0.00	Convergence Failure	Convergence Failure	Convergence Failure	Convergence Failure	Convergence Failure
8.00	Convergence Failure	Convergence Failure	Convergence Failure	Convergence Failure	Convergence Failure
0.00	Convergence Failure	Convergence Failure	Convergence Failure	Convergence Failure	Convergence Failure



Multiples of  $p_y$  - Transversely Loaded

b [mm]	450	450	450	450	450
t [mm]	37.5	37.5	37.5	37.5	37.5
$\sigma_y$ [N/mm <sup>2</sup> ]	355	355	355	355	355
$\alpha$	1	2	3	4	5
e/b	infinite	infinite	infinite	infinite	infinite
f/b	0.667	0.667	0.667	0.667	0.667
$p_y$ [N/mm <sup>2</sup> ]	8.2393	7.1777	7.1777	7.1777	7.1777

Run ID >	226	227	228	229	230
0.00	0.00	0.00	0.00	0.00	0.00
0.50	0.47	0.50	0.50	0.50	0.50
0.00	0.00	0.00	0.00	0.00	0.00
1.00	0.93	1.00	1.00	1.00	1.00
0.00	0.00	0.00	0.00	0.00	0.00
1.50	1.41	1.52	1.52	1.52	1.52
0.00	0.01	0.02	0.02	0.02	0.02
2.00	1.93	2.12	2.12	2.12	2.12
0.00	0.07	0.12	0.13	0.13	0.13
2.50	2.66	3.08	3.09	3.09	3.09
0.00	0.33	0.59	0.59	0.59	0.59
3.00	3.63	4.53	4.54	4.54	4.54
0.00	0.82	1.53	1.54	1.54	1.54
3.50	5.49	7.22	7.25	7.25	7.25
0.00	2.22	3.76	3.79	3.79	3.79
4.00	11.13	11.06	11.10	11.11	11.11
0.00	7.64	7.30	7.35	7.35	7.35
4.50	17.38	16.37	16.44	16.44	16.44
0.00	13.98	12.64	12.71	12.71	12.71
5.00	22.31	21.47	21.55	21.55	21.55
0.00	19.03	17.90	18.00	18.00	18.00
5.50	26.22	25.74	25.83	25.83	25.83
0.00	23.04	22.34	22.44	22.44	22.44
6.00	29.50	29.27	29.37	29.37	29.37
0.00	26.40	25.99	26.11	26.11	26.11
6.50	32.49	32.41	32.52	32.52	32.52
0.00	29.45	29.23	29.36	29.36	29.36
7.00	35.19	35.20	35.33	35.33	35.33
0.00	32.22	32.09	32.24	32.24	32.24
7.50	37.78	37.77	37.91	37.91	37.91
0.00	34.85	34.73	34.88	34.88	34.88
8.00	40.27	40.29	40.43	40.43	40.43
0.00	Convergence Failure	37.30	37.46	37.46	37.46



Multiples of  $p_y$  - Transversely Loaded

b [mm]	500	500	500	500	500
t [mm]	25.0	25.0	25.0	25.0	25.0
$\sigma_y$ [N/mm <sup>2</sup> ]	355	355	355	355	355
$\alpha$	1	2	3	4	5
e/b	infinite	infinite	infinite	infinite	infinite
f/b	0.600	0.600	0.600	0.600	0.600
$p_y$ [N/mm <sup>2</sup> ]	3.1394	2.7299	2.7295	2.7295	2.7295

Run ID >	231	232	233	234	235
0.00	0.00	0.00	0.00	0.00	0.00
0.50	0.45	0.48	0.48	0.48	0.48
0.00	0.00	0.00	0.00	0.00	0.00
1.00	0.89	0.96	0.96	0.96	0.96
0.00	0.00	0.00	0.00	0.00	0.00
1.50	1.35	1.45	1.46	1.46	1.46
0.00	0.01	0.02	0.02	0.02	0.02
2.00	1.86	2.06	2.06	2.06	2.06
0.00	0.08	0.15	0.15	0.15	0.15
2.50	2.55	2.97	2.97	2.97	2.97
0.00	0.34	0.61	0.61	0.61	0.61
3.00	3.47	4.24	4.25	4.25	4.25
0.00	0.84	1.47	1.47	1.47	1.47
3.50	4.92	5.97	5.99	5.99	5.99
0.00	1.92	2.87	2.88	2.88	2.88
4.00	7.22	7.84	7.86	7.86	7.86
0.00	4.04	4.54	4.56	4.56	4.56
4.50	10.16	10.02	10.05	10.05	10.05
0.00	7.10	6.72	6.76	6.76	6.76
5.00	12.71	12.37	12.40	12.40	12.40
0.00	9.84	9.24	9.28	9.28	9.28
5.50	14.76	14.52	14.56	14.56	14.56
0.00	12.03	11.57	11.62	11.62	11.62
6.00	16.51	16.37	16.41	16.41	16.41
0.00	13.88	13.57	13.62	13.62	13.62
6.50	18.03	17.98	18.03	18.03	18.03
0.00	15.48	15.29	15.35	15.35	15.35
7.00	19.41	19.44	19.50	19.50	19.50
0.00	16.92	16.84	16.91	16.91	16.91
7.50	20.69	20.79	20.86	20.86	20.86
0.00	18.25	18.26	18.35	18.35	18.35
8.00	21.89	22.05	22.13	22.13	22.13
0.00	19.49	19.58	19.67	19.67	19.67



Multiples of  $p_y$  - Transversely Loaded

b [mm]	350	350	350	350	350
t [mm]	12.5	12.5	12.5	12.5	12.5
$\sigma_y$ [N/mm <sup>2</sup> ]	355	355	355	355	355
$\alpha$	1	2	3	4	5
e/b	infinite	infinite	infinite	infinite	infinite
f/b	0.571	0.571	0.571	0.571	0.571
$p_y$ [N/mm <sup>2</sup> ]	1.6306	1.4237	1.4235	1.4235	1.4235

Run ID >	236	237	238	239	240
0.00	0.00	0.00	0.00	0.00	0.00
0.50	0.73	0.79	0.79	0.79	0.79
0.00	0.00	0.00	0.00	0.00	0.00
1.00	1.46	1.57	1.57	1.57	1.57
0.00	0.00	0.00	0.00	0.00	0.00
1.50	2.19	2.36	2.36	2.36	2.36
0.00	0.02	0.03	0.03	0.03	0.03
2.00	3.02	3.33	3.33	3.33	3.33
0.00	0.15	0.26	0.26	0.26	0.26
2.50	4.08	4.67	4.67	4.67	4.67
0.00	0.56	0.95	0.95	0.95	0.95
3.00	5.41	6.31	6.32	6.32	6.32
0.00	1.30	2.06	2.07	2.07	2.07
3.50	7.14	8.20	8.21	8.21	8.21
0.00	2.55	3.58	3.60	3.60	3.60
4.00	9.06	10.05	10.07	10.07	10.07
0.00	4.20	5.24	5.26	5.26	5.26
4.50	11.48	11.97	11.99	11.99	11.99
0.00	6.71	7.15	7.18	7.18	7.18
5.00	13.92	13.90	13.93	13.93	13.93
0.00	9.43	9.21	9.24	9.24	9.24
5.50	16.03	15.83	15.86	15.86	15.86
0.00	11.81	11.34	11.37	11.37	11.37
6.00	17.86	17.62	17.65	17.65	17.65
0.00	13.85	13.34	13.38	13.38	13.38
6.50	19.48	19.25	19.29	19.29	19.28
0.00	15.62	15.15	15.19	15.19	15.19
7.00	20.94	20.75	20.80	20.80	20.80
0.00	17.21	16.80	16.86	16.86	16.86
7.50	22.29	22.19	22.25	22.25	22.24
0.00	18.67	18.37	18.44	18.44	18.43
8.00	23.56	23.55	23.62	23.62	23.62
0.00	20.01	19.84	19.92	19.92	19.92



Multiples of  $p_y$  - Transversely Loaded

b [mm]	450	450	450	450	450
t [mm]	12.5	12.5	12.5	12.5	12.5
$\sigma_y$ [N/mm <sup>2</sup> ]	355	355	355	355	355
$\alpha$	1	2	3	4	5
e/b	infinite	infinite	infinite	infinite	infinite
f/b	0.556	0.556	0.556	0.556	0.556
$p_y$ [N/mm <sup>2</sup> ]	0.9989	0.8737	0.8736	0.8736	0.8736



Run ID >	241	242	243	244	245
0.00	0.00	0.00	0.00	0.00	0.00
0.50	0.24	0.25	0.25	0.25	0.25
0.00	0.00	0.00	0.00	0.00	0.00
1.00	0.48	0.51	0.51	0.51	0.51
0.00	0.00	0.00	0.00	0.00	0.00
1.50	0.72	0.76	0.76	0.76	0.76
0.00	0.00	0.00	0.00	0.00	0.00
2.00	0.98	1.04	1.04	1.04	1.04
0.00	0.01	0.02	0.02	0.02	0.02
2.50	1.27	1.36	1.36	1.36	1.36
0.00	0.06	0.09	0.09	0.09	0.09
3.00	1.65	1.83	1.83	1.83	1.83
0.00	0.20	0.30	0.30	0.30	0.30
3.50	2.22	2.58	2.58	2.58	2.58
0.00	0.53	0.79	0.79	0.79	0.79
4.00	3.33	4.17	4.17	4.17	4.17
0.00	1.38	2.11	2.11	2.11	2.11
4.50	10.58	9.74	9.75	9.75	9.75
0.00	8.44	7.45	7.47	7.47	7.47
5.00	17.59	16.38	16.41	16.41	16.41
0.00	15.34	13.98	14.01	14.01	14.01
5.50	24.80	23.44	23.49	23.49	23.49
0.00	Convergence Failure	Convergence Failure	Convergence Failure	Convergence Failure	Convergence Failure
6.00	Convergence Failure	Convergence Failure	Convergence Failure	Convergence Failure	Convergence Failure
0.00	Convergence Failure	Convergence Failure	Convergence Failure	Convergence Failure	Convergence Failure
6.50	Convergence Failure	Convergence Failure	Convergence Failure	Convergence Failure	Convergence Failure
0.00	Convergence Failure	Convergence Failure	Convergence Failure	Convergence Failure	Convergence Failure
7.00	Convergence Failure	Convergence Failure	Convergence Failure	Convergence Failure	Convergence Failure
0.00	Convergence Failure	Convergence Failure	Convergence Failure	Convergence Failure	Convergence Failure
7.50	Convergence Failure	Convergence Failure	Convergence Failure	Convergence Failure	Convergence Failure
0.00	Convergence Failure	Convergence Failure	Convergence Failure	Convergence Failure	Convergence Failure
8.00	Convergence Failure	Convergence Failure	Convergence Failure	Convergence Failure	Convergence Failure
0.00	Convergence Failure	Convergence Failure	Convergence Failure	Convergence Failure	Convergence Failure



Multiples of  $p_y$  - Transversely Loaded

b [mm]	450	450	450	450	450
t [mm]	37.5	37.5	37.5	37.5	37.5
$\sigma_y$ [N/mm <sup>2</sup> ]	355	355	355	355	355
$\alpha$	1	2	3	4	5
e/b	infinite	infinite	infinite	infinite	infinite
f/b	0.333	0.333	0.333	0.333	0.333
$p_y$ [N/mm <sup>2</sup> ]	12.1053	11.0702	11.0702	11.0702	11.0702

Run ID >	246	247	248	249	250
0.00	0.00	0.00	0.00	0.00	0.00
0.50	0.41	0.43	0.43	0.43	0.43
0.00	0.00	0.00	0.00	0.00	0.00
1.00	0.81	0.86	0.86	0.86	0.86
0.00	0.00	0.00	0.00	0.00	0.00
1.50	1.22	1.30	1.30	1.30	1.30
0.00	0.00	0.01	0.01	0.01	0.01
2.00	1.64	1.76	1.76	1.76	1.76
0.00	0.02	0.04	0.04	0.04	0.04
2.50	2.19	2.38	2.38	2.38	2.38
0.00	0.17	0.23	0.23	0.23	0.23
3.00	2.89	3.22	3.22	3.22	3.22
0.00	0.46	0.63	0.63	0.63	0.63
3.50	4.14	4.66	4.66	4.66	4.66
0.00	1.30	1.65	1.65	1.65	1.65
4.00	6.06	7.04	7.04	7.04	7.04
0.00	2.83	3.63	3.63	3.63	3.63
4.50	10.88	10.81	10.81	10.81	10.81
0.00	7.44	7.12	7.12	7.12	7.12
5.00	16.25	15.67	15.68	15.68	15.68
0.00	12.84	11.97	11.98	11.98	11.98
5.50	20.72	20.13	20.15	20.15	20.15
0.00	17.37	16.50	16.52	16.52	16.52
6.00	24.52	24.20	24.23	24.23	24.23
0.00	21.24	20.68	20.71	20.71	20.71
6.50	28.07	27.76	27.80	27.80	27.80
0.00	24.88	24.34	24.39	24.39	24.39
7.00	31.27	30.89	30.95	30.95	30.95
0.00	Convergence Failure	Convergence Failure	Convergence Failure	Convergence Failure	Convergence Failure
7.50	Convergence Failure	Convergence Failure	Convergence Failure	Convergence Failure	Convergence Failure
0.00	Convergence Failure	Convergence Failure	Convergence Failure	Convergence Failure	Convergence Failure
8.00	Convergence Failure	Convergence Failure	Convergence Failure	Convergence Failure	Convergence Failure
0.00	Convergence Failure	Convergence Failure	Convergence Failure	Convergence Failure	Convergence Failure



Multiples of  $p_y$  - Transversely Loaded

b [mm]	500	500	500	500	500
t [mm]	25.0	25.0	25.0	25.0	25.0
$\sigma_y$ [N/mm <sup>2</sup> ]	355	355	355	355	355
$\alpha$	1	2	3	4	5
e/b	infinite	infinite	infinite	infinite	infinite
f/b	0.200	0.200	0.200	0.200	0.200
$p_y$ [N/mm <sup>2</sup> ]	6.5265	5.9902	5.9899	5.9898	5.9898

Run ID >	251	252	253	254	255
0.00	0.00	0.00	0.00	0.00	0.00
0.50	0.38	0.41	0.41	0.41	0.41
0.00	0.00	0.00	0.00	0.00	0.00
1.00	0.76	0.81	0.81	0.81	0.81
0.00	0.00	0.00	0.00	0.00	0.00
1.50	1.14	1.22	1.22	1.22	1.22
0.00	0.00	0.01	0.01	0.01	0.01
2.00	1.54	1.66	1.66	1.66	1.66
0.00	0.03	0.04	0.04	0.04	0.04
2.50	2.06	2.24	2.24	2.24	2.24
0.00	0.17	0.23	0.23	0.23	0.23
3.00	2.76	3.03	3.03	3.03	3.03
0.00	0.51	0.63	0.63	0.63	0.63
3.50	3.85	4.25	4.26	4.26	4.26
0.00	1.26	1.50	1.51	1.51	1.51
4.00	5.30	5.84	5.84	5.85	5.85
0.00	2.41	2.81	2.81	2.81	2.81
4.50	7.17	7.58	7.58	7.58	7.58
0.00	4.10	4.36	4.36	4.36	4.36
5.00	9.62	9.67	9.68	9.68	9.68
0.00	6.58	6.43	6.43	6.43	6.43
5.50	11.87	11.87	11.88	11.88	11.88
0.00	8.96	8.74	8.75	8.75	8.75
6.00	13.78	13.85	13.86	13.86	13.86
0.00	10.96	10.84	10.85	10.85	10.85
6.50	15.44	15.62	15.64	15.64	15.64
0.00	12.69	12.72	12.74	12.74	12.74
7.00	16.94	17.20	17.22	17.22	17.22
0.00	14.25	14.39	14.41	14.41	14.41
7.50	18.37	18.61	18.64	18.64	18.64
0.00	15.75	15.86	15.89	15.89	15.89
8.00	19.72	19.90	19.93	19.93	19.93
0.00	17.15	17.20	17.24	17.24	17.24



Multiples of  $p_y$  - Transversely Loaded

b [mm]	350	350	350	350	350
t [mm]	12.5	12.5	12.5	12.5	12.5
$\sigma_y$ [N/mm <sup>2</sup> ]	355	355	355	355	355
$\alpha$	1	2	3	4	5
e/b	infinite	infinite	infinite	infinite	infinite
f/b	0.143	0.143	0.143	0.143	0.143
$p_y$ [N/mm <sup>2</sup> ]	4.4356	4.0868	4.0866	4.0866	4.0866

Run ID >	256	257	258	259	260
0.00	0.00	0.00	0.00	0.00	0.00
0.50	0.61	0.66	0.66	0.66	0.66
0.00	0.00	0.00	0.00	0.00	0.00
1.00	1.22	1.31	1.31	1.31	1.31
0.00	0.00	0.00	0.00	0.00	0.00
1.50	1.83	1.96	1.96	1.96	1.96
0.00	0.01	0.01	0.01	0.01	0.01
2.00	2.47	2.66	2.66	2.66	2.66
0.00	0.05	0.07	0.07	0.07	0.07
2.50	3.27	3.56	3.56	3.56	3.56
0.00	0.28	0.37	0.37	0.37	0.37
3.00	4.36	4.72	4.72	4.72	4.72
0.00	0.82	0.97	0.97	0.97	0.97
3.50	5.85	6.29	6.29	6.29	6.29
0.00	1.86	2.08	2.08	2.08	2.08
4.00	7.52	8.03	8.03	8.03	8.03
0.00	3.17	3.50	3.51	3.51	3.51
4.50	9.23	9.79	9.79	9.79	9.79
0.00	4.66	5.07	5.08	5.08	5.08
5.00	11.27	11.66	11.66	11.66	11.66
0.00	6.70	6.90	6.91	6.91	6.91
5.50	13.38	13.57	13.58	13.58	13.58
0.00	8.96	8.91	8.92	8.92	8.92
6.00	15.28	15.47	15.48	15.48	15.48
0.00	11.03	10.98	10.99	10.99	10.99
6.50	16.97	17.24	17.25	17.25	17.25
0.00	12.85	12.92	12.93	12.93	12.93
7.00	18.49	18.85	18.87	18.87	18.87
0.00	14.47	14.68	14.70	14.70	14.70
7.50	19.88	20.32	20.34	20.34	20.34
0.00	15.95	16.26	16.28	16.28	16.28
8.00	21.17	21.66	21.69	21.69	21.69
0.00	17.30	17.68	17.71	17.71	17.71



Multiples of  $p_y$  - Transversely Loaded

b [mm]	450	450	450	450	450
t [mm]	12.5	12.5	12.5	12.5	12.5
$\sigma_y$ [N/mm <sup>2</sup> ]	355	355	355	355	355
$\alpha$	1	2	3	4	5
e/b	infinite	infinite	infinite	infinite	infinite
f/b	0.111	0.111	0.111	0.111	0.111
$p_y$ [N/mm <sup>2</sup> ]	3.3570	3.0985	3.0983	3.0983	3.0983

Run ID >	301	302	303	304	305
0.00	0.00	0.00	0.00	0.00	0.00
0.50	0.18	0.39	0.46	0.47	0.48
0.00	0.00	0.00	0.00	0.00	0.00
1.00	0.36	0.78	0.92	0.95	0.96
0.00	0.00	0.00	0.00	0.00	0.00
1.50	0.55	1.17	1.40	1.47	1.48
0.00	0.00	0.00	0.03	0.04	0.05
2.00	0.74	1.63	2.01	2.22	2.32
0.00	0.02	0.07	0.18	0.33	0.41
2.50	1.01	2.32	4.92	8.76	10.42
0.00	0.10	0.38	2.65	6.47	8.16
3.00	1.33	6.65	13.74	15.79	16.76
0.00	0.24	4.35	11.23	13.27	14.25
3.50	2.06	15.41	20.87	22.88	23.85
0.00	0.77	12.95	18.22	20.22	21.19
4.00	10.02	22.46	27.35	28.73	29.14
0.00	8.59	19.91	24.64	25.98	26.36
4.50	16.19	28.33	32.47	33.73	34.09
0.00	14.66	25.75	29.74	30.94	31.27
5.00	22.03	33.84	37.98	39.02	39.21
0.00	Convergence Failure	31.30	Convergence Failure	36.29	36.43
5.50	Convergence Failure	38.65	Convergence Failure	42.44	42.53
0.00	Convergence Failure	36.17	Convergence Failure	Convergence Failure	39.70
6.00	Convergence Failure	42.33	Convergence Failure	Convergence Failure	45.36
0.00	Convergence Failure	39.87	Convergence Failure	Convergence Failure	42.48
6.50	Convergence Failure	45.53	Convergence Failure	Convergence Failure	47.88
0.00	Convergence Failure	43.06	Convergence Failure	Convergence Failure	Convergence Failure
7.00	Convergence Failure	48.78	Convergence Failure	Convergence Failure	Convergence Failure
0.00	Convergence Failure	Convergence Failure	Convergence Failure	Convergence Failure	Convergence Failure
7.50	Convergence Failure	Convergence Failure	Convergence Failure	Convergence Failure	Convergence Failure
0.00	Convergence Failure	Convergence Failure	Convergence Failure	Convergence Failure	Convergence Failure
8.00	Convergence Failure	Convergence Failure	Convergence Failure	Convergence Failure	Convergence Failure
0.00	Convergence Failure	Convergence Failure	Convergence Failure	Convergence Failure	Convergence Failure



Multiples of  $p_y$  - Longitudinally Loaded

b [mm]	450	450	450	450	450
t [mm]	37.5	37.5	37.5	37.5	37.5
$\sigma_y$ [N/mm <sup>2</sup> ]	235	235	235	235	235
$\alpha$	1	2	3	4	5
e/b	infinite	infinite	infinite	infinite	infinite
f/b	1.000	1.000	1.000	1.000	1.000
$p_y$ [N/mm <sup>2</sup> ]	5.0792	3.6953	3.6381	3.6351	3.6349

Run ID >	306	307	308	309	310
0.00	0.00	0.00	0.00	0.00	0.00
0.50	0.32	0.71	0.85	0.88	0.89
0.00	0.00	0.00	0.00	0.00	0.00
1.00	0.64	1.42	1.70	1.77	1.78
0.00	0.00	0.00	0.00	0.00	0.00
1.50	0.97	2.14	2.60	2.73	2.76
0.00	0.01	0.01	0.06	0.09	0.10
2.00	1.34	2.98	3.92	4.47	4.71
0.00	0.05	0.14	0.55	0.99	1.20
2.50	1.86	4.55	8.68	11.16	12.25
0.00	0.25	1.03	4.71	7.25	8.41
3.00	2.60	9.90	14.81	16.69	17.53
0.00	0.67	5.97	10.66	12.57	13.44
3.50	5.09	16.24	20.68	22.21	22.91
0.00	2.84	12.28	16.54	18.07	18.78
4.00	12.02	21.92	26.23	27.50	27.94
0.00	9.71	18.08	22.30	23.52	23.93
4.50	17.47	26.70	29.59	30.34	30.60
0.00	15.22	23.07	25.69	26.29	26.49
5.00	21.66	29.76	31.99	32.60	32.81
0.00	19.46	26.18	28.03	28.45	28.58
5.50	25.01	32.22	34.31	34.90	35.11
0.00	22.85	28.64	30.33	30.72	30.85
6.00	27.93	34.48	36.41	36.93	37.11
0.00	25.80	30.91	32.42	32.72	32.80
6.50	30.52	36.54	38.19	38.63	38.79
0.00	28.42	32.97	34.14	34.34	34.38
7.00	32.79	38.41	39.90	40.24	40.32
0.00	30.70	34.82	35.78	35.83	35.77
7.50	34.94	40.45	42.05	42.37	42.29
0.00	32.87	36.86	37.93	37.96	37.71
8.00	37.11	42.73	44.70	45.14	45.14
0.00	35.06	39.17	40.66	Convergence Failure	40.70



Multiples of  $p_y$  - Longitudinally Loaded

b [mm]	500	500	500	500	500
t [mm]	25.0	25.0	25.0	25.0	25.0
$\sigma_y$ [N/mm <sup>2</sup> ]	235	235	235	235	235
$\alpha$	1	2	3	4	5
e/b	infinite	infinite	infinite	infinite	infinite
f/b	1.000	1.000	1.000	1.000	1.000
$p_y$ [N/mm <sup>2</sup> ]	1.8472	1.3395	1.3183	1.3173	1.3172

Run ID >	311	312	313	314	315
0.00	0.00	0.00	0.00	0.00	0.00
0.50	0.31	0.69	0.83	0.86	0.87
0.00	0.00	0.00	0.00	0.00	0.00
1.00	0.62	1.38	1.65	1.72	1.73
0.00	0.00	0.00	0.00	0.00	0.00
1.50	0.93	2.06	2.50	2.62	2.65
0.00	0.01	0.01	0.05	0.08	0.09
2.00	1.30	2.85	3.64	4.04	4.20
0.00	0.07	0.14	0.44	0.76	0.91
2.50	1.81	4.15	6.36	7.41	7.88
0.00	0.28	0.84	2.72	3.83	4.35
3.00	2.53	6.87	9.27	10.06	10.39
0.00	0.70	3.26	5.55	6.37	6.71
3.50	4.35	9.90	12.18	12.85	13.10
0.00	2.26	6.32	8.51	9.15	9.39
4.00	7.56	12.72	14.83	15.55	15.79
0.00	5.47	9.30	11.31	11.98	12.19
4.50	10.40	15.16	16.96	17.48	17.64
0.00	8.43	11.95	13.56	13.97	14.07
5.00	12.60	17.08	18.45	18.88	19.00
0.00	10.72	14.00	15.08	15.35	15.40
5.50	14.49	18.52	19.66	20.03	20.13
0.00	12.68	15.50	16.27	16.45	16.47
6.00	16.08	19.71	20.75	21.06	21.15
0.00	14.33	16.71	17.33	17.44	17.44
6.50	17.49	20.75	21.72	22.02	22.10
0.00	15.79	17.75	18.27	18.35	18.34
7.00	18.78	21.73	22.60	22.86	22.94
0.00	17.12	18.71	19.10	19.14	19.12
7.50	19.94	22.68	23.50	23.73	23.79
0.00	18.31	19.66	19.98	19.97	19.90
8.00	21.02	23.67	24.39	24.58	24.63
0.00	19.41	20.66	20.84	Convergence Failure	20.67



Multiples of  $p_y$  - Longitudinally Loaded

b [mm]	350	350	350	350	350
t [mm]	12.5	12.5	12.5	12.5	12.5
$\sigma_y$ [N/mm <sup>2</sup> ]	235	235	235	235	235
$\alpha$	1	2	3	4	5
e/b	infinite	infinite	infinite	infinite	infinite
f/b	1.000	1.000	1.000	1.000	1.000
$p_y$ [N/mm <sup>2</sup> ]	0.9397	0.6814	0.6705	0.6700	0.6699

Run ID >	316	317	318	319	320
0.00	0.00	0.00	0.00	0.00	0.00
0.50	0.50	1.14	1.37	1.42	1.44
0.00	0.00	0.00	0.00	0.00	0.00
1.00	1.01	2.25	2.68	2.79	2.81
0.00	0.00	0.00	0.00	0.00	0.00
1.50	1.52	3.33	3.99	4.16	4.20
0.00	0.01	0.01	0.07	0.11	0.12
2.00	2.13	4.52	5.52	5.87	6.00
0.00	0.13	0.20	0.52	0.74	0.85
2.50	2.95	6.18	8.07	8.90	9.28
0.00	0.48	1.00	2.41	3.30	3.73
3.00	4.07	8.75	10.97	11.77	12.13
0.00	1.14	3.17	5.26	6.12	6.50
3.50	6.04	11.39	13.58	14.39	14.54
0.00	2.76	5.85	7.94	8.74	8.85
4.00	8.83	14.15	16.15	16.95	17.08
0.00	5.56	8.89	10.71	11.43	11.50
4.50	11.61	16.51	18.46	19.17	19.24
0.00	8.55	11.54	13.23	13.79	13.76
5.00	13.85	18.57	20.23	20.87	20.91
0.00	10.96	13.84	15.11	15.56	15.48
5.50	15.75	20.24	21.69	22.22	22.26
0.00	13.00	15.67	16.61	16.92	16.82
6.00	17.43	21.60	22.88	23.35	23.37
0.00	14.79	17.11	17.79	18.00	17.87
6.50	18.93	22.77	23.96	24.41	24.42
0.00	16.39	18.29	18.84	19.01	18.86
7.00	20.32	23.80	24.94	25.37	25.38
0.00	17.87	19.33	19.78	19.91	19.74
7.50	21.60	24.77	25.88	26.28	26.27
0.00	19.21	20.29	20.66	20.74	20.56
8.00	22.79	25.70	26.79	27.18	27.16
0.00	20.45	21.20	21.54	21.59	21.38



Multiples of  $p_y$  - Longitudinally Loaded

b [mm]	450	450	450	450	450
t [mm]	12.5	12.5	12.5	12.5	12.5
$\sigma_y$ [N/mm <sup>2</sup> ]	235	235	235	235	235
$\alpha$	1	2	3	4	5
e/b	infinite	infinite	infinite	infinite	infinite
f/b	1.000	1.000	1.000	1.000	1.000
$p_y$ [N/mm <sup>2</sup> ]	0.5680	0.4118	0.4052	0.4049	0.4049



Run ID >	321	322	323	324	325
0.00	0.00	0.00	0.00	0.00	0.00
0.50	0.18	0.38	0.44	0.46	0.46
0.00	0.00	0.00	0.00	0.00	0.00
1.00	0.35	0.75	0.88	0.91	0.92
0.00	0.00	0.00	0.00	0.00	0.00
1.50	0.53	1.13	1.35	1.41	1.43
0.00	0.00	0.00	0.03	0.04	0.05
2.00	0.72	1.57	1.92	2.10	2.18
0.00	0.01	0.06	0.15	0.27	0.34
2.50	0.96	2.22	3.88	6.69	8.90
0.00	0.08	0.34	1.68	4.45	6.69
3.00	1.26	4.53	12.47	14.62	15.51
0.00	0.20	2.28	10.00	12.14	13.04
3.50	1.87	13.82	19.77	21.90	22.86
0.00	0.62	11.39	17.16	19.27	20.23
4.00	7.52	21.03	26.08	27.62	28.14
0.00	6.11	18.50	23.39	24.88	25.39
4.50	14.33	26.64	30.98	32.27	32.62
0.00	12.83	24.05	28.22	29.44	29.76
5.00	19.88	32.05	35.98	37.09	37.41
0.00	18.29	29.46	33.22	Convergence Failure	Convergence Failure
5.50	25.55	36.88	40.67	Convergence Failure	Convergence Failure
0.00	23.94	34.32	Convergence Failure	Convergence Failure	Convergence Failure
6.00	30.46	41.40	Convergence Failure	Convergence Failure	Convergence Failure
0.00	Convergence Failure	Convergence Failure	Convergence Failure	Convergence Failure	Convergence Failure
6.50	Convergence Failure	Convergence Failure	Convergence Failure	Convergence Failure	Convergence Failure
0.00	Convergence Failure	Convergence Failure	Convergence Failure	Convergence Failure	Convergence Failure
7.00	Convergence Failure	Convergence Failure	Convergence Failure	Convergence Failure	Convergence Failure
0.00	Convergence Failure	Convergence Failure	Convergence Failure	Convergence Failure	Convergence Failure
7.50	Convergence Failure	Convergence Failure	Convergence Failure	Convergence Failure	Convergence Failure
0.00	Convergence Failure	Convergence Failure	Convergence Failure	Convergence Failure	Convergence Failure
8.00	Convergence Failure	Convergence Failure	Convergence Failure	Convergence Failure	Convergence Failure
0.00	Convergence Failure	Convergence Failure	Convergence Failure	Convergence Failure	Convergence Failure



### Multiples of $p_y$ - Longitudinally Loaded

b [mm]	450	450	450	450	450
t [mm]	37.5	37.5	37.5	37.5	37.5
$\alpha_y$ [N/mm <sup>2</sup> ]	235	235	235	235	235
$\alpha$	1	2	3	4	5
e/b	infinite	infinite	infinite	infinite	infinite
f/b	0.667	0.667	0.667	0.667	0.667
$p_y$ [N/mm <sup>2</sup> ]	5.4542	4.0329	3.9740	3.9709	3.9707

Run ID >	326	327	328	329	330
0.00	0.00	0.00	0.00	0.00	0.00
0.50	0.31	0.68	0.82	0.85	0.85
0.00	0.00	0.00	0.00	0.00	0.00
1.00	0.62	1.37	1.63	1.69	1.70
0.00	0.00	0.00	0.00	0.00	0.00
1.50	0.94	2.06	2.49	2.61	2.64
0.00	0.01	0.01	0.06	0.08	0.09
2.00	1.28	2.86	3.76	4.27	4.49
0.00	0.04	0.13	0.53	0.93	1.14
2.50	1.76	4.31	7.50	9.95	11.15
0.00	0.22	0.92	3.62	6.10	7.36
3.00	2.42	8.32	13.63	15.36	16.16
0.00	0.55	4.42	9.52	11.27	12.10
3.50	3.74	14.81	19.57	21.47	22.11
0.00	1.55	10.82	15.43	17.33	17.98
4.00	9.74	20.57	24.90	26.30	26.80
0.00	7.39	16.67	20.87	22.23	22.72
4.50	15.68	25.41	28.76	29.65	29.93
0.00	13.37	21.68	24.83	25.58	25.80
5.00	20.08	28.89	31.37	32.01	32.20
0.00	17.82	25.26	27.38	27.83	27.93
5.50	23.66	31.41	33.46	34.00	34.16
0.00	21.44	27.77	29.38	29.70	29.76
6.00	26.67	33.58	35.54	36.07	36.21
0.00	24.47	29.91	31.39	31.69	31.73
6.50	29.39	35.69	37.77	38.36	38.52
0.00	27.22	32.01	33.60	33.96	34.01
7.00	31.86	37.87	39.70	40.18	40.31
0.00	29.70	Convergence Failure	35.51	35.71	35.70
7.50	34.17	Convergence Failure	41.49	41.84	41.88
0.00	32.03	Convergence Failure	37.23	37.26	37.14
8.00	36.37	Convergence Failure	43.20	43.54	43.57
0.00	Convergence Failure	Convergence Failure	38.88	38.89	38.75



Multiples of  $p_y$  - Longitudinally Loaded

b [mm]	500	500	500	500	500
t [mm]	25.0	25.0	25.0	25.0	25.0
$\sigma_y$ [N/mm <sup>2</sup> ]	235	235	235	235	235
$\alpha$	1	2	3	4	5
e/b	infinite	infinite	infinite	infinite	infinite
f/b	0.600	0.600	0.600	0.600	0.600
$p_y$ [N/mm <sup>2</sup> ]	2.0782	1.5377	1.5152	1.5140	1.5139

Run ID >	331	332	333	334	335
0.00	0.00	0.00	0.00	0.00	0.00
0.50	0.30	0.66	0.79	0.82	0.83
0.00	0.00	0.00	0.00	0.00	0.00
1.00	0.59	1.32	1.57	1.64	1.65
0.00	0.00	0.00	0.00	0.00	0.00
1.50	0.89	1.98	2.39	2.51	2.53
0.00	0.01	0.01	0.06	0.08	0.09
2.00	1.24	2.73	3.51	3.91	4.07
0.00	0.06	0.13	0.45	0.77	0.92
2.50	1.71	3.99	5.77	6.76	7.23
0.00	0.23	0.80	2.20	3.23	3.75
3.00	2.35	6.23	8.69	9.56	9.93
0.00	0.58	2.67	4.99	5.91	6.30
3.50	3.51	9.08	11.53	12.32	12.60
0.00	1.46	5.47	7.84	8.63	8.92
4.00	6.18	12.01	14.33	15.03	15.27
0.00	4.02	8.54	10.77	11.42	11.64
4.50	9.25	14.54	16.42	16.95	17.12
0.00	7.17	11.25	12.95	13.37	13.49
5.00	11.69	16.47	18.01	18.43	18.55
0.00	9.71	13.30	14.56	14.83	14.89
5.50	13.61	17.99	19.30	19.64	19.75
0.00	11.71	14.88	15.83	16.00	16.02
6.00	15.28	19.23	20.40	20.72	20.82
0.00	13.44	16.14	16.90	17.01	17.02
6.50	16.76	20.33	21.45	21.79	21.89
0.00	14.97	17.23	17.91	18.03	18.04
7.00	18.09	21.34	22.43	22.71	22.79
0.00	16.33	18.23	18.85	18.89	18.87
7.50	19.29	22.34	23.34	23.57	23.63
0.00	17.57	19.22	19.71	19.67	19.61
8.00	20.41	23.34	24.13	24.36	24.43
0.00	18.71	20.21	20.44	20.38	20.32



Multiples of  $p_y$  - Longitudinally Loaded

b [mm]	350	350	350	350	350
t [mm]	12.5	12.5	12.5	12.5	12.5
$\sigma_y$ [N/mm <sup>2</sup> ]	235	235	235	235	235
$\alpha$	1	2	3	4	5
e/b	infinite	infinite	infinite	infinite	infinite
f/b	0.571	0.571	0.571	0.571	0.571
$p_y$ [N/mm <sup>2</sup> ]	1.0794	0.8008	0.7891	0.7885	0.7884

Run ID >	336	337	338	339	340
0.00	0.00	0.00	0.00	0.00	0.00
0.50	0.48	1.09	1.30	1.35	1.36
0.00	0.00	0.00	0.00	0.00	0.00
1.00	0.97	2.15	2.56	2.65	2.68
0.00	0.00	0.00	0.00	0.00	0.00
1.50	1.46	3.19	3.82	3.98	4.03
0.00	0.01	0.01	0.08	0.11	0.12
2.00	2.02	4.34	5.33	5.71	5.86
0.00	0.10	0.19	0.53	0.79	0.93
2.50	2.78	5.97	7.72	8.41	8.71
0.00	0.40	0.99	2.26	2.95	3.26
3.00	3.78	8.23	10.42	11.24	11.60
0.00	0.95	2.75	4.75	5.64	6.03
3.50	5.32	10.67	12.83	13.58	13.86
0.00	2.10	5.09	7.14	7.89	8.16
4.00	7.54	13.39	15.68	16.42	16.68
0.00	4.14	8.02	10.20	10.87	11.08
4.50	10.34	15.89	18.09	18.76	18.97
0.00	7.06	10.79	12.79	13.33	13.46
5.00	12.80	18.01	19.86	20.40	20.56
0.00	9.72	13.15	14.62	14.96	15.01
5.50	14.81	19.68	21.32	21.84	21.98
0.00	11.88	14.94	16.10	16.39	16.42
6.00	16.56	21.08	22.59	23.07	23.21
0.00	13.76	16.41	17.37	17.59	17.60
6.50	18.13	22.30	23.70	24.13	24.25
0.00	15.43	17.66	18.44	18.56	18.55
7.00	19.59	23.40	24.76	25.17	25.28
0.00	16.97	18.75	19.45	19.53	19.50
7.50	20.92	24.40	25.75	26.15	26.26
0.00	18.38	19.75	20.39	20.44	20.40
8.00	22.15	25.35	26.66	27.02	27.13
0.00	19.65	20.68	21.24	21.24	21.18



Multiples of  $p_y$  - Longitudinally Loaded

b [mm]	450	450	450	450	450
t [mm]	12.5	12.5	12.5	12.5	12.5
$\sigma_y$ [N/mm <sup>2</sup> ]	235	235	235	235	235
$\alpha$	1	2	3	4	5
e/b	infinite	infinite	infinite	infinite	infinite
f/b	0.556	0.556	0.556	0.556	0.556
$p_y$ [N/mm <sup>2</sup> ]	0.6612	0.4912	0.4840	0.4837	0.4837

Run ID >	341	342	343	344	345
0.00	0.00	0.00	0.00	0.00	0.00
0.50	0.16	0.34	0.40	0.41	0.42
0.00	0.00	0.00	0.00	0.00	0.00
1.00	0.32	0.69	0.80	0.83	0.83
0.00	0.00	0.00	0.00	0.00	0.00
1.50	0.48	1.03	1.22	1.27	1.28
0.00	0.00	0.00	0.02	0.03	0.03
2.00	0.65	1.42	1.71	1.79	1.82
0.00	0.01	0.05	0.11	0.14	0.16
2.50	0.84	1.93	2.78	3.34	4.08
0.00	0.04	0.21	0.78	1.27	2.01
3.00	1.09	3.00	8.59	11.73	12.89
0.00	0.13	0.95	6.25	9.38	10.56
3.50	1.47	9.48	15.93	18.59	19.59
0.00	0.35	7.15	13.41	16.07	17.07
4.00	2.21	17.25	22.63	24.54	25.29
0.00	0.92	14.82	20.01	21.89	22.64
4.50	9.22	23.03	27.76	29.16	29.65
0.00	7.80	20.50	25.05	26.40	26.87
5.00	14.90	27.75	32.35	33.62	34.06
0.00	13.39	25.15	29.58	30.78	31.19
5.50	19.76	32.85	36.78	37.82	38.20
0.00	18.17	Convergence Failure	34.00	34.94	35.27
6.00	25.11	Convergence Failure	40.63	41.35	41.58
0.00	Convergence Failure	Convergence Failure	37.81	38.40	38.57
6.50	Convergence Failure	Convergence Failure	44.46	45.15	45.23
0.00	Convergence Failure	Convergence Failure	Convergence Failure	Convergence Failure	Convergence Failure
7.00	Convergence Failure	Convergence Failure	Convergence Failure	Convergence Failure	Convergence Failure
0.00	Convergence Failure	Convergence Failure	Convergence Failure	Convergence Failure	Convergence Failure
7.50	Convergence Failure	Convergence Failure	Convergence Failure	Convergence Failure	Convergence Failure
0.00	Convergence Failure	Convergence Failure	Convergence Failure	Convergence Failure	Convergence Failure
8.00	Convergence Failure	Convergence Failure	Convergence Failure	Convergence Failure	Convergence Failure
0.00	Convergence Failure	Convergence Failure	Convergence Failure	Convergence Failure	Convergence Failure



Multiples of  $p_y$  - Longitudinally Loaded

b [mm]	450	450	450	450	450
t [mm]	37.5	37.5	37.5	37.5	37.5
$\sigma_y$ [N/mm <sup>2</sup> ]	235	235	235	235	235
$\alpha$	1	2	3	4	5
e/b	infinite	infinite	infinite	infinite	infinite
f/b	0.333	0.333	0.333	0.333	0.333
$p_y$ [N/mm <sup>2</sup> ]	8.0134	6.1441	6.0651	6.0609	6.0606

Run ID >	346	347	348	349	350
0.00	0.00	0.00	0.00	0.00	0.00
0.50	0.27	0.60	0.71	0.74	0.74
0.00	0.00	0.00	0.00	0.00	0.00
1.00	0.54	1.20	1.42	1.47	1.48
0.00	0.00	0.00	0.00	0.00	0.00
1.50	0.81	1.80	2.18	2.27	2.30
0.00	0.00	0.01	0.05	0.07	0.08
2.00	1.09	2.49	3.21	3.60	3.76
0.00	0.02	0.11	0.38	0.68	0.82
2.50	1.45	3.71	5.54	6.73	7.73
0.00	0.11	0.74	2.08	3.18	4.21
3.00	1.92	5.81	10.59	12.81	13.75
0.00	0.31	2.29	6.72	9.00	9.99
3.50	2.77	10.77	15.86	17.77	18.67
0.00	0.88	6.94	11.85	13.79	14.72
4.00	4.16	16.34	21.41	22.93	23.45
0.00	2.00	12.47	17.42	18.90	19.40
4.50	9.47	21.31	25.25	26.38	26.78
0.00	7.15	17.50	21.22	22.27	22.63
5.00	14.60	24.97	28.27	29.13	29.39
0.00	12.30	21.18	24.20	24.92	25.12
5.50	18.38	28.00	30.72	31.38	31.57
0.00	16.07	24.23	26.57	27.05	27.16
6.00	21.71	30.59	32.97	33.62	33.87
0.00	19.41	26.82	28.76	29.21	29.37
6.50	24.94	32.90	35.22	35.87	36.06
0.00	22.67	29.12	Convergence Failure	31.41	31.49
7.00	28.07	35.09	Convergence Failure	37.57	37.72
0.00	25.85	31.31	Convergence Failure	Convergence Failure	37.61
7.50	30.80	37.11	Convergence Failure	Convergence Failure	Convergence Failure
0.00	Convergence Failure	33.32	Convergence Failure	Convergence Failure	Convergence Failure
8.00	Convergence Failure	39.04	Convergence Failure	Convergence Failure	Convergence Failure
0.00	Convergence Failure	35.23	Convergence Failure	Convergence Failure	Convergence Failure



Multiples of  $p_y$  - Longitudinally Loaded

b [mm]	500	500	500	500	500
t [mm]	25.0	25.0	25.0	25.0	25.0
$\sigma_y$ [N/mm <sup>2</sup> ]	235	235	235	235	235
$\alpha$	1	2	3	4	5
e/b	infinite	infinite	infinite	infinite	infinite
f/b	0.200	0.200	0.200	0.200	0.200
$p_y$ [N/mm <sup>2</sup> ]	4.3203	3.3624	3.3210	3.3188	3.3187

Run ID >	351	352	353	354	355
0.00	0.00	0.00	0.00	0.00	0.00
0.50	0.25	0.57	0.68	0.70	0.71
0.00	0.00	0.00	0.00	0.00	0.00
1.00	0.50	1.14	1.35	1.40	1.41
0.00	0.00	0.00	0.00	0.00	0.00
1.50	0.76	1.71	2.06	2.14	2.17
0.00	0.00	0.01	0.04	0.06	0.07
2.00	1.02	2.35	3.08	3.44	3.58
0.00	0.02	0.10	0.44	0.72	0.85
2.50	1.37	3.54	4.97	5.58	5.86
0.00	0.12	0.78	1.84	2.41	2.70
3.00	1.86	5.14	7.33	8.29	8.71
0.00	0.35	1.97	3.91	4.92	5.38
3.50	2.65	7.28	9.61	10.49	10.87
0.00	0.90	3.86	6.09	7.00	7.39
4.00	3.82	9.93	12.48	13.34	13.68
0.00	1.83	6.50	9.02	9.89	10.23
4.50	5.93	12.48	14.83	15.47	15.68
0.00	3.82	9.17	11.42	11.99	12.17
5.00	8.57	14.50	16.39	16.86	17.01
0.00	6.50	11.26	12.92	13.28	13.37
5.50	10.79	16.10	17.68	18.10	18.23
0.00	8.79	12.88	14.15	14.43	14.49
6.00	12.47	17.44	18.90	19.28	19.40
0.00	10.51	14.22	15.33	15.54	15.58
6.50	14.02	18.64	19.99	20.35	20.45
0.00	12.08	15.41	16.37	16.54	16.57
7.00	15.48	19.72	21.00	21.35	21.46
0.00	13.59	16.49	17.33	17.48	17.49
7.50	16.85	20.71	21.93	22.26	22.37
0.00	14.99	17.46	18.20	18.29	18.29
8.00	18.11	21.63	22.76	23.09	23.21
0.00	16.28	18.35	18.96	19.02	19.02



Multiples of  $p_y$  - Longitudinally Loaded

b [mm]	350	350	350	350	350
t [mm]	12.5	12.5	12.5	12.5	12.5
$\sigma_y$ [N/mm <sup>2</sup> ]	235	235	235	235	235
$\alpha$	1	2	3	4	5
e/b	infinite	infinite	infinite	infinite	infinite
f/b	0.143	0.143	0.143	0.143	0.143
$p_y$ [N/mm <sup>2</sup> ]	2.9362	2.3030	2.2754	2.2738	2.2738

Run ID >	356	357	358	359	360
0.00	0.00	0.00	0.00	0.00	0.00
0.50	0.41	0.92	1.10	1.14	1.15
0.00	0.00	0.00	0.00	0.00	0.00
1.00	0.81	1.83	2.18	2.26	2.28
0.00	0.00	0.00	0.00	0.00	0.00
1.50	1.22	2.74	3.27	3.41	3.45
0.00	0.00	0.02	0.06	0.09	0.10
2.00	1.65	3.74	4.76	5.20	5.37
0.00	0.04	0.17	0.62	0.97	1.13
2.50	2.20	5.43	7.09	7.66	7.88
0.00	0.19	1.14	2.36	2.91	3.13
3.00	2.99	7.33	9.31	10.05	10.36
0.00	0.60	2.54	4.23	4.99	5.32
3.50	4.18	9.34	11.43	12.21	12.55
0.00	1.43	4.25	6.16	6.97	7.33
4.00	5.68	11.54	14.01	14.90	15.07
0.00	2.62	6.35	8.76	9.68	9.81
4.50	7.47	13.99	16.46	17.28	17.43
0.00	4.24	8.95	11.35	12.12	12.20
5.00	9.78	16.14	18.48	19.19	19.31
0.00	6.56	11.27	13.41	13.99	14.03
5.50	12.01	17.89	19.96	20.55	20.65
0.00	8.93	13.10	14.82	15.22	15.23
6.00	13.89	19.38	21.17	21.70	21.78
0.00	10.92	14.62	15.92	16.23	16.19
6.50	15.44	20.65	22.31	22.81	22.86
0.00	12.54	15.87	16.98	17.22	17.14
7.00	16.86	21.77	23.40	23.89	23.93
0.00	14.01	16.97	18.00	18.22	18.13
7.50	18.20	22.83	24.41	24.88	24.93
0.00	15.41	18.00	18.95	19.13	19.02
8.00	19.48	23.82	25.34	25.80	25.84
0.00	16.73	18.96	19.80	19.95	19.83



Multiples of  $p_y$  - Longitudinally Loaded

b [mm]	450	450	450	450	450
t [mm]	12.5	12.5	12.5	12.5	12.5
$\sigma_y$ [N/mm <sup>2</sup> ]	235	235	235	235	235
$\alpha$	1	2	3	4	5
e/b	infinite	infinite	infinite	infinite	infinite
f/b	0.111	0.111	0.111	0.111	0.111
$p_y$ [N/mm <sup>2</sup> ]	2.2222	1.7510	1.7302	1.7292	1.7291



Run ID >	401	402	403	404	405
0.00	0.00	0.00	0.00	0.00	0.00
0.50	0.28	0.59	0.69	0.72	0.72
0.00	0.00	0.00	0.00	0.00	0.00
1.00	0.55	1.18	1.38	1.43	1.44
0.00	0.00	0.00	0.00	0.00	0.00
1.50	0.83	1.77	2.12	2.21	2.23
0.00	0.00	0.00	0.04	0.07	0.07
2.00	1.12	2.45	3.03	3.34	3.48
0.00	0.02	0.10	0.26	0.49	0.60
2.50	1.52	3.49	6.98	10.65	12.38
0.00	0.14	0.56	3.59	7.26	9.03
3.00	2.01	8.60	15.75	18.12	19.10
0.00	0.36	5.16	12.07	14.44	15.43
3.50	3.11	17.52	23.18	25.43	26.41
0.00	1.16	13.90	19.33	21.58	22.57
4.00	11.52	25.41	31.41	33.51	34.27
0.00	9.39	21.74	27.62	29.71	30.46
4.50	19.15	33.08	38.00	39.36	39.74
0.00	16.91	29.53	34.33	35.60	35.93
5.00	27.16	39.13	43.03	44.07	44.33
0.00	Convergence Failure	Convergence Failure	39.43	40.35	40.54
5.50	Convergence Failure	Convergence Failure	46.81	47.57	47.71
0.00	Convergence Failure	Convergence Failure	43.21	Convergence Failure	43.87
6.00	Convergence Failure	Convergence Failure	50.05	Convergence Failure	50.68
0.00	Convergence Failure	Convergence Failure	46.41	Convergence Failure	46.76
6.50	Convergence Failure	Convergence Failure	53.42	Convergence Failure	53.71
0.00	Convergence Failure	Convergence Failure	Convergence Failure	Convergence Failure	Convergence Failure
7.00	Convergence Failure	Convergence Failure	Convergence Failure	Convergence Failure	Convergence Failure
0.00	Convergence Failure	Convergence Failure	Convergence Failure	Convergence Failure	Convergence Failure
7.50	Convergence Failure	Convergence Failure	Convergence Failure	Convergence Failure	Convergence Failure
0.00	Convergence Failure	Convergence Failure	Convergence Failure	Convergence Failure	Convergence Failure
8.00	Convergence Failure	Convergence Failure	Convergence Failure	Convergence Failure	Convergence Failure
0.00	Convergence Failure	Convergence Failure	Convergence Failure	Convergence Failure	Convergence Failure



Multiples of  $p_y$  - Longitudinally Loaded

b [mm]	450	450	450	450	450
t [mm]	37.5	37.5	37.5	37.5	37.5
$\sigma_y$ [N/mm <sup>2</sup> ]	355	355	355	355	355
$\alpha$	1	2	3	4	5
e/b	infinite	infinite	infinite	infinite	infinite
f/b	1.000	1.000	1.000	1.000	1.000
$p_y$ [N/mm <sup>2</sup> ]	7.6729	5.5822	5.4959	5.4913	5.4910

Run ID >	406	407	408	409	410
0.00	0.00	0.00	0.00	0.00	0.00
0.50	0.48	1.08	1.29	1.34	1.35
0.00	0.00	0.00	0.00	0.00	0.00
1.00	0.97	2.15	2.56	2.66	2.68
0.00	0.00	0.00	0.00	0.00	0.00
1.50	1.46	3.22	3.90	4.08	4.13
0.00	0.01	0.01	0.08	0.13	0.14
2.00	2.02	4.46	5.75	6.44	6.72
0.00	0.08	0.21	0.73	1.27	1.54
2.50	2.79	6.61	10.86	13.13	14.12
0.00	0.38	1.37	5.06	7.43	8.51
3.00	3.89	11.92	16.67	18.28	18.93
0.00	0.99	6.14	10.68	12.34	13.01
3.50	6.80	18.09	22.25	23.63	24.16
0.00	3.45	12.32	16.28	17.64	18.14
4.00	13.47	23.47	27.53	28.92	29.41
0.00	10.06	17.88	21.80	23.14	23.59
4.50	19.28	28.33	31.55	32.46	32.75
0.00	15.99	23.07	26.00	26.72	26.91
5.00	23.92	31.85	34.37	35.14	35.36
0.00	20.77	26.75	28.80	29.32	29.42
5.50	27.64	34.73	37.09	37.82	38.03
0.00	Convergence Failure	29.71	31.54	32.00	32.09
6.00	Convergence Failure	37.32	39.39	40.01	40.19
0.00	Convergence Failure	32.36	33.83	34.16	34.19
6.50	Convergence Failure	39.50	41.32	41.88	42.03
0.00	Convergence Failure	34.57	35.69	35.92	35.92
7.00	Convergence Failure	41.44	43.14	43.62	43.72
0.00	Convergence Failure	Convergence Failure	37.44	37.56	37.49
7.50	Convergence Failure	Convergence Failure	45.12	45.60	45.68
0.00	Convergence Failure	Convergence Failure	39.38	39.49	Convergence Failure
8.00	Convergence Failure	Convergence Failure	47.35	47.78	Convergence Failure
0.00	Convergence Failure	Convergence Failure	41.63	Convergence Failure	Convergence Failure



Multiples of  $p_y$  - Longitudinally Loaded

b [mm]	500	500	500	500	500
t [mm]	25.0	25.0	25.0	25.0	25.0
$\sigma_y$ [N/mm <sup>2</sup> ]	355	355	355	355	355
$\alpha$	1	2	3	4	5
e/b	infinite	infinite	infinite	infinite	infinite
f/b	1.000	1.000	1.000	1.000	1.000
$p_y$ [N/mm <sup>2</sup> ]	2.7904	2.0235	1.9915	1.9899	1.9898

Run ID >	411	412	413	414	415
0.00	0.00	0.00	0.00	0.00	0.00
0.50	0.47	1.05	1.25	1.30	1.31
0.00	0.00	0.00	0.00	0.00	0.00
1.00	0.93	2.07	2.47	2.56	2.58
0.00	0.00	0.00	0.00	0.00	0.00
1.50	1.40	3.07	3.68	3.84	3.88
0.00	0.01	0.01	0.07	0.10	0.11
2.00	1.95	4.17	5.15	5.48	5.63
0.00	0.10	0.18	0.51	0.72	0.85
2.50	2.70	5.77	7.69	8.55	8.94
0.00	0.41	0.95	2.43	3.36	3.80
3.00	3.72	8.34	10.59	11.39	11.73
0.00	1.00	3.14	5.28	6.14	6.50
3.50	5.57	11.05	13.25	13.90	14.14
0.00	2.51	5.88	8.01	8.64	8.85
4.00	8.46	13.78	15.74	16.38	16.63
0.00	5.38	8.86	10.65	11.21	11.42
4.50	11.38	16.10	18.00	18.54	18.73
0.00	8.50	11.44	13.10	13.49	13.60
5.00	13.70	18.14	19.75	20.19	20.35
0.00	10.99	13.71	14.96	15.21	15.27
5.50	15.66	19.75	21.16	21.56	21.70
0.00	13.08	15.46	16.41	16.58	16.62
6.00	17.31	21.11	22.37	22.72	22.85
0.00	14.83	16.89	17.61	17.70	17.71
6.50	18.75	22.30	23.53	23.86	23.98
0.00	16.35	18.11	18.77	18.82	18.81
7.00	20.08	23.38	24.55	24.86	24.97
0.00	17.73	19.20	19.76	19.78	19.75
7.50	21.32	24.37	25.49	25.77	25.86
0.00	19.03	20.18	20.65	20.62	20.57
8.00	22.51	25.34	26.43	26.70	26.78
0.00	20.26	21.14	21.56	21.50	21.43



Multiples of  $p_y$  - Longitudinally Loaded

b [mm]	350	350	350	350	350
t [mm]	12.5	12.5	12.5	12.5	12.5
$\alpha_y$ [N/mm <sup>2</sup> ]	355	355	355	355	355
$\alpha$	1	2	3	4	5
e/b	infinite	infinite	infinite	infinite	infinite
f/b	1.000	1.000	1.000	1.000	1.000
$p_y$ [N/mm <sup>2</sup> ]	1.4195	1.0293	1.0129	1.0121	1.0120

Run ID >	416	417	418	419	420
0.00	0.00	0.00	0.00	0.00	0.00
0.50	0.76	1.71	2.05	2.13	2.15
0.00	0.00	0.00	0.00	0.00	0.00
1.00	1.52	3.35	3.95	4.09	4.12
0.00	0.00	0.00	0.00	0.00	0.00
1.50	2.28	4.86	5.68	5.89	5.96
0.00	0.02	0.01	0.06	0.10	0.12
2.00	3.17	6.40	7.47	7.81	7.93
0.00	0.19	0.22	0.47	0.64	0.71
2.50	4.31	8.28	9.86	10.40	10.64
0.00	0.66	1.04	1.97	2.44	2.67
3.00	5.74	10.63	12.52	13.26	13.60
0.00	1.51	2.82	4.43	5.22	5.58
3.50	7.72	12.96	14.81	15.52	15.86
0.00	3.08	5.13	6.79	7.47	7.78
4.00	10.04	15.34	17.42	18.07	18.31
0.00	5.33	7.76	9.66	10.18	10.34
4.50	12.59	17.64	19.70	20.41	20.66
0.00	8.11	10.45	12.21	12.73	12.89
5.00	14.88	19.73	21.68	22.28	22.49
0.00	10.68	12.90	14.39	14.71	14.80
5.50	16.86	21.53	23.29	23.85	24.05
0.00	12.89	14.96	16.12	16.36	16.42
6.00	18.60	23.07	24.73	25.25	25.44
0.00	14.83	16.69	17.65	17.82	17.84
6.50	20.13	24.41	25.97	26.46	26.63
0.00	16.50	18.14	18.90	19.01	19.02
7.00	21.54	25.62	27.12	27.58	27.75
0.00	18.04	19.40	20.04	20.10	20.08
7.50	22.87	26.70	28.17	28.62	28.78
0.00	19.47	20.49	21.05	21.08	21.05
8.00	24.13	27.74	29.18	29.60	29.75
0.00	20.81	21.53	22.02	22.01	21.96



Multiples of  $p_y$  - Longitudinally Loaded

b [mm]	450	450	450	450	450
t [mm]	12.5	12.5	12.5	12.5	12.5
$\sigma_y$ [N/mm <sup>2</sup> ]	355	355	355	355	355
$\alpha$	1	2	3	4	5
e/b	infinite	infinite	infinite	infinite	infinite
f/b	1.000	1.000	1.000	1.000	1.000
$p_y$ [N/mm <sup>2</sup> ]	0.8580	0.6221	0.6122	0.6116	0.6116

Run ID >	421	422	423	424	425
0.00	0.00	0.00	0.00	0.00	0.00
0.50	0.27	0.57	0.67	0.69	0.70
0.00	0.00	0.00	0.00	0.00	0.00
1.00	0.53	1.14	1.33	1.38	1.39
0.00	0.00	0.00	0.00	0.00	0.00
1.50	0.80	1.71	2.04	2.13	2.15
0.00	0.00	0.00	0.04	0.06	0.07
2.00	1.09	2.37	2.89	3.16	3.28
0.00	0.02	0.10	0.23	0.41	0.51
2.50	1.45	3.34	5.68	8.86	10.83
0.00	0.12	0.50	2.38	5.52	7.54
3.00	1.90	6.51	14.58	16.68	17.68
0.00	0.30	3.14	10.95	13.06	14.07
3.50	2.82	15.78	21.79	24.24	25.31
0.00	0.94	12.19	17.97	20.40	21.48
4.00	8.89	23.71	29.75	31.79	32.63
0.00	6.77	20.04	25.92	27.94	28.78
4.50	16.68	31.06	36.70	38.22	38.76
0.00	14.44	27.44	32.97	34.41	34.92
5.00	24.73	37.44	41.58	42.53	42.79
0.00	22.45	33.93	37.86	38.67	Convergence Failure
5.50	31.36	42.30	45.90	46.80	Convergence Failure
0.00	Convergence Failure	38.85	Convergence Failure	Convergence Failure	Convergence Failure
6.00	Convergence Failure	46.67	Convergence Failure	Convergence Failure	Convergence Failure
0.00	Convergence Failure	43.28	Convergence Failure	Convergence Failure	Convergence Failure
6.50	Convergence Failure	50.35	Convergence Failure	Convergence Failure	Convergence Failure
0.00	Convergence Failure	46.97	Convergence Failure	Convergence Failure	Convergence Failure
7.00	Convergence Failure	53.85	Convergence Failure	Convergence Failure	Convergence Failure
0.00	Convergence Failure	Convergence Failure	Convergence Failure	Convergence Failure	Convergence Failure
7.50	Convergence Failure	Convergence Failure	Convergence Failure	Convergence Failure	Convergence Failure
0.00	Convergence Failure	Convergence Failure	Convergence Failure	Convergence Failure	Convergence Failure
8.00	Convergence Failure	Convergence Failure	Convergence Failure	Convergence Failure	Convergence Failure
0.00	Convergence Failure	Convergence Failure	Convergence Failure	Convergence Failure	Convergence Failure



Multiples of  $p_y$  - Longitudinally Loaded

b [mm]	450	450	450	450	450
t [mm]	37.5	37.5	37.5	37.5	37.5
$\sigma_y$ [N/mm <sup>2</sup> ]	355	355	355	355	355
$\alpha$	1	2	3	4	5
e/b	infinite	infinite	infinite	infinite	infinite
f/b	0.667	0.667	0.667	0.667	0.667
$p_y$ [N/mm <sup>2</sup> ]	8.2393	6.0922	6.0032	5.9985	5.9982

Run ID >	426	427	428	429	430
0.00	0.00	0.00	0.00	0.00	0.00
0.50	0.47	1.03	1.23	1.28	1.29
0.00	0.00	0.00	0.00	0.00	0.00
1.00	0.93	2.06	2.45	2.55	2.57
0.00	0.00	0.00	0.00	0.00	0.00
1.50	1.41	3.10	3.74	3.91	3.96
0.00	0.01	0.01	0.09	0.12	0.14
2.00	1.93	4.28	5.53	6.19	6.47
0.00	0.07	0.20	0.71	1.23	1.48
2.50	2.66	6.33	9.77	11.95	12.99
0.00	0.33	1.28	4.08	6.33	7.45
3.00	3.63	10.62	15.74	17.41	18.08
0.00	0.82	4.90	9.80	11.53	12.24
3.50	5.49	16.64	21.22	22.85	23.51
0.00	2.22	10.82	15.26	16.89	17.56
4.00	11.13	22.19	26.40	27.66	28.09
0.00	7.64	16.53	20.53	21.70	22.08
4.50	17.38	27.17	30.68	31.74	32.06
0.00	13.98	21.76	25.00	25.92	26.15
5.00	22.31	30.96	33.81	34.61	34.83
0.00	19.03	25.75	28.17	28.74	28.85
5.50	26.22	33.89	36.27	36.95	37.14
0.00	23.04	28.75	30.56	30.96	31.01
6.00	29.50	36.30	38.43	39.07	39.25
0.00	26.40	31.16	32.63	32.96	32.99
6.50	32.49	38.56	40.61	41.22	41.38
0.00	29.45	33.42	Convergence Failure	35.03	35.04
7.00	35.19	40.70	Convergence Failure	43.21	43.36
0.00	32.22	Convergence Failure	Convergence Failure	Convergence Failure	36.90
7.50	37.78	Convergence Failure	Convergence Failure	Convergence Failure	45.18
0.00	34.85	Convergence Failure	Convergence Failure	Convergence Failure	38.58
8.00	40.27	Convergence Failure	Convergence Failure	Convergence Failure	46.94
0.00	Convergence Failure	Convergence Failure	Convergence Failure	Convergence Failure	Convergence Failure



Multiples of  $p_y$  - Longitudinally Loaded

b [mm]	500	500	500	500	500
t [mm]	25.0	25.0	25.0	25.0	25.0
$\sigma_y$ [N/mm <sup>2</sup> ]	355	355	355	355	355
$\alpha$	1	2	3	4	5
e/b	infinite	infinite	infinite	infinite	infinite
f/b	0.600	0.600	0.600	0.600	0.600
$p_y$ [N/mm <sup>2</sup> ]	3.1394	2.3228	2.2888	2.2871	2.2869

Run ID >	431	432	433	434	435
0.00	0.00	0.00	0.00	0.00	0.00
0.50	0.45	1.00	1.19	1.24	1.25
0.00	0.00	0.00	0.00	0.00	0.00
1.00	0.89	1.98	2.36	2.44	2.46
0.00	0.00	0.00	0.00	0.00	0.00
1.50	1.35	2.95	3.53	3.68	3.72
0.00	0.01	0.01	0.07	0.11	0.12
2.00	1.86	4.01	4.97	5.34	5.49
0.00	0.08	0.17	0.51	0.77	0.92
2.50	2.55	5.57	7.33	8.04	8.34
0.00	0.34	0.94	2.23	2.95	3.27
3.00	3.47	7.84	10.07	10.89	11.25
0.00	0.84	2.72	4.79	5.68	6.07
3.50	4.92	10.33	12.56	13.29	13.56
0.00	1.92	5.13	7.27	8.01	8.26
4.00	7.22	13.06	15.28	16.03	16.29
0.00	4.04	8.05	10.15	10.85	11.08
4.50	10.16	15.56	17.60	18.18	18.37
0.00	7.10	10.81	12.64	13.08	13.20
5.00	12.71	17.61	19.32	19.83	19.99
0.00	9.84	13.06	14.41	14.73	14.80
5.50	14.76	19.24	20.76	21.23	21.37
0.00	12.03	14.80	15.86	16.11	16.15
6.00	16.51	20.64	22.07	22.50	22.63
0.00	13.88	16.26	17.17	17.36	17.37
6.50	18.03	21.85	23.20	23.60	23.72
0.00	15.48	17.49	18.27	18.41	18.40
7.00	19.41	22.93	24.21	24.59	24.69
0.00	16.92	18.57	19.23	19.32	19.29
7.50	20.69	23.93	25.16	25.52	25.62
0.00	18.25	19.55	20.12	20.18	20.13
8.00	21.89	24.87	26.08	26.41	26.49
0.00	19.49	20.48	20.99	20.99	20.92



Multiples of  $p_y$  - Longitudinally Loaded

b [mm]	350	350	350	350	350
t [mm]	12.5	12.5	12.5	12.5	12.5
$\sigma_y$ [N/mm <sup>2</sup> ]	355	355	355	355	355
$\alpha$	1	2	3	4	5
e/b	infinite	infinite	infinite	infinite	infinite
f/b	0.571	0.571	0.571	0.571	0.571
$p_y$ [N/mm <sup>2</sup> ]	1.6306	1.2097	1.1920	1.1911	1.1910

Run ID >	436	437	438	439	440
0.00	0.00	0.00	0.00	0.00	0.00
0.50	0.73	1.64	1.95	2.02	2.04
0.00	0.00	0.00	0.00	0.00	0.00
1.00	1.46	3.20	3.77	3.91	3.94
0.00	0.00	0.00	0.00	0.00	0.00
1.50	2.19	4.67	5.48	5.69	5.75
0.00	0.02	0.02	0.08	0.12	0.13
2.00	3.02	6.18	7.28	7.62	7.74
0.00	0.15	0.22	0.52	0.70	0.77
2.50	4.08	8.06	9.57	10.12	10.35
0.00	0.56	1.05	1.90	2.41	2.63
3.00	5.41	10.22	12.11	12.79	13.10
0.00	1.30	2.56	4.13	4.82	5.14
3.50	7.14	12.42	14.35	15.09	15.43
0.00	2.55	4.55	6.30	7.04	7.38
4.00	9.06	14.72	16.89	17.70	17.96
0.00	4.20	7.00	9.05	9.79	9.99
4.50	11.48	17.20	19.36	20.19	20.46
0.00	6.71	9.89	11.79	12.49	12.67
5.00	13.92	19.33	21.42	22.13	22.36
0.00	9.43	12.37	14.04	14.52	14.63
5.50	16.03	21.19	23.03	23.68	23.89
0.00	11.81	14.48	15.70	16.06	16.13
6.00	17.86	22.72	24.45	25.07	25.26
0.00	13.85	16.14	17.16	17.44	17.49
6.50	19.48	24.06	25.73	26.32	26.51
0.00	15.62	17.56	18.43	18.67	18.70
7.00	20.94	25.29	26.88	27.44	27.62
0.00	17.21	18.83	19.56	19.75	19.75
7.50	22.29	26.41	27.96	28.49	28.66
0.00	18.67	19.97	20.60	20.73	20.70
8.00	23.56	27.45	28.98	29.49	29.65
0.00	20.01	21.00	21.57	21.65	21.61



Multiples of  $p_y$  - Longitudinally Loaded

b [mm]	450	450	450	450	450
t [mm]	12.5	12.5	12.5	12.5	12.5
$\sigma_y$ [N/mm <sup>2</sup> ]	355	355	355	355	355
$\alpha$	1	2	3	4	5
e/b	infinite	infinite	infinite	infinite	infinite
f/b	0.556	0.556	0.556	0.556	0.556
$p_y$ [N/mm <sup>2</sup> ]	0.9989	0.7420	0.7312	0.7307	0.7306



Run ID >	441	442	443	444	445
0.00	0.00	0.00	0.00	0.00	0.00
0.50	0.24	0.52	0.61	0.63	0.63
0.00	0.00	0.00	0.00	0.00	0.00
1.00	0.48	1.03	1.21	1.25	1.26
0.00	0.00	0.00	0.00	0.00	0.00
1.50	0.72	1.55	1.84	1.92	1.94
0.00	0.00	0.00	0.02	0.04	0.05
2.00	0.98	2.15	2.58	2.71	2.75
0.00	0.01	0.08	0.16	0.21	0.24
2.50	1.27	2.90	4.17	4.94	5.82
0.00	0.06	0.32	1.16	1.83	2.71
3.00	1.65	4.50	10.53	13.84	15.08
0.00	0.20	1.41	7.03	10.39	11.66
3.50	2.22	11.38	17.98	20.22	21.39
0.00	0.53	7.91	14.29	16.52	17.70
4.00	3.33	19.04	25.59	27.69	28.58
0.00	1.38	15.44	21.79	23.86	24.76
4.50	10.58	26.31	32.31	34.40	35.21
0.00	8.44	22.66	28.51	30.57	31.36
5.00	17.59	32.99	38.44	39.85	40.37
0.00	15.34	29.40	34.70	36.01	36.48
5.50	24.80	38.71	42.82	43.83	44.17
0.00	Convergence Failure	Convergence Failure	39.05	39.90	40.16
6.00	Convergence Failure	Convergence Failure	46.26	46.95	47.19
0.00	Convergence Failure	Convergence Failure	42.39	42.86	43.00
6.50	Convergence Failure	Convergence Failure	49.53	49.99	50.06
0.00	Convergence Failure	Convergence Failure	Convergence Failure	45.76	45.70
7.00	Convergence Failure	Convergence Failure	Convergence Failure	53.73	53.65
0.00	Convergence Failure	Convergence Failure	Convergence Failure	Convergence Failure	Convergence Failure
7.50	Convergence Failure	Convergence Failure	Convergence Failure	Convergence Failure	Convergence Failure
0.00	Convergence Failure	Convergence Failure	Convergence Failure	Convergence Failure	Convergence Failure
8.00	Convergence Failure	Convergence Failure	Convergence Failure	Convergence Failure	Convergence Failure
0.00	Convergence Failure	Convergence Failure	Convergence Failure	Convergence Failure	Convergence Failure



Multiples of  $p_y$  - Longitudinally Loaded

b [mm]	450	450	450	450	450
t [mm]	37.5	37.5	37.5	37.5	37.5
$\sigma_y$ [N/mm <sup>2</sup> ]	355	355	355	355	355
$\alpha$	1	2	3	4	5
e/b	infinite	infinite	infinite	infinite	infinite
f/b	0.333	0.333	0.333	0.333	0.333
$p_y$ [N/mm <sup>2</sup> ]	12.1053	9.2815	9.1622	9.1559	9.1554

Run ID >	446	447	448	449	450
0.00	0.00	0.00	0.00	0.00	0.00
0.50	0.41	0.90	1.07	1.11	1.12
0.00	0.00	0.00	0.00	0.00	0.00
1.00	0.81	1.81	2.14	2.22	2.24
0.00	0.00	0.00	0.00	0.00	0.00
1.50	1.22	2.71	3.27	3.41	3.45
0.00	0.00	0.01	0.07	0.10	0.11
2.00	1.64	3.74	4.76	5.29	5.51
0.00	0.02	0.16	0.53	0.93	1.12
2.50	2.19	5.50	7.90	9.05	9.68
0.00	0.17	1.06	2.80	3.86	4.50
3.00	2.89	8.26	12.89	14.95	15.83
0.00	0.46	3.07	7.27	9.44	10.39
3.50	4.14	12.88	17.65	19.42	20.15
0.00	1.30	7.27	11.87	13.69	14.45
4.00	6.06	18.27	23.13	24.80	25.40
0.00	2.83	12.66	17.39	19.05	19.64
4.50	10.88	23.28	27.58	28.72	29.09
0.00	7.44	17.79	21.87	22.89	23.20
5.00	16.25	27.40	30.92	31.87	32.16
0.00	12.84	22.03	25.19	25.94	26.15
5.50	20.72	30.63	33.69	34.51	34.76
0.00	17.37	25.30	27.90	28.47	28.61
6.00	24.52	33.49	36.16	36.85	37.06
0.00	21.24	28.20	30.28	30.68	30.76
6.50	28.07	36.05	38.34	38.93	39.12
0.00	24.88	30.77	32.35	32.60	32.63
7.00	31.27	38.27	40.37	40.92	41.12
0.00	Convergence Failure	32.96	34.28	34.43	34.44
7.50	Convergence Failure	40.27	42.26	42.85	43.07
0.00	Convergence Failure	34.92	36.03	36.20	36.22
8.00	Convergence Failure	42.25	44.08	44.66	44.89
0.00	Convergence Failure	Convergence Failure	Convergence Failure	37.85	37.88



Multiples of  $p_y$  - Longitudinally Loaded

b [mm]	500	500	500	500	500
t [mm]	25.0	25.0	25.0	25.0	25.0
$\sigma_y$ [N/mm <sup>2</sup> ]	355	355	355	355	355
$\alpha$	1	2	3	4	5
e/b	infinite	infinite	infinite	infinite	infinite
f/b	0.200	0.200	0.200	0.200	0.200
$p_y$ [N/mm <sup>2</sup> ]	6.5265	5.0793	5.0168	5.0136	5.0134

Run ID >	451	452	453	454	455
0.00	0.00	0.00	0.00	0.00	0.00
0.50	0.38	0.86	1.02	1.06	1.07
0.00	0.00	0.00	0.00	0.00	0.00
1.00	0.76	1.71	2.03	2.10	2.12
0.00	0.00	0.00	0.00	0.00	0.00
1.50	1.14	2.55	3.06	3.18	3.21
0.00	0.00	0.01	0.06	0.08	0.09
2.00	1.54	3.48	4.40	4.80	4.96
0.00	0.03	0.14	0.51	0.83	0.97
2.50	2.06	5.03	6.63	7.19	7.42
0.00	0.17	0.99	2.15	2.68	2.92
3.00	2.76	6.89	8.90	9.66	10.00
0.00	0.51	2.34	4.08	4.86	5.23
3.50	3.85	8.90	11.04	11.82	12.16
0.00	1.26	4.05	6.05	6.87	7.22
4.00	5.30	11.19	13.65	14.45	14.72
0.00	2.41	6.28	8.70	9.51	9.77
4.50	7.17	13.69	16.06	16.80	17.04
0.00	4.10	8.95	11.22	11.90	12.10
5.00	9.62	15.78	17.93	18.52	18.70
0.00	6.58	11.17	13.10	13.55	13.66
5.50	11.87	17.53	19.41	19.92	20.08
0.00	8.96	12.99	14.52	14.86	14.92
6.00	13.78	18.99	20.70	21.19	21.33
0.00	10.96	14.48	15.75	16.02	16.06
6.50	15.44	20.28	21.86	22.32	22.45
0.00	12.69	15.77	16.83	17.04	17.06
7.00	16.94	21.45	22.94	23.35	23.48
0.00	14.25	16.93	17.83	17.96	17.96
7.50	18.37	22.53	23.96	24.36	24.47
0.00	15.75	17.99	18.78	18.89	18.87
8.00	19.72	23.53	24.90	25.28	25.39
0.00	17.15	18.95	19.65	19.71	19.67



Multiples of  $p_y$  - Longitudinally Loaded

b [mm]	350	350	350	350	350
t [mm]	12.5	12.5	12.5	12.5	12.5
$\sigma_y$ [N/mm <sup>2</sup> ]	355	355	355	355	355
$\alpha$	1	2	3	4	5
e/b	infinite	infinite	infinite	infinite	infinite
f/b	0.143	0.143	0.143	0.143	0.143
$p_y$ [N/mm <sup>2</sup> ]	4.4356	3.4790	3.4373	3.4349	3.4349


Run ID >	456	457	458	459	460
0.00	0.00	0.00	0.00	0.00	0.00
0.50	0.61	1.39	1.65	1.72	1.73
0.00	0.00	0.00	0.00	0.00	0.00
1.00	1.22	2.74	3.23	3.35	3.38
0.00	0.00	0.00	0.00	0.00	0.00
1.50	1.83	4.04	4.76	4.94	4.99
0.00	0.01	0.02	0.08	0.11	0.12
2.00	2.47	5.40	6.53	6.91	7.07
0.00	0.05	0.21	0.59	0.85	0.99
2.50	3.27	7.34	9.03	9.60	9.83
0.00	0.28	1.21	2.40	2.94	3.16
3.00	4.36	9.42	11.21	11.88	12.18
0.00	0.82	2.72	4.17	4.84	5.14
3.50	5.85	11.39	13.33	14.06	14.37
0.00	1.86	4.37	6.06	6.78	7.09
4.00	7.52	13.37	15.34	15.92	16.23
0.00	3.17	6.18	7.94	8.43	8.72
4.50	9.23	15.54	17.74	18.44	18.73
0.00	4.66	8.45	10.48	11.08	11.32
5.00	11.27	17.65	19.89	20.61	20.90
0.00	6.70	10.77	12.75	13.31	13.53
5.50	13.38	19.46	21.68	22.34	22.60
0.00	8.96	12.71	14.54	14.99	15.15
6.00	15.28	21.05	23.14	23.74	23.97
0.00	11.03	14.38	15.94	16.25	16.37
6.50	16.97	22.48	24.41	24.97	25.19
0.00	12.85	15.84	17.09	17.33	17.42
7.00	18.49	23.76	25.57	26.11	26.31
0.00	14.47	17.11	18.14	18.32	18.38
7.50	19.88	24.91	26.65	27.16	27.36
0.00	15.95	18.24	19.10	19.23	19.27
8.00	21.17	25.99	27.69	28.18	28.37
0.00	17.30	19.28	20.05	20.12	20.14



Multiples of  $p_y$  - Longitudinally Loaded

b [mm]	450	450	450	450	450
t [mm]	12.5	12.5	12.5	12.5	12.5
$\sigma_y$ [N/mm <sup>2</sup> ]	355	355	355	355	355
$\alpha$	1	2	3	4	5
e/b	infinite	infinite	infinite	infinite	infinite
f/b	0.111	0.111	0.111	0.111	0.111
$p_y$ [N/mm <sup>2</sup> ]	3.3570	2.6451	2.6138	2.6122	2.6120

Run ID >	508	518	528	538	548	558
0.00	0.00	0.00	0.00	0.00	0.00	0.00
0.50	0.71	1.13	0.62	0.97	0.50	0.77
0.00	0.00	0.00	0.00	0.00	0.00	0.00
1.00	1.41	2.24	1.23	1.93	1.01	1.53
0.00	0.00	0.00	0.00	0.00	0.00	0.00
1.50	2.12	3.30	1.85	2.85	1.51	2.28
0.00	0.00	0.01	0.00	0.00	0.00	0.00
2.00	2.93	4.43	2.52	3.82	2.04	3.04
0.00	0.11	0.14	0.06	0.08	0.03	0.04
2.50	4.17	5.88	3.36	4.94	2.63	3.88
0.00	0.68	0.70	0.29	0.37	0.12	0.17
3.00	6.95	7.84	4.88	6.44	3.49	4.96
0.00	2.84	2.02	1.22	1.14	0.48	0.60
3.50	11.72	9.95	7.85	8.26	4.87	6.33
0.00	7.27	3.83	3.68	2.47	1.38	1.40
4.00	17.26	12.25	12.85	10.22	7.46	7.89
0.00	12.81	6.17	8.46	4.18	3.52	2.54
4.50	22.36	14.58	18.17	12.49	12.00	9.65
0.00	18.09	8.78	13.86	6.57	7.88	4.06
5.00	26.64	16.66	22.63	14.69	16.71	11.81
0.00	22.59	11.17	18.48	9.08	12.59	6.28
5.50	29.76	18.51	26.36	16.63	20.59	13.81
0.00	25.82	13.31	22.35	11.31	16.55	8.49
6.00	32.43	20.11	29.48	18.35	24.04	15.59
0.00	28.56	15.12	25.58	13.29	20.09	10.50
6.50	34.80	21.47	32.23	19.87	27.11	17.10
0.00	30.99	16.62	28.42	15.00	23.25	12.19
7.00	36.95	22.63	34.62	21.22	29.99	18.50
0.00	33.17	17.87	30.88	16.50	26.23	13.72
7.50	39.08	23.69	36.85	22.47	32.68	19.79
0.00	35.35	18.98	33.16	17.87	29.02	15.14
8.00	41.30	24.71	39.05	23.64	35.13	20.99
0.00	37.62	20.05	35.42	19.15	31.55	16.44

 Multiples of  $p_y$  - Transversely Loaded

b [mm]	500	450	500	450	500	450
t [mm]	25.0	12.5	25.0	12.5	25.0	12.5
$\sigma_y$ [N/mm <sup>2</sup> ]	235	235	235	235	235	235
$\alpha$	3	3	3	3	3	3
e/b	1.000	1.000	1.000	1.000	1.000	1.000
f/b	1.000	1.000	0.600	0.556	0.200	0.111
$p_y$ [N/mm <sup>2</sup> ]	1.4569	0.4465	1.8069	0.5783	3.9652	2.0510

Run ID >	608	618	628	638	648	658
0.00	0.00	0.00	0.00	0.00	0.00	0.00
0.50	0.64	1.03	0.62	0.98	0.54	0.84
0.00	0.00	0.00	0.00	0.00	0.00	0.00
1.00	1.28	2.03	1.23	1.94	1.08	1.66
0.00	0.00	0.00	0.00	0.00	0.00	0.00
1.50	1.91	3.01	1.84	2.88	1.62	2.47
0.00	0.00	0.00	0.00	0.00	0.00	0.00
2.00	2.61	4.01	2.51	3.86	2.21	3.33
0.00	0.06	0.07	0.06	0.08	0.06	0.08
2.50	3.45	5.14	3.34	4.99	2.95	4.48
0.00	0.28	0.36	0.29	0.38	0.27	0.50
3.00	5.09	6.68	4.81	6.48	4.27	6.03
0.00	1.31	1.17	1.17	1.18	1.07	1.47
3.50	8.34	8.59	7.46	8.22	5.91	7.52
0.00	4.07	2.64	3.30	2.41	2.20	2.48
4.00	13.06	10.54	11.61	9.99	8.61	9.01
0.00	8.58	4.39	7.15	3.90	4.45	3.62
4.50	18.02	12.65	16.49	12.03	12.47	10.69
0.00	13.59	6.61	12.01	5.92	8.09	5.06
5.00	22.60	14.75	21.20	14.11	16.92	12.46
0.00	18.35	8.98	16.86	8.20	12.56	6.79
5.50	26.46	16.63	25.23	16.07	20.74	14.19
0.00	22.40	11.14	21.06	10.44	16.44	8.60
6.00	29.36	18.32	28.38	17.77	24.21	15.82
0.00	25.40	13.09	24.35	12.37	19.99	10.36
6.50	31.82	19.81	30.85	19.26	27.08	17.22
0.00	27.94	14.78	26.88	14.05	22.91	11.85
7.00	34.04	21.10	33.01	20.53	29.60	18.47
0.00	30.21	16.21	29.07	15.45	25.48	13.17
7.50	36.05	22.20	35.14	21.65	31.96	19.62
0.00	32.27	17.41	31.23	16.65	27.90	14.37
8.00	37.96	23.19	37.23	22.66	34.13	20.67
0.00	34.20	18.46	33.38	17.72	30.11	15.44



Multiples of  $p_y$  - Longitudinally Loaded

b [mm]	500	450	500	450	500	450
t [mm]	25.0	12.5	25.0	12.5	25.0	12.5
$\sigma_y$ [N/mm <sup>2</sup> ]	235	235	235	235	235	235
$\alpha$	3	3	3	3	3	3
e/b	1.000	1.000	1.000	1.000	1.000	1.000
f/b	1.000	1.000	0.600	0.556	0.200	0.111
$p_y$ [N/mm <sup>2</sup> ]	1.3183	0.4052	1.5152	0.4840	3.3210	1.7302

Run ID >	708	718	728	738	748	758
0.00	0.00	0.00	0.00	0.00	0.00	0.00
0.50	0.83	1.34	0.80	1.27	0.70	1.08
0.00	0.00	0.00	0.00	0.00	0.00	0.00
1.00	1.66	2.63	1.59	2.50	1.39	2.13
0.00	0.00	0.00	0.00	0.00	0.00	0.00
1.50	2.53	3.89	2.43	3.73	2.12	3.20
0.00	0.05	0.05	0.05	0.06	0.04	0.05
2.00	3.68	5.33	3.54	5.15	3.04	4.55
0.00	0.38	0.41	0.37	0.42	0.27	0.47
2.50	7.13	7.58	6.29	7.30	5.10	6.75
0.00	3.15	1.88	2.42	1.83	1.70	2.04
3.00	12.79	10.28	11.73	9.76	8.86	8.80
0.00	8.50	4.39	7.49	3.94	4.92	3.66
3.50	18.34	12.68	17.15	12.01	13.53	10.78
0.00	13.99	6.80	12.80	6.09	9.34	5.39
4.00	23.98	15.23	22.61	14.66	18.80	12.95
0.00	19.83	9.56	18.35	8.92	14.61	7.47
4.50	28.19	17.47	27.17	17.00	23.22	15.32
0.00	24.21	12.04	23.11	11.48	19.05	9.96
5.00	30.87	19.36	30.19	18.94	26.57	17.30
0.00	26.89	14.11	26.17	13.59	22.40	12.04
5.50	33.28	20.92	32.44	20.46	29.32	18.89
0.00	29.29	15.80	28.38	15.17	25.12	13.62
6.00	35.48	22.17	34.53	21.76	31.69	20.18
0.00	31.51	17.09	30.42	16.51	27.46	14.85
6.50	37.36	23.27	36.63	22.92	33.88	21.34
0.00	33.37	18.19	32.50	17.67	29.63	15.96
7.00	39.11	24.26	38.79	23.98	35.93	22.41
0.00	35.08	19.15	34.66	18.70	31.66	16.97
7.50	41.27	25.20	40.75	24.94	37.70	23.41
0.00	37.24	20.06	36.60	19.63	33.37	17.92
8.00	43.77	26.10	42.52	25.85	39.51	24.34
0.00	39.81	20.94	38.33	20.50	35.12	18.79



Multiples of  $p_y$  - Longitudinally Loaded

b [mm]	500	450	500	450	500	450
t [mm]	25.0	12.5	25.0	12.5	25.0	12.5
$\sigma_y$ [N/mm <sup>2</sup> ]	235	235	235	235	235	235
$\alpha$	3	3	3	3	3	3
e/b	2.000	2.000	2.000	2.000	2.000	2.000
f/b	1.000	1.000	0.600	0.556	0.200	0.111
$p_y$ [N/mm <sup>2</sup> ]	1.3183	0.4052	1.5152	0.4840	3.3210	1.7302

Run ID >	808	818	828	838	848	858
0.00	0.00	0.00	0.00	0.00	0.00	0.00
0.50	0.86	1.38	0.82	1.32	0.72	1.11
0.00	0.00	0.00	0.00	0.00	0.00	0.00
1.00	1.72	2.72	1.65	2.59	1.44	2.20
0.00	0.00	0.00	0.00	0.00	0.00	0.00
1.50	2.64	4.04	2.53	3.87	2.20	3.31
0.00	0.06	0.08	0.06	0.08	0.05	0.07
2.00	4.03	5.61	3.87	5.41	3.30	4.87
0.00	0.63	0.56	0.60	0.56	0.44	0.70
2.50	8.98	8.21	7.82	7.86	5.72	7.22
0.00	4.98	2.52	3.91	2.35	2.21	2.46
3.00	14.89	11.05	13.72	10.51	10.80	9.43
0.00	10.68	5.27	9.57	4.79	6.89	4.30
3.50	20.70	13.63	19.58	12.87	15.89	11.50
0.00	16.50	7.90	15.38	7.09	11.82	6.17
4.00	26.24	16.18	24.92	15.69	21.41	14.01
0.00	22.25	10.63	20.81	10.10	17.35	8.67
4.50	29.58	18.48	28.76	18.08	25.23	16.44
0.00	25.61	13.14	24.75	12.68	21.13	11.22
5.00	31.98	20.24	31.35	19.85	28.25	18.44
0.00	27.94	15.01	27.28	14.50	24.10	13.26
5.50	34.30	21.69	33.42	21.30	30.69	19.90
0.00	30.24	16.51	29.26	15.97	26.46	14.65
6.00	36.38	22.87	35.50	22.57	32.93	21.10
0.00	32.31	17.68	31.28	17.23	28.64	15.74
6.50	38.14	23.95	37.74	23.67	35.18	22.23
0.00	34.00	18.72	33.50	18.29	Convergence Failure	16.77
7.00	39.85	24.92	39.65	24.72	Convergence Failure	23.30
0.00	35.64	19.65	35.37	19.29	Convergence Failure	17.78
7.50	42.04	25.85	41.42	25.70	Convergence Failure	24.30
0.00	37.84	20.53	37.08	20.22	Convergence Failure	18.71
8.00	44.71	26.75	43.14	26.60	Convergence Failure	25.22
0.00	40.60	21.39	38.72	21.06	Convergence Failure	19.55



Multiples of  $p_y$  - Longitudinally Loaded

b [mm]	500	450	500	450	500	450
t [mm]	25.0	12.5	25.0	12.5	25.0	12.5
$\alpha_y$ [N/mm <sup>2</sup> ]	235	235	235	235	235	235
$\alpha$	3	3	3	3	3	3
e/b	3.000	3.000	3.000	3.000	3.000	3.000
f/b	1.000	1.000	0.600	0.556	0.200	0.111
$p_y$ [N/mm <sup>2</sup> ]	1.3183	0.4052	1.5152	0.4840	3.3210	1.7302



Run ID >	906	907	908	909	910
0.00	0.00	0.00	0.00	0.00	0.00
0.50	0.32	0.34	0.35	0.35	0.35
0.00	0.00	0.00	0.00	0.00	0.00
1.00	0.64	0.69	0.69	0.69	0.69
0.00	0.00	0.00	0.00	0.00	0.00
1.50	0.96	1.05	1.05	1.05	1.05
0.00	0.01	0.02	0.02	0.02	0.02
2.00	1.32	1.50	1.50	1.50	1.50
0.00	0.05	0.12	0.13	0.13	0.13
2.50	1.83	2.27	2.28	2.28	2.28
0.00	0.24	0.55	0.56	0.56	0.56
3.00	2.56	3.60	3.63	3.63	3.63
0.00	0.64	1.52	1.55	1.55	1.55
3.50	4.50	6.40	6.49	6.49	6.49
0.00	2.26	3.99	4.08	4.08	4.08
4.00	11.47	11.09	11.23	11.23	11.23
0.00	9.15	8.55	8.69	8.69	8.69
4.50	17.07	16.36	16.50	16.50	16.50
0.00	14.80	13.89	14.05	14.05	14.05
5.00	21.32	20.79	20.91	20.91	20.91
0.00	19.11	18.42	18.55	18.55	18.55
5.50	Convergence Failure	24.62	24.73	24.73	24.73
0.00	Convergence Failure	22.34	22.46	22.46	22.46
6.00	Convergence Failure	27.77	27.89	27.89	27.89
0.00	Convergence Failure	25.56	25.68	25.68	25.68
6.50	Convergence Failure	30.65	30.78	30.78	30.78
0.00	Convergence Failure	28.50	28.63	28.63	28.63
7.00	Convergence Failure	33.22	33.36	33.35	33.35
0.00	Convergence Failure	31.11	31.26	31.26	31.26
7.50	Convergence Failure	35.46	35.60	35.60	35.60
0.00	Convergence Failure	33.39	33.54	33.54	33.54
8.00	Convergence Failure	37.71	37.84	37.84	37.84
0.00	Convergence Failure	35.67	35.80	35.80	35.80



Multiples of  $p_y$  - Transversely Loaded

b [mm]	500	500	500	500	500
t [mm]	25.0	25.0	25.0	25.0	25.0
$\sigma_y$ [N/mm <sup>2</sup> ]	235	235	235	235	235
$\alpha$	1	2	3	4	5
e/b	infinite	infinite	infinite	infinite	infinite
f/b	0.800	0.800	0.800	0.800	0.800
$p_y$ [N/mm <sup>2</sup> ]	1.8915	1.5757	1.5754	1.5754	1.5754

Run ID >	916	917	918	919	920
0.00	0.00	0.00	0.00	0.00	0.00
0.50	0.50	0.55	0.55	0.55	0.55
0.00	0.00	0.00	0.00	0.00	0.00
1.00	1.00	1.09	1.09	1.09	1.09
0.00	0.00	0.00	0.00	0.00	0.00
1.50	1.51	1.65	1.66	1.66	1.66
0.00	0.01	0.03	0.03	0.03	0.03
2.00	2.11	2.44	2.44	2.44	2.44
0.00	0.13	0.28	0.29	0.29	0.29
2.50	2.91	3.61	3.62	3.62	3.62
0.00	0.46	0.97	0.98	0.98	0.98
3.00	4.00	5.25	5.27	5.27	5.27
0.00	1.09	2.20	2.23	2.23	2.23
3.50	5.79	7.15	7.19	7.19	7.19
0.00	2.51	3.83	3.88	3.88	3.88
4.00	8.45	9.16	9.22	9.22	9.22
0.00	5.12	5.74	5.82	5.82	5.82
4.50	11.27	11.26	11.32	11.32	11.32
0.00	8.14	7.92	8.00	8.00	8.00
5.00	13.58	13.30	13.36	13.36	13.36
0.00	10.62	10.11	10.19	10.19	10.19
5.50	15.52	15.18	15.24	15.24	15.24
0.00	12.72	12.16	12.23	12.23	12.23
6.00	17.24	16.87	16.93	16.93	16.93
0.00	14.55	14.00	14.08	14.08	14.08
6.50	18.76	18.39	18.46	18.46	18.46
0.00	16.18	15.64	15.73	15.73	15.73
7.00	20.15	19.82	19.90	19.90	19.90
0.00	17.65	17.18	17.28	17.28	17.28
7.50	21.45	21.19	21.28	21.28	21.28
0.00	19.01	18.65	18.76	18.75	18.75
8.00	22.67	22.48	22.59	22.59	22.59
0.00	20.28	20.02	20.14	20.14	20.14



Multiples of  $p_y$  - Transversely Loaded

b [mm]	450	450	450	450	450
t [mm]	12.5	12.5	12.5	12.5	12.5
$\sigma_y$ [N/mm <sup>2</sup> ]	235	235	235	235	235
$\alpha$	1	2	3	4	5
e/b	infinite	infinite	infinite	infinite	infinite
f/b	0.778	0.778	0.778	0.778	0.778
$p_y$ [N/mm <sup>2</sup> ]	0.5851	0.4886	0.4885	0.4885	0.4885

Run ID >	926	927	928	929	930
0.00	0.00	0.00	0.00	0.00	0.00
0.50	0.29	0.31	0.31	0.31	0.31
0.00	0.00	0.00	0.00	0.00	0.00
1.00	0.59	0.62	0.62	0.62	0.62
0.00	0.00	0.00	0.00	0.00	0.00
1.50	0.88	0.94	0.94	0.94	0.94
0.00	0.01	0.01	0.01	0.01	0.01
2.00	1.20	1.30	1.30	1.30	1.30
0.00	0.03	0.05	0.05	0.05	0.05
2.50	1.63	1.82	1.82	1.82	1.82
0.00	0.17	0.26	0.26	0.26	0.26
3.00	2.22	2.57	2.57	2.57	2.57
0.00	0.45	0.69	0.69	0.69	0.69
3.50	3.29	4.01	4.02	4.01	4.01
0.00	1.23	1.81	1.82	1.82	1.82
4.00	6.89	6.98	7.00	6.98	6.98
0.00	4.57	4.49	4.50	4.49	4.49
4.50	13.05	11.88	11.91	11.91	11.91
0.00	10.71	9.29	9.33	9.32	9.32
5.00	17.76	16.73	16.78	16.77	16.77
0.00	15.45	14.21	14.26	14.25	14.25
5.50	21.49	20.74	20.80	20.79	20.79
0.00	19.21	18.27	18.33	18.32	18.32
6.00	24.87	24.25	24.32	24.31	24.31
0.00	22.62	21.83	21.90	21.89	21.89
6.50	27.84	27.33	27.41	27.40	27.40
0.00	25.62	24.95	25.03	25.03	25.03
7.00	30.50	30.03	30.11	30.11	30.11
0.00	28.30	27.69	27.78	27.77	27.77
7.50	32.89	32.51	32.59	32.59	32.59
0.00	30.72	30.20	30.29	30.28	30.28
8.00	35.12	34.88	34.96	34.96	34.96
0.00	32.96	32.61	32.69	32.69	32.69



Multiples of  $p_y$  - Transversely Loaded

b [mm]	500	500	500	500	500
t [mm]	25.0	25.0	25.0	25.0	25.0
$\sigma_y$ [N/mm <sup>2</sup> ]	235	235	235	235	235
$\alpha$	1	2	3	4	5
e/b	infinite	infinite	infinite	infinite	infinite
f/b	0.400	0.400	0.400	0.400	0.400
$p_y$ [N/mm <sup>2</sup> ]	2.5817	2.3178	2.3178	2.3176	2.3176

Run ID >	936	937	938	939	940
0.00	0.00	0.00	0.00	0.00	0.00
0.50	0.45	0.49	0.49	0.49	0.49
0.00	0.00	0.00	0.00	0.00	0.00
1.00	0.91	0.97	0.97	0.97	0.97
0.00	0.00	0.00	0.00	0.00	0.00
1.50	1.36	1.46	1.46	1.46	1.46
0.00	0.01	0.01	0.01	0.01	0.01
2.00	1.87	2.03	2.03	2.03	2.03
0.00	0.07	0.11	0.11	0.11	0.11
2.50	2.55	2.85	2.85	2.85	2.85
0.00	0.31	0.46	0.46	0.46	0.46
3.00	3.46	3.95	3.95	3.95	3.95
0.00	0.79	1.13	1.14	1.14	1.14
3.50	4.85	5.54	5.54	5.54	5.54
0.00	1.80	2.35	2.35	2.35	2.35
4.00	6.60	7.31	7.32	7.32	7.32
0.00	3.27	3.87	3.88	3.88	3.88
4.50	9.03	9.22	9.23	9.23	9.23
0.00	5.67	5.68	5.69	5.69	5.69
5.00	11.59	11.38	11.39	11.39	11.39
0.00	8.39	7.92	7.93	7.93	7.93
5.50	13.72	13.51	13.52	13.52	13.52
0.00	10.69	10.21	10.23	10.23	10.23
6.00	15.53	15.41	15.43	15.43	15.43
0.00	12.62	12.28	12.30	12.30	12.30
6.50	17.12	17.14	17.17	17.17	17.17
0.00	14.29	14.15	14.18	14.18	14.18
7.00	18.55	18.67	18.71	18.71	18.71
0.00	15.81	15.78	15.82	15.82	15.82
7.50	19.90	20.06	20.10	20.10	20.10
0.00	17.23	17.25	17.30	17.30	17.30
8.00	21.16	21.32	21.37	21.37	21.37
0.00	18.54	18.57	18.63	18.63	18.63



Multiples of  $p_y$  - Transversely Loaded

b [mm]	450	450	450	450	450
t [mm]	12.5	12.5	12.5	12.5	12.5
$\alpha_y$ [N/mm <sup>2</sup> ]	235	235	235	235	235
$\alpha$	1	2	3	4	5
e/b	infinite	infinite	infinite	infinite	infinite
f/b	0.333	0.333	0.333	0.333	0.333
$p_y$ [N/mm <sup>2</sup> ]	0.8986	0.8120	0.8119	0.8119	0.8119

Run ID >	946	947	948	949	950
0.00	0.00	0.00	0.00	0.00	0.00
0.50	0.32	0.71	0.84	0.87	0.88
0.00	0.00	0.00	0.00	0.00	0.00
1.00	0.64	1.41	1.68	1.75	1.76
0.00	0.00	0.00	0.00	0.00	0.00
1.50	0.96	2.12	2.57	2.70	2.73
0.00	0.01	0.01	0.06	0.09	0.10
2.00	1.32	2.95	3.87	4.41	4.65
0.00	0.05	0.14	0.54	0.97	1.18
2.50	1.83	4.46	8.31	10.81	11.95
0.00	0.24	0.97	4.36	6.91	8.11
3.00	2.56	9.46	14.43	16.34	17.13
0.00	0.64	5.53	10.28	12.22	13.03
3.50	4.50	15.88	20.42	22.07	22.79
0.00	2.26	11.90	16.27	17.91	18.63
4.00	11.47	21.69	26.03	27.35	27.78
0.00	9.15	17.84	22.08	23.35	23.75
4.50	17.07	26.48	29.45	30.27	30.50
0.00	14.80	22.83	25.54	26.22	26.38
5.00	21.32	29.62	31.84	32.47	32.64
0.00	19.11	26.03	27.86	28.29	28.38
5.50	24.70	32.06	34.14	34.74	34.91
0.00	22.51	28.45	30.11	30.52	30.59
6.00	27.64	34.34	36.27	36.83	36.99
0.00	25.48	30.74	32.22	32.57	32.62
6.50	30.29	36.46	38.27	38.79	38.91
0.00	28.17	32.86	34.20	34.48	34.49
7.00	32.61	38.38	40.03	40.46	40.52
0.00	30.50	34.77	Convergence Failure	36.05	Convergence Failure
7.50	34.78	40.40	Convergence Failure	42.50	Convergence Failure
0.00	32.68	Convergence Failure	Convergence Failure	38.06	Convergence Failure
8.00	36.93	Convergence Failure	Convergence Failure	44.60	Convergence Failure
0.00	34.85	Convergence Failure	Convergence Failure	40.15	Convergence Failure



Multiples of  $p_y$  - Longitudinally Loaded

b [mm]	500	500	500	500	500
t [mm]	25.0	25.0	25.0	25.0	25.0
$\sigma_y$ [N/mm <sup>2</sup> ]	235	235	235	235	235
$\alpha$	1	2	3	4	5
e/b	infinite	infinite	infinite	infinite	infinite
f/b	0.800	0.800	0.800	0.800	0.800
$p_y$ [N/mm <sup>2</sup> ]	1.8915	1.3792	1.3578	1.3567	1.3567

Run ID >	956	957	958	959	960
0.00	0.00	0.00	0.00	0.00	0.00
0.50	0.50	1.13	1.35	1.40	1.42
0.00	0.00	0.00	0.00	0.00	0.00
1.00	1.00	2.23	2.65	2.75	2.78
0.00	0.00	0.00	0.00	0.00	0.00
1.50	1.51	3.30	3.94	4.11	4.16
0.00	0.01	0.01	0.07	0.11	0.12
2.00	2.11	4.47	5.47	5.82	5.96
0.00	0.13	0.19	0.52	0.74	0.86
2.50	2.91	6.11	7.95	8.71	9.07
0.00	0.46	0.97	2.33	3.11	3.52
3.00	4.00	8.59	10.80	11.61	11.97
0.00	1.09	3.01	5.08	5.95	6.33
3.50	5.79	11.18	13.37	14.18	14.44
0.00	2.51	5.61	7.70	8.50	8.73
4.00	8.45	13.96	16.05	16.88	17.15
0.00	5.12	8.64	10.59	11.36	11.58
4.50	11.27	16.41	18.39	19.08	19.27
0.00	8.14	11.40	13.12	13.66	13.77
5.00	13.58	18.47	20.12	20.74	20.90
0.00	10.62	13.69	14.94	15.37	15.44
5.50	15.52	20.12	21.59	22.14	22.29
0.00	12.72	15.49	16.46	16.78	16.82
6.00	17.24	21.50	22.82	23.31	23.44
0.00	14.55	16.94	17.68	17.91	17.92
6.50	18.76	22.69	23.89	24.33	24.44
0.00	16.18	18.16	18.71	18.86	18.83
7.00	20.15	23.74	24.92	25.36	25.45
0.00	17.65	19.22	19.70	19.83	19.77
7.50	21.45	24.72	25.90	26.34	26.43
0.00	19.01	20.18	20.64	20.76	20.69
8.00	22.67	25.68	26.87	27.28	27.36
0.00	20.28	21.13	21.58	21.65	21.56



Multiples of  $p_y$  - Longitudinally Loaded

b [mm]	450	450	450	450	450
t [mm]	12.5	12.5	12.5	12.5	12.5
$\sigma_y$ [N/mm <sup>2</sup> ]	235	235	235	235	235
$\alpha$	1	2	3	4	5
e/b	infinite	infinite	infinite	infinite	infinite
f/b	0.778	0.778	0.778	0.778	0.778
$p_y$ [N/mm <sup>2</sup> ]	0.5851	0.4270	0.4204	0.4201	0.4200

Run ID >	966	967	968	969	970
0.00	0.00	0.00	0.00	0.00	0.00
0.50	0.29	0.65	0.77	0.80	0.81
0.00	0.00	0.00	0.00	0.00	0.00
1.00	0.59	1.30	1.54	1.60	1.61
0.00	0.00	0.00	0.00	0.00	0.00
1.50	0.88	1.95	2.36	2.47	2.49
0.00	0.01	0.01	0.06	0.08	0.09
2.00	1.20	2.70	3.56	4.03	4.23
0.00	0.03	0.12	0.50	0.87	1.05
2.50	1.63	4.10	6.47	8.65	9.89
0.00	0.17	0.89	2.75	4.92	6.21
3.00	2.22	6.99	12.43	14.27	15.01
0.00	0.45	3.22	8.42	10.30	11.06
3.50	3.29	13.06	18.10	20.13	21.04
0.00	1.23	9.11	14.01	16.07	17.00
4.00	6.89	18.87	23.26	24.56	25.06
0.00	4.57	14.98	19.19	20.42	20.90
4.50	13.05	23.48	27.14	28.22	28.62
0.00	10.71	19.66	23.09	24.08	24.44
5.00	17.76	27.17	30.24	31.03	31.30
0.00	15.45	23.42	26.21	26.86	27.05
5.50	21.49	30.18	32.63	33.30	33.56
0.00	19.21	26.49	28.56	29.03	29.21
6.00	24.87	32.61	34.78	35.42	35.66
0.00	22.62	28.93	30.63	31.06	31.21
6.50	27.84	34.68	36.70	37.22	37.41
0.00	25.62	30.97	32.48	32.74	32.81
7.00	30.50	36.63	38.35	38.78	38.97
0.00	28.30	32.87	34.01	34.15	34.20
7.50	32.89	38.50	39.97	40.38	40.55
0.00	30.72	34.71	35.54	35.62	35.65
8.00	35.12	40.39	41.78	42.08	42.24
0.00	32.96	36.57	37.29	37.24	37.24



Multiples of  $p_y$  - Longitudinally Loaded

b [mm]	500	500	500	500	500
t [mm]	25.0	25.0	25.0	25.0	25.0
$\sigma_y$ [N/mm <sup>2</sup> ]	235	235	235	235	235
$\alpha$	1	2	3	4	5
e/b	infinite	infinite	infinite	infinite	infinite
f/b	0.400	0.400	0.400	0.400	0.400
$p_y$ [N/mm <sup>2</sup> ]	2.5817	1.9541	1.9275	1.9262	1.9261

Run ID >	976	977	978	979	980
0.00	0.00	0.00	0.00	0.00	0.00
0.50	0.45	1.02	1.22	1.26	1.27
0.00	0.00	0.00	0.00	0.00	0.00
1.00	0.91	2.02	2.40	2.49	2.51
0.00	0.00	0.00	0.00	0.00	0.00
1.50	1.36	3.01	3.60	3.76	3.80
0.00	0.01	0.02	0.08	0.11	0.12
2.00	1.87	4.10	5.12	5.55	5.72
0.00	0.07	0.19	0.59	0.93	1.09
2.50	2.55	5.80	7.47	8.10	8.38
0.00	0.31	1.10	2.31	2.93	3.21
3.00	3.46	7.89	9.93	10.73	11.09
0.00	0.79	2.68	4.47	5.32	5.71
3.50	4.85	10.08	12.17	12.92	13.26
0.00	1.80	4.65	6.60	7.37	7.71
4.00	6.60	12.63	15.03	15.78	16.04
0.00	3.27	7.27	9.61	10.33	10.55
4.50	9.03	15.15	17.39	18.14	18.38
0.00	5.67	10.03	12.10	12.75	12.94
5.00	11.59	17.25	19.33	19.95	20.14
0.00	8.39	12.33	14.12	14.56	14.67
5.50	13.72	19.01	20.81	21.35	21.51
0.00	10.69	14.21	15.58	15.90	15.96
6.00	15.53	20.46	22.09	22.61	22.76
0.00	12.62	15.71	16.82	17.09	17.12
6.50	17.12	21.70	23.24	23.71	23.85
0.00	14.29	16.96	17.91	18.10	18.11
7.00	18.55	22.83	24.32	24.75	24.87
0.00	15.81	18.09	18.93	19.05	19.03
7.50	19.90	23.87	25.31	25.73	25.85
0.00	17.23	19.11	19.85	19.94	19.91
8.00	21.16	24.84	26.23	26.63	26.74
0.00	18.54	20.05	20.70	20.75	20.71



Multiples of  $p_y$  - Longitudinally Loaded

b [mm]	450	450	450	450	450
t [mm]	12.5	12.5	12.5	12.5	12.5
$\sigma_y$ [N/mm <sup>2</sup> ]	235	235	235	235	235
$\alpha$	1	2	3	4	5
e/b	infinite	infinite	infinite	infinite	infinite
f/b	0.333	0.333	0.333	0.333	0.333
$p_y$ [N/mm <sup>2</sup> ]	0.8986	0.6854	0.6762	0.6758	0.6757







